DESIGN AND ANALYSIS OF DISTRIBUTED COOPERATIVE ALGORITHMS FOR OPTIMISING THE PERFORMANCE OF FUTURE WIRELESS NETWORKS

A thesis submitted to the University of Manchester
for the degree of Doctor of Philosophy
in the Faculty of Science and Engineering

2017

By
Mohammed S Bahbahani
School of Electrical and Electronic Engineering
Information Engineering Division

Contents

Abstract **4**

Declaration **6**

Copyright **7**

Acknowledgements **8**

List of Abbreviations **10**

1 Introduction **15**
1.1 Overview 15
1.2 Motivations 18
1.3 Aims and Objectives 19
1.4 Methodology 20
1.5 Contributions of the Thesis 21
1.6 List of Publications 24
1.6.1 Journal Papers 24
1.6.2 Conference Papers 24
1.7 Structure of the Thesis 25

2 Background and Literature Review **26**
2.1 Overview 26
2.2 Introduction to Game Theory 26
2.2.1 Coalitional Games 27
2.2.2 Stackelberg Games 28
2.2.3 Repeated Games 28
2.2.4 Bayesian Games 29
2.2.5 Large Games 30

2.3 Cooperative Communication 30
2.3.1 Relaying Protocols 30
2.3.2 Relay Selection and Resource Allocation Schemes 32
2.3.3 Energy Harvesting Relay Networks 34
2.3.4 Cooperative MAC Protocols 35
2.3.5 Cooperative Routing Protocols 36
2.4 Stadium Connectivity 37
2.4.1 Distributed Antenna Systems and Small Cells 37
2.4.2 High-Density WiFi 38
2.4.3 Wireless Ad-hoc Mesh Networks 39
2.4.4 Software Defined Networks 40
2.5 Summary 40

3 A Distributed Political Coalition Formation Framework for Multi-Relay Selection in Cooperative Wireless Networks 41

4 A Repeated Game Technique for Power and Relay Management in Energy Harvesting Based Networks 42

5 A Cooperative Clustering Protocol With Duty Cycling for Energy Harvesting Enabled Wireless Sensor Networks 43

6 CrowdConnect: A Network Connectivity Enhancement Solution for Crowded Sport Venues 44

7 Conclusions and Future Work 45
7.1 Conclusions 45
7.2 Future Work 47

References 51

Word Count: 41,344

Abstract

Cooperative communication networks, in which nodes share their resources to maximise the overall network performance, have recently attracted significant interests. Traditionally, the nodes only collaborated in multi-hop transmission at the network (NET) layer. However, cooperative diversity at the physical (PHY) layer can achieve capacity gains from the already wasted power in broadcast channels. Meanwhile, energy-efficient designs that enable perpetual network operation are crucial for future wireless applications, such as the Internet of Things (IoT). Hence, the thesis in hand concerns the design and analysis of cooperative techniques to enhance performance and lifetime of future wireless networks while addressing the practical aspects, such as algorithm complexity, decentralisation and cooperation incentives. To fulfil the above, we apply game theory to model the actions of autonomous nodes as they compete or cooperate in maximising their utilities, and in turn, the aggregate network performance. Our research includes a comprehensive analysis of cooperation at the various layers of the communication stack.

At the physical layer, we solve the relay selection problem in a one-to-many decode-and-forward relay channel as a political coalition formation game. This algorithm is shown to yield a stable set of relays that achieves near-optimal sum-rate performance while allowing for a trade-off between performance and complexity through the formation of parties. In the next problem, the power-level selection in amplify-and-forward energy harvesting relay networks is approached via a repeated Bayesian Stackelberg game, in which the source (seller) and the relays (buyers) iteratively negotiate the price that maximises their utilities. The scheme only requires a statistical knowledge of channel, energy and data side information.

The third problem concerns a cross-layer cooperative protocol, which integrates duty-cycling, clustering, energy harvesting and cooperative diversity to

enhance the throughput while maintaining perpetual operation. In addition, a cooperative medium access control (MAC) protocol is designed, in which the relay node forwards the source's packet during a designated sub-slot. The optimal cluster size is also optimised based on the application requirements. The protocol is evaluated and compared against other benchmark schemes using the realistic network simulator OMNET++.

Finally, we present a novel cooperative application-layer protocol, in which smartphone users in a crowded stadium coordinate their cellular network usage to improve their average quality of experience (QoE). Besides, a cluster-based mesh network is designed using the phones' Peer-to-Peer (P2P) connectivity to exchange common match-specific application data. Additionally, the selfish behaviour of users is modelled as a finitely repeated game, where each stage game is played with symmetric near-Nash strategies. Simulations performed in MATLAB confirm the improvement in QoE achieved by the proposed scheme, particularly when it is adopted by more than half of the fans.

Declaration

No portion of the work referred to in this thesis has been submitted in support of an application for another degree or qualification of this or any other university or other institute of learning.

Copyright

Acknowledgements

All praise is due to Allah Almighty for all the blessings he has laid upon me throughout the journey of my PhD programme. I would like to express my sincere gratitude to my supervisor, Dr Emad Alsusa for his constant support and valuable guidance, which have ultimately lead to the accomplishment of this thesis. Also, I would like to thank Dr Mohammed Baidas for his collaboration and the inspiration he provided me with during the first year of my PhD course. Finally, I would like to thank my beloved wife, Zahraa, my parents and the rest of my family for their continuous support and love.

To my parents, wife, and sons.

List of Abbreviations

ACK	Acknowledgement
AF	Amplify-and-Forward
AP	Access Point
AWGN	Additive White Gaussian Noise
BER	Bit Error Rate
BNE	Bayesian Nash Equilibrium
BP	Blocking Probability
BPMP	Blocking Probability Minimising Policy
BPSK	Binary Phase Shift Keying
BT	Bluetooth
C-LEACH	Conventional LEACH
CC	Crowd Connect
CD	Connected Device
CDF	Commulative Density Function
CE	Cellular Enabled
CF	Compress-and-Forward
CH	Cluster Head
CM	Cluster Member

CR	Cognetive Radio
CTS	Cooperative Transmission Subslot
CSI	Channel State Information
CSMA	Carrier Sense Multiple Access
D2D	Device-to-device
DAS	Distributed Antenna System
DC	Duty Cycle
DD	Disconnected Device
DECI	Data/Energy/Channel Side Information
DF	Decode-and-Forward
DSI	Data Side Information
DTS	Direct Transmission Subslot
EA-LEACH	Energy-aware LEACH
EC	Ergodic Capacity
ECO-LEACH	Energy harvesting and Cooperative LEACH
EH	Energy Harvesting
EMWA	Exponentially Weighted Moving Average
ENCO-LEACH	Energy Harvesting Non-Cooperative LEACH
ENO	Energy Neutral Operation
ESI	Energy Side Information
HD-WiFi	High Density Wireless Fidelity
IoT	Internet of Things

IoV	Internet of Vehicles
LAN	Local Area Network
LEACH	Low-energy Adaptive Clustering Hierarchy
LOS	Line of Sight
LTE	Long Term Evolution
MAC	Medium Access Control
MIMO	Multi Input Multi Output
MINLP	Mixed Integer Non-Linear Programming
MMSE	Minimum Mean Square Error
MRC	Maximum Ratio Combining
MRS	Multiple Relay Selection
NACK	Non-acknowledgement
NCH	Non-cluster Head
NE	Nash Equilibrium
NET	Network Layer
OCHP	Optimal Cluster Head Percentage
OFDMA	Orthogonal Frequency Division Multiple Access
OS	Operating System
OSI	Open System Interconnection Model
P2P	Peer-to-Peer
PBE	Perfect Bayesian Equilibrium
PDF	Probability Density Function

PHY Physical Layer

QAM Quadrature Amplitude Modulation

QoE Quality of Experience

QoS Quality of Service

QPSK Quadrature Phase Shift Keying

RAB Relay Advertisement Beacon

RB Resource Block

RACK Relay Acknowledgement Beacon

RBSG Repeated Bayesian Stackelberg Game

RO Relay Ordering Algorithm

RPLS Relay Power Level Selection

RRS Random Relay Selection Algorithm

RSS Relay SNR Strength

RSSI Recieved Signal Strength Indicator

SC Selection Combining

SE Stackelberg Equilibrium

SER Symbol Error Rate

SINR Signal to Interference Plus Noise Ratio

SNR Signal to Noise Ratio

SPMP Source Performance Maximising Policy

SPNE Subgame Perfect Nash Equilibrium

SRS Single Relay Selection

STBC Space-time Block Code

SWDE Sequentially Weakly Dominant Equilibrium

TDMA Time Division Multiple Access

URC Ultimate Ruling Coalition

WAN Wide Area Network

WMN Wireless Mesh Network

WSN Wireless Sensor Network

Chapter 1

Introduction

1.1 Overview

Wireless communications are becoming increasingly popular driven by the widespread of smartphones and the emergence of new wireless applications and technologies. For instance, the fifth generation of wireless networks ($5G$) is expected to improve the peak data rate, the round-trip latency, the number of connected devices, and the energy efficiency of an order of magnitude compared to the current LTE system [1–3]. Moreover, application-specific wireless systems, such as the Internet of Things (IoT) [4], the Internet of Vehicles (IoV), wireless sensor networks (WSN) [5], and e-healthcare systems [6], will bring stringent latency, energy and reliability constraints unsupported by the current wireless designs. Specifically, the IoT will connect billions of objects most of which have no constant supply of energy. Vehicular communications, on the other hand, cannot afford delays longer than a millisecond to avoid accidents, whereas medical sensor networks must be highly reliable and secure so that the patient vitals are continuously monitored.

To fulfil the above requirements of the next generation of wireless systems, two major challenges will be encountered. On the one hand, the aggregate power consumption of billions of wireless devices, as in IoT, will contribute significantly to the global carbon emission footprint demanding the use of renewable energy resources [7], which are unpredictable. On the other hand, the high interference in many proposed ultra-dense network deployments will be too complex to manage given the scarce frequency spectrum, limiting the achievable throughput.

Over the past three decades, different generations of cellular systems have already exploited the time, frequency, code and space domains of the wireless channel to meet the ever-increasing demands of the user applications. Any further enhancement, using conventional techniques, will be limited as the wireless channel theoretical capacity has been already reached. Hence, alternative techniques that exploit other dimensions are expected to lead the next evolution of wireless technology. Among these schemes, massive multiple-input-multiple-output (MIMO) employs a large number of antennas per transceiver to mitigate the channel impairments and to increase the capacity by manyfold, thanks to the millimeter wave frequency band [8]. Future networks may employ cognitive radios that intelligently switch to unoccupied frequencies to improve the spectral efficiency. Besides, network virtualisation based on cloud computing and software-defined networking (SDN) can result in further energy savings as well as in enhanced flexibility by splitting the data plane from the control plane [9]. Another promising scheme is beamforming, which allows for non-orthogonal communication by spatially isolating the radio beams of each receiver [10]. Moreover, machine-learning, device-to-device (D2D) [7], and cooperative communications are other potential technologies of futuristic wireless networks.

Cooperative communication, the focus of this thesis, targets the efficient sharing of the wireless network resources to maximise the overall network performance by leveraging its broadcast nature [11]. Specifically, an intermediate node (relay) overhearing the source node transmission can retransmit the received signal to the destination node, which can then apply a diversity combining scheme improving the channel capacity. Besides the physical layer diversity, the nodes can also collaborate at the upper layers. For example, a cooperative time division multiple access (TDMA) based MAC protocol may allocate special time slots to the relay nodes with better data rates compared to the direct link, whereas a cooperative routing protocol jointly minimises the energy consumption through multi-hop transmissions, while maximising the physical layer diversity gain [12]. Finally, the network nodes can also cooperate by sharing application layer data among themselves in a peer-to-peer fashion achieving energy savings through data aggregation and broadcasting.

The optimal allocation of relays, power levels and channel resources has

been extensively investigated in the literature to maximise the cooperative diversity gains, mainly via centralised optimisation tools [13]. In these schemes, a relay node is assumed to always devote its resources for the sake of maximising the overall network performance. However, when the nodes belong to independent authorities or when future encounters are not guaranteed, a selfish node, also known as a free-rider, may choose to conserve its resources anticipating good behaviour from the other nodes. Thus, incentives, in the form of payments or reputations, are necessary to maintain user cooperation [14]. Recently, game theory has been employed to model the user incentives in cooperative wireless networks and to facilitate distributed solutions required by future ad-hoc wireless applications [15].

In this work, distributed algorithmic designs based on user cooperation are proposed to enhance the network performance at the different layers of the network protocol stack under various scenarios and applications. The first problem considered tackles the multi-relay selection and power allocation in a one-to-many relay channel. Specifically, a political coalition formation game is proposed, where relays form political parties then coalitions of parties to be part of the ultimate ruling coalition that will deliver the source's message to the destinations and win the promised payment.

The scenario is then extended by considering energy harvesting relays with self-generated traffic. Since energy and channel states are not known a priori, a repeated Bayesian Stackelberg game model is proposed to determine the optimal relay power levels. The third problem expands the scenario further to a multi-hop cluster-based network of energy harvesting WSN nodes. A novel cross-layer protocol is designed combining duty-cycling, clustering, energy harvesting and cooperative diversity to not only extend the network lifetime, but also to enable perpetual operation.

The last problem involves a cost-effective software-defined network solution to enhance the fans' quality of experience (QoE) in highly dense sports venues using the ideas developed in the above problems. By disabling the cellular connectivity of a random group of users, the remaining users can acquire common application data at a higher data rate then share it with the disconnected users through a dynamic cluster-based Wi-Fi/Bluetooth P2P network. To eliminate free-riders, we formulate a finitely repeated game with

limited punishment, and extensively analyse its equilibria. The results, obtained through MATLAB simulations, show that the proposed scheme promotes the average user QoE even when it is adopted by nearly half of the fans, and when the human error in following the recommended strategies is as high as 20%.

The following sections explain the motivations, objectives, methodologies and contributions of the thesis.

1.2 Motivations

The motivations behind the work presented in this thesis are summarised as follows:

- Cooperative Diversity

Future wireless networks have many characteristics that can leverage the full benefits of the cooperative diversity. As most IoT applications will be indoors, where the path loss exponent is in the range of $4-6$ [16], splitting the source-destination link by an intermediate relay can mitigate the large scale channel attenuation. Notably, the high density of nodes in such applications ensures the continuous availability of beneficial relays. Additionally, by utilising the antennas of the neighbouring nodes, the diversity gains of MIMO can be realised despite a single antenna per node. This configuration is convenient when a node is constrained by cost, size and complexity as in a WSN. Moreover, the channel correlation between the scattered antennas is much lower, compared to MIMO, leading to even higher diversity gains.

In $5G$ cellular systems, energy harvesting relay stations can be deployed to improve cell edge user's experience through spatial diversity and path loss mitigation in a sustainable manner, as the relays harvest energy from the environment. Furthermore, by being off-grid, such nodes can be more flexibly installed in places that can optimise the coverage enrichment.

- Energy Harvesting

In WSNs and the IoT, the frequent replacement of nodes' batteries will be impractical. Meanwhile, future cellular networks will consume more energy to cope with the growing data traffic and processing costs. A promising technology to extend the lifetime of future systems with minimum environmental

damage is the harvesting of ambient energy [17]. With a careful power management, by which the harvesting rate limits the energy consumption, an energy neutral operation can sustain an indefinitely operating network.

When combined with relaying, EH nodes may act as relays using the excess harvested energy that would be wasted otherwise. This scheme brings incentives for cooperation, and thus will be considered in two problems for this thesis.

- Dense Networks

Highly dense wireless networks (with more than one device per square meter) will be widespread in the future. Consequently, the perceived quality of service (QoS) will suffer as a result of the interference and the limited resources available to each user. Currently, advanced cellular techniques, such as distributed antenna systems (DAS) and high-density WiFi (HD-WiFi), are being deployed at many crowded venues, such as sports stadia and musical concerts. These solutions are expensive, inflexible and inefficiently utilised when these dense situations only occur for short periods of time. Alternatively, software-based solutions that exploit the existing ad-hoc network capabilities of current smartphones should be investigated to enhance the user experience at low cost, as demonstrated in [18].

1.3 Aims and Objectives

The aim of the thesis is to investigate and develop novel strategies based on user cooperation to enhance the performance of future dense and energy constrained wireless networks in terms of data rates, coverage, lifetime and energy efficiency. In light of the above motivations, the research will aim to achieve the following objectives:

- To design distributed algorithms, based on the game theory, to efficiently solve the resource allocation problem while accounting for the node's selfish behaviour. The proposed schemes must also yield a performance comparable to that of centralised optimal schemes with minimum associated computational costs, given the limited resources of tiny network elements.

- To investigate cross-layer cooperative designs that consider the practicality of cooperative diversity from the MAC, NET and Application layers perspectives.
- To develop distributed algorithms for energy harvesting based networks that either maximise the network lifetime or facilitate perpetual operation.
- To solve the stadium connectivity problem using software defined networking concepts that address the free-rider behaviour. The solutions must be cost-effective, practical, and adaptive to the particular match scenario.
- To verify the uniqueness, convergence, and complexity properties of the Nash equilibrium (NE), the stable outcome of the proposed game solution, through rigorous mathematical proof.
- To design and program realistic network simulators needed to verify the performance of cross-layer protocols traversing the whole OSI communication stack.

1.4 Methodology

In this section, we explain the approaches we follow to achieve the above targets and the rationale behind them. First of all, we choose to investigate the node cooperation in a bottom-up manner. In more details, we start by studying capacity maximising designs of a single cooperative link. Following, we examine a network of multiple cooperation-enabled links in terms of the packet delivery rate. Finally, we employ the previous designs in a cooperative application-layer protocol to improve the user's perception of the network performance under realistic scenarios.

Each of the studied problems is approached using the following procedure. First, a system model states the mathematical signal representations, problem settings as well as proper boundaries and assumptions. Secondly, we investigate optimal solutions, where applicable, either in exact or approximate form depending on the problem complexity using MIDACO software package [19]. Since these upper-bounds are based on unrealistic assumptions,

such as the availability of global channel knowledge, and users' altruism, we, then, present the proposed distributed designs that address the above practicality issues using game theory (except from the problem in Chapter 5).

The construction of a game theoretic model starts by defining its components; the players, their strategies, and utilities. The game dynamics are then formulated by adapting existing game models in the literature. In the first problem (Chapter 3), we modify the coalitional game in [20] by redefining its utility and coalitional strength functions according to the proposed scenario. The proofs of equilibrium properties are then directly adapted from the same reference paper. In the second and forth problems (Chapters 4 and 6), we present original mathematical proofs of the game equilibria that are specific to the proposed game model.

Finally, comparisons against other distributed benchmark solutions are performed using extensive simulations. The investigated performance metrics of the proposed PHY schemes are the ergodic capacity and the energy efficiency, whereas the packet delivery rate and the latency are used in evaluating the clustering protocol ECO-LEACH in Chapter 5. Besides, for each game solution, the player utility and the number of iterations until convergence are obtained. As for CrowdConnect (Chapter 6), the player utility is made to reflect the user QoE, which is simply taken as the number of supported applications given the realised throughput.

The MATLAB software is used to simulate the PHY layer problems (Chapters 3 and 4) due to its simplicity in modelling the relay channel performance, whereas the network protocol ECO-LEACH is simulated using GreenCastalia that extends Castalia and OMNET++. This event-driven network simulator emulates the different layers of the network protocol stack producing authentic evaluation of the proposed protocol.

1.5 Contributions of the Thesis

The contributions of this thesis to the literature, as listed in Chapters 3 to 6 in the form of journal papers, are explained as follows:

- A Distributed Political Coalition Formation Framework for Multi-Relay Selection in Cooperative Wireless Networks (Published in IEEE Transactions on Wireless Communications).

In this work, a political coalition and party formation algorithm are designed to solve the network sum-rate maximising multi-relay selection problem. Also, a low complexity iterative algorithm is proposed to efficiently compute the ultimate ruling coalition mapping to be used by players when taking their best response actions. Moreover, an algorithm with linear complexity is designed to eliminate redundant relays and speed-up the convergence of the proposed solution. The proposed solution features stability of the selected relays compared to other schemes in the literature. This work was a result of a collaboration with Dr Mohammed Baidas, an associate professor at Kuwait University, Kuwait. He has participated in the problem formulation and system model. He has also helped in maintaining the quality of the paper in terms of its presentation and accuracy.

- A Repeated Game Technique for Power and Relay Management in Energy Harvesting Based Networks (Submitted to Elsevier Computer Networks Journal).

This work first proposes a low-complexity sub-optimal scheme for the centralised relay power level selection (RPLS). Then, a distributed solution based on a repeated Bayesian Stackelberg game (RBSG) is suggested that only requires causal knowledge of channel, energy and data traffic states. This scheme is spectrally efficient, as the source and relays interact in the game only through the broadcast signals. The proposed solution also provides a trade-off between the throughput and the overheads as the repeated game can be terminated whenever the stage game cost factor outweighs the expected gain from any continuation play. This feature makes the proposed scheme compatible with applications of different latency and throughput requirements. Additionally, the perfect Bayesian equilibrium (PBE) of the game is proven to exist and shown to converge in a finite number of iterations. To the best of our knowledge, an RBSG with an infinite strategy space and uniformly distributed beliefs is unique.

- A Cooperative Clustering Protocol With Duty Cycling for Energy Harvesting Enabled Wireless Sensor Networks (Accepted in IEEE Transactions of Wireless Communications)

The optimal cluster head percentage problem for EH clustering based networks is formulated that guarantees ENO, while fulfilling the bandwidth and

latency requirements. The problem is then solved using an iterative method for which complexity is bounded by the number of nodes in the network. Additionally, a distributed CH selection scheme is proposed based on duty cycling and the energy harvesting rate. The deterministic CH selection in ECO-LEACH is compatible with rapidly changing energy sources such that the required CH percentage can be maintained over a few number of rounds. In contrast, LEACH needs some rounds equal to the number of nodes before the required number of CHs is maintained. Another feature of the proposed CH selection is the absence of harvesting rate information exchanged between the nodes. Instead, only the average nodes' harvesting rates are required. Moreover, the proposed protocol is applicable in non-homogeneous networks, in which nodes have different capabilities and QoS requirements. Another component of the proposed protocol is the data transmission duty cycle, which ensures ENO when the OCHP problem has no feasible solution. Moreover, a novel TDMA-based cooperative mechanism is suggested based on sub-slots along with a relaying duty cycle design that utilises the energy unconsumed in data transmission. The sub-slot based relaying scheme has a low latency, as the relayed transmission starts immediately after the direct one.

- CrowdConnect: A Network Connectivity Enhancement Solution for Crowded Sport Venues (Prepared for a Patent proposal)

A novel technique based on software-defined networking concepts is proposed to enhance the QoE in crowded sports stadia at minimum cost. To facilitate the sharing of match-specific application data, a dynamic cluster-based topology algorithm is designed that adapts to specific situation and the predicted behaviour of fans. Then, a novel game strategy with limited punishment in finitely repeated games is created to discourage the free-riding behaviour. The occasional irrationality of fans is modelled as game noise and incorporated within the repeated game equilibrium. Due to the commercial potential of the proposed solution, the intellectual property, in the form of a patent, is being pursued. Once the patent is filed, this work will be submitted to a distinguished journal for publication.

Besides the contributions of Dr Baidas in the first problem as stated above, I would like to state that the rest of the research work including the problem

formulation, mathematical analysis, simulation, result analysis and discussion of all the other problems are all my own work.

1.6 List of Publications

1.6.1 Journal Papers

1. M. S. Bahbahani, M. W. Baidas and E. Alsusa, "A distributed political coalition formation framework for multi-relay selection in cooperative wireless networks" IEEE Trans. Wireless Commun., vol. 14, no. 12, pp. 6869–6882, Dec. 2015.

2. M. S. Bahbahani and E. Alsusa, "A cooperative clustering protocol with duty cycling for energy harvesting enabled wireless sensor networks" IEEE Trans. Wireless Commun., doi: 10.1109/TWC.2017.2762674.

1.6.2 Conference Papers

1. M. S. Bahbahani, M. W. Baidas and E. Alsusa, "Distributed multi-relay selection via political coalition formation in cooperative wireless networks", IEEE Wireless Common. Netw. Conf. (WCNC), Apr. 2016.

2. M. S. Bahbahani and E. Alsusa, "Joint cost-sharing and multi-relay selection for two-way relay networks using a pricing game", IEEE Wireless Common. Netw. Conf. (WCNC), Apr. 2016.

3. M. S. Bahbahani and E. Alsusa, "Relay selection for energy harvesting relay networks using a repeated game", IEEE Wireless Common. Netw. Conf. (WCNC), Apr. 2016.

4. M. S. Bahbahani and E. Alsusa, "DC-LEACH: A duty-cycle based clustering protocol for energy harvesting WSNs", 13th International Wireless Communications and Mobile Computing Conference (IWCMC), Jun. 2017.

1.7 Structure of the Thesis

This thesis is written in the university approved journal format, in which the conducted research is presented in a suitable publication form. Minor modifications were made to the published journal in order to conform with the university thesis submission guidelines. Hence, the thesis structure is organised as follows: the first chapter lists the contributions, motivations and approaches used to conduct the research work in the thesis. The second chapter reviews the recent literature concerning the areas covered by the thesis. Chapters 3 to 6 contains the main research contributions of this PhD thesis in the form of journal papers. Finally, Chapter 7 concludes the thesis with a summary of the main contributions and a discussion of possible future work.

Chapter 2

Background and Literature Review

2.1 Overview

This chapter presents a comprehensive survey of the recent advancements in the areas investigated by this thesis. The first section provides the reader with the essential knowledge of the basic concepts of game theory, particularly, the game equilibrium notions investigated in the chapters to follow. In the second section, we explain the concept of cooperative diversity by reviewing the literature of the relaying protocols, relay selection and power allocation schemes of battery-powered and energy harvesting based networks. The literature on contention and scheduling-based cooperative MAC protocols as well as cooperative routing protools are also reviewed. Lastly, we compare different approaches used to enhance the network performance in sports stadia.

2.2 Introduction to Game Theory

Game theory is a mathematical tool that analyses the strategic interaction among several decision-making individuals as each strives to maximise his benefit in the game [21]. Besides its wide popularity in economics and political sciences, game theory has been recently introduced to solve many wireless communication network problems from resource allocation to network security. Instead of solving complex optimisation problems centrally, a game allows for a distributed solution, whereby each player in the game contributes to the overall solution using local information.

Primarily, a game is composed of a set of players, a set of permissible actions, and a set of player utilities. Players are usually assumed to be rational, that is, they always strive to maximise their utilities being the payoffs earned minus the costs incurred by taking any possible action in the game. The actions can be either *pure*, that is, a single action played with certainty or *mixed*, where the player assigns probabilities to each possible action.

A special outcome of any game is the equilibrium state known as the *Nash Equilibrium* (NE). The NE is the state of the game in which no player benefits by unilaterally deviating to any other action given the other player' actions remain unchanged [21]. Games can have multiple equilibria or no equilibrium at all. However, it is shown in [21], using fixed point theorems, that a NE always exists for mixed strategy games. In pure strategy games, the existence of a NE depends on whether the payoff function is continuous and quasi-concave in the player action space.

Even when a state of equilibrium exists, the convergence to this state is not always guaranteed especially when players start from a non-equilibrium state and have limited knowledge about the utilities of each other. Besides, the game equilibrium may be computationally expensive making the game solution impractical. Hence, it is always desirable for a game theoretic solution to maintain a unique NE, which its convergence is guaranteed with minimum complexity. The different types of games and their equilibrium notions that will be encountered in this thesis are discussed in the following subsections.

2.2.1 Coalitional Games

With the lack of coordination, the selfishness of players entails a non-cooperative behaviour that may compromise the social welfare, such as the network sum-rate. For instance, in a file sharing game, the non-cooperative action profile, in which all the peers defer from uploading any files is an inefficient NE, as none will obtain any resources, yet no player will benefit by unilaterally starting to upload files. However, in a cooperative game, a group of players can form a coalition (a binding agreement) to strengthen their positions in the game against the remaining players and to obtain higher rewards. The coalition utility can be either distributed among the coalition members arbitrarily (transferrable utility) or deterministically (non-transferrable utility) [22]. The formation of coalitions can be implemented by a sequence of

merge and split operations, such that a player only merges to a coalition if the merger results in a higher utility. Similarly, the player will split from a coalition when the split is more beneficial. It is shown in [23] that a merge and split algorithm always converges to a stable coalition structure.

Besides coalition formation games, cooperative game theory also includes bargaining games in which players negotiate upon the terms of cooperation [24]. A real-life example of a coalitional game is the interaction among politicians in governmental elections. A framework for analysing political coalition formation games is presented by Acemoglu *et al.* in [20], where a dynamic non-cooperative coalition formation algorithm is proposed, in which players sequentially propose then vote over coalitions.

2.2.2 Stackelberg Games

In a Stackelberg game, a player can be either a leader or a follower. The leader player makes the first move then the follower player responds optimally. This scenario creates an advantage for the leader since the follower's best response action depends on the leader's move, which the latter can anticipate in advance [25]. An example of a Stackelberg situation is when a large firm (leader) decides on a price, then a smaller firm (follower) decides to enter or to exit the market.

Due to the sequential play in a Stackelberg interaction, a special equilibrium, named the Stackelberg Equilibrium (SE), exists when each player is best responding to the opponent's strategy. This SE pair of leader/follower actions can be induced through *backward induction* as follows. Starting at the follower turn, the follower's utility maximising action is determined, given any leader action, then the leader's best action, given the follower's best response, is found. Stackelberg interactions with multiple leaders/followers may also exist as will be demonstrated in Chapter 4.

2.2.3 Repeated Games

When binding agreements cannot be enforced, cooperation among players can be sustained through repeated interactions, where a series of *stage games* are played consecutively and the player utility becomes the sum of the utilities obtained in each stage game. Punishment strategies, such as the grim-trigger,

can support cooperative equilibria when players have sufficient beliefs that the interaction will continue, as outlined by the *folk theorems* [21]. In the grim-trigger strategy, a player in the file sharing game above will play the cooperative action (upload files) in every stage game until a defection by an opponent player triggers the player to play the non-cooperative action (refuse to upload) thereafter.

The NE discussed above is no longer adequate in repeated games, as it does not prevent incredible threats. In other words, given a player actually deviated in the first stage, it is not beneficial for the other player to conduct the punishment in the next stage. Hence, a stronger equilibrium notion called the sub-game perfect Nash equilibrium (SPNE) is introduced for repeated games, which demands that each sub-game (the continuation play following any history of play) itself constitutes a NE.

2.2.4 Bayesian Games

In the above games, the players' identities, their strategy spaces and utility functions, also referred to as the player *type*, were assumed to be common knowledge among all players. In many practical scenarios, the player types may not be available to all players. For example, the channel state information (CSI) of every link in a wireless network may not be available to all the nodes. These games are referred to as *incomplete information* or *Bayesian* games [26]. In such games, each player forms a belief (probability distribution) over the possible *types* of the other players.

An appropriate equilibrium concept that addresses the uncertainty in game components is known as the *Bayesian Nash Equilibrium* (BNE) [27]. This equilibrium requires each player to play a best response that maximises the expected utility by applying Baye's rule. When a Bayesian game is played repeatedly, a refinement to the SPNE, termed the *Perfect Bayesian Equilibrium* (PBE), emerges as a stronger game solution. This equilibrium demands that player's strategies are sequentially rational and that the beliefs are consistent, as will be explained in detail in Chapter 4.

2.2.5 Large Games

Many real-life interactions, such as political elections and stock markets, involve a finite but large number of players, in which the effect of each player on the game outcome is negligible. Game theorists have invented different models to represent and analyse such situations. For instance, Aumann, in [28], imagined a continuum of players that approximates the true situation, so that powerful mathematical solutions can be directly applied. The work by Schmeidler [29] proves that a complete information continuum game has a pure strategy Nash equilibrium. On the other hand, Kalai in [30] followed an asymptotic approach, where the number of players tends to infinity. The equilibrium of such game model was shown to be robust even with incomplete information. In [31], Kalai *et al.* extends the model to include Bayesian repeated games of anonymous players. The concept of compressed equilibrium is proposed, in which a player simply replaces the distributions of the unknown player types by their expected values according to the law of large numbers. Approximate Nash equilibria in large games have been analysed in [32], where players learn to play a near Nash equilibrium.

2.3 Cooperative Communication

Cooperative diversity exploits the broadcast nature of the wireless channel [11], [33]. Specifically, when a source node's message is overheard by a node (relay), other than the destination, the node may support the transmission by retransmitting (relaying) the message to the destination. The destination may combine the signals received from the relay(s) and the source (if the direct link exists) to realise cooperative diversity. Thus, the cooperative relay channel is effectively a single-input multi-output (SIMO) and a multi-input single-output (MISO) systems connected back-to-back with the multiple antennas distributed over the relay nodes. Depending on how the relays process the received signal, different relaying protocols are obtained as discussed below.

2.3.1 Relaying Protocols

Amplify-and-forward (AF) and decode-and-forward (DF) are popular relaying protocols in the literature. An AF relay receives the source's transmission

in the first time-slot, then simply amplifies and retransmits the unprocessed signal in the second time-slot. As a result, the capacity of the relay channel depends on the combination of the backward (source-to-relay) and the forward (relay-to-destination) channel gains as well as the direct channel gain (source-to-destination). For a mathematical representation of the AF relay channel and its theoretical capacity bounds, the reader may refer to Section 3.2 of the thesis.

On the other hand, a DF relay attempts to decode the received message before retransmission. Hence, two variations of DF relaying can be achieved, as discussed in [34]. In a fixed DF protocol, the relay always forwards the decoded signal, whereas, in a selective DF protocol, the relay attempts to decode the signal only if the signal to noise ratio (SNR) is above a certain threshold. Since the relay may incorrectly decode the message, the mutual information and hence the capacity of any of the above DF schemes is limited by the minimum of the source-relay link mutual information and the combined mutual information of the source-destination and the relay-destination channels. The fixed DF scheme has a diversity order of 1, as the mutual information is the minimum of both forward and backward links. The selective DF relaying (with a single relay and the direct link), however, achieves a diversity order of 2 by only forwarding the correctly decoded symbols [34]. The diversity order is defined as the slope of the outage probability curve in the high SNR region [33].

The performance of the above protocols has been well analysed in the literature. For example, a comparison of DF and AF protocols in a multi-hop coded transmission is given in [35], which concludes that the capacity and the SNR gains of DF over AF is no more than $\log_2 N$ and N respectively, where N is the number of hops. In contrast, Boyer et al. in [36] have demonstrated, using uncoded binary phase shift keying (BPSK), that AF is superior to DF in a multi-hop relay channel as DF is limited by the performance of the weakest hop. Another work by Yu and Li in [37] has considered practicality issues when comparing the two protocols. Specifically, it was found that when the inter-user link is in outage, the performance of both protocols is similar. Generally speaking, AF is cheaper, simple to implement and it introduces less latency compared to DF relaying. However, once a DF relay correctly decodes a symbol, a noise-free version of the symbol is relayed to the destination,

preventing noise propagation, as in AF. Despite that, when DF incorrectly decodes the symbol, AF becomes superior despite the amplification of noise. Hence, adaptive relaying schemes were developed to opportunistically select the appropriate protocol according to the channel conditions [38].

Besides AF and DF protocols, compress and forward (CF) and incremental relaying (IR) are other protocols in the literature that may excel over AF and DF schemes under particular conditions [39]. In CF, the relay only sends a quantised version of the decoded symbol instead of the exact symbol as in DF, whereas the IR protocol relies on a feedback channel, by which the destination requests the relay to forward the decoded signal only if the destination fails to decode the source's symbol [40]. This technique improves the latency and the spectral efficiency at the cost of a feedback link. The IR protocol is demonstrated in Chapter 5 of the thesis.

2.3.2 Relay Selection and Resource Allocation Schemes

Despite the direct relationship between the diversity order and the number of available relays, selecting a single best relay at a time is shown to yield the full diversity order. Thus, single relay selection (SRS) techniques have been well explored in the literature due to the reduced interference and synchronisation issues compared with the $all - participate$ or the multi-relay selection (MRS) schemes. For instance, the best-worst channel SRS has been studied in [41], and then, shown in [42] to achieve the full diversity order. In [13], an optimal SRS in multi-user multi-relay networks is analysed, which is shown to have quadratic complexity in the number of users and relays. In turn, the authors propose a suboptimal SRS scheme with linear complexity in the number of relays but quadratic complexity in the number of users. Another SRS scheme that maximises the end-to-end signal-to-noise ratio (SNR) is studied in [43].

Multi-relay selection (MRS), in which a subset of relays collectively relay the source's signal, was shown in [42] to yield a better performance than SRS under separate power constraint per node using AF relays. Moreover, a suboptimal distributed algorithm for MRS is proposed based on relay ordering, which has linear complexity. In [44], the MRS is modelled as a knapsack problem considering both short-term and long-term relay selection. A threshold-based MRS technique is proposed in [45], where the destination selects the most reliable relays based on the relay-destination SNR only. The impact of

outdated CSI on relay selection was compared in [46] showing a better performance of SRS under CSI error. Also, a performance comparison shows that MRS outperforms SRS when more relays are introduced. On the other hand, MRS leads to more packet collisions and requires stringent synchronisation schemes [14].

In the papers above, a relay either transmits at full power or remains silent. However, allowing relays to transmit at any feasible power level can further enhance the SNR as demonstrated in [47]. In particular, upper bounds and approximations of the symbol error rate (SER) performance are derived for both quadrature phase-shift keying (QPSK) and quadrature amplitude modulation (QAM), in the cases of AF and DF relaying, assuming a direct link between the source and destination nodes. In addition, the optimal power distribution between the source and relay nodes is determined for different channel gains of the source-relay and relay-destination channels. Many important results are outlined as follows. First, the DF protocol is shown to be generally superior to the AF protocol, with the performance gain being related to the modulation used. Secondly, the whole power should be allocated to the source when the source-relay channel gain is much greater than that of the relay-destination channel. In contrast, an equal power split is optimal when the channels have comparable gains.

To find the optimal set of relays and power levels, a complex optimisation problem must be solved that requires the knowledge of all channel gains. Due to the absence of a central station in many future wireless applications such as WSNs and IoT, distributed RS using game theory has recently gained attention as it spreads the computational burden across the relay network. For example, a distributed RS technique with power control using a Stackelberg game is studied in [48], where, in the buyer-seller game, each relay negotiates with the source the relaying price that maximises the benefit of both nodes. The authors in [49] propose a distributed SRS based on the Chinese restaurant game model, taking into account the negative network externality, which is the effect of the node's action on the utilities of the other nodes. Additionally, it is demonstrated that the proposed algorithm converges to a Nash Equilibrium grouping and yields a sum-rate comparable to that of centralised relay selection. An auction game is utilised in [50] to design a distributed MRS algorithm to select the best subset of relays for each source in the uplink of

a cellular network. In [51], a distributed relay assignment approach is modelled as a non-cooperative repeated game with mixed strategy, where players randomise between the available actions.

Coalitional game theory has also been applied to address the RS problem by modelling the interaction as a cooperative game. In [52], the stability of the coalition formation is analysed using a Markov chain model. Distributed merge-and-split algorithms based on coalition formation are studied in [23], [22] and [53]. Specifically, the algorithm in [22] allows network nodes to form disjoint coalitions, while that proposed in [53] optimises power allocation, taking into account the interference between coalition members. Finally, in [23], an altruistic coalition formation game is proposed for many-to-one networks, which analyses the effect of different power allocation criteria as well as mobility on the coalition formation.

2.3.3 Energy Harvesting Relay Networks

Green communication networks operated by renewable energy have recently emerged to maximise the network lifetime without harming the environment. The network nodes can have rechargeable batteries continuously replenished with energy harvested from the surrounding environment, such as solar, vibration or thermal energies [17]. Energy may also be harvested from the received RF signal; thus, nodes can exchange energy packets in a technique named simultaneous wireless information and power transfer (SWIPT) [54]. If optimally designed, the energy transfer among nodes may greatly improve the resource utilisation and extend the network lifetime, particularly in self-sustained WSNs.

Relay nodes with energy harvesting capabilities have been recently suggested for EH cooperative networks. However, the relay selection problem with EH relays is further complicated due to the random arrival of energy packets. Specifically, the optimal relay selection is only achieved by investing the harvested energy in the time-slots where the channel gains are at a maximum. This requires a non-causal knowledge of energy arrivals and channel conditions in the future time slots, which is impractical. Several works have considered both causal and non-causal RS using optimisation techniques [55–59]. In [60], the non-causal selection problem is first formulated as an assignment problem, which is shown to be NP-hard. Then, a

sub-optimal and low-complexity algorithm for the causal scenario, based on the relative throughput gain, is proposed. Later, in [55], the joint relay selection and power allocation problem for EH systems with DF relays is studied. Again, finding the performance upper bound for outage minimisation requires solving a dynamic programming problem. Alternatively, suboptimal causal policies with low complexity are simulated and shown to yield substantial improvements over non-energy-aware selection schemes.

Similar to RS in battery powered networks, distributed EH-RS schemes can also be implemented using the theory of games as follows. A coalitional game is adopted in [61], where a set of source-destination pairs form a coalition to share their transmitted and relayed powers under a total power constraint. Interestingly, it was shown that the grand coalition (the coalition of all relays) is always preferred by the players in the game. Another game theoretic EH-RS technique is discussed in [62], which models the interaction between sources and relays as a college admission market, whereas the interaction between the different sources is modelled as an interactive, partially observable, Markov decision process. The results showed that, with the adopted selection policy, the solution maximises the long-term players' utilities. The authors in [54] considers a Stackelberg game to incentivise the relays to forward the sources message, while harvesting RF energy from the received transmissions.

2.3.4 Cooperative MAC Protocols

Cooperation-enabled MAC protocols, when combined with the diversity schemes above, can provide a higher transmission rate and a lower latency in fading channels [63]. The contention-based cooperative protocol in [64] brings throughput and latency enhancements, while maintaining compatibility with the IEEE 802.11 standard. Because relaying consumes additional energy, the protocol in [65] maximises the network lifetime by assigning scores that quantify the relays' availability. Another protocol in [66] incorporates two relays per source node such that the total transmission time when using both relays is less than that of the direct link. Also, a cross layer protocol that leverages cooperation at MAC and PHY simultaneously is presented in [67]. Specifically, a source node broadcasts its coded data bits in the first half of a time-slot, which is overheard by a potential relay node.

Scheduling based cooperative MAC protocols based on TDMA were also

investigated in the literature. In [68], the inactive nodes (not allocated a time slot) can overhear the transmission of the active node and the non-acknowledgement (NACK) of the destination. Only, if a NACK is received and the active node's packet was decoded correctly, the relay node will re-transmit the packet in the next allocated time slot of the following TDMA frame. A different technique is proposed in [69], where mini-slots are used to reserve cooperative resources and avoid conflicts between sources, relays and destinations.

2.3.5 Cooperative Routing Protocols

Apart from the multi-hop transmission, layer-3 protocols can also exploit co-operative diversity to boost the network performance further. In this regard, we focus on cluster-based routing protocols due to their associated energy savings. A famous clustering protocol is LEACH [70] (explained in Chapter 5), which elects cluster heads (CH) to aggregate and then forward data packets of their cluster members to a sink node.

The EH clustering extensions to LEACH were proposed in [71–74]. Unlike LEACH, which evenly distributes the CH role among the nodes, the above schemes select CHs based on their residual energies and forecasted harvesting rates. For instance, in [72], a CH decision threshold termed the energy potential (EP) function is computed for each node in terms of its energy harvesting rate and currently available energy as well as the EP functions of neighbouring nodes. In [72], the optimal percentage of CHs is incorporated into a new CH threshold function that gets updated by the sink throughout the operation of the protocol. Specifically, a search algorithm is used by the sink to compare the current round's average throughput against that of the last round, and then a regulation factor is updated accordingly.

The above solutions do not guarantee a perpetual operation and require the exchange of information among the nodes, which creates additional overheads. The protocol in [74] proposes cluster head groups (CHG), in which nodes take turns in becoming the CH to minimise the overheads of the CH selection process. In [71], Yang et al. analysed an optimal multi-hop clustering architecture to achieve a perpetual operation in EH-WSNs. Particularly, energy neutrality constraints were defined and used to obtain the minimum network data transmission cycle using convex optimisation. Lastly, an EH

aware routing protocol based on the gradient model is proposed in [75] for WSNs. Also, a CH selection scheme based on the residual energy of nodes and their relative positions is suggested. Then, a packet forwarding mechanism to balance the energy consumption among the EH nodes is presented.

Cooperation enabled clustering protocols were discussed in [76], [77], and [78]. The protocol in [76] introduces cooperative cluster heads (CCH) that are selected to maximise the spatial diversity. Non-cluster members may become CCHs to participate in relaying the CH packet to the sink using the space-time block code (STBC) technique [33]. In [78], the lifetime of a battery-powered WSN is extended using an optimised clustering algorithm that determines the optimal locations of CH nodes. Then, EH nodes can be used to relay the NCH packets to the CHs.

2.4 Stadium Connectivity

In many crowded venues, wireless networks often fail to deliver the expected user quality of experience, defined as the human perception of the provided quality of service (QoS) [79]. A common crowded network situation is the football stadium, where the number of active users normally exceeds the capacity of the cellular network. Hence, we review the most recent approaches in the literature and the industry that attempt to either enhance the performance of the stadium cellular/WiFi network or to propose alternative schemes as we explain next.

2.4.1 Distributed Antenna Systems and Small Cells

A distributed antenna system (DAS) is a MIMO system, in which multiple antennas are co-located at one side of the radio link and spatially scattered access points (AP), connected with optical fibre, comprise the other end of the link [80]. As a result, the DAS system extends the coverage of the macro base station to the inside of the RF signal attenuating stadium structure. Despite being limited by the cell capacity, the SINR performance is enhanced through the diversity-multiplexing tradeoff of MIMO [81]. Therefore, performance optimised designs for the stadium DAS have been recently investigated in the literature. In [82], the optimal distributed antenna selection is studied by

considering both signal and interference strengths. The stadium scenario investigated shows that power allocation can further enhance the capacity. The optimal designs of a 2D antenna system including beam pointing directions is analysed in [83]. The results show that it is sufficient to use four antennas with sectoring by pointing the beams towards the nearest stadium stands.

Another distributed antenna system, designed at Bell Labs, is shown to outperform legacy DAS in both indoor and outdoor stadia [84]. By constructing a 3D stadium model, the optimal number, location, orientation and transmit power level were investigated and simulated using OPNET, which is based on the LTE system. In practice, DAS systems have been widely used by network operators to enhance cellular coverage in stadia, besides small cells and WiFi offloading. Claimed as the most connected stadium in the world, the Wembley Stadium in London has an advanced DAS system installed by EE to boost 4G internet access to all fans [85].

2.4.2 High-Density WiFi

In a high-density (HD) WiFi network, a large number of users and access points coexist in the same coverage area, thus, limiting the user capacity due to interference and collisions. Unlike a coverage-based WiFi design, an HD-WiFi benefits from the 5GHz band of WiFi due to its shorter range and more non-overlapping channels. To mitigate interference and maximise the user's QoE, the number of APs, their locations, power levels, frequency channel reuse and application requirements must all be optimised. For instance, the number of APs should neither be too high, increasing the co-channel interference, nor too low, sacrificing the wireless coverage. In addition, the channel frequency assignment to APs should minimise the interference as explained in [86].

Among the several HD WiFi networks deployed across sports stadia, Agile Stadium Solution [86], developed by Huawei, is implemented at Borussia Dortmund's stadium in Germany. By utilising 3D site planning, 5GHz RF and MIMO, over 80,000 fans can enjoy the speed of a 1.75 Gbps broadband Internet backhaul connection. Cisco has developed another HD-WiFi solution based on their own components. The proposed design is scalable, reliable, secure and includes specially designed algorithms for services including video replays, ticketing and secure point-of-sale infrastructure [87].

2.4.3 Wireless Ad-hoc Mesh Networks

Wireless mesh networks (WMN) can be temporarily deployed to mitigate dead zones and increase the capacity of cellular and WiFi hotspots at low cost [88]. In a mesh network, each node connects to its surrounding nodes, thus, data packets can traverse the network in a multi-hop fashion through distributed algorithms and protocols until the packets reach Internet gateway nodes. Applications of mesh networks vary from public emergency control, social networks and other situations with absent network infrastructure. Cisco has developed a mesh network system based on Cisco Aironet APs for secure enterprise, campus and metropolitan WiFi networks [89]. Particularly, a mesh network is created among WiFi APs running the Cisco Adaptive Wireless Path Protocol (AWPP) to carry wireless LAN client traffic.

On the other hand, a mesh network can be established between the mobile devices themselves (Device-to-Device) using WiFi-Direct technology without the need for fixed mesh APs [90]. Initially called WiFi P2P, the WiFi-Direct standard facilitates the seamless setup of infrastructure or ad-hoc WiFi hotspots and the discovery of nearby services on the go without an actual AP. In detail, a node can create a group and become a group owner (GO) or join other groups using the WiFi-Direct protocol. Access credentials are exchanged through the protocol setup phase granting access to specific services declared by the group. Legacy WiFi devices may still join the groups as legacy APs. With this technology, scalable and secure P2P mesh networks have been demonstrated by many applications including chatting Apps and stadium solutions. For instance, TribeHive [18], allows fans to share their cellular data connections to obtain match specific information using WiFi P2P connectivity by employing a delay-tolerant protocol. Specifically, when a device cannot receive the match data from the cellular network due to congestion or poor signal, the data is requested from a nearby device with better signal strength. However, this scheme was only demonstrated to support low data rate text-based in-match applications and not a general Internet access.

2.4.4 Software Defined Networks

A newly proposed strategy for future networks is the decoupling of the network control plane (routing decisions) from the data flow plane (forwarding decisions) through virtualisation. In a software-defined network (SDN), routers and switches are only responsible for the forwarding of packets, whereas the routing of packets is controlled externally by a centralised controller [9], [91]. This technique improves the WAN link utilisation through dynamic routing and traffic engineering and also enables efficient protocol evolution. In wireless mesh networks, many design challenges can be overcome by using SDN concepts. Efficient resource allocation, congestion control and load balancing are among the major problems that require a global network view, which is hard to obtain in conventional distributed algorithms. However, the centralised control of an SDN suffers from compromised network reliability as a result of link failure or network partitioning. Thus, fault tolerance support using fault detection and redundancy is essential [91]. For a detailed comparison of existing SDN schemes for WMN, the reader may refer to [91].

2.5 Summary

In this chapter, a comprehensive review of game theory and cooperative communication techniques was presented. Cooperative relaying achieves the full diversity without the associated hardware complexity of MIMO. The optimal utilisation of resources can further improve the network performance but requires full CSI availability at a central station. Thus, distributed algorithms based on game theoretic models can eliminate the need for a central node in future ad-hoc networks, while creating incentives to the relay nodes in the form of payments or reputations, as will be explained in the following chapters.

Chapter 3

A Distributed Political Coalition Formation Framework for Multi-Relay Selection in Cooperative Wireless Networks

A Distributed Political Coalition Formation Framework for Multi-Relay Selection in Cooperative Wireless Networks

Mohammed S. Bahbahani, *Student Member, IEEE*, Mohammed W. Baidas, *Member, IEEE* and Emad Alsusa, *Senior Member, IEEE*

Abstract

In this paper, the problem of multi-relay selection in one-to-many cooperative wireless networks is studied via a political coalition formation game approach. Specifically, each relay node is endowed with some *coalitional strength* and the selected coalition consists of a subset of the available relays in the network that is powerful enough to win against any other potential coalition. In addition, the formed "ruling" coalition must be self-enforcing (and hence stable) such that none of its members would split and become the new ruling coalition. A distributed ruling coalition formation algorithm is proposed that selects such stable set of relays with a marginal compromise on network sum-rate performance. Moreover, our proposed algorithm offers a network sum-rate performance/stability tradeoff through formation of political parties of relays, which also reduces complexity and communication overheads. The proposed algorithm is compared with centralized multi-relay selection as well as other multi-relay relay selection algorithms from the literature, and is shown to provide comparable network sum-rate with the added advantage of network stability.

Index Terms

Centralized, coalition formation, cooperation, distributed, relay selection, stability, sum-rate

I. Introduction

Cooperative communication using wireless relays has attracted much attention in the past few years. The basic idea of cooperative relaying is that nodes which overhear a source node's broadcast may help mitigate shadowing and path-loss, extend coverage area, and exploit spatial diversity gains by forwarding its signal to its intended destination node(s) [1]. Specifically, with multiple relays, spatial diversity can be further exploited; hence, improving network performance without the need for multiple antennas at each node [2]. Recently, several research works have considered single-relay selection (SRS) as well as multi-relay selection (MRS) to achieve bandwidth efficiency and full diversity gains. For instance, best-worst channel SRS has been studied in [3], then shown in [4] to achieve full diversity. In [5], an optimal SRS scheme that achieves full diversity in

multi-user multi-relay networks is proposed and shown to have quadratic complexity in the number of users and relays. Additionally, the authors propose a suboptimal SRS scheme with linear complexity in the number of relays but quadratic in the number of users. A SRS scheme that maximizes the end-to-end signal-to-noise ratio (SNR) has been studied in [6]. In [7], the authors propose an output-threshold MRS scheme that selects a set of relays the combined SNR of which exceeds a certain threshold. Such a scheme has been shown to outperform other single- and multi-relay selection schemes in low to moderately high SNRs as well as providing flexibility in utilizing bandwidth and spatial diversity. In [4], the achievable diversity orders of several single- and multi-relay selection schemes have been studied. In addition, it was shown that MRS can yield better performance than SRS under separate power constraint per node with amplify-and-forward relays. Moreover, a suboptimal distributed algorithm for MRS that achieves full diversity with linear complexity is proposed based on relay ordering. Also, an MRS scheme with quadratic complexity but improved SNR performance is studied. All these relay selection schemes are based on the assumption that a centralized controller exists to perform relay selection and that the relays are always willing to cooperate and share their transmission resources. However, this is not the case in practical ad-hoc wireless networks, as network nodes are naturally selfish and may be unwilling to share their transmission resources to help other nodes without a reward/payoff [8].

Game theory has recently been applied by many researchers to wireless relay networks to address the problem of distributed relay selection [9]. For example, a distributed single-relay selection technique with power control using a Stackelberg game is studied in [10], where in this buyer-seller game, the source node and the relays negotiate a price for relaying the source's packets such that their utilities are maximized. The authors in [11] proposed a distributed single-relay selection based on the Chinese restaurant game model, taking into account negative network externality. Additionally, it was demonstrated that the proposed algorithm converges to a Nash Equilibrium grouping and yields a sum-rate that is comparable with that of centralized relay selection. An auction game is utilized in [12] to design a distributed algorithm to select the best subset of relays for each source in the uplink of cellular networks. In [13], a distributed relay assignment approach is studied and modeled as a non-cooperative and mixed strategy repeated game. Coalitional game theory has recently been applied by many researchers to address the problem of distributed relay selection. For instance, in [14], the stability under uncertainty of coalition formation is analyzed using a Markov chain-based model. Distributed merge-and-split algorithms based on coalition formation were studied in [15]–[17]. Specifically, the algorithm in [15] allows network nodes to form disjoint coalitions; while that proposed in [16] optimizes power allocation taking into account the interference between coalition members. Finally, in [17], an altruistic coalition formation

game is proposed for many-to-one networks, which analyzes the effect of different power allocation criteria as well as mobility on coalition formation.

In this work, the problem of distributed multi-relay selection in one-to-many cooperative wireless networks is studied and formulated as a political coalition formation game [18], [19]. Specifically, a distributed algorithm for the selection of a network sum-rate maximizing stable set of relays is designed. The selected relays must be part of the unique ultimate "ruling" coalition, which is self-enforcing and stable, such that none of its members would split (unilaterally or multilaterally) and form a new ruling coalition. To appreciate the tradeoff between network sum-rate performance and stability, a party formation algorithm is proposed, where it is shown that higher network sum-rate and lower computational complexity can be achieved at the expense of lower stability. Our proposed algorithm is compared with centralized multi-relay selection as well as other multi-relay selection schemes from the literature, yielding comparable network sum-rate performance. The existence, uniqueness, convergence and stability properties of the proposed algorithm have also been studied and verified via extensive simulations. Most published multi-relay selection schemes are assumed to be centralized and do not consider the stability of the selected relays set. Also, in contrast to other coalitional game theory-based solutions in the literature, our proposed distributed algorithm considers one-to-many (e.g. downlink) communications.

The motivation behind the application of a political coalition formation game for multi-relay selection is explained as follows. Because of the conflict of interest among relays—as each relay prefers to participate in cooperative transmission to gain the highest reward from the destination nodes, and given that the inclusion of other relays improves the network sum-rate but also reduces the reward to every other participating relay—a dynamic game model is necessary. The political aspect of the proposed coalition formation game conforms with a scenario in which there is no rule to enforce a decision except the rule of majority. This scenario is most compatible with a decentralized "ad-hoc" network where no central controller can enforce the selection of relays. In turn, the selected set of relays has to emerge through an agreement by the relays on a single coalition based on their relative strengths, where the relative strength of each relay in the game is characterized by a sum-rate maximizing value that reflects its overall SNR contribution to all destination nodes. As a result, the game always converges to a sub-optimal set of relays—in terms of network sum-rate—but is stable, as none of its members would split since they cannot constitute a majority either by themselves or by joining any other possible set of relays. To the best of our knowledge, no prior work has applied political coalition formation for distributed multi-relay selection in ad-hoc wireless networks.

The main contributions of this work can be listed as follows:

- Proposed a distributed algorithm based on a political coalition formation game for network sum-rate maximizing multi-relay selection.
- Designed a iterative/non-recursive algorithm for ultimate ruling coalition mapping, as opposed to the recursive algorithm in [19], and characterized its computational complexity.
- Designed an algorithm with linear complexity to eliminate redundant relays to speed-up the convergence of the proposed distributed algorithm.
- Proposed a distributed party formation algorithm to study the tradeoff between ruling coalition stability and network sum-rate performance.

The remainder of this paper is organized as follows. The network model is presented in Section II. In Section III, multi-relay selection is modeled as a political coalition formation game; while Section IV presents the distributed coalition formation algorithm and its properties. Simulation results are presented in Section V along with a discussion on some related properties. Finally, conclusions are drawn in Section VI.

II. Network Model

In this work, a one-to-many ad-hoc wireless network is studied, where a source node wishes to broadcast its data symbol x_s to N destination nodes through a set of K intermediate decode-and-forward relay nodes. Communication between the source node and destination nodes is performed over two phases: (1) broadcasting phase (1 time-slot), and (2) cooperation phase (1 time-slot). Between any two nodes, the channel is given by $h = e^{\jmath\theta}\sqrt{d^{-\nu}}$, where d is the inter-node distance, ν is the path-loss exponent and θ is the channel's phase shift, which is uniformly distributed in $[0, 2\pi]$. It is also assumed that there is no direct link between the source and destination nodes and that there is a total power constraint P per time-slot.

Fig. 1 shows an ad-hoc cooperative wireless network with $K = 7$ intermediate relays and $N = 3$ destination nodes, where only three relays have been selected to forward the source's symbol to the destination nodes.

A. Broadcasting Phase

The received signal at each of the K relay nodes from the source node is written as

$$y_{s,k} = \sqrt{P} h_{s,k} x_s + n_{s,k}, \tag{1}$$

where $h_{s,k}$ is the channel fading coefficient between the source node and relay R_k, for $k \in \{1, 2, \ldots, K\}$. Also, $n_{s,k}$ is the zero-mean N_0-variance complex additive white Gaussian noise (AWGN) at relay node R_k. The signal-to-noise ratio (SNR) at the output of the matched-filter of relay R_k is given by

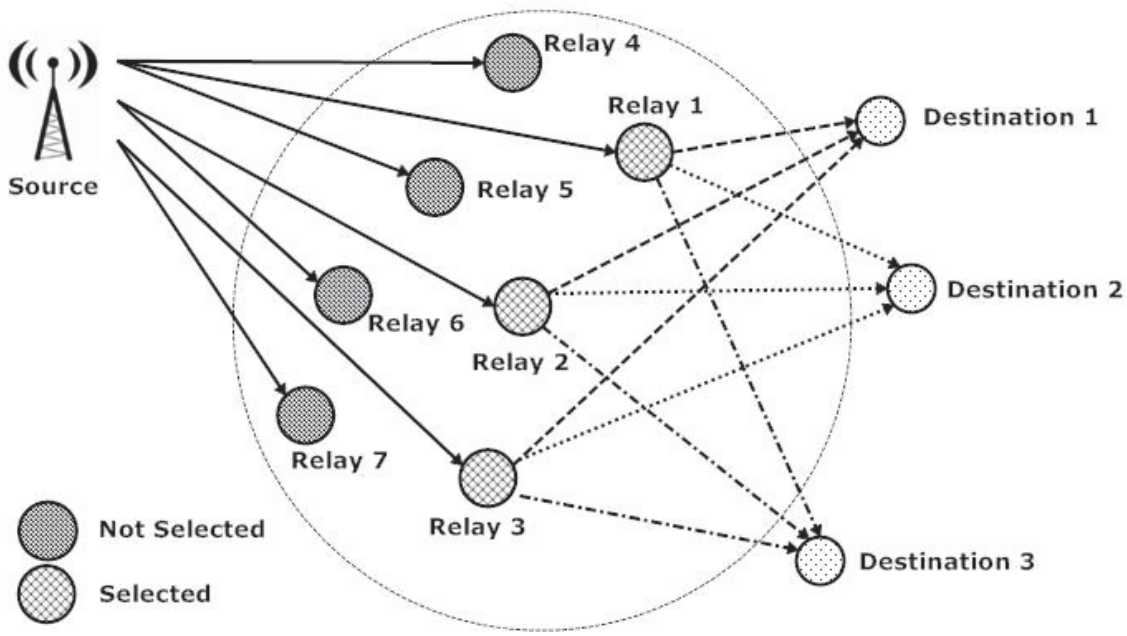

Fig. 1. Multi-Relay Selection in Ad-hoc Cooperative Wireless Networks

$$\gamma_{s,k} = \frac{P|h_{s,k}|^2}{N_0}. \tag{2}$$

For the source node's symbol to be decoded correctly at a relay node, then $\gamma_{s,k} \geq \gamma_{th}$, where γ_{th} is the target SNR, which is assumed to be common to all relay nodes in the network.

B. Cooperation Phase

Let $\mathcal{D}$ denote the subset of relay nodes that decoded the source node's symbol correctly, where $1 \leq |\mathcal{D}| \leq K$, and $|\cdot|$ denotes the cardinality of the parameter set[1]. The aim is to select at least one relay that will forward the source's symbol to the N destination nodes. Let $\mathcal{S}$ be the set of selected relays, where $1 \leq |\mathcal{S}| \leq |\mathcal{D}|$. The total power per time-slot P is split equally over the selected relays. That is, relay R_k for $k \in \mathcal{S}$ is allocated a transmit power of $P_{R_k} = \frac{P}{|\mathcal{S}|}$. Now, all selected relay nodes—assuming perfect timing synchronization—simultaneously transmit the source node's symbol to all destinations. The received signal at each destination node D_j, for $j \in \{1, 2, \ldots, N\}$, is given by

$$y_j = \sum_{k \in \mathcal{S}} \sqrt{P_{R_k}} h_{k,j} x_s + n_j, \tag{3}$$

[1]It is assumed that there is at least one relay node that decodes the source node's symbol correctly.

where n_j is the zero-mean AWGN with variance N_0, at destination node D_j. The received SNR at destination node D_j is expressed as [17]

$$\gamma_j = \sum_{k \in \mathcal{S}} \gamma_{k,j} = \sum_{k \in \mathcal{S}} \frac{P_{R_k} |h_{k,j}|^2}{N_0}. \tag{4}$$

Hence, the achievable rate at destination node D_j is given by

$$\mathcal{R}_j = \frac{1}{2} \log_2 \left(1 + \sum_{k \in \mathcal{S}} \frac{P_{R_k} |h_{k,j}|^2}{N_0} \right). \tag{5}$$

Remark 1: The achievable rate function of each destination node is a strictly monotonically increasing concave function. Therefore, the greater the sum-SNR γ_j at each destination node D_j is, the higher the achievable rate is.

III. Multi-Relay Selection As a Political Coalition Formation Game

The problem of multi-relay selection is modeled as a political coalition formation game [18]. In this case, the players are the relay nodes, which strive to form and be part of a stable coalition with sufficient "political power" to guarantee a majority and become the winning coalition. The outcome of this game will be termed the *ultimate ruling coalition* (as will be defined later in this section), which includes the set of relays that are powerful enough to win against any other competing coalition. Such set is fixed and all selected relays simultaneously forward the source node's symbol to all N destination nodes.

The political coalition formation game in hand requires each relay to have a value specifying its political coalition formation power. To eliminate any potential confusion with the relay's transmit power, in the remainder of this paper, this value is referred to as the *coalitional strength*. There are several possible metrics that can be used to characterize a relay's coalitional strength. For instance, a relay's coalitional strength may be defined in terms of its channel gain or the received SNR at the destination nodes. Since the aim of this work is to select the network sum-rate maximizing set of relays, it is straightforward to show from (6) that maximizing $\prod_{j=1}^{N} (1 + \gamma_j)$ across all destination nodes maximizes the network sum-rate. Moreover, note that the network sum-rate due to relay R_k's transmission only is

$$\frac{1}{2} \sum_{j=1}^{N} \log_2 (1 + \gamma_{k,j}) = \frac{1}{2} \log_2 \left(\prod_{j=1}^{N} (1 + \gamma_{k,j}) \right). \tag{7}$$

Clearly, $\prod_{j=1}^{N} (1 + \gamma_{k,j})$ is relay R_k's SNR contribution to the network sum-rate. Therefore, the following metric is proposed as a measure of the relative strength of each relay in terms of its resulting SNR at all destination nodes.

$$\begin{aligned}\frac{1}{2}\sum_{j=1}^{N}\log_2(1+\gamma_j) &= \frac{1}{2}\log_2\left(\prod_{j=1}^{N}(1+\gamma_j)\right)\\ &= \frac{1}{2}\log_2\left(1+\sum_{j=1}^{N}\gamma_j+\sum\sum_{i<j}\gamma_i\gamma_j+\sum\sum_{i<j<k}\sum\gamma_i\gamma_j\gamma_k+\ldots+\prod_{j=1}^{N}\gamma_j\right).\end{aligned} \tag{6}$$

Definition 1 (Relay SNR Strength (RSS)): Let ω_k be relay R_k's *RSS* (for $k \in \mathcal{D}$), which is given by

$$\omega_k = \prod_{j=1}^{N}(1+\gamma_{k,j}) = \prod_{j=1}^{N}\left(1+\frac{P_{R_k}}{N_0}|h_{k,j}|^2\right), \tag{8}$$

where $P_{R_k} = \frac{P}{|\mathcal{D}|}, \forall k \in \mathcal{D}$.

It is noteworthy that each relay can calculate its RSS value locally, which means that the relays will only need to exchange their RSS values during the coalition formation process, instead of all their channel coefficients, ultimately reducing communication overheads.

The characteristics of the political coalition formation game are outlined in the following definitions [19].

Definition 2 (Degree of Majority α): $\alpha \in [0.5, 1)$ is a majority factor that specifies the minimum strength required for a subset of set $\mathcal{D}$ to become a winning coalition[2].

Definition 3 (Power Mapping ω): The power mapping ω is a correspondence $\omega : \mathcal{D} \rightarrow \mathbb{R}_{++}$ that assigns a positive and non-zero real number ω_k as the coalitional strength of relay R_k in $\mathcal{D}$. Also, $\omega_{\mathcal{C}} = \sum_{k\in\mathcal{C}}\omega_k$ denotes the total coalitional strength of coalition $\mathcal{C}$.

Definition 4 (Winning Coalition): A coalition $\mathcal{C} \subset \mathcal{Q}$ is winning in $\mathcal{Q}$ if and only if $\omega_{\mathcal{C}} > \alpha \cdot \omega_{\mathcal{Q}}$ where $\omega_{\mathcal{C}}$ and $\omega_{\mathcal{Q}}$ are the coalitional strength values of coalitions $\mathcal{C}$ and $\mathcal{Q}$, respectively.

Definition 5 (Self-Enforcement): A coalition $\mathcal{C}$ is recursively defined as self-enforcing if and only if it does not contain any winning sub-coalition that can split from it and become the winning coalition.

Definition 6 (Ultimate Ruling Coalition): The ultimate ruling coalition (URC) is defined as the coalition that is winning, self-enforcing and yields the maximum sum-utility to its members. Moreover, the URC is a mapping from the initial set of relays

[2]For a coalition to be winning, the total coalitional strength of its relays must be at least greater than α times the total coalitional strength of all relays. Moreover, it will be shown in Section V that the value of α defines the network sum-rate, average URC size and number of iterations required for convergence. Hence, depending on the network application and required network sum-rate or latency constraint, the value of α will be agreed upon by all the destination nodes, before the coalition formation algorithm is initiated.

$$\mathcal{U}(\Psi) = \left\{ \boldsymbol{\mathcal{U}}(\Psi) \in \mathbb{R}^{|\Psi|} | \forall R_k \in \Psi, \mathcal{U}_k = \frac{\omega_k}{\omega_\Psi} \mathcal{R}_\Psi - \zeta P_{R_k}, \text{ if } P_{R_k} > 0, \text{ and } \mathcal{U}_k = 0, \text{ otherwise} \right\}. \tag{11}$$

$\mathcal{D}$ to a winning and self-enforcing coalition, based on power mapping ω and majority degree α, as denoted by $\Psi = \Psi(\mathcal{D}, \omega, \alpha)$.

To illustrate the above concepts and definitions, consider the following examples.

Example 1: Let the set of relays be $\mathcal{D} = \{R_1, R_2, R_3, R_4\}$ with RSS values $\omega_1 = 1$, $\omega_2 = 2$, $\omega_3 = 3$, $\omega_4 = 4$. Then, $\omega_\mathcal{D} = \sum_{k \in \mathcal{D}} \omega_k = 10$. Also, let $\alpha = 0.5$. Clearly, the winning sub-coalitions in $\mathcal{D}$ are $\{R_2, R_4\}$, $\{R_3, R_4\}$, and the four sub-coalitions of size 3. Any sub-coalition of size 2 is not self-enforcing, because any of its members forms a majority on its own, which is also self-enforcing being a singleton. Consequently, all sub-coalitions of size 3 are self-enforcing, except $\{R_1, R_2, R_4\}$, because relay R_4 can form a winning coalition on its own (since $\omega_4 > \alpha \cdot (\omega_1 + \omega_2 + \omega_4)$), and also because R_4 as a singleton is self-enforcing. Also, the grand coalition $\{R_1, R_2, R_3, R_4\}$ is not self-enforcing, as it contains winning and self-enforcing sub-coalitions. As a result, the URC will be the winning and self-enforcing coalition that yields the maximum utility to its members. In other words, $\Psi(\mathcal{D}, \omega, \alpha) = \{R_1, R_2, R_3\}$ or $\{R_1, R_3, R_4\}$, or $\{R_2, R_3, R_4\}$, whichever achieves the maximum sum-utility.

Example 2: Let $\mathcal{C} = \{R_1, R_2, R_3\}$ with $\omega = \{3, 5, 7\}$. Coalition $\mathcal{C}$ is self-enforcing when $\alpha = 0.5$; however, is not self-enforcing for $7/12 < \alpha < 12/15$, because $\{R_2, R_3\}$ becomes a self-enforcing and winning coalition.

Example 3: Let $\alpha = 0.5$ and $\mathcal{D} = \{R_1, R_2, R_3, R_4, R_5\}$ with $\omega = \{2, 10, 15, 20, 21\}$, and $\omega' = \{2, 10, 15, 20, 40\}$ [19]. Then, $\Psi(\mathcal{D}, \omega, \alpha) = \{R_1, R_4, R_5\}$; while $\Psi(\mathcal{D}, \omega', \alpha) = \{R_2, R_3, R_4\}$. Clearly, R_5, which is the relay with the highest RSS value, belongs to $\Psi(\mathcal{D}, \omega, \alpha)$ but not $\Psi(\mathcal{D}, \omega', \alpha)$.

Based on the stated definitions and given examples, the following remarks are made [19].

Remark 2: If $\alpha = 0.5$, coalitions of two relays are never self-enforcing, provided relays cannot have equal coalitional strengths[3].

Remark 3: When $\alpha = 0.5$, the URC needs to be more powerful than the rest of the network nodes; whereas, when $\alpha > 0.5$, the URC needs to contain majority of "powerful" enough network nodes.

Remark 4: The resulting URC may contain any number of relays and may include or exclude the relays with the highest RSS values in the network.

[3]The probability of two relays having equal coalitional strengths is virtually zero, as nodes' locations/channel conditions are randomly generated.

Proposition 1: Given that no two relays can have equal coalitional strengths in the coalition formation game, if a single relay is winning in $\mathcal{D}$, then it is the only winning relay and it forms by itself the only URC of the game.

Proof: This proposition is proved by contradiction. Suppose there two relays R_i and R_j for $i \neq j$ with RSS values ω_i and $\omega_j = \omega_i - \delta$, respectively, where δ is a small positive number. If each of these two relays forms a majority in the coalition formation game, then

$$\begin{aligned} \omega_j > \alpha \cdot \sum_{k=1}^{|\mathcal{D}|} \omega_k &> \alpha \cdot \left(\omega_i + \omega_j + \sum_{k=1, k \neq i,j}^{|\mathcal{D}|-2} \omega_k \right) \\ &> \alpha \cdot (2 \cdot \omega_j) + \alpha \cdot \left(\delta + \sum_{k=1, k \neq i,j}^{|\mathcal{D}|-1} \omega_k \right). \end{aligned} \tag{9}$$

Note that $\alpha \cdot \left(\delta + \sum_{k=1, k \neq i,j}^{|\mathcal{D}|-1} \omega_k \right)$ is positive for any $\alpha = [0.5, 1)$; thus, the inequality yields a contradiction. Also, since a singleton is self-enforcing by definition, a winning singleton, if exists, forms by itself the only URC of the game. ■

Although the URC can recursively be induced based on the definitions above, in this work, an alternative iterative/non-recursive algorithm is proposed, which coincides with the recursive one in[4] [18]. The idea of this algorithm is to iteratively go through all possible sub-coalitions of the initial relay set $\mathcal{D}$, starting from singletons up to coalitions of size $|\mathcal{D}| - 1$. However, a simple check is performed in the beginning to determine if a single relay $R_k \in \mathcal{D}$ is winning in $\mathcal{D}$, so the iterative procedure may be avoided, such that $R_k = \Psi(\mathcal{D}, \omega, \alpha)$ and the algorithm terminates. Otherwise, the iterative procedure takes place as follows. Let $\mathcal{T}$ denote the list of self-enforcing coalitions (not necessarily winning in $\mathcal{D}$). For each coalition $\mathcal{C}$, if there is no coalition in $\mathcal{T}$ that is contained and also winning in $\mathcal{C}$, then coalition $\mathcal{C}$ is added to $\mathcal{T}$. If $\mathcal{C}$ also happens to be winning in the grand coalition $\mathcal{D}$ (i.e. set of all relays), then it is also added to the set of potential URCs $\mathcal{L}$. Eventually, the URC with maximum sum-utility is returned as the URC Ψ. The proposed iterative URC-inducing algorithm is given in Algorithm 1.

To incentivize relays to compete and be part of the URC, a payoff proportional to the total sum-rate achieved can be offered to the relays in the URC. Specifically, the payoff is divided among the relays in the coalition according to their relative coalitional strengths. However, the cost for each relay is fixed and equal to the power allocated to that relay in the URC Ψ. Thus, the utility of relay R_k can be given as

[4]It will be shown in Section V that our proposed iterative algorithm performs faster than the recursive URC algorithm under certain scenarios.

Algorithm 1 Non-Recursive URC-Inducing Algorithm

Input: initial relay set $\mathcal{D}$, power mapping ω, and majority degree α.

```
Initialize 𝒯 = ϕ and ℒ = ϕ.
IF there exists a relay R_k ∈ 𝒟 and is winning in 𝒟
  Output: R_k = Ψ(𝒟, ω, α)
ELSE
  FOR i = 1 : |𝒟| − 1
    Set 𝒟_i = set of all possible subcoalitions of 𝒟 of size i;
      FOR each coalition 𝒞 ∈ 𝒟_i
        Self_enforcing ← TRUE;
        FOR each coalition 𝒬 ∈ 𝒯
          IF 𝒬 ⊆ 𝒞 AND 𝒬 is winning in 𝒞
            Self_enforcing ← FALSE;
          END IF
        END FOR
        IF Self_enforcing = TRUE
          𝒯 = 𝒯 ∪ 𝒞;
          IF 𝒞 is winning in 𝒟
            ℒ = ℒ ∪ 𝒞;
          END IF
        END IF
      END FOR
  END FOR
  Output: Ψ = Ψ(𝒟, ω, α).
END IF
```

$$\mathcal{U}_k = \begin{cases} \frac{\omega_k}{\omega_\Psi}\mathcal{R}_\Psi - \zeta P_{R_k}, & k \in \Psi \\ 0, & \text{otherwise} \end{cases}, \tag{10}$$

where $\zeta > 0$ is the price per unit power; whereas, ω_Ψ and $\mathcal{R}_\Psi$ are the RSS value and the network sum-rate achieved by the URC Ψ. Clearly, any relay R_k that is not part of the URC should not participate in the cooperative transmission (i.e. its best strategy is to remain silent, such that $\mathcal{U}_k = 0$); otherwise, it will incur the cost of power P_{R_k} (i.e. $\mathcal{U}_k = -\zeta P_{R_k}$).

Proposition 2: The URC is the winning and self-enforcing coalition that maximizes the network sum-rate.

Proof: The sum-utility of the relays in the URC is given by $\sum_{k\in\Psi}\mathcal{U}_k = \mathcal{R}_\Psi - \zeta P$. Since the total power constraint P is fixed for all winning and self-enforcing coalitions, then the URC is the coalition that maximizes the network sum-rate. ■

Remark 5: Due to the "fixed" total power constraint, the network sum-rate $\mathcal{R}_\Psi$ is proportional to $\frac{\omega_\Psi}{|\Psi|}$, where $|\Psi|$ denotes the number of relays in the URC. Hence, the

URC is the ruling coalition with maximum $\frac{\omega_{\Psi}}{|\Psi|}$.

It is noteworthy that the political coalition formation game model in hand is an example of a non-transferable utility (NTU) game, as the total utility of the emerging URC (i.e. network sum-rate) cannot be arbitrarily distributed among the selected relays in the URC, since a specific utility is given to each relay, as per the following remark.

Remark 6: The political coalition formation game in hand is a NTU game, defined by a pair $(\mathcal{D},\mathcal{U})$, where $\mathcal{D}$ is the set of relays that have decoded the source node's symbol correctly, and $\mathcal{U} : \Psi \rightarrow \mathbb{R}^{|\Psi|}$ is a set-valued function, such that for $\Psi \subseteq \mathcal{D}$, where $\mathcal{U}(\Psi)$ is a closed convex set of $\mathbb{R}^{|\Psi|}$ that contains the payoff vectors the relays in Ψ can achieve. Moreover, the coalition set-valued function $\mathcal{U}$ of URC Ψ is given by (11).

It should also be noted that the grand coalition may not emerge as the URC, since a winning and stable sub-coalition, if exists, will always split from the larger coalition and declare itself as the URC. The split is due to the fact that this new sub-coalition may result in a higher network sum-rate than that produced by the grand coalition, as the power P now is divided among a smaller set of stronger relays (i.e. relays with higher RSS values). In addition, this higher reward (i.e. network sum-rate) will now be shared by fewer relays, which means higher utility to each relay in this new URC. Thus, due to the selfish nature of the relays, the smallest winning and self-enforcing coalition is more likely to emerge as the URC than the grand coalition.

IV. Distributed Coalition Formation Algorithm

The proposed distributed coalition formation algorithm is outlined in Table I. Each of the algorithm's three phases will be discussed in the following subsections.

TABLE I
Phases of Proposed Distributed Coalition Formation Algorithm

Phase 1: Redundant Relay Elimination.
Phase 2: Party Formation.
Phase 3: Dynamic Ultimate Ruling Coalition Formation.

A. Redundant Relay Elimination

Relays that do not improve the resulting sum-rate can be determined and eliminated before the ruling coalition formation process is started, so as to reduce computational complexity and speed-up convergence. Mathematically speaking, removing a positive number below the average value does not reduce the average value. Additionally, note that the sum-SNR at a destination node is proportional to the average channel gains

from all relays, since the power is equally divided among the potential relays. Thus, if a relay does not reduce the sum-SNR simultaneously at all destination nodes when removed, then such relay is redundant and the total power is better invested in the other relays. That is, a relay with received SNR that is lower than the average SNR at *each* destination node is a redundant relay[5].

Redundant relay elimination can be implemented in a distributed fashion. Specifically, each destination node calculates the received sum-SNR value of all potential relays and feeds it back to the relays. After that, each relay compares its received SNR at each destination node against the received sum-SNR value at that destination node. If the SNR of a relay is lower than the received sum-SNR for all the destination nodes, that relay declares itself as redundant and notifies all the destination nodes[6]. Consequently, all destination nodes recalculate their received sum-SNR excluding the redundant relay, and the process repeats until there are no more redundant relays. The resulting set of potential relays after this phase is denoted $\mathcal{D}_R$, where $|\mathcal{D}_R| \leq |\mathcal{D}|$ and the total power is distributed evenly over the remaining relays in $\mathcal{D}_R$.

B. Party Formation

In this phase, the relays are allowed to form parties in order to increase their chances of being part of the URC. Specifically, relays sequentially propose parties according to their ordered RSS values, according to the following rules.

Definition 7 (Proposing Rule - Party Formation): A relay proposes the party which includes itself and the sum-utility maximizing set of relays, not committed to other parties, that make the proposed party the winning set.

Definition 8 (Acceptance Rule - Party Formation): A relay accepts a proposal to form a party with other relays if and only if the received proposal is the same as what the relay would have proposed prior to the reception of the proposal.

A party of relays is treated as a single player with its coalitional strength being the sum of its members' RSS values. In addition, all relays in a party enter into a binding agreement, in which they are guaranteed not to be eliminated in case the party emerges in the URC. Also, the achieved utility by the party will be divided proportionally among its members. By referring back to Example 1 in Section III, relays R_3 and R_4 may both receive a better utility in coalition $\{R_3, R_4\}$ than $\{R_2, R_3, R_4\}$. However, relay R_3 will reject the former coalition, knowing that relay R_4 will have enough power to eliminate R_3 when R_2 is not present. Anticipating this, relay R_4 may offer R_3 the chance to form

[5]It has been verified via extensive exhaustive searches that the optimally selected set of relays (in the network sum-rate sense) is always a subset of the resulting set of relays at the end of the redundant relay elimination phase.

[6]Such relay has no incentive to falsify its weakness, because otherwise, it will undergo the coalition formation phase and still not become part of the URC due to its low coalitional strength.

Algorithm 2 Party Formation Algorithm

Input: relay set $\mathcal{D}_R$, majority degree α, and maximum party size ξ.

```
Initialize: 𝒴 = 𝒟_R, ℱ = ϕ, and 𝒲 = ϕ.
WHILE 𝒴 ≠ ϕ
   R_max = relay with highest RSS value in 𝒴 \ 𝒲;
   𝒫 = propose_party (𝒴, R_max, ξ, α);
    IF vote_party (𝒴, R_k, ξ, α) = TRUE, ∀R_k ∈ 𝒫
        ℱ = ℱ ∪ 𝒫;
        𝒴 = 𝒴 \ 𝒫;
     ELSE
        𝒲 = 𝒲 ∪ R_max;
        IF |𝒲| = |𝒟_R|
           𝒲 = ϕ;
        END IF
     END IF
END WHILE
```

Output: Set of formed parties, $\mathcal{D}_P$.

a party together in which R_3 is guaranteed not to be eliminated even when $\{R_3, R_4\}$ emerges as the URC.

Based on the above rules, a distributed algorithm for party formation (outlined in Algorithm 2) is proposed, in which the relay with the highest RSS value is the first to propose a party $\mathcal{P}$, such that $|\mathcal{P}| \leq \xi$, where ξ is the maximum allowed party size. This proposal is then multicast only to the relays in that proposal. Each relay $R_k \in \mathcal{P}$ either accepts or rejects the proposal. If the proposal is accepted by all relays in $\mathcal{P}$, a party is formed and added to the set of formed parties $\mathcal{F}$ and its members are removed from the set $\mathcal{Y}$, which is the set of relays to propose a party. Otherwise, the proposing relay R_k is added to $\mathcal{W}$, which is the set of relays with rejected proposals. Only after all relays have taken their chances to propose, the relays with rejected proposals are allowed to propose again. This process repeats until all relays have formed parties or remained as singletons (i.e. parties of a single relay). The final set of parties is denoted $\mathcal{D}_P$, where $|\mathcal{D}_P| \leq |\mathcal{D}_R|$.

Based on the proposed party formation algorithm, the following propositions are made.

Proposition 3: The proposed party contains the minimum number of relays with highest RSS values that make the party the winning set.

Proof: Suppose the relays are ordered such that $\omega_1 > \omega_2 > \omega_3 > \ldots > \omega_{|\mathcal{D}_\mathcal{R}|}$, where ω_j is the RSS value of relay R_j, for $j \in \{1, 2, \ldots, |\mathcal{D}_R|\}$. Consequently, $\frac{\omega_1}{1} > \frac{\omega_1+\omega_2}{2} > \frac{\omega_1+\omega_2+\omega_3}{3} > \cdots > \frac{\sum_{k\in\mathcal{D}_R}\omega_k}{|\mathcal{D}_R|}$ and since the utility of any coalition $\mathcal{C}$ is proportional to $\frac{\sum_{k\in\mathcal{C}}\omega_k}{|\mathcal{C}|}$, thus, the smallest set of relays satisfying the majority constraint is the sum-utility maximizing one. ■

Proposition 4: When relays propose sequentially in a descending order according to their RSS values, their proposals are always accepted.

Proof: Suppose relay R_1 is the first to propose a party. It will propose the party $\mathcal{P} = \{R_1, R_2, \ldots, R_j\}$ with minimum j such that $(\omega_1 + \omega_2 + \ldots + \omega_j) > \alpha \cdot \omega_{\mathcal{D}_R}$ and $j \leq \xi$. Now, since $\mathcal{P}$ includes the minimum set of relays with the highest RSS values, it is easy to show that there is no party $\bar{\mathcal{P}} \neq \mathcal{P}$ that yields a better utility to any relay R_k in $\mathcal{P} \setminus \{R_1\}$ than $\mathcal{P}$, given that ξ is fixed for $\bar{\mathcal{P}}$ and $\mathcal{P}$. Hence, the proposal of R_1 is always accepted forming the party $\mathcal{P}$. Relay R_{j+1} in $\mathcal{D}_R \setminus \mathcal{P}$ (the currently highest RSS) will be the second to propose, where its proposal is recursively proved to be always accepted. The last relay $R_{|\mathcal{D}_R|}$ either will have joined a party proposed by its preceding relays, or be left to propose the party $\{R_{|\mathcal{D}_R|}\}$, which is always accepted. ■

Remark 7: If a weaker relay is permitted to propose before a more powerful relay, the proposal is likely to be rejected, requiring the relay to propose again.

Remark 8: When $\xi = 1$, no party formation occurs.

Proposition 5: When $\xi = |\mathcal{D}_R|$, there is always a party that is winning in $\mathcal{D}_R$ for any $\alpha \in [0.5, 1)$.

Proof: Since no limit on the party size exists, the party that includes all relays in $\mathcal{D}_R$ is possible to be formed. This set of relays is winning by definition, since $\omega_{\mathcal{D}_R} > \alpha \cdot \omega_{\mathcal{D}_R}$ for any $\alpha \in [0.5, 1)$. ■

C. Dynamic Ruling Coalition Formation

Before the dynamic ruling coalition formation algorithm can be described, the following two rules must be stated.

Definition 9 (Proposing Rule - Coalition Formation): A party proposes the winning and self-enforcing coalition with maximum utility that includes itself. If no such coalition exists, it proposes the grand coalition.

Definition 10 (Voting Rule - Coalition Formation): A party votes against a proposal that will eventually excludes it from the URC or one that does not yield a better utility than accepting a future proposal. Otherwise, the party will vote for the proposal.

Following the redundant relay elimination and party formation phases, the dynamic ruling coalition formation algorithm—adapted from [19] and listed in Algorithm 3—is initiated. In this algorithm, the formed parties (and also possibly singletons) negotiate and propose the URC, using an appropriate iterative (as in Algorithm 1) or recursive (as the one given in [18]) URC-inducing algorithm. The algorithm emulates a dynamic game where at each stage, a subset of relays forms a coalition and eliminates those outside it, such that any relay that is eliminated at any point cannot join future coalitions. This game ends when a URC, which does not engage in further elimination, emerges. Specifically, each stage j of the game starts with some ruling coalition $\mathcal{X}_j \subset \mathcal{D}_P$ as the

Algorithm 3 Dynamic Ruling Coalition Formation Algorithm

Input: relay set $\mathcal{D}_P$, power mapping ω, and majority degree α.

1) Initialize: $j = 0$, $\mathcal{Z} = \phi$, $\mathcal{X}_j = \mathcal{D}_P$.
2) Set $q = 1$;
3) Choose a random relay $R^{(j,q)} \in \mathcal{X}_j$;
4) $\mathcal{Z} = \mathcal{Z} \cup R^{(j,q)}$;
5) $\mathcal{C}_{j,q} = propose\_coalition\left(R^{(j,q)}\right)$;
6) IF $\sum_{k \in \mathcal{C}_{j,q}} \left(vote\_coalition\left(R_k^{(j,q)}\right) \cdot \omega_k\right) > \alpha \cdot \omega_{\mathcal{X}_j}$
7) Go to (11);
8) ELSE
9) Go to (18);
10) END IF
11) IF $\mathcal{C}_{j,q} = \mathcal{X}_j$
12) Go to (23);
13) ELSE
14) $j = j + 1$;
15) $\mathcal{X}_j = \mathcal{C}_{j,q}$;
16) Go to (2);
17) END IF
18) IF $q < |\mathcal{X}_j|$
19) $q = q + 1$;
20) Choose a random relay $R^{(j,q)}$ from the set $\mathcal{X}_j \backslash \mathcal{Z}$;
21) Go to (5);
22) END IF
23) $\Psi = \mathcal{X}_j$;
24) $\mathcal{U}_k = \frac{\omega_k}{\omega_\Psi} \mathcal{R}_\Psi - P_{R_k}, \quad \forall k \in \Psi$.

Output: $\Psi = \Psi\left(\mathcal{D}_P, \omega, \alpha\right)$.

initial coalition (where initially, $\mathcal{X}_0 = \mathcal{D}_P$). Then, a randomly selected relay (or party) $R^{(j,q)}$ proposes a coalition $\mathcal{C}_{j,q}$ from $\mathcal{X}_j$ and each relay in $\mathcal{C}_{j,q}$ votes either for or against that proposal[7]. If the relays voting 'yes' are winning in $\mathcal{X}_j$ and the proposal is $\mathcal{X}_j$, then the game stage ends with the current proposal as the URC. The process then repeats with the proposal $\mathcal{C}_{j,q}$ as the new initial set $\mathcal{X}_j$ with j incremented by 1. In case the proposal fails to attain a winning majority of the votes, another relay from $\mathcal{X}_j \setminus \mathcal{Z}$, where $\mathcal{Z}$ is the set of players which already have proposed coalitions in the current elimination stage, will be randomly selected to propose a coalition. If no proposal is accepted after all relays have made their proposals, the game terminates with the current $\mathcal{X}_j$ as the URC Ψ. Finally, each relay in Ψ receives its payoff according to (10), proportionally to its RSS value.

[7]A party-head may randomly be selected and is responsible for message exchange, timing synchronization among party members as well as accepting or rejecting a URC proposal.

D. Properties of Proposed Distributed Algorithm

In the following subsections, the properties of the proposed distributed coalition formation algorithm are discussed.

1) Existence and Uniqueness: The existence of a subgame perfect Nash Equilibrium (SPNE) in the dynamic coalition formation game of the proposed algorithm is guaranteed and proved in [18]. Specifically, this game is guaranteed to have at least one SPNE and that an ultimate ruling coalition always exists. In addition, such game may also have several equilibria, which may be inefficient, in the sense that the network sum-rate is not necessarily maximized. For instance, a possible inefficient equilibrium would be to propose randomly and the parties always reject any proposal. However, such equilibrium is not a reasonable outcome for a network of rational relays that aim at maximizing their utilities (and hence, maximizing network sum-rate). This has been shown in [18] to be eliminated through the notion of *sequentially weakly dominant equilibrium* (SWDE), which is based on backward induction and equilibrium in weakly dominant strategies.

The uniqueness of the resulting URC can intuitively be established by noting that, if no two different coalitions can have exactly the same coalitional strength then there is only one possible URC that maximizes the network sum-rate. It has also been proved that this game has a SWDE in pure strategy if the proposing and voting strategies defined above are adopted, leading to the same URC in alls SWDEs. For a detailed proof, the reader is referred to [18].

Corollary 1: In our distributed coalition formation game, the resulting ultimate ruling coalition is "generically" unique.

2) Convergence: The convergence of each phase of the proposed distributed algorithm is discussed separately. First, the redundant elimination phase is guaranteed to converge since in each iteration, a relay is eliminated until there is only a single relay or no redundant relays are found. The sequentially ordered proposing scheme of the party formation phase is also guaranteed to converge in a maximum of $|\mathcal{D}_R|$ iterations, since proposals are always accepted (see Proposition 4). Finally, the convergence of the dynamic ruling coalition formation phase has been proved in [18], where it is shown that in pure strategy SWDE, the ultimate ruling coalition is guaranteed to emerge after a maximum of one elimination stage. This can also be proved by noting that parties play their best response strategies, having the URC previously been predicted using the mapping $\Psi\left(\mathcal{D}_P, \omega, \alpha\right)$. Precisely, if a randomly selected party predicts that it is not going to be in the URC, its best response would be to propose the grand coalition, which will be refused by the URC parties that form a majority. Another party will be given the chance to propose until a party in the URC is selected, which proposes the URC. This proposal will definitely be accepted as the URC parties form a majority; while all parties

not in the URC will be eliminated in this first elimination stage. Thus, all parties in the next stage will be in the URC; hence, any proposal will be accepted and the game will end without any further eliminations.

Corollary 2: The proposed algorithm converges in a finite number of iterations to the stable and unique ultimate ruling coalition.

3) Stability: It is essential to determine the conditions at which the URC may no longer be self-sustaining, which require the distributed algorithm to be re-invoked. It has previously been shown that the URC in our game is self-enforcing, which implies that at equilibrium, no relay would want to deviate from the URC to form another coalition to maximize its utility because no such coalition exists. In addition, it can be shown that a small perturbation in the coalitional strength of any relay may still leave the URC stable. That is, if ω and ω' are two power mappings defined over the set $\mathcal{D}_P$. Then, there exists a sufficiently small $\epsilon > \max_{\forall k \in \mathcal{D}_P} |\omega_i - \omega'_i| > 0$, such that $\Psi\left(\mathcal{D}_P, \omega, \alpha\right) = \Psi\left(\mathcal{D}_P, \omega', \alpha\right)$ [19]. Also, it can be shown that the URC may be fragile when a relay is added or removed from the URC. That is, if a relay joins/leaves the URC, the resulting coalition may no longer constitute a stable self-enforcing and winning coalition (i.e. no longer the URC); particularly for $\alpha = 0.5$, where the addition/removal of a single relay always destroys the URC [18]. In general, if two coalitions are self-enforcing, their union is not; as one the coalition with higher RSS value will be the self-enforcing and winning coalition.

4) Complexity: To evaluate the complexity of the proposed distributed coalition formation algorithm, the complexity of each phase must be analyzed. First of all, the complexity of the redundant relay elimination phase is bounded between 0 and $|\mathcal{D}|$, where $\mathcal{D}$ is the initial set of relays. The worst case complexity happens when the minimum required SNR at any destination is not satisfied after eliminating all relays while the lower bound occurs when SNR requirement is met initially. As for the party formation phase, since proposals are always accepted, each party will either propose once or vote once resulting in linear complexity in the number of parties.

Now, to calculate the complexity of the dynamic ruling coalition formation phase, one must determine the complexity of $\Psi\left(\mathcal{D}_P, \omega, \alpha\right)$, which has a complexity that is lower-bounded by $|\mathcal{D}_P|$ (based on the initial check to determine if a singleton is a winning and hence is the URC), and upper-bounded by $\sum_{i=1}^{|\mathcal{D}_P|-1} \frac{|\mathcal{D}_P|!}{(|\mathcal{D}_P|-i)!\cdot i!}$, since every possible sub-coalition has to be tested. Additionally, the complexity burden on each party/singleton when making a proposal is equal to that of $\Psi\left(\mathcal{D}_P, \omega, \alpha\right)$. On the other hand, voting requires evaluating all the proposals, leading to a complexity of $\left(\sum_{i=1}^{|\mathcal{D}_P|-1} \frac{|\mathcal{D}_P|!}{(|\mathcal{D}_P|-i)!\cdot i!}\right)\cdot|\mathcal{D}_P|$. The last step is to find out how many proposals or voting actions a party/singleton has to perform until convergence occurs. The best case scenario occurs when a party makes a proposal and it is accepted by all parties, ending the game; while the worst case scenario

takes place when all parties' proposals are rejected except for the last party causing each party to propose and then vote $|\mathcal{D}_P| - 1$ times. Clearly, eliminating redundant relays as well as reducing the number of players in the dynamic URC formation phase through party formation may significantly speed-up the convergence of the distributed algorithm, as will be illustrated in the following section.

V. Simulation Results and Discussion

A. Simulation Results

In this subsection, the proposed distributed coalition formation algorithm (CFA) is numerically evaluated and compared to the following multi-relay selection algorithms.

1) **Centralized Multi-Relay Selection:** The centralized multi-relay selection is formulated as a mixed integer nonlinear programming (MINLP) problem. This optimization problem, although non-practical due to its centralized nature and high complexity, will be used as a reference for comparison. Now, let ℓ denote the number of selected relays. Also, let $\mathcal{I}_k$ for $k \in \mathcal{D}$ be a binary decision variable defined as $\mathcal{I}_k = 1$, if relay R_k is selected, and $\mathcal{I}_k = 0$, otherwise. The optimization problem is then given by

$$\max \quad \frac{1}{2}\sum_{j=1}^{N} \log_2\left(1 + \sum_{k=1}^{|\mathcal{D}|} \mathcal{I}_k \frac{P_{R_k}|h_{k,j}|^2}{N_0}\right)$$

$$\text{s.t.} \quad \sum_{k=1}^{|\mathcal{D}|} \mathcal{I}_k = \ell, \tag{12a}$$

$$\ell \cdot P_{R_k} \leq P, \qquad \forall k \in \{1, 2, \ldots, |\mathcal{D}|\}, \tag{12b}$$

$$P_{R_k} \geq 0, \qquad \forall k \in \{1, 2, \ldots, |\mathcal{D}|\}, \tag{12c}$$

$$\mathcal{I}_k \in \{0, 1\}, \qquad \forall k \in \{1, 2, \ldots, |\mathcal{D}|\}, \tag{12d}$$

$$\ell \in \{1, 2, \ldots, |\mathcal{D}|\}. \tag{12e}$$

The first constraint defines the number of selected relays; while the second constraint ensures that the total power constraint is equally split across the selected relays. The third and fourth constraints define the range of values of the relay's transmit power R_k and the associated binary indicator variable $\mathcal{I}_k$, respectively. The last constraint defines the range of possible number of selected relays. Finally, the formulated MINLP problem is, in general, NP-hard and often quite difficult to solve.

2) **Relay Ordering (RO):** This algorithm is a modified version of the relay ordering scheme in [4], where relays are initially sorted in a descending order according to their channel strengths and then sequentially added to the set of selected relays with

the resulting sum-rate calculated after each inclusion. The set of relays resulting in the maximum sum-rate is then selected. The RO algorithm is modified to accommodate multiple destinations and utilizes the RSS value as a metric of relay ordering. Also, a total power constraint is applied in contrast to the separate power constraints in the original RO algorithm.

3) **Multi-Relay Selection with Quadrature Complexity (QC)**: This multi-relay selection algorithm is based on the recursive relay selection scheme outlined in [4], which offers a complexity/network sum-rate tradeoff. This algorithm is also modified as explained in the RO algorithm.
4) **Random Relay Selection (RRS):** In this scheme, multiple relays are selected randomly/uniformly, without any respect to their RSS values.

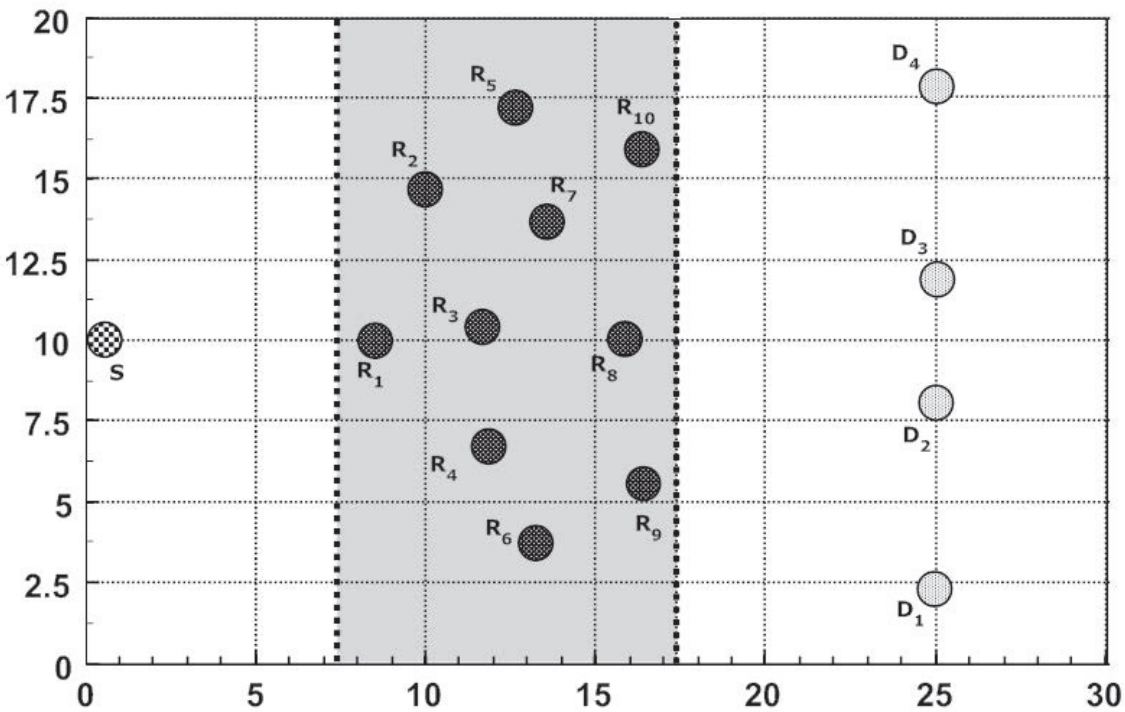

Fig. 2. Network Topology

The following simulations assume a network of $K = 10$ relay and $N = 4$ destination nodes, with a total constraint per time-slot $P = 0.5$ W and price per unit power of $\zeta = 1$. The path loss exponent ν is 3.5 and noise variance is $N_0 = 10^{-5}$. The SNR threshold between any two nodes is set to $\gamma_{th} = 3$ dB [1]. The simulated quasi-static network topology is shown in Fig. 2, where the relay nodes positions are randomly generated and uniformly distributed over the shaded region (of network density of 0.05 nodes/unit square area), while the locations of the source and destination nodes are fixed.

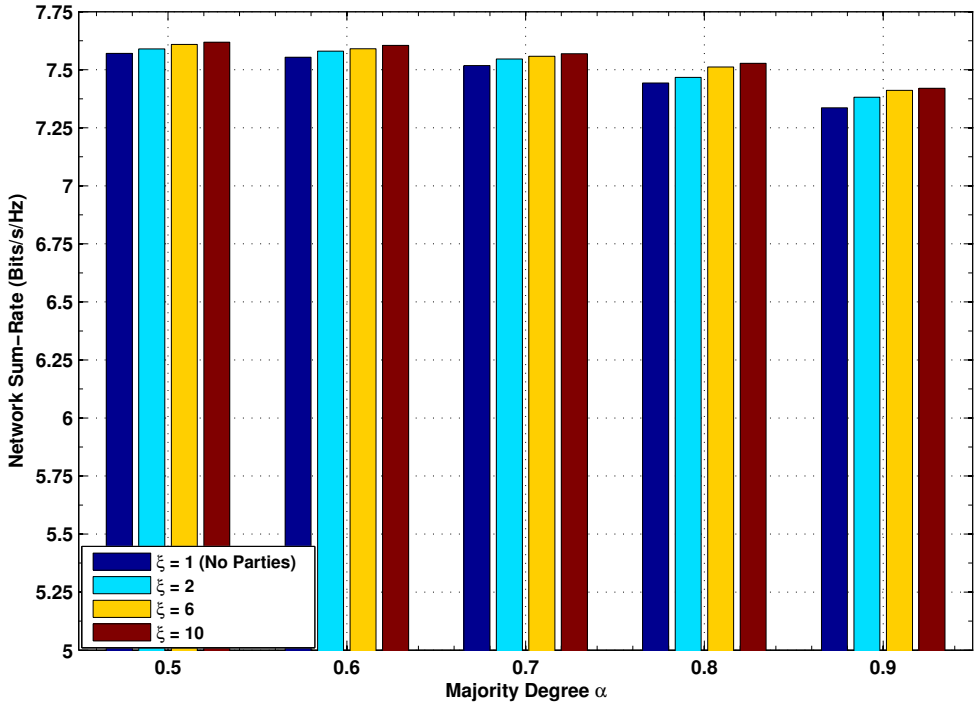

Fig. 3. Network Sum-Rate vs. Majority Degree α of the Proposed CFA - Network Density = 0.05 Nodes/Unit Square Area

Fig. 3 depicts the achievable network sum-rate for different values of α of the proposed distributed algorithm. It can be seen that for any value of α, increasing the party size ξ increases the network sum-rate. However, as the value of α increases, the sum-rate for any maximum party size decreases. Intuitively, increasing the value of α makes the network more stable, at the price of lower network sum-rate, with the value of $\alpha = 0.5$ being the least stable/most fragile but with the highest achievable network sum-rate.

The achievable network sum-rate of the centralized multi-relay selection algorithm[8] as well as the different multi-relay selection algorithms listed above are compared against the proposed distributed algorithm in Fig. 4 for different network densities[9]. Although the network sum-rate of the distributed algorithm is worse than the centralized, QC and RO algorithms, the degradation is at most 0.2 bits/sec/Hz for the different network densities. As expected, the RRS algorithm is by far the worst among all the multi-relay selection algorithms, particularly at low network densities, where the relays are confined

[8]The centralized MINLP multi-relay selection problem is solved using MIDACO, with optimization tolerance set to 0.01 [20].

[9]Network density is increased by shrinking the shaded area in the network topology diagram (see Fig. 2) towards the destinations.

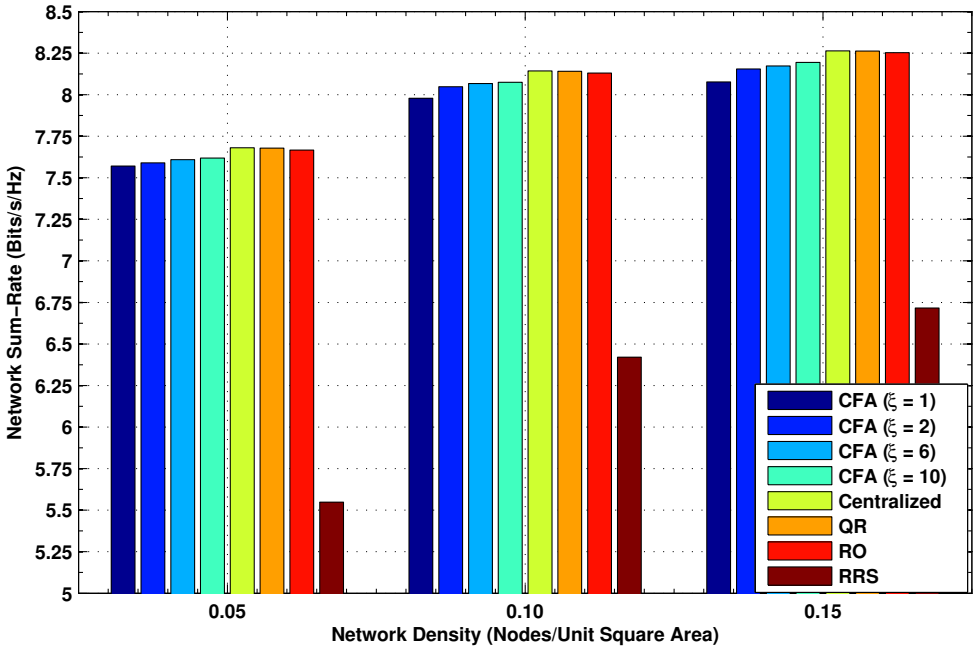

Fig. 4. Network Sum-Rate vs. Network Density for the Different Algorithms for Majority Degree α = 0.5

in a larger area. It is also observed that party formation increases the network sum-rate, especially at high network densities.

In Fig. 5a, the average URC size of the proposed algorithm as a function of α is illustrated. Clearly, increasing α increases the average URC size, as formed coalitions tend to contain more relays so as to become a majority and win (especially in the case of no parties). Also, increasing ξ decreases the average URC size; this is because having less restriction on the party size makes it more possible for a single party to win on its own, and such party will only contain the strongest relays. Moreover, with larger values of α, this party will have more relays compared to lower values of α. Fig. 5b shows the average number of selected relays of the different algorithms, where it is clear that the centralized, QR and RO algorithms yield almost the same number of selected relays. The RRS algorithm shows the largest average number of selected relays, which is due to its randomness/uniformity in selecting a set of relays from the 10 available relays.

The percentage of the numbers of selected relays of the proposed algorithm for $\alpha = 0.5$ is compared with those of the other relay selection algorithms in illustrated in Fig. 6. It is evident that for all multi-relay selection algorithms (except for RRS), most relay selections occur for relay sets of sizes 3 or less, with single-relay selections occurring more than 60% of the time. Also, it can be seen that for the proposed algorithm with $\xi = 1$ (i.e. no parties), no URC of two relays occurs, in agreement with Remark 2. This is also observed when $\xi = 2$, as three relays are never selected, because a URC of

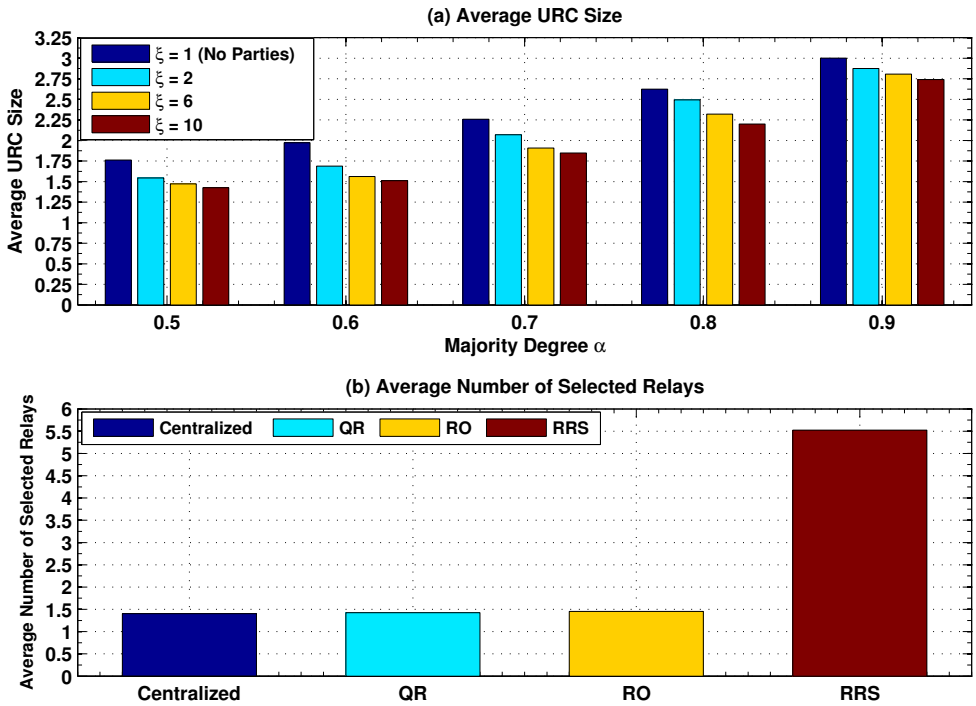

Fig. 5. (a) Average URC Size and (b) Number of Selected Relays of the Different Algorithms

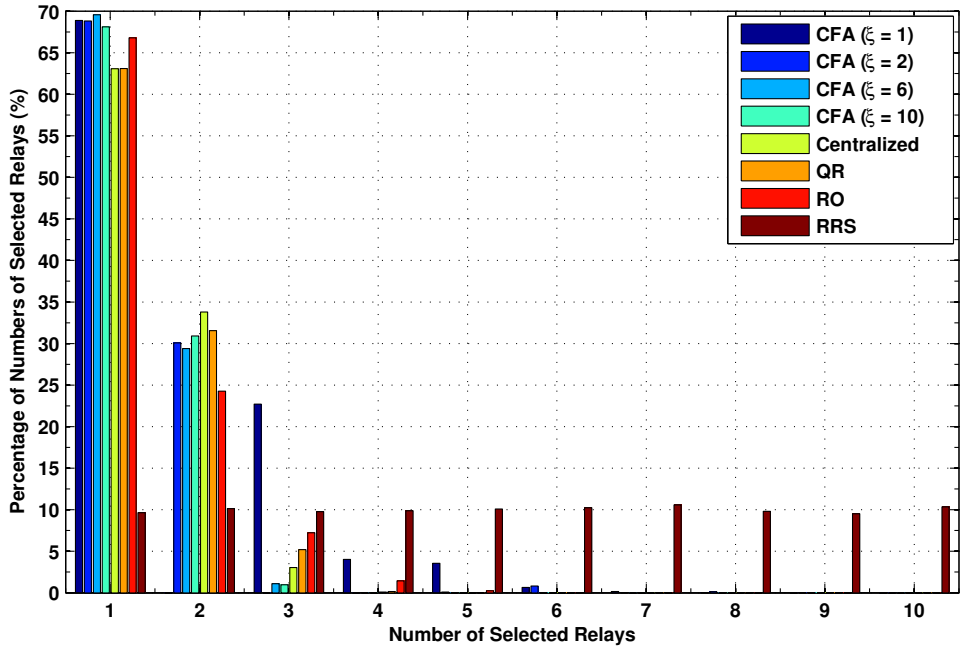

Fig. 6. Percentage of Numbers of Selected Relays of the Different Algorithms for Majority Degree α = 0.5 - Network Density = 0.05 Nodes/Unit Square Area

size two is composed of a singleton and a party of two relays (which are treated as a single entity). It is also noticed that the selection of four or more relays rarely occurs (except for RRS). As for the RRS algorithm, a uniform distribution of relay selection is observed.

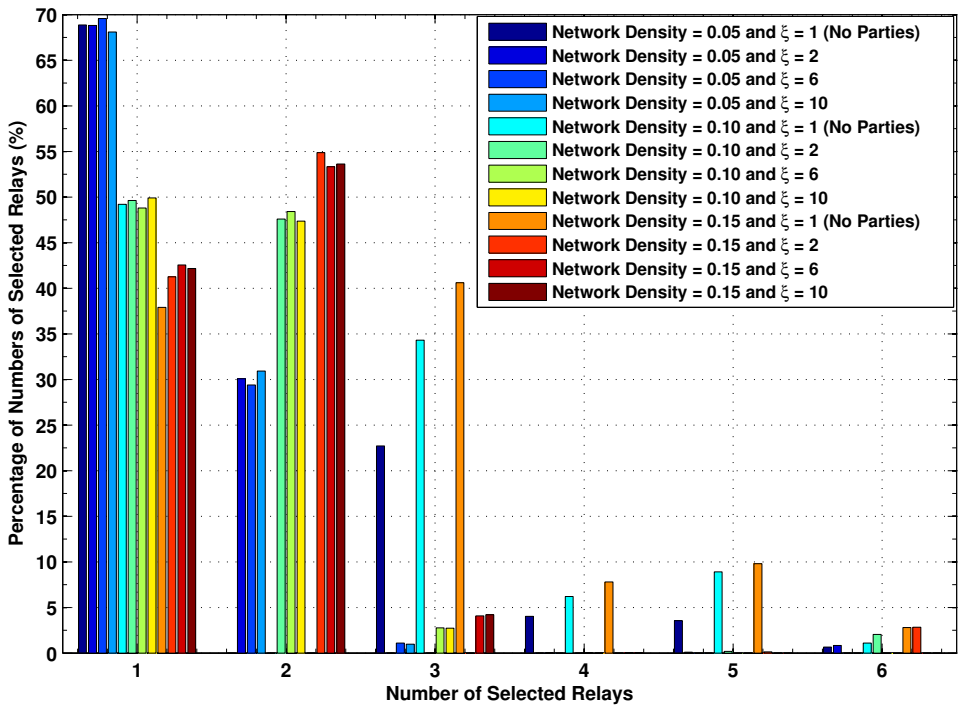

Fig. 7. Percentage of Numbers of Selected Relays of the Proposed CFA for Majority Degree α = 0.5 and Different Network Densities (Nodes/Unit Square Area) and Maximum Allowed Party Sizes ξ

Fig. 7 illustrates the percentage of numbers of selected relays of the proposed algorithm for $\alpha = 0.5$ for different network densities and maximum party sizes[10]. It is evident that increasing network density decreases single-relay selections and gives rise to multi-relay selections of two or more relays. This is because, with a smaller network area, the RSS values of the different relays are relatively similar. Therefore, for a party to form a majority and win, it would need to include more relays. As before, it is noticed that for $\xi = 1$ ($\xi = 2$), two (three) relays are never selected, as per Remark 2. It is noteworthy that for $\alpha > 0.5$ and different values of ξ, the observations made in Figs. 6 and 7 do not change, except that Remark 2 no longer applies.

[10]Percentages for 7 or more selected relays are negligibly small and thus not shown in Fig. 7.

B. Discussion

In this subsection, some properties related to the proposed distributed coalition formation algorithm are discussed.

1) Complexity of Proposed Algorithm: The complexity in terms of the average number of iterations of our proposed iterative/non-recursive URC-inducing algorithm (see Algorithm 1) against that of the recursive algorithm in [18] is shown in Fig. 8 for different values of α and numbers of relays. While both algorithms are shown to have exponential complexities, our proposed algorithm's complexity (see Fig. 8a)—for more than four relays—can be seen to be independent of α. As for four or less relays, there is a negligibly small difference in the number of iterations for the different values of α. The complexity of the recursive algorithm is illustrated in Fig. 8b, where it can be seen that the average number of iterations increases at a much higher rate with number of relays, compared with the proposed iterative algorithm. Particularly, for $\alpha < 0.9$, the proposed iterative algorithm requires less number of iterations than the recursive algorithm. This is due to the fact that for large enough values of α, the number of winning coalitions decreases, which suggests that the recursive algorithm may be less complex. Finally, it has also been verified via extensive simulations that our proposed iterative algorithm always coincides with the URC of the recursive algorithm.

It is noteworthy that the proposing and voting rules of the dynamic ruling coalition formation algorithm, which both rely on any of the URC-inducing algorithms, are highly complex in the number of relays, limiting network scalability. This explains why the redundant relay elimination and party formation phases have been proposed, which is to significantly reduce complexity and improve convergence speed, ultimately reducing communication overheads. Fig. 9 compares the average number of proposals/votes as a function of the majority degree and the maximum allowed party size. It can be seen that increasing α and ξ decreases the average number of proposals/votes. However, a less significant decrease is noted for the case for party sizes greater than 6, since the size of 6 may be sufficient for winning parties to be formed.

For practical implementation of the proposed distributed multi-relay selection algorithm appropriate modifications to the physical, data link and network layers must be implemented. Additionally, experimentation and multi-layer simulation must take place, taking into account potential overheads, delays, packet losses and retransmissions. However, these will be investigated in future work.

2) Stability and Network Sum-Rate Performance Tradeoff: The lower sum-rate of the URC with respect to the optimal centralized multi-relay selection algorithm is explained by the fact that the URC must be stable and self-enforcing, before the sum-rate maximizing coalition is selected, which may restrict the possible set of coalitions to one that excludes the optimum sum-rate maximizing relays set. For example, it is possible

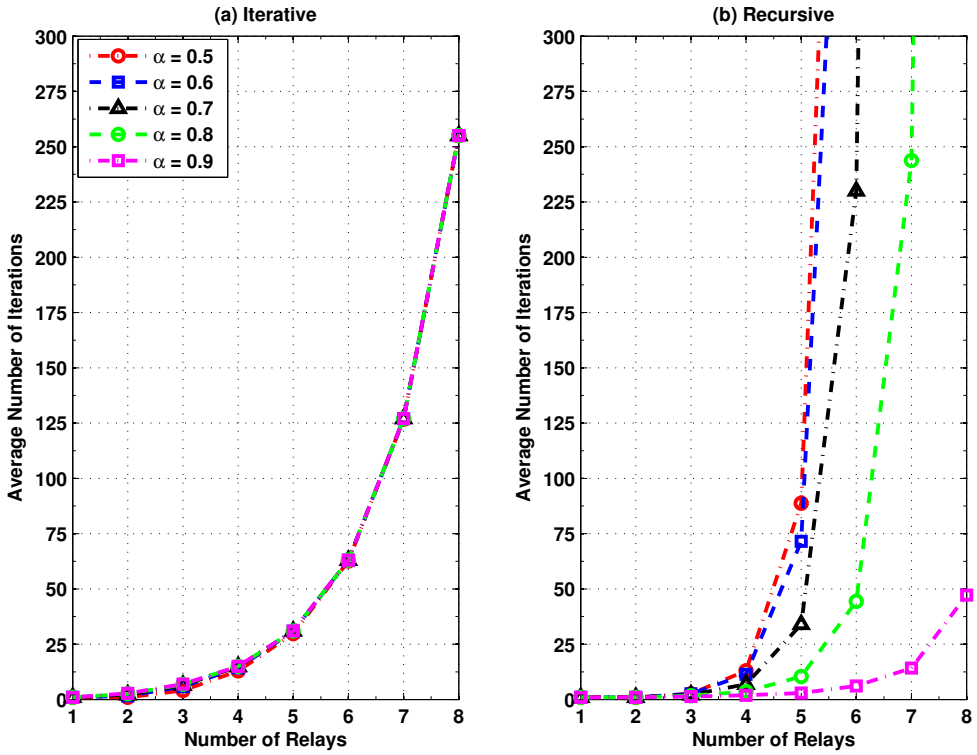

Fig. 8. Average Number of Iterations of the (a) Iterative, and (b) Recursive URC-Inducing Algorithms for Different Numbers of Relays and Values of α.

for the relay with the highest coalitional strength to be excluded from a stable coalition of less powerful relays unless the former relay has enough strength to rule out that stable coalition (see Remarks 3 and 4). On the other hand, the URC must posses a relatively high coalitional strength to emerge; explaining the comparable network sum-rate with the other multi-relay selection algorithms. This also demonstrates the effectiveness of our chosen RSS metric. If the coalitional strengths of the selected sets of relays by the other algorithms were to be considered, most likely they would not be stable.

The stability of the URC is degraded with party formation, since some relays may not abide to the binding agreement and eliminate weak relays. To address this issue, a reputation system may be enforced, in which untruthful relays are punished by receiving a bad reputation, preventing them from joining parties in the future [21]. Despite this, relays may still choose to betray their party members with positive probability. Intuitively, the larger the party is, the more likely the party will be destroyed by a single relay choosing to deviate. Hence, a means for trading off stability for performance can be realized by setting a maximum possible size on the formed parties, which also affects the network sum-rate and convergence speed, as explained earlier.

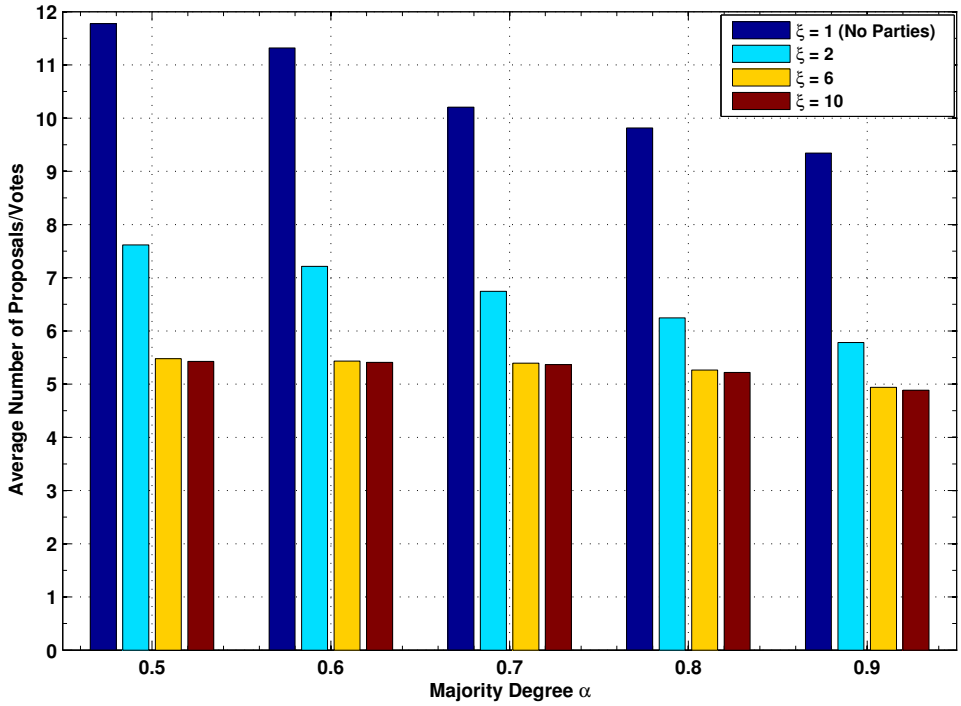

Fig. 9. Average Number of Proposals/Votes of the Proposed CFA for Different Values of α - Network Density = 0.05 Nodes/Unit Square Area

3) Power Allocation: In this work, equal power allocation among the relays in the emerging URC is assumed for simplicity and to reduce computational complexity and communication overheads. On the other hand, optimal power allocation requires all channel state information (CSI) to be available at a relay node (possibly an elected coalition-head) to determine the power allocation fractions and share them with the other relays in that coalition. Now, the proposed URC-inducing algorithm (see Algorithm 1) iteratively goes through all possible sub-coalitions of the initial relay set $\mathcal{D}$, starting from singletons up to coalitions of size $|\mathcal{D}| - 1$. Consequently, for each potential sub-coalition, all the CSI of its participating relays must be communicated to an elected coalition-head, which solves an optimization problem and then assigns power fractions to the different relays in the coalition. Doing so in a distributed manner incurs significant communication overheads and delays, in addition to the computational complexity at the elected coalition-head.

Alternatively, power may be allocated proportionally over all the nodes in the resulting URC according to the relays' RSS values (i.e. RSS-based power allocation, or RSS-PA) without having to exchange complete CSI. Fig. 10 compares the network sum-rate with equal power allocation (EPA) and RSS-PA for the proposed algorithm against the

centralized algorithm with EPA and "global" optimal joint multi-relay selection and power allocation. It can be seen that the RSS-PA improves the network sum-rate of the proposed algorithm for different combinations of α and ξ. However, the improvement for $\alpha = 0.5$ is relatively marginal; while for $\alpha = 0.9$ is more significant. This is attributed to the relatively larger average URC size, which leads to higher diversity gains. Comparing the proposed algorithm with its centralized counterpart, it is clear that centralized multi-relay selection with EPA is still superior. Additionally, the global optimal centralized shows an improvement of about 0.05 bits/s/Hz over the centralized algorithm with EPA. However, as stated before, the selected relays under the centralized algorithms are not necessarily stable and are difficult to compute in ad-hoc networks.

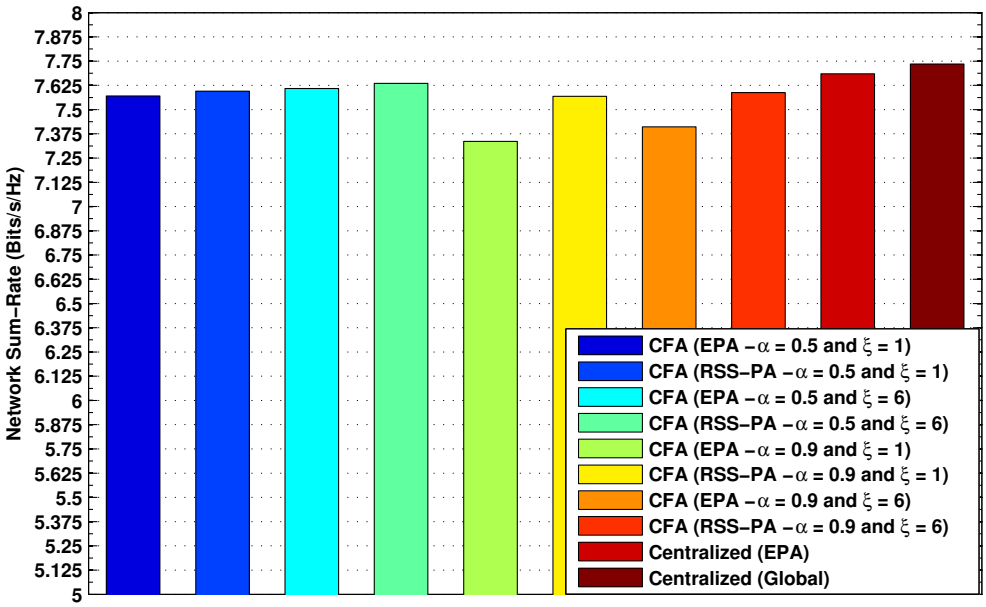

Fig. 10. Network Sum-Rate of the Proposed CFA (EPA and RSS-PA) vs. Centralized Algorithm (EPA and Global) - Network Density = 0.05 Nodes/Unit Square Area

4) Similarity to Matching Models: The proposed political coalition formation algorithm is similar "in principle" to, but more general than the deferred acceptance (DA) algorithm, proposed by Gale and Shapley to find stable matchings [22]. Moreover, the coalition formation game can be thought of as a one-sided matching model [23], where the agents' preferences are defined over their power set (e.g. RSS values). Our game model can also be considered as a two-sided matching problem between two disjoint sets of agents, relays and destinations, with preferences based on the RSS values. Particularly, it encompasses cases such as that if only one relay is matched to multiple destinations (i.e. one-to-many matching), or if multiple relays are matched to a single destination

(i.e. many-to-one matching), or if individual relays are matched to individual destination nodes (i.e. one-to-one matching). Nevertheless, several works have considered the DA algorithm. For instance, in [24], the DA algorithm is proposed to determine the sum-rate maximizing stable one-to-one matching of transmitters and receivers in ad-hoc networks. In [25], the authors apply a novel "priority-based" DA algorithm to find a stable many-to-one matching of users and base-stations in the downlink of wireless small-cell networks. An extension of the DA algorithm has been proposed in [26] to address the caching problem in small-cell networks, in a many-to-many matching game of small base-stations and service providers' servers.

VI. Conclusion

A distributed algorithm based on political coalition formation game theory is proposed to solve the problem of multi-relay selection in one-to-many ad-hoc wireless networks. The proposed algorithm yields a subset of relays that is self-enforcing and stable enough to win against any other potential coalition; while maximizing the network sum-rate. A party formation solution has been proposed to study the network sum-rate performance and stability, where it has been shown that higher network sum-rate can be achieved at the expense of lower stability. The tradeoff between network sum-rate performance and stability has been demonstrated by altering the value of the majority degree and the maximum allowed party size, which directly affect the computational complexity and communication overheads. Finally, simulation results show comparable network sum-rate performance of the proposed distributed algorithm with centralized multi-relay selection as well as other existing multi-relay selection schemes.

References

[1] K. J. R. Liu, A. K. Sadek, W. Su, and A. Kwasinski, *Cooperative Communications and Networking*. Cambridge University Press, 2008.

[2] J. N. Laneman, D. N. C. Tse, and G. W. Wornell, "Cooperative diversity in wireless networks: Efficient protocols and outage behavior," *IEEE Trans. Information Theory*, vol. 50, no. 12, pp. 3062–3080, Dec. 2004.

[3] A. Bletsas, A. Khisti, D. Reed, and A. Lippman, "A simple cooperative diversity method based on network path selection," *IEEE Journal on Selected Areas in Comms*, vol. 24, no. 3, pp. 659–672, March 2006.

[4] Y. Jing and H. Jafarkhani, "Single and multiple relay selection schemes and their achievable diversity orders," *IEEE Transactions in Wireless Communcations*, vol. 8, pp. 1414 – 1423, March 2009.

[5] S. Atapattu, Y. Jing, H. Jiang, and C. Tellambura, "Relay selection and performance analysis in multi-user networks," *IEEE Journal on Selected Areas in Communications*, vol. 31, no. 8, pp. 740—753, Aug. 2013.

[6] Y. Zhao, R. Adve, and T. J. Lim, "Improving amplify-and-forward relay networks: Optimal power allocation versus selection," *IEEE Trans. on Wireless Communications*, vol. 6, pp. 3114 – 3123, Aug. 2007.

[7] G. Amarasuriya, M. Ardakani, and C. Tellambura, "Adaptive multiple relay selection scheme for cooperative wireless networks," *Proc. of IEEE Wireless Communications and Networking Conference (WCNC)*, pp. 1—6, Apr. 2010.

[8] P. Ju, W. Song, and D. Zhou, "Survey on cooperative medium access control protocols," *IET Communications*, vol. 7, no. 9, pp. 893–902, Jun. 2013.

[9] A. B. MacKenzie and L. A. DaSilva, *Game Theory for Wireless Engineers*. Morgan and Claypool Publishers, 2006.

[10] B. Wang, Z. Han, and K. J. R. Liu, "Distributed relay selection and power control for multiuser cooperative communication networks using Stackelberg game," *IEEE Trans. on Mobile Computing*, vol. 8, pp. 975–990, Jul. 2009.

[11] M. W. Baidas and M. S. Bahbahani, "A game-theoretic approach to relay selection in cooperative wireless networks," *Proc. of IEEE International Wireless Communications and Mobile Computing Conference*, pp. 375—380, Aug. 2014.

[12] C.-H. Yu, B. Mume, and O. Tirkkonen, "Distributed multiple relay selection by an auction mechanism," in *Proc. of IEEE Global Communications Conference (GLOBECOM)*, Dec 2012, pp. 4392–4397.

[13] X. Liang, M. Chen, and V. C. M. Leung, "A game-theoretic approach for relay assignment over distributed wireless networks," *Proc. of IEEE Wireless Communications and Networking Conference*, pp. 1557—1562, Jul. 2011.

[14] D. Niyato, P. Wang, W. Saad, Z. Han, and A. Hjorungnes, "Coalition formation games for relay transmission: Stability analysis under uncertainty," pp. 920–925, March 2011.

[15] W. Saad, Z. Han, M. Debbah, and A. Hjorungnes, "A distributed coalition formation framework for fair user cooperation in wireless networks," *IEEE Trans. on Wireless Comms*, vol. 8, no. 9, pp. 4580 – 4593, Sept. 2009.

[16] H. Khayatian, R. Saadat, and J. Abouei, "Coalition-based approaches for joint power control and relay selection in cooperative networks," *IEEE Trans. on Vehicular Technology*, vol. 62, no. 2, pp. 835–842, Feb 2013.

[17] M. W. Baidas and A. B. MacKenzie, "Altruistic coalition formation in cooperative wireless networks," *IEEE Transactions on Communications*, vol. 61, no. 11, pp. 4678–4689, Nov. 2013.

[18] D. Acemoglu, G. Egorov, and K. Sonin, "Coalition formation in political games," *NBER Working Paper No. 12749*, Dec. 2004, Online: http://www.nber.org/papers/w12749.

[19] ——, "Coalition formation in non-demoncracies," *Revew of Economic Studies*, vol. 75, pp. 987—1009, 2008.

[20] M. Schluter, M. Gerdts, and J. J. Ruckmann, "MIDACO: New global optimization software for MINLP," 2011, Online: http://www.midaco-solver.com.

[21] Y. Gao, Y. Chen, and K. J. R. Liu, "Cooperation stimulation for multiuser cooperative communications using indirect reciprocity game," *IEEE Trans. on Communications*, vol. 60, no. 12, pp. 3650—3661, Dec. 2012.

[22] A. E. Roth, "Deferred acceptance algorithms: History, theory, practive, and open questions," *International Journal of Game Theory*, vol. 36, no. 3, pp. 537–569, 2008.

[23] J. Alcalde and P. Revilla, "Tops responsiveness, strategy-proofness, and coalition formation problems," *Instituto Valenciano de Investigaciones Económicas, S.A.* - IVIE *Working Paper Series* AD, no. 11, Apr. 2001.

[24] E. A. Jorswieck, "Stable matchings for resource allocaion in wireless networks," *Proc. of IEEE International Conference on Digital Signal Processing (*DSP*)*, pp. 1—8, Jul. 2011.

[25] S. V. M. B. O. Semiari, W. Saad and B. Maham, "Matching theory for priority-based cell association in the downlink of wireless small cell networks," *Proc. of IEEE Int. Conference on Acoustics, Speech and Signal Processing (*ICASSP*)*, pp. 444—448, May 2014.

[26] K. Hamidouche, W. Saad, and M. Debbah, "Many-to-many matching games for proactive social-caching in wireless small cell netowrks," *Proc. of IEEE Int. Symposium on Modeling and Optimization in Mobile, Ad Hoc, and Wireless Networks (*W*i*O*pt)*, pp. 569–574, May 2014.

Chapter 4

A Repeated Game Technique for Power and Relay Management in Energy Harvesting Based Networks

A Repeated Game Technique for Power and Relay Management in Energy Harvesting Based Networks

Mohammed S. Bahbahani and Emad Alsusa

Abstract

In this paper, a repeated game model is used to jointly optimise multi-relay selection and power control in energy harvesting cooperative communication networks with non-orthogonal channels. Specifically, a repeated Bayesian Stackelberg game is proposed in which the source, as the lead player, updates its price offer to sequentially induce a single power-level transition that maximises its utility gain. The relays, as followers, concurrently respond to the submitted price and SNR from the source, such that each relay transmits at a power-level that maximises its own stage utility. Since the relays are assumed to have their own data traffic, the relay cost function is derived in terms of its energy, data profiles and channel conditions. Using only statistical characteristics of such information, the source applies Bayesian inference to select its price and updates its beliefs after each stage game is played. It will be shown that the Perfect Bayesian Equilibrium of the dynamic Bayesian game exists and that convergence is controlled by the stage cost factor. The performance of the proposed technique, including the impact of channel estimation errors, is evaluated and compared against other benchmark schemes.

Index Terms

Relay selection, energy harvesting, Bayesian inference, Stackelberg game, game theory.

I. Introduction

Cooperative communication and energy harvesting (EH) have been recently explored as means to provide performance gains and extend the lifetime of future green wireless networks. For example, in a cellular network, EH relays can be deployed to improve cell edge user's experience through spacial diversity and path loss mitigation in a sustainable manner, as the relays harvest energy from the environment. Furthermore, by being off-grid, such nodes can be more flexibly installed in places that can optimise the coverage enrichment. To fully reap the benefits of cooperation, relay selection (RS) and power allocation have been well studied in the literature, where various techniques were proposed to maximise the achievable gains [1], [2] ,[3], [4] (and references therein). One of the most common of these includes a distributed single relay selection (SRS)

scheme based on timers [2], which was shown to yield the maximum diversity order. Although SRS avoids the overhead of time synchronisation, multiple relay selection (MRS) was shown in [3] to outperform SRS under individual relay power constraints.

In certain applications, nodes may extract energy from the surrounding environment to maintain a virtually infinite network lifetime [5]. Optimal strategies of an EH transmitter to, either, maximise the short-term throughput or minimise the transmission duration, have been derived in [6] when the channel state information (CSI) and the energy side information (ESI) of future time-slots are known a priori. A low complexity scheme, based on the directional water-filling algorithm, was proposed in [7] with a causal knowledge of CSI and ESI. In cooperative EH networks, appropriate RS and resource allocation schemes are required, as the energy harvested by the relays must be optimally invested in the time-slots with the best channel gains [8]. For example, without selection (all relays participate), a relay's channel gain may be as good as the other relays', hence, its participation will be redundant towards the received SNR. Even worse, the relay may degrade the performance when it contributes to a lower SNR. On the other hand, in SRS, unselected relays may waste their harvested energy when their batteries overflow. That wasted energy could have been utilised in improving the SNR at certain time-slots. Therefore, the optimal investment of the harvested energy can only be realised through MRS with power control.

To enforce cooperation among independent and selfish nodes, providing incentives to the relays is necessary. Pricing, reputation and punishment systems are among various game theoretic solutions that have been developed to take into consideration the node's selfish behavior [9]. In pricing games, nodes use virtual credits to trade network resources at the optimal price. Repeated games were also considered to model the continuous interactions among nodes, as they aim to maximise their long term benefit.

In this paper, the MRS problem is extended to the relay power-level selection problem (RPLS), in which a relay node selects from a finite set of power levels, as it is the case in real transceiver circuits. In addition, a new relaying model is considered, whereby the relays have data traffic of their own. This adds a further complexity to the RPLS problem, as relays should not only save energy for time slots with best channel conditions but should also consider the effect of relaying on their own throughput. To formulate the optimal RPLS we examine two policies. In the first policy, the relays' energy and time resources are first invested in maximizing the average source's capacity and only any unconsumed energy is used for the relay's own transmissions. In contrast, the second policy gives priority to the relay's own traffic. These upper bound solutions are impractical as they are centralised, complex and assume dedicated relays with non-causal data, energy and channel side information (NC-DECI) of future time slots. Thus, we propose a distributed solution, with incentives to the relays, based on a repeated

Bayesian Stackelberg Game (RBSG) [10], that only requires causal information (C-DECI). Specifically, a series of Stackelberg stage games are played, in which the source, as the leader, broadcasts a price factor that maximises its utility and also the SNR. Each relay, as a follower player, responds to the committed price by selecting the power level that maximises its utility. This interaction repeats until no player deviates from its previous action, ending the RBSG process so that data transmission may commence. Since the source has incomplete information about the relays' cost functions that combine their DECIs, equilibrium strategies based on Bayesian inference [11], [12] along with a belief update system are derived and shown to yield a $perfect\ Bayesian\ equilibrium$ (PBE). The convergence of the RBSG is also analyzed and its relationship to the stage cost factor is established.

The contribution of this work can be summarised as follows:

- Proposed a low-complexity sub-optimal scheme to solve the centralised RPLS with NC-DECI that helps in comparisons involving large number of relays, power levels and time-slots.
- Propose a distributed solution with incentives based on an RBSG that only requires C-DECI. That is, only partial information (distributions) of the energy and channel profiles of nodes are required at the source node. The proposed scheme is spectrally efficient with lower overheads compared to [13] as the source and relays interact in the game through broadcast signals. The proposed solution also provides a trade off between throughput and overhead as the repeated game can be terminated whenever the cost of the overhead, represented by a stage game cost factor, outweighs the expected gain from any continuation play. This feature makes the proposed scheme compatible with many applications of different latency and throughput requirements.
- The PBE of the game is proven to exist and shown to converge in a finite number of iterations. To the best of our knowledge, an RBSG with an infinite strategy space and uniformly distributed beliefs is unique.

The rest of the paper is organised as follows. Relevant literature on EH relay selection and cooperative game theory is discussed in Section II. The relevant network and energy models are explained in Section III. Optimal relay power-level selection with NC-DECI is formulated in Section IV. The RPLS problem with causal CSI/ESI/DSI is then modelled as a repeated Bayesian Stackelberg game in Section V. In Section VI, the proposed game is evaluated and compared against other benchmark schemes. Practical aspects of the proposed scheme are discussed in Section VII before conclusions are finally drawn in Section VIII.

II. Related Work

Many EH-RS techniques were proposed in the literature with different energy/channel causality assumptions [6], [8], [14], [15], [16]. Due to the high complexity of the non-causal RS assignment problem, a sub-optimal and low-complexity algorithm for the causal scenario was proposed in [8]. Later in [14], the authors studied the joint relay selection and power allocation problem, where the upper bound performance was formulated as a dynamic programming problem. In addition, different low complexity and sub-optimal policies for causal CSI/ESI were designed and shown to yield improvements over other non-energy aware selection schemes.

To address the selfishness of nodes in relaying each others' packets, a buyer-seller Stackelberg game model was adopted in [13] to solve the MRS and power allocation problems in battery powered wireless networks. On the other hand, a political coalition formation game was utilised in [17], where the stable and sum-rate maximizing set of relays is selected based on a majority rule. Many repeated game solutions for resource allocation in cooperative networks were reviewed in [18]; for example, a repeated game is applied in [19] to enforce the cooperation between selfish nodes without any extrinsic incentive mechanisms. In [20], Ju and Song studied a slotted-based cooperative MAC scenario using a repeated game approach. It was shown that cooperation yields a Nash equilibrium (NE) in the two-stage game, while playing a non-cooperative strategy is the NE in the single stage game. The authors in [21] presented a fully distributed relay management strategy based on a repeated game model with imperfect information.

Despite the aforementioned progress, only a few papers have considered game theory in EH scenarios. For instance, a coalitional game is adopted in [22], where source-destination pairs can form a coalition to share their transmitted and relayed powers under a total power constraint. The authors in [23] considered a scenario where the source may share its energy with relays to incentivise their cooperation. Another game theoretic EH RS technique is presented in [24], which models the interaction between sources and relays as a college admission market, whereas the interaction among the different sources is modelled as an interactive partially observable Markov decision process. Finally, a competitive market with uncertainty is applied in [25] to model the user association in small cell networks. In our work in [10], a repeated Bayesian Stackelberg game is proposed to solve the MRS in EH cooperative networks with non-orthogonal channels.

III. System Model

A. Network Model

The proposed network model illustrated in Fig. 1 consists of a single source node S, a single destination node D and K amplify-and-forward (AF) relay nodes. A flat fading

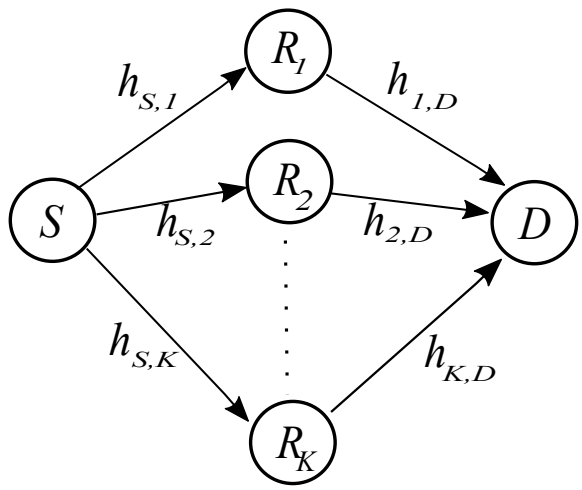

Fig. 1. Network Model

channel model is assumed. The channel coefficient between two nodes i and j is denoted by $h_{i,j} = e^{j\theta}\sqrt{d^{-\nu}}$, where d is the inter-node distance, ν is the path-loss exponent and θ is the channel's phase shift, which is uniformly distributed in [0, 2π] [17]. Also, an individual power constraint P is assumed at each node. In the first half of a time-slot T^{slot}, the source broadcasts its message x_s to the relays. Hence, each relay k receives the signal:

$$y_{s,k} = \sqrt{P} h_{s,k} x_s + n_{s,k}, \tag{1}$$

where $n_{s,k}$ is a zero-mean N_0-variance complex additive white Gaussian noise at relay node R_k. In the second half of the time-slot, assuming perfect timing synchronisation [17], each relay amplifies then broadcasts the received signal yielding the following signal at the destination:

$$y_D = \sum_{k=1}^{K} \beta_k h_{k,D} y_{s,k} + n_D = \tag{2}$$

$$\underbrace{\sum_{k=1}^{K} \beta_k \sqrt{P} h_{s,k} h_{k,D} x_s}_{signal} + \underbrace{\sum_{k=1}^{K} \beta_k \cdot h_{k,D} n_{s,k} + n_D}_{noise}. \tag{3}$$

In the above equation, $\beta_k = \sqrt{P_k/(P|h_{s,k}|^2)}$ maintains the transmit power of relay R_k at $P_k \in \mathcal{P} = \{0, \frac{P}{L-1}, \frac{2P}{L-1}, \ldots, P\}$, where L is the number of permissible transmit

power levels. Hence, the received SNR at the destination node becomes[1]:

$$\gamma_{\mathbf{P_R}} = \frac{P(\sum_{k=1}^{K} \beta_k |h_{s,k}||h_{k,D}|)^2}{N_o(1+\sum_{r=1}^{K} \beta_k^2 |h_{k,D}^2|)}, \tag{4}$$

where $\mathbf{P_R} = \{P_1, \ldots, P_K\}$ are the relays' selected power levels. The normalised capacity is then found using Shannon's capacity theorem as:

$$\mathfrak{R}_{\mathbf{P_R}} = \frac{1}{2} \log_2(1+\gamma_{\mathbf{P_R}}), \tag{5}$$

where the term $\frac{1}{2}$ comes from the two-hop transmission.

B. Energy Model

In this work, we adopt the discrete energy model, [14], illustrated in Fig. 2, where T^{hor} is the time horizon over which the performance is optimised. Also, the harvested energy is assumed to be quantised into packets of size $E^{pac} = PT^{slot}$ such that a single packet of harvested energy may arrive at the beginning of time-slot z of relay k, indicated by the binary variable $I_{k,z}^{ene}$, according to an i.i.d $Bernoulli\ process$ [26] given as[2]:

$$I_{k,z}^{ene} = \begin{cases} 1 & with \quad probability \quad \xi_k^{ene} \\ 0 & with \quad probability \quad 1-\xi_k^{ene} \end{cases}, \tag{6}$$

where the probability ξ_k^{ene} may vary for each relay but remains fixed for all time-slots. Similarly, the data traffic of relay R_k is modelled as another $Bernoulli\ process$ with parameter ξ_k^{data}, such that the binary variable $I_{k,z}^{data}$ indicates the event of a data packet generated in slot z by relay R_k. Each relay has a battery of size $E_k^{max} > E^{pac}$ with an initial charge of $e_{k,0}$. A relay node k is considered $active$ to relay if its residual energy at slot z ($e_{k,z} \in [0, E_k^{max}]$) is at least $\frac{E^{pac}}{(L-1)} + E^{pac}$ Joules. Otherwise, the relay becomes $inactive$ and will not participate in the relaying process in slot z. Further, if the relay has less than E^{pac} of energy, its own data transmission, if it exists, will be blocked. Unless the analysis is independent of z, the selected power of relay k at time slot z will be denoted by $P_{k,z}$.

IV. Centralised Relay Power-Level Selection with Non-causal Information

In this section, the centralised optimal RPLS in EH relay channels is formulated as a non-linear integer programming problem such that the average performance is maximised

[1]It is assumed that relays compensate for the channel phase using full CSI of the forward and backward channels [3].

[2]Note that E^{pac} is the energy needed by a source node to transmit its packet at full power.

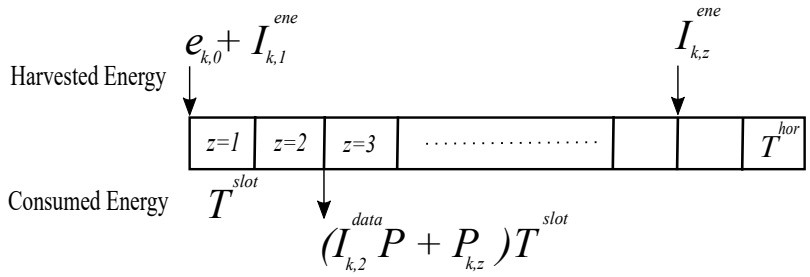

Fig. 2. Energy Model

over T^{hor} time-slots, assuming NC-DECI availability. Since maximizing the source's throughput comes at the expense of a higher relay blocking probability, two benchmark selection policies are proposed as follows.

A. Source Performance Maximizing Policy (SPMP)

In this policy, the relay's own data packet can only be transmitted using the excess energy left after allocating relaying power to all time slots in T^{hor} to maximise the source's average performance, as formulated in (7)-(13) below. The energy causality constraint in (8) ensures, for all time slots, that energy consumed through relaying does not exceed the harvested energy, while (9) guarantees that the battery constraint is never violated. The third constraint restricts the total relay transmit power in each time slot to P. Constraints (11) to (13) define the range of values of the optimisation parameters.

B. Blocking Probability Minimizing Policy (BPMP)

In the BPMP policy, the harvested energy packets over T^{hor} are first reserved for the relays' own data transmissions. Then, unconsumed energy is optimally allocated to relaying the source's message. The same optimisation formulation is adopted except from the causality constraint in (8), which is updated to:

$$e_{k,z-1} + E^{pac} I_{k,z}^{ene} - P_{k,z} T^{slot} - I_{k,z}^{data} E^{pac} \geq 0,$$

$$I_{k,z}^{data} \in \{0,1\}, \forall z \in \mathcal{T}, \forall k \in \mathcal{K}. \tag{14}$$

An illustrative example of the above policies is shown in Fig. 3. In the first time slot, a packet of energy is harvested by the relay, which has a data packet to send in the second time slot. In SPMP, the first slot may be allocated to relaying leaving no energy for the relay's own packet in the second time slot. On the other hand, BPMP reserves the harvested energy for the relay's own transmission turning it inactive in the first time slot.

$$\max_{P_{k,z}\forall z\in\mathcal{T},\forall k\in\mathcal{K}} \frac{1}{T^{hor}}\sum_{z=1}^{T^{hor}} \mathfrak{R}_{\mathbf{P_R}}(z), \tag{7}$$

s.t.

$$e_{k,z-1} + E^{pac} I^{ene}_{k,z} - P_{k,z} T^{slot} \geq 0, \forall z \in \mathcal{T}, \forall k \in \mathcal{K}, \tag{8}$$

$$e_{k,z} \leq E^{max}_k, \qquad \forall z \in \mathcal{T}, \forall k \in \mathcal{K}, \tag{9}$$

$$\sum_{k=1}^{K} P_{k,z} \leq P, \qquad \forall z \in \mathcal{T}, \tag{10}$$

$$P_{k,z} \in \mathcal{P}, \quad \mathcal{T} = \{1, 2, \ldots, T^{hor}\}, \mathcal{K} = \{1, 2, \ldots, K\}, \tag{11}$$

$$e_{k,z} \in \{0, \frac{E^{pac}}{(L-1)}, \frac{2E^{pac}}{(L-1)}, \ldots, E^{max}_k\}, \tag{12}$$

$$I^{ene}_{k,z} \in \{0, 1\}. \tag{13}$$

$$\mathcal{U}_s(t, \mathbf{P_R}, f_s) = \mu_s \mathfrak{R}_{\mathbf{P_R}}(t) - \lambda_s \pi(t) - \varrho_s t. \tag{15}$$

$$\mathcal{U}_k(t, \pi(t), P_k(t), \pi^{res}(t-1)) =$$

$$\begin{cases} \mu_k(\frac{\pi^{exc}(t)}{K'} + \pi^{res}_k(t-1)) - \lambda_k P_k(t) & P_k(t) \geq P_k(t-1) \geq P \\ \mu_k(\frac{\pi^{exc}(t)}{K'}) - \lambda_k P_k(t) & 0 < P_k(t) < P_k(t-1) \\ 0 & P_k(t) = 0 \end{cases}. \tag{16}$$

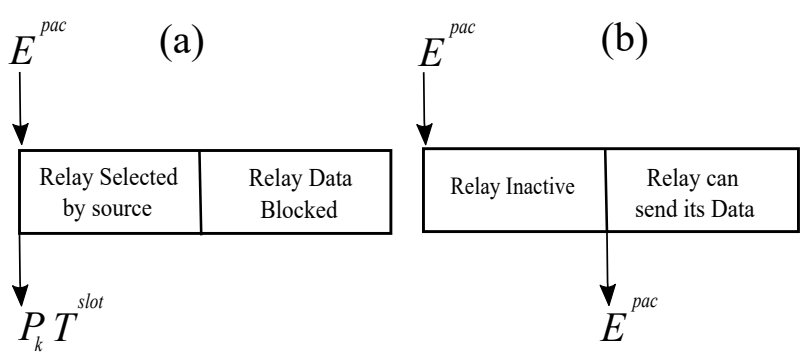

Fig. 3. (a) SPMP , (b) BPMP

Algorithm 1 Sub-optimal RPLS Algorithm for NC-DECI

```
FOR EACH k ∈ K
    γ_k^sorted = SORT_decending({γ_k(1), ..., γ_k(T)})
    FOR EACH z ∈ γ_k^sorted
        I_{k,z}^res ← 1 %Reserve slot
        FOR EACH z ∈ T
            IF min(E_k^max, e_{k,z-1} + E^pac(I_{k,z}^ene − I_{k,z}^res − I_{k,z}^data)) < 0 %Check Causality
                I_{k,z}^res ← 0 %Unreserved slot
                BREAK
            END IF
        END FOR
    END FOR
END FOR
FOR EACH z ∈ T
    P_R(z) ← arg max_{P_{k,z} ∈ P, ∀k ∈ K, ∀z ∈ T, P_{k,z} ≤ P I_{k,z}^res} ℜ_{P_R(z)}
END FOR
```

C. Sub-optimal SPMP and BPMP Solutions

As the complexity of the RPLS problem grows exponentially with the number of relays, power levels and time slots, we propose a low-complexity greedy sub-optimal algorithm (listed in Algorithm 1) described as follows. For each relay k, the time-slots are sorted in a descending order according to their channel gains. Starting with the best SNR slot $\gamma_k(1)$, if allocating this slot to relaying does not violate the constraints above (omitting $I_{k,z}^{data}$ for SPMP), the slot is marked as reserved by $I_{k,z}^{res} \in \{0,1\}$. Having obtained all reservations, the best set of power levels is sequentially obtained for each time slot z, where the energy unused at a reserved slot is carried to the next slot updating its reservation status accordingly. The optimal power levels at each slot are obtained based on the iterative relay ordering technique in [3] such that in each iteration the best transition of power level $l \in \mathcal{P}$ and relay k, denoted by the pair (k,l), that maximises the current SNR is selected until no transition improves the SNR. To enable a distributed solution, an SNR updating function is proposed to determine the new SNR of transition (k,l) by replacing old relay terms $\gamma_{P_k}^{nom} = \sqrt{P}\beta_k h_{s,k} h_{k,D}$ and $\gamma_{P_k}^{denom} = \beta_k^2 h_{s,k}^2$ in (4) with new terms corresponding to the transition (k,l) as [10]:

$$\gamma_{\mathbf{P_R}}^{new}(k,l) = \frac{(\gamma_{\mathbf{P_R}}^{nom} - \gamma_{P_k}^{nom} + \gamma_{P_k^{new}}^{nom})^2}{N_{\mathrm{o}}(1 + \gamma_{\mathbf{P_R}}^{denom} - \gamma_{P_k}^{denom} + \gamma_{P_k^{new}}^{denom})}, \tag{17}$$

where $\gamma_{\mathbf{P_R}}^{nom} = \sqrt{P}\sum_{k=1}^{K}\beta_k h_{s,k} h_{k,D}$ and $\gamma_{\mathbf{P_R}}^{denom} = \sum_{k=1}^{K}\beta_k^2 h_{k,D}^2$. Note that $\gamma_{\mathbf{P_R}}^{nom}$ and $\gamma_{\mathbf{P_R}}^{denom}$ need to be separately conveyed to the relay in order to compute $\gamma_{\mathbf{P_R}}^{new}(k,l)$.

$$\lambda_k(e_{k,z}, \xi_k^{ene}, \xi_k^{data}, E^{max}, \gamma_{\mathbf{P_R}}^{nom}, \gamma_{\mathbf{P_R}}^{denom}, z)$$

$$= \psi \cdot \frac{1 - \prod_{i=z}^{T^{hor}} Pr(e_{k,z} \geq E^{pac} | I_{k,z}^{data} = 1 \ldots I_{k,T^{hor}}^{data} = 1)}{\gamma_{\mathbf{P_R}}^{new}(k,l)}. \tag{18}$$

$$\Lambda_k^L = \lambda_k(E^{pac}, \xi_k^{ene^H}, \xi_k^{data^L}, E_k^{max^H}, \gamma_{\mathbf{P_R}}^{nom^H}, \gamma_{\mathbf{P_R}}^{denom^H}, z),$$

$$\Lambda_k^H = \lambda_k(0, \xi_k^{ene^L}, \xi_k^{data^H}, E_k^{max^L}, \gamma_{\mathbf{P_R}}^{nom^L}, \gamma_{\mathbf{P_R}}^{denom^L}, z) \tag{19}$$

The complexity of the first phase of the sub-optimal RPLS scheme (slot reservation) is KT^{hor^2}, whereas the second phase (power-level selection) requires a maximum of $K(L-1)$ iterations per time slot. Thus, the total number of steps is upper bounded by $KT^{hor^2} + K(L-1)T^{hor}$ compared to $L^{K^{T^{hor}}}$ steps required by the optimal solution.

V. Relay Power-level Selection as a Repeated Bayesian Stackelberg Game

Due to the impracticality of the centralised solution above and the absence of NC-DECI in practical scenarios, in this section, we present a distributed solution to the RPLS problem as an RBSG process wherein each time slot a series of Stackelberg interactions (stage games) are played between the source and the relays with incomplete information. The game indefinitely repeats between the selfish players until no one deviates from his last stage action yielding the selected power levels, after which data transmission may commence. A single stage of the RBSG is formulated as follows.

A. Stage Game Formulation

In each stage t of the repeated game, a single-leader/multiple-follower Stackelberg game is played. The source (leader) makes the first move by broadcasting a price factor $f_s(t) \in \mathbb{R}^+$ that constitutes a payment of $\pi(t) = f_s(t)\gamma(t)$ to be shared by the relays, where $\gamma(t)$ is the SNR that would result from the relays' overall response actions at the end of stage t. As the followers, relays simultaneously respond to the committed price $f_s(t)$ and the predicted SNR $\gamma^{new}(t)$, using the last stage SNR $\gamma(t-1)$, by transmitting short beacons indicating their selected power levels $\mathbf{P_R}(t)$.

At the end of the stage, the utilities of the source and the relays obtained (per transmitted bit) are expressed in (15) and (16) respectively. As for the source, a payoff of $\mathfrak{R}_{\mathbf{P_R}}(t)$ multiplied by a gain of μ_s is obtained, whereas a cost of the payment submitted multiplied by a cost gain of λ_s is incurred. Additionally, the source incurs a

cost of $\varrho_s t$ that resembles the overhead, computation and delay costs associated with the number of stages played up to stage t. The relay utility function is explained as follows. First, the relays that do not decrease their transmit powers in the current stage will receive the payments they had obtained (reserved) in the previous stage, denoted by $\pi^{res}(t-1) = \{\pi_1^{res}(t-1), \ldots, \pi_K^{res}(t-1)\}$, from the submitted payment $\pi(t)$[3]. Any excess payment $\pi^{exc}(t) = max(\pi(t) - \sum_{k=1}^{K} \pi_k^{res}(t-1)$,0) will be equally shared by the K' relays that strictly increased their power levels in stage t. The obtained stage utility of a relay k will be the payment received times its payoff gain μ_k, while the cost incurred is the power transmitted times the relay's cost factor λ_k.

The sharing of relay payments in the manner explained above allows for the pricing game to occur over a single broadcast channel. In other words, the source does not require orthogonal channels per relay as in [13]. It is assumed that the proposed payment sharing scheme is enforced by the source and the game rule.

Remark 1 : The allocated relay payments at each stage may not be equal, as they depend on payments reserved in the previous stage.

B. Relay Cost Function

In this section, we propose a function for updating the relay's cost factor at each time slot in terms of its data, channel and energy profiles as given in (18), shown at the top of the previous page. Specifically, the cost at a given slot z is inversely proportional to the SNR contribution of the relay when transmitting at full power. Additionally, the cost is directly proportional to the relay's blocking probability, where $Pr(e_{k,i} \geq E^{pac} | I_{k,i}^{data} = 1 \ldots I_{k,T^{hor}}^{data} = 1)$ is the probability that the relay is $active$ in slot i given it had packets to transmit in all previous slots. This probability is calculated by sequentially deducing that the probability of the battery level is $\ell \in \{0, E^{pac}, 2E^{pac}, \ldots, E_k^{max}\}$ using $Pr(e_{k,i} = \ell) = Pr(e_{k,i-1} = \ell) \cdot \xi_k^{ene} + Pr(e_{k,i-1} = \ell + E^{pac}) \cdot (1 - \xi_k^{ene})$. It is worth noting that the battery capacity affects the relay cost, as $Pr(e_{k,i-1} = \ell + E^{pac}) = 0$ when $\ell + E^{pac} > E_k^{max}$. Finally, a cost tuning factor ψ is used to optimise the network performance as will be explained in Section V-G below. Thus, the suggested cost function promotes the selection of relays with better channel conditions, higher energy availability and lower data traffic.

Remark 2 : Relays with higher cost factors/lower SNR contributions will require higher payments to stimulate their cooperation at the targeted power level.

C. Game Equilibrium Strategies

In repeated games, players strive to maximise their sum utilities gained over the stages of the game. Because the actual data transmission occurs after the last stage of

[3]Reserved payments are allocated in the order they were obtained.

$$f_s^*(\mathbf{P}_{\mathbf{R}}^{SE}, k, l, t) = \max_{f_s \in [f_s^L, f_s^H]} E[\mathcal{U}_s(t+1, \mathbf{P}_{\mathbf{R}}^{SE}, f_s; \Lambda_{\mathbf{R}}) - \mathcal{U}_s(t)] \tag{20}$$

$$= \max_{f_s \in [f_s^L, f_s^H]} \int_{\Lambda_{\mathbf{R}}} Pr(d\Lambda_{\mathbf{R}})(\mathcal{U}_s(t{+}1, \mathbf{P}_{\mathbf{R}}^{SE}, f_s; \Lambda_{\mathbf{R}}) - \mathcal{U}_s(t)),$$

$$f_s^*(\mathbf{P}_{\mathbf{R}}^{SE}, k, l, t) = \max_{f_s \in [f_s^L, f_s^H]} Pr(Y_{k,l}^{f_s})(\mathcal{U}_s(t+1, \mathbf{P}_{\mathbf{R}}^{SE}, f_s) - \mathcal{U}_s(t)) + (1 - Pr(Y_{k,l}^{f_s}))(-\varrho_s t). \tag{21}$$

---

the repeated game, a player's utility gained from all stages preceding the last stage is negligible since only short beacons are exchanged. As players do not know the number of stage games in advance, each player will aim to maximise the current stage utility gain. Hence, we propose an optimal strategy pair that yields a Stackelberg equilibrium (SE) at each stage and also constitutes a perfect equilibrium of the repeated game. The SE strategies are derived by backward induction as the following.

1) Follower (Relay) Strategy: At each stage t, a relay k, determines its obtained payment in the last stage using the SNR and $K^{'}$ fed back from the source. As relays make their actions simultaneously, each relay computes the SNR achieved upon unilaterally selecting every possible power level using (17) then selects the one that maximises its current stage utility in (16). Thus, the relay's proposed SE strategy becomes:

$$P_k^{SE} = \max_{P_k \in \mathcal{P}} \mathcal{U}_k(t, \pi(t), P_k, \pi^{res}(t-1)). \tag{22}$$

2) Leader (Source) Strategy: The source is assumed to have initial beliefs (distributions) over each relay's cost factor uniformly distributed between Λ_k^L and Λ_k^H as in (19). The values $(E_k^{max^H}, \xi_k^{ene^H}, \xi_k^{data^H})$ and $(E_k^{max^L}, \xi_k^{ene^L}, \xi_k^{data^L})$ define the upper and lower limits on the possible values of the battery size, energy harvesting and data arrival probabilities respectively, whereas $\gamma_{\mathbf{P_R}}^{nom^H} = \gamma_{\mathbf{P_R}}^{nom} + \kappa\gamma_{\mathbf{P_R}}^{nom}$ and $\gamma_{\mathbf{P_R}}^{nom^L} = \gamma_{\mathbf{P_R}}^{nom} - \kappa\gamma_{\mathbf{P_R}}^{nom}$ (and similarly $\gamma_{\mathbf{P_R}}^{denom^H}$ and $\gamma_{\mathbf{P_R}}^{denom^L}$) represent the range of estimated CSI parameters around the actual values $\gamma_{\mathbf{P_R}}^{nom}$ and $\gamma_{\mathbf{P_R}}^{denom}$ with $\kappa \in [0, 1]$ being the error factor. The PDF and CDF functions of the source beliefs are defined respectively as:

$$Pr(\Lambda_k) = \begin{cases} 0 & \Lambda_k \notin [\Lambda_k^L, \Lambda_k^H] \\ \frac{1}{\Lambda_k^H - \Lambda_k^L} & \Lambda_k \in [\Lambda_k^L, \Lambda_k^H] \end{cases}, \tag{23}$$

$$F(\Lambda_k) = \begin{cases} 0 & \Lambda_k < \Lambda_k^L \\ \frac{\Lambda_k - \Lambda_k^L}{\Lambda_k^H - \Lambda_k^L} & \Lambda_k^L \leq \Lambda_k < \Lambda_k^H \\ 1 & \Lambda_k \geq \Lambda_k^H \end{cases}. \tag{24}$$

$$Pr(\hat{X}_{k,l,v}^{f_s}) = Pr(\mathcal{U}_k(f_s,l) \geq \mathcal{U}_k(f_s,v) =$$

$$\begin{cases} Pr(\lambda_k > \frac{\mu_k f_s(\gamma_{\mathbf{P_R}}^{new}(k,l)-\gamma_{\mathbf{P_R}}^{new}(k,v))}{\mathcal{P}(l)-\mathcal{P}(v)}) & P_k(t-1) \leq v \leq P \\ Pr(\lambda_k < \frac{\mu_k f_s(\gamma_{\mathbf{P_R}}^{new}(k,l)-\sum_{i=1}^{K}\pi_i^{res}+\pi_k^{res})}{\mathcal{P}(l)}) & v = 0 \\ Pr(\lambda_k < \frac{\mu_k f_s(\gamma_{\mathbf{P_R}}^{new}(k,l)-\gamma_{\mathbf{P_R}}^{new}(k,v))+\mu_k\pi_k^{res}}{\mathcal{P}(l)-\mathcal{P}(v)}) & 0 < v < P_k(t-1) \end{cases}. \tag{27}$$

$$Pr(X_{k,l}^{f_s}) = Pr(max_{P_k(t-1)\leq v\leq P})(\frac{\mu_k f_s(\gamma_{\mathbf{P_R}}^{new}(k,l)-\gamma_{\mathbf{P_R}}^{new}(k,v))}{\mathcal{P}(l)-\mathcal{P}(v)}) <$$

$$\lambda_k < min_{0\leq v<P_k(t-1)}(\frac{\mu_k f_s(\gamma_{\mathbf{P_R}}^{new}(k,l)-\gamma_{\mathbf{P_R}}^{new}(k,v))+\mu_k\pi_k^{res}}{\mathcal{P}(l)-\mathcal{P}(v)}))$$

$$= F(max_{P_k(t-1)\leq v\leq P})(\frac{\mu_k f_s(\gamma_{\mathbf{P_R}}^{new}(k,l)-\gamma_{\mathbf{P_R}}^{new}(k,v))}{\mathcal{P}(l)-\mathcal{P}(v)})-$$

$$F(min_{0\leq v<P_k(t-1)}(\frac{\mu_k f_s(\gamma_{\mathbf{P_R}}^{new}(k,l)-\gamma_{\mathbf{P_R}}^{new}(k,v))+\mu_k\pi_k^{res}}{\mathcal{P}(l)-\mathcal{P}(v)})$$

$$= \frac{max_{P_k(t-1)\leq v\leq P}(\frac{\mu_k f_s(\gamma_{\mathbf{P_R}}^{new}(k,l)-\gamma_{\mathbf{P_R}}^{new}(k,v))}{\mathcal{P}(l)-\mathcal{P}(v)}) - min_{0\leq v<P_k(t-1)}(\frac{\mu_k f_s(\gamma_{\mathbf{P_R}}^{new}(k,l)-\gamma_{\mathbf{P_R}}^{new}(k,v))+\mu_k\pi_k^{res}}{\mathcal{P}(l)-\mathcal{P}(v)})}{\Lambda_k^H - \Lambda_k^L}. \tag{28}$$

$$f_s^{SE}(t) = \begin{cases} f_{max}^* & E[\mathcal{U}_s(t+1,\mathbf{P_R^{SE}},f_{max}^*;\Lambda_{\mathbf{R}}) - \mathcal{U}_s(t)] > 0 \\ f_s^{SE}(t-1) & otherwise \end{cases}. \tag{29}$$

Also, the feasible range of prices is defined by:

$$f_s^L(\mathbf{P_R},k,l) = (\frac{\Lambda_k^L\mathcal{P}(l)}{\mu_k} + \sum_{i=1}^{K}\pi_i^{res} - \pi_k^{res})/\gamma_{\mathbf{P_R}}^{new^H}(k,l), \tag{25}$$

$$f_s^H(\mathbf{P_R},k,l) = (\frac{\Lambda_k^H\mathcal{P}(l)}{\mu_k} + \sum_{i=1}^{K}\pi_i^{res} - \pi_k^{res})/\gamma_{\mathbf{P_R}}^{new^L}(k,l), \tag{26}$$

where $\gamma_{\mathbf{P_R}}^{new^H}$ and $\gamma_{\mathbf{P_R}}^{new^L}$ are the upper and lower possible values of the new SNR given the CSI estimation error.

In each stage game, the source determines the optimal price factor, between f_s^L and f_s^H, that maximises the expected utility gain upon targeting transition (k,l) as given in (20) above [11], where $\mathbf{P_R^{SE}} = \{P_1^{SE},\ldots,P_K^{SE}\}$ and $\Lambda_{\mathbf{R}} = \{\Lambda_1,\ldots,\Lambda_K\}$ in which Λ_k is a typical type of relay k. Since an increase in the source utility only occurs if a single relay adjusts its power level (as will be proven in Section V-E), the above equation can

be rewritten as (21) shown above, where $Pr(Y_{k,l}^{f_s})$ represents the probability that the transition (k, l) occurs when f_s is submitted. In other words, it is the probability that k is the only relay that will deviate to select level l, while all other relays will keep their power levels fixed. Due to the independence the relays' cost factors, $Pr(Y_{k,l}^{f_s})$ can be expressed as:

$$Pr(Y_{k,l}^{f_s}) = Pr(X_{k,l}^{f_s}) \cdot (\prod_{i=1, i \neq k}^{K-1} Pr(X_{i,P_i}^{f_s})), \tag{30}$$

where $Pr(X_{k,l}^{f_s}) = \prod_{v=1, v \neq l}^{L} Pr(\hat{X}_{k,l,v}^{f_s})$ is the probability that the cost factor of relay k will turn its utility upon selecting level l to be at least equal to that obtained by selecting any other power level $v \neq l$ as given in (27) below. By using (16), (23) and (27), $Pr(X_{k,l}^{f_s})$ can be computed as (28) shown above.

The optimal price $f_s^*(\mathbf{P}_{\mathbf{R}}^{SE}, k, l, t)$ is found by taking the derivative of the expected utility gain with respect to f_s and equating it to zero. Apparently, this derivative is intractable and thus the closed form of (21) is left for future work. Alternatively, a sub-optimal price may be found by evaluating (21) at fixed intervals between f_s^L and f_s^H. Having determined the optimal price when targeting every possible transition, the source selects the price factor corresponding to the transition with the highest expected utility gain $f_{max}^*(\mathbf{P}_{\mathbf{R}}^{SE}, k^{max}, l^{max}, t)$, where $(k^{max}, l^{max}) = \arg\max_{k \in \mathcal{K} \quad l \in \mathcal{P}} f_s^*(\mathbf{P}_{\mathbf{R}}^{SE}, k, l, t)$. If the maximum expected gain in utility is non-positive, the source re-submits the last stage price factor. Thus, the source's best response strategy in the RBSG is summarised as (29) below.

D. Belief Update System

At every stage of the RBSG, the source applies the Bayes' theorem [27] to update its beliefs upon realizing the relays' best response actions as follows [4]. The source's belief over the type of relay k $(Pr(\Lambda_k))$ at the beginning of the stage game is termed the $prior\ probability$. The observation of the relay's action after the stage game is played gives the $likelihood\ function$ $Pr(X_{k,l}^{f_s^{SE}}|\Lambda_k)$. Given these probabilities and the $marginal\ likelihood$ in (31), the $posterior\ probability$ $Pr(\lambda_k|X_{k,l}^{f_s^{SE}})$ is found using (32).

$$Pr(X_{k,l}^{f_s^{SE}}) = \int_{\Lambda_k \in [\Lambda_k^L, \Lambda_k^H]} Pr(X_{k,l}^{f_s^{SE}}|\Lambda_k) Pr(\Lambda_k) \tag{31}$$

$$Pr(\Lambda_k|X_{k,l}^{f_s^{SE}}) =$$

[4]Note that $\mathbf{P}_{\mathbf{R}}^{SE}$ can be inferred by comparing the received SNR with that resulting from each possible combination of relay actions.

$$\Lambda_k \begin{cases} > \Lambda_k^{L^{new}} = \max(\Lambda_k^L, \max_{\mathcal{P}(i)\in\mathcal{P}\setminus\mathcal{P}(l)} \frac{f_s^{SE}(\gamma_{\mathbf{P_R}}^{new}(k,l)-\gamma_{\mathbf{P_R}}^{new}(k,i))}{(\mathcal{P}(l)-\mathcal{P}(i))} & if \quad l<i) \\ < \Lambda_k^{H^{new}} = \min(\Lambda_k^H, \min_{\mathcal{P}(i)\in\mathcal{P}\setminus\mathcal{P}(l)} \frac{f_s^{SE}(\gamma_{\mathbf{P_R}}^{new}(k,l)-\gamma_{\mathbf{P_R}}^{new}(k,i))}{(\mathcal{P}(l)-\mathcal{P}(i))} & if \quad l>i) \end{cases} . \tag{33}$$

$$Pr(\Lambda_k|X_{k,l}^{f_s^{SE}}) =$$

$$\begin{cases} 0 & \Lambda_k \notin [\Lambda_k^{L^{new}}, \Lambda_k^{H^{new}}] \\ \frac{1\cdot\frac{1}{\Lambda_k^H-\Lambda_k^L}}{\int_{\Lambda_k^L}^{\Lambda_k^{L^{new}}} 0\cdot\frac{1}{\Lambda_k^H-\Lambda_k^L}d(\Lambda_k)+\int_{\Lambda_k^{L^{new}}}^{\Lambda_k^{H^{new}}} 1\cdot\frac{1}{\Lambda_k^H-\Lambda_k^L}d(\Lambda_k)+\int_{\Lambda_k^{H^{new}}}^{\Lambda_k^H} 0\cdot\frac{1}{\Lambda_k^H-\Lambda_k^L}d(\Lambda_k)} & \Lambda_k \in [\Lambda_k^{L^{new}}, \Lambda_k^{H^{new}}] \end{cases}$$

$$= \begin{cases} 0 & \Lambda_k \notin [\Lambda_k^{L^{new}}, \Lambda_k^{H^{new}}] \\ \frac{1}{\Lambda_k^{H^{new}}-\Lambda_i^{L^{new}}} & \Lambda_k \in [\Lambda_k^{L^{new}}, \Lambda_k^{H^{new}}] \end{cases} . \tag{34}$$

$$\frac{Pr(X_{k,l}^{f_s^{SE}}|\Lambda_k)Pr(\Lambda_k)}{Pr(X_{k,l}^{f_s^{SE}})} \quad if \;\; Pr(X_{k,l}^{f_s^{SE}}) > 0 \; . \tag{32}$$

The optimal strategy of relay k upon transmitting at level l, as explained in the previous section, leads to the inequality $f_s^{SE}(t)\gamma^{new}(\mathbf{P_R},k,l)-\lambda_k\mathcal{P}(l) > f_s^{SE}(t)\gamma^{new}(\mathbf{P_R},k,i)-\lambda_k\mathcal{P}(i)\ \forall\mathcal{P}(i)\in\mathcal{P}\setminus\mathcal{P}(l)$. With some manipulations, the source's belief over the relay's cost factor is bounded in (33) above. Consequently, the probability $Pr(X_{k,l}^{f_s^{SE}}|\Lambda_k)$ is exactly 1 if Λ_k conforms with (33), and 0 otherwise. By substituting these results into (32) and using (23), the posterior probability is obtained as shown in (34). The posterior probability with the updated limits $\Lambda_k^{L^{new}}$ and $\Lambda_k^{H^{new}}$ is then used as the prior probability in the next stage of the RBSG. This process is then repeated for all the relays.

E. Existence of a Perfect Bayesian Equilibrium

The appropriate notion of equilibrium for repeated games with incomplete information is the perfect Bayesian equilibrium (PBE), which demands that strategy profiles are sequentially rational while beliefs are consistent [28]. In other words, the source strategy should always maximise the expected utility given the beliefs, which are updated after realizing the relays' actions by applying Bayes' rule. To prove the existence of a PBE of the proposed game, the two properties above are verified in the following propositions:

Proposition 1 : The proposed belief update system is consistent.

Proof : To show that Bayes rule is always satisfied, one needs to prove that the denominator in (32) is always non-zero. Assuming a valid initial belief ($\Lambda_k^L > \lambda_k > \Lambda_k^H$) and that the uniform distribution parameters (Λ_k^L and Λ_k^H) are updated according to (34),

then λ_k must always remain between Λ_k^L and Λ_k^H after any stage leading to $Pr(\Lambda_k)$ being positive for a given value $\Lambda_k \in [\Lambda_k^L, \Lambda_k^H]$, and hence $Pr(X_{k,l}^{f_s^{SE}})$ is always non-zero. Therefore, Bayes' rule is always satisfied for any belief update at any information set reached with a positive probability. ■

Proposition 2 : The proposed strategy pair in (22) and (29) is sequentially rational.

Proof : First, to show that submitting the minimum payment to induce a single relay transition at each stage is a best response strategy of the source, suppose otherwise. If the submitted payment is lower than f_s^{SE}, then $\mathbf{P_R}$ will remain unchanged, but a game stage cost will be incurred that will reduce the utility of the source node. However, if the payment is above f_s^{SE} but insufficient to induce multiple transitions, the source will only commit to an unnecessarily higher payment for the same achieved performance again reducing the utility. In addition, if the payment is high enough to cause multiple transitions then the deviating relays will eventually receive lower payments than predicted (divided by $K^{'}$), causing them to revert their actions in the following stage. This again results in nothing but an additional stage cost $\varrho_s t$. Since any strategy other than f_s^{SE} strictly decreases the sources' utility gain, f_s^{SE} is the best response of the source in the stage game.

Therefore, the proposed strategy pair of the source and relays that maximises their expected utilities upon inducing the optimal transition given the belief over the relay types at every information set is sequentially rational. Although a closed form solution to maximise (21) is not derived in this work, a global maximum is proven to exist since the function is continuous and defined over the closed interval $[f_s^L, f_s^H]$. ■

Remark 3 : The proposed strategy pair and belief system form a perfect Bayesian equilibrium.

F. Convergence of the Proposed Game

The convergence to the selected set of power levels is another important property of the game equilibrium, which is proven as follows:

Proposition 3 : The proposed RBSG converges in a finite number of iterations.

Proof: Given that the number of relays and power levels are finite and that only the SNR maximizing transitions are induced by the rational players, the optimal relay power vector must be reached in a finite number of unilateral transitions from the initial state $\mathbf{P_R} = \{0, \ldots, 0\}$. After each stage game is played to target the next best transition, the updated belief distribution intervals $[\Lambda_k^L,\ \Lambda_k^H]$ are always reduced for at least one relay, increasing the likelihood of achieving the targeted transition, that is, $\exists k \in \mathcal{K}$: $\Lambda_k^{L^{new}} > \Lambda_k^L$ or $\Lambda_k^{H^{new}} < \Lambda_k^H$. Eventually, either the transition will occur or the source will choose to end the game when the iteration cost exceeds the expected utility gain

in causing the targeted transition. Hence, the game converges in a finite number of iterations. ■

G. Complexity of the Proposed Game

The complexity of the proposed game theoretic algorithm is analyzed by evaluating the complexity of players' strategies in each stage game. Despite its infinite strategy space, the source only targets a finite set of relay/level transitions that maximise the channel capacity. Hence, the source needs to evaluate the maxima of its utility function (21) for every possible transition leading to a complexity of $RL\mathcal{C}$, where $\mathcal{C}$ is the complexity of finding the maximum of (21). The relay, on the other hand, needs to evaluate the utility associated with L possible levels, hence the complexity of its best response strategy is linear. The convergence speed of the RBSG depends on the game parameters μ_s, ϱ_s, ψ and κ as follows. At higher values of μ_s and lower values of ψ, more stage games will be played as the source will afford to purchase relatively higher SNR values that are associated with more transitions. Conversely, a higher CSI error κ will extend the belief intervals leading to more multilateral transitions that will be eventually reverted, hence, leading to more iterations. Finally, a low stage cost factor ϱ_s will lower the source's expected utility gain in playing additional stage games. The effect of the aforementioned parameters on the convergence speed and the performance of the proposed solution will be illustrated in the following section.

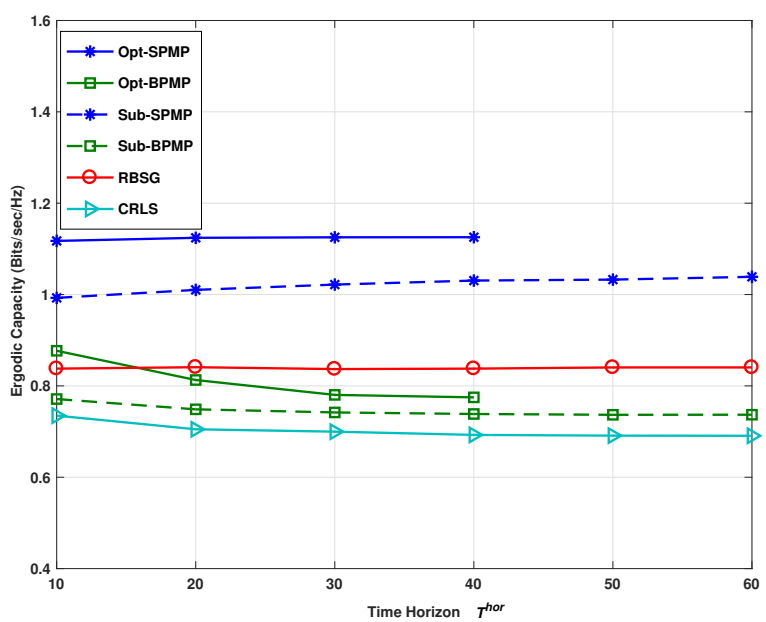

Fig. 4. Ergodic Capacity vs. Number of Time-slots (Time horizon) ($K = 4$,$L = 2$)

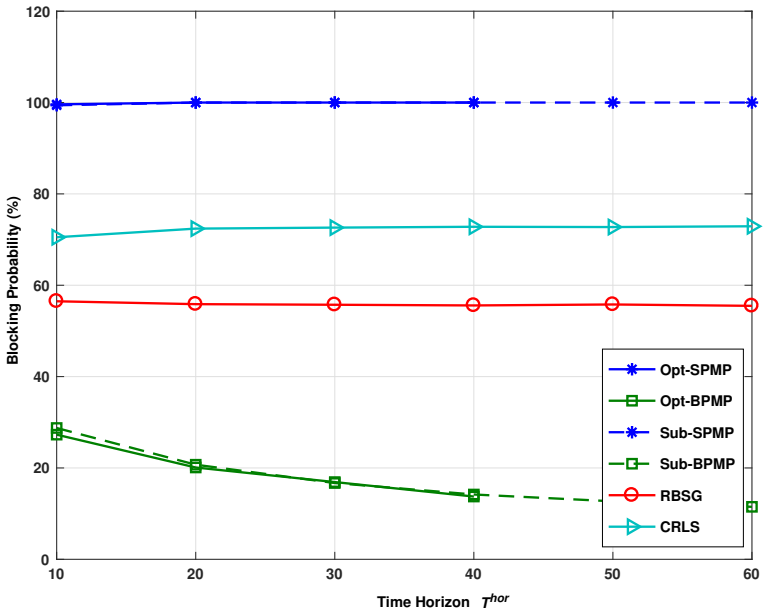

Fig. 5. Blocking Probability (BP) vs. Number of Time-slots (Time horizon) ($K = 4$,$L = 2$)

VI. Numerical Evaluation

The proposed selection scheme based on the RBSG is evaluated using extensive Matlab simulations and compared against the RPLS with NC-DECI approaches formulated in Section IV. In addition, the conventional non-energy-aware relay power-level selection (CRLS) is simulated, in which power levels that maximise the instantaneous SNR and satisfy the causality constraints are selected. In the simulated topology, the source and the destination nodes are positioned at coordinates (0,2m) and (6m,2m) respectively, while the relays are randomly positioned in a square with vertices (1m,0), (5m,0), (1m,4m) and (5m,4m). The simulation parameters (listed in Table I) are specified such that $P = 100mW$, $N_o = 10^{-5}$W/Hz, $\upsilon = 3.5$, $\mu_s = 10$, $\lambda_s = 10$ and $\psi = 5$. All simulations were averaged over 10,000 iterations wherein each iteration the energy model parameters are randomly and uniformly selected from the intervals $[E_k^{max^L} = 0J, E_k^{max^H} = 4E^{pac}J]$, $[\xi_k^{ene^L} = 0.2, \xi_k^{ene^H} = 0.3]$ and $[\xi_k^{data^L} = 0, \xi_k^{data^H} = 0.2]$.

Figures 4 and 5 depict the performance of the different schemes in terms of capacity and blocking probability with 4 relays and 2 power levels (On/Off relaying). Due to the high complexity of the optimal schemes (obtained using MIDACO solver [29]), only a maximum of 40 time slots were simulated beyond which the performance is seen to saturate. The capacity of the sub-optimal NC-DECI schemes (Sub-SPMP and Sub-BPMP) falls by around 6% with respect to their optimal counterparts (Opt-SPMP and Opt-BPMP), while no degradation is seen in BP. The slight improvement in capacity

Table I
LIST OF KEY NOTATIONS

$\mathfrak{R}$	Channel Capacity
P	Node Power Constraint
K	Total Number of Relays
L	Number of Power Levels
γ	SNR
N_o	Noise Spectral Density
υ	Path loss Exponent
ξ	Bernoulli Process Parameter
T^{hor}	Time horizon (no. time slots)
T^{slot}	Time slot duration
E^{max}	Relay Battery Capacity
μ	Player Payoff Gain
ϱ	Iteration Cost
ψ	Relay Cost Tuning Factor
f_s	Source Price Factor
π	Submitted Relay Payment
λ	Player Cost Factor
κ	CSI Error Factor

for RBSG and SPMP at high T^{hor} is due to the higher likelihood of harvesting energy packets and traversing more channel gains that are efficiently utilised in these schemes. In contrast, CRLS falls with T^{hor} as it does not utilise time slots of high channel gains hence the performance degrades when averaged over a large T^{hor}. Eventually, the performance in all schemes saturates at high T^{hor} due to the uniform energy arrival rates and the diminished effect of the initial energy. In general, the proposed RBSG is seen to offer a compromise between the two optimal policies where each policy achieves either maximum capacity and worse BP or vice versa. For example, at $T^{hor} = 60$ the RBSG data rate is only 13% below that of Sub-SPMP, while in BP it outperforms the former scheme by 66%. Conversely, the proposed solution is superior to Sub-BPMP in capacity but lags behind in BP. CRLS, however, is the worst in both capacity and BP since it is not an energy aware scheme.

To further demonstrate the effectiveness of the proposed protocol, simulations of the average throughput of the source and relays were performed, as shown in Fig. 6, where the throughput is defined as the rate of packet delivery assuming a minimum detection SNR of $3dB$ [17]. The proposed game outperforms both sub-optimal policies, for $K = 4$, as it offers a compromise between the source's capacity and relay BP. By increasing the number of relays, the BPMP results in a better throughput than RBSG as the source's throughput now has a lower effect on the average network throughput.

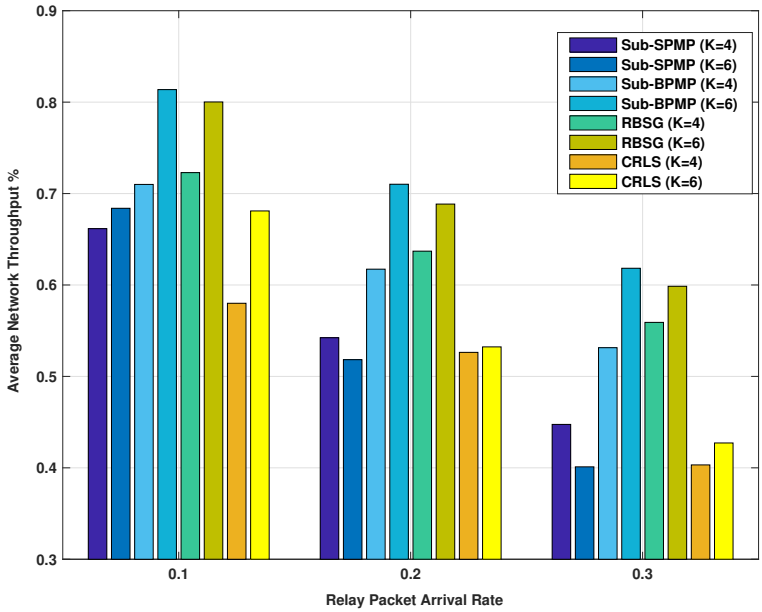

Fig. 6. Average Network Throughput vs. Relay Packet Arrival Rate ξ_k^{data} ($L = 2$, $\xi_k^{ene^L} = 0.3, \xi_k^{ene^H} = 0.5$)

It is also observed that increasing the relay packet arrival rate reduces the throughput for all schemes because of the limited harvesting rate being insufficient to deliver the increased number of data packets.

In Fig. 7, the effect of increasing the number of relays and power levels is illustrated for the different schemes. As expected, all schemes benefit from increasing the number of power levels as the harvested energy is more efficiently utilised. Introducing more relays also improves the performance because of the higher achievable diversity order. Meanwhile, the gap between RBSG and CRLS falls from 21% to 16% when K is increased from 4 to 6. This is due to the higher $energy\ diversity$; that is, the more relays with independent energy arrivals, the more likely an active relay exists. In addition, the iteration cost prevents the RBSG from achieving a better performance due to the higher number of iterations associated with more transition levels reducing the obtained utility.

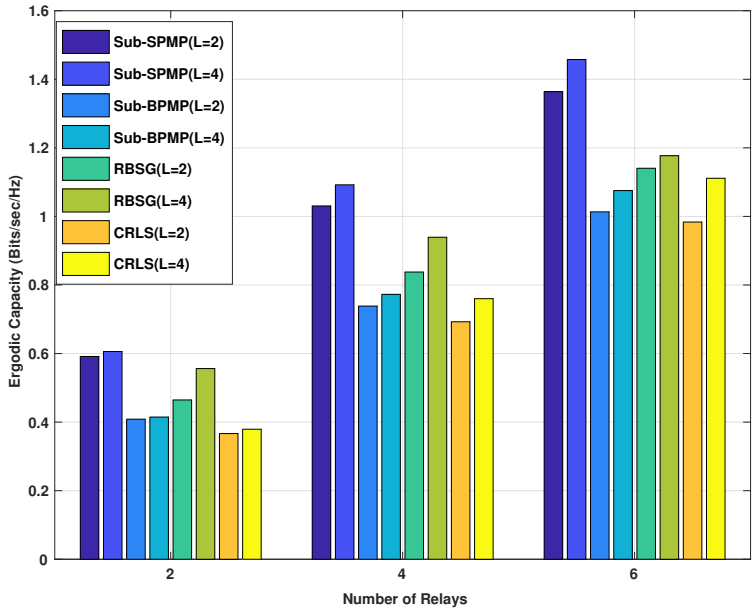

Fig. 7. Ergodic Capacity vs. Number of Relays ($T^{hor} = 40$)

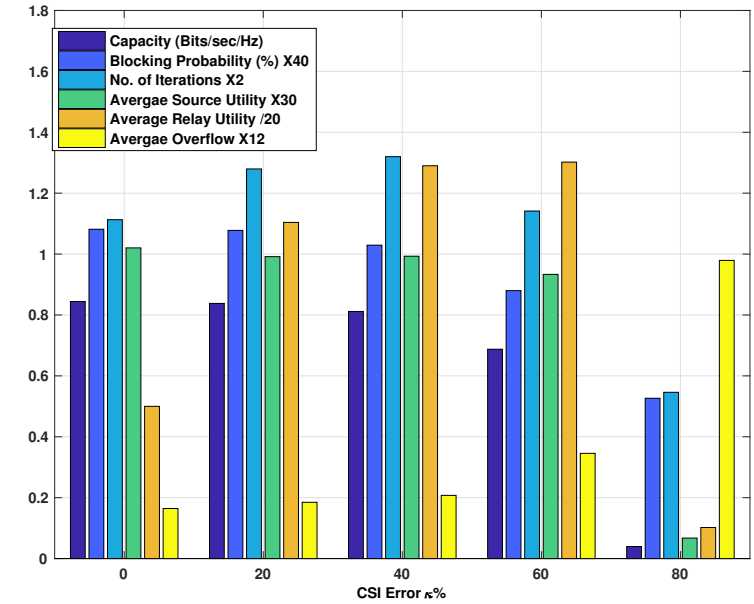

Fig. 11. Performance vs. CSI Estimation Error κ ($K = 4$, $L = 2$, $T^{hor} = 20$)

The relationship between the stage cost factor ϱ_s and the network performance represented by the ergodic capacity (EC), complexity (number of iterations), blocking probability and the source node utility are shown in Fig. 8 for different power levels,

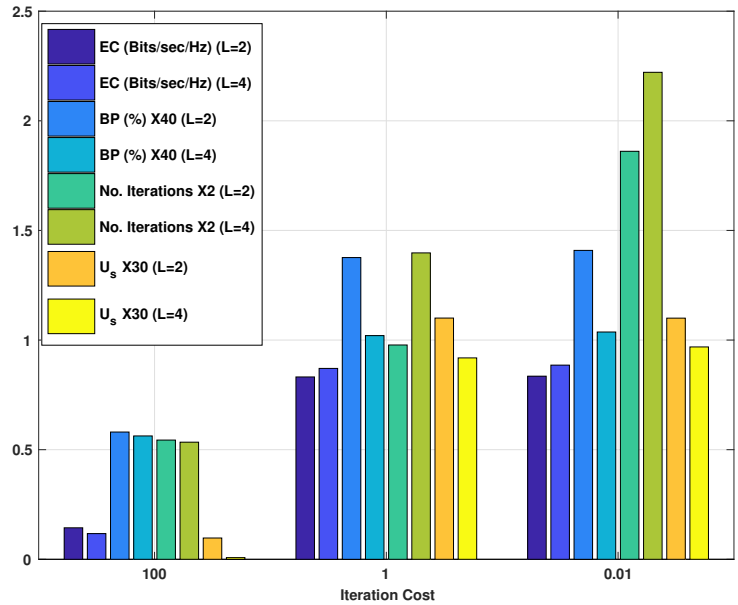

Fig. 8. Performance vs. Iteration Cost Factor ϱ_s for $K = 4$, $T^{hor} = 20$

4 relay nodes and a time horizon of 20 slots. The number of iterations increases with the number of levels but falls with the stage cost factor, as discussed in the complexity analysis above. At the same time, the average capacity and source utility drop with higher cost per stage hence a trade off between complexity and performance can be realised. However, the variations in the above metrics remain almost constant as the iteration cost is increased from 0.01 to 1 while the complexity is greatly reduced. A high iteration cost factor is also shown to improve the blocking probability, since it reduces the number of selected relays.

The convergence of the RBSG and hence the selected power levels is illustrated in figures 9 and 10 for different number of relays and game parameters respectively. With 2 relay nodes, the algorithm requires 3 iterations to converge, while it takes 4 iterations when K is increased to 4. Increasing K further does not affect the convergence speed significantly since only a subset of the relays with best channels are selected. As predicted in Section V-G above, by keeping the source gain factor μ_s fixed and increasing the cost tuning factor ψ, the capacity is seen to drop as the repeated game terminates after a fewer stage games. Conversely, when the source gain factor is increased the capacity improves at the cost of more stage games (iterations) played.

Lastly, the effect of increasing the CSI estimation error κ on the source node's performance in the proposed scheme is depicted in Fig. 11 for the case of ($K = 4$, $L = 2$, $T^{hor} = 20$, $\varrho_s = 0.1$). It is seen that the performance is only marginally degraded

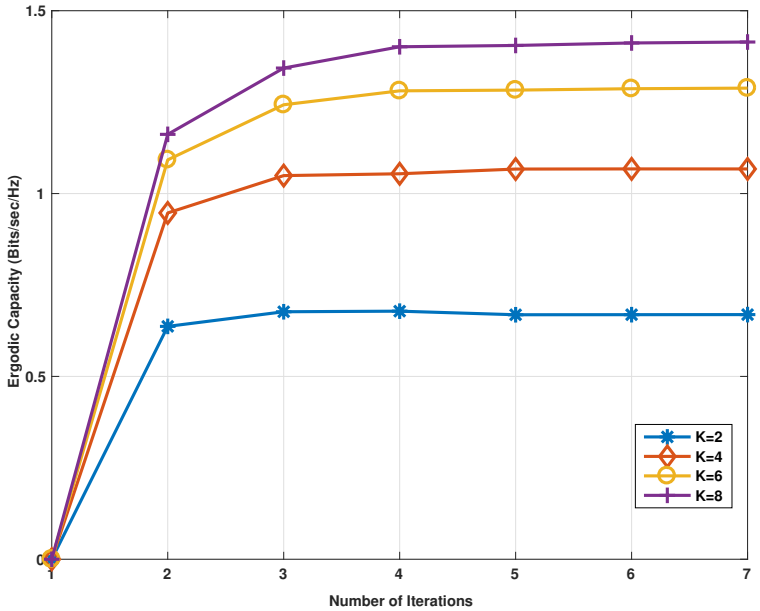

Fig. 9. Convergence of the Proposed RBSG ($L = 2$, $T^{hor} = 20$)

as the error is increased to 20%. This is explained by the fact that the same number of iterations (stage games) needed to infer the energy parameters can also help in learning the CSI. The performance in terms of the capacity and BP is seen to sharply drop as the error reaches 80%. Although the complexity increases with higher error margins due to more multiple (reverted) transitions, the number of iterations eventually falls with very high CSI errors. This is due to the very low expected utility gained causing the source to end the RBSG before the capacity maximizing transitions are induced. Interestingly, the relay's average utility improves with high CSI errors, as the source may wrongly infer the relay's cost resulting in more relay overpay.

VII. Discussion

A. *Capacity/Overhead Tradeoff*

The tradeoff between the capacity and the overhead associated with the RPLS process, controlled by the game parameters, makes the proposed scheme suitable for varying applications and scenarios. For instance, a real time system such as a vehicular ad hoc network may opt for a degraded throughput with a low overhead as small data packets need to be delivered with a very low latency. In a cellular data network, the RBSG can be tuned for maximum throughput, since large data packets are exchanged between users without stringent latency constraints.

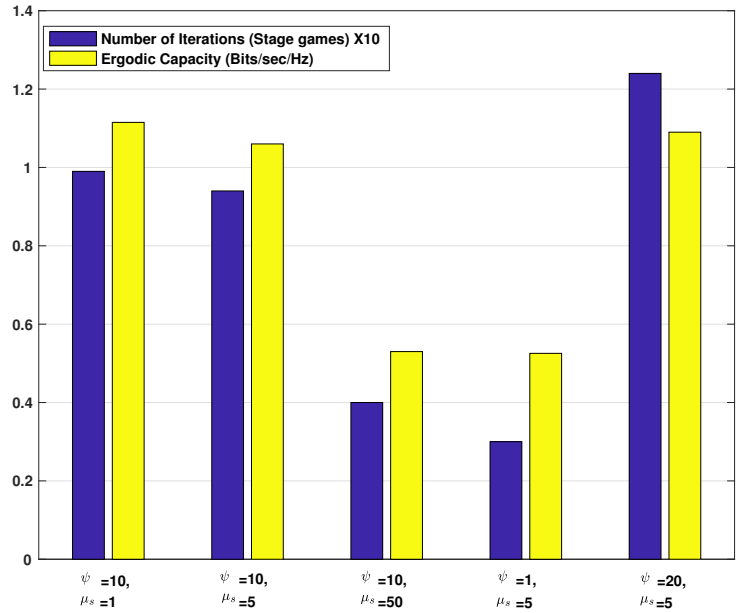

Fig. 10. Complexity of the Proposed RBSG for Different Game Parameters ($K = 4$, $L = 4$, $T^{hor} = 20$)

B. Practical Considerations

Among the practical issues associated with the proposed solution is the acquisition of the initial distributions. In a heterogeneous ad hoc network, such as the IoT, nodes may have different battery storage and energy harvesting capabilities. In this situation, nodes may obtain the initial distributions based on the minimum/maximum possible values that may be encountered. For instance, it can be known that the minimum possible battery capacity is 1 mAh or that the harvesting rate cannot exceed 10 mW/s. Another issue is the practical implementation of the power allocation among the competing players. A relay node can simply maintain a record of the payments earned from each source node it had encountered. A source node can then deduct the submitted payments from the payments received when it acted as a relay. However, the assumption of truth telling or a reputation system will be necessary, which is out of the scope of this study.

C. Multiple Source-Destination Pairs

In multiple access cooperative networks with many source-destination pairs, the described RBSG can still be applied with decode and forward relays. Specifically, in the first time slot the sources encode then transmit their data packets using spreading sequences known to the relays and corresponding destination nodes. Each relay separately decodes the received signals, forms a combined signal then broadcasts it, at the selected power level to the destinations in the second time slot. Each destination decodes its

intended message using the combined signal received from the relays. Since relays are simultaneously helping the source-pairs with optimal power levels being the same for all sources, the sources can fairly distribute the cost of payments to the relays in a round robin fashion. That is, in each transmission slot, a single source plays the RBSG with the relays by reimbursing them for their relaying costs. Because of multiple access transmission, the SNR function in (17) has to account for the cross interference.

VIII. Conclusion

A game theoretic resource management scheme for multi-relay energy harvesting cooperative networks is proposed. A relay cost function that encapsulates energy, data and channel information is designed. The distributed game theoretic solution is shown to yield a capacity enhancement of up to 21% with respect to other conventional selection schemes even when only statistical CSI is available at the source. Meanwhile, the proposed scheme shows a compromise between the source capacity and the BP of the relays in contrast to the two extreme upper bound policies. In addition, the proposed technique brings incentives to the relays and does not require NC-DECI. The proposed scheme is compatible with non-orthogonal relay channels and provides a good means for trading off complexity for performance by means of the stage cost factor.

References

[1] J. N. Laneman, D. N. C. Tse, and G. W. Wornell, "Cooperative diversity in wireless networks: Efficient protocols and outage behavior," *IEEE Trans. Information Theory*, vol. 50, no. 12, pp. 3062–3080, Dec. 2004.

[2] A. Bletsas, A. Khisti, D. Reed, and A. Lippman, "A simple cooperative diversity method based on network path selection," *IEEE J. Sel. Areas Commun.*, vol. 24, no. 3, pp. 659–672, Mar. 2006.

[3] Y. Jing and H. Jafarkhani, "Single and multiple relay selection schemes and their achievable diversity orders," *IEEE Trans. Wireless Commun.*, vol. 8, pp. 1414 – 1423, Mar. 2009.

[4] W. Su, A. K. Sadek, and K. J. R. Liu, "Cooperative communication protocols in wireless networks: Performance analysis and optimal power allocation," *Wireless Pers Commun*, pp. 181—217, Aug. 2007.

[5] D. Niyato, E. Hossain, M. Rashid, and V. Bhargava, "Wireless sensor networks with energy harvesting technologies: a game-theoretic approach to optimal energy management," *Wireless Commun.*, vol. 14, no. 4, pp. 90–96, Aug. 2007.

[6] K. Tutuncuoglu and A. Yener, "Optimum transmission policies for battery limited energy harvesting nodes," *IEEE Trans. Wireless Commun.*, vol. 11, no. 3, pp. 1180–1189, Mar. 2012.

[7] O. Ozel, K. Tutuncuoglu, J. Yang, S. Ulukus, and A. Yener, "Transmission with energy harvesting nodes in fading wireless channels: Optimal policies," *IEEE J. Sel. Areas Commun.*, vol. 29, no. 8, pp. 1732–1743, Sep. 2011.

[8] Y. Luo, J. Zhang, and K. Letaief, "Relay selection for energy harvesting cooperative communication systems," in *IEEE Global Telecommun. Conf. (GLOBECOM)*, Dec. 2013, pp. 2514–2519.

[9] P. Ju, W. Song, and D. Zhou, "Survey on cooperative medium access control protocols," *IET Communications*, vol. 7, no. 9, pp. 893–902, Jun. 2013.

[10] M. S. Bahbahani and E. Alsusa, "Relay selection for energy harvesting relay networks using a repeated game," *IEEE Wireless Commun. Netw. Conf. (WCNC)*, Apr. 2016.

[11] C. Kiekintveld, J. Marecki, and M. Tambe, "Approximation methods for infinite bayesian stackelberg games: modeling distributional payoff uncertainty." in *AAMAS*, L. Sonenberg, P. Stone, K. Tumer, and P. Yolum, Eds. IFAAMAS, 2011, pp. 1005–1012. [Online]. Available: http://dblp.uni-trier.de/db/conf/atal/aamas2011.html

[12] J. Marecki, G. Tesauro, and R. Segal, "Playing repeated stackelberg games with unknown opponents." in *AAMAS*, W. van der Hoek, L. Padgham, V. Conitzer, and M. Winikoff, Eds. IFAAMAS, 2012, pp. 821–828. [Online]. Available: http://dblp.uni-trier.de/db/conf/atal/aamas2012.html

[13] B. Wang, Z. Han, and K. J. R. Liu, "Distributed relay selection and power control for multiuser cooperative communication networks using Stackelberg game," *IEEE Trans. Mobile Computing*, vol. 8, pp. 975–990, Jul. 2009.

[14] Y. Mao, J. Zhang, S. Song, and K. Letaief, "Joint link selection and relay power allocation for energy harvesting relaying systems," in *IEEE Global Telecommun. Conf. (GLOBECOM)*, Dec. 2014, pp. 2568–2573.

[15] M. Kashef and A. Ephremides, "Optimal partial relaying for energy-harvesting wireless networks," *IEEE/ACM Trans. Netw.*, vol. PP, no. 99, pp. 1–1, Feb. 2016.

[16] T. Li, P. Fan, and K. Letaief, "Outage probability of energy harvesting relay-aided cooperative networks over rayleigh fading channel," *IEEE Trans. Veh. Technol.*, vol. PP, no. 99, pp. 1–1, Feb. 2016.

[17] M. Bahbahani, M. Baidas, and E. Alsusa, "A distributed political coalition formation framework for multi-relay selection in cooperative wireless networks," *IEEE Trans. Wireless Commun.*, vol. 14, no. 12, pp. 6869–6882, Dec. 2015.

[18] D. T. Hoang, X. Lu, D. Niyato, P. Wang, D. I. Kim, and Z. Han, "Applications of repeated games in wireless networks: A survey," *Commun. Surveys Tuts.*, vol. 17, no. 4, pp. 2102–2135, 2015.

[19] D. R. Brown and F. Fazel, "A game theoretic study of energy efficient cooperative wireless networks," *J. Commun. Netw.*, vol. 13, no. 3, pp. 266–276, Jun. 2011.

[20] P. Ju and W. Song, "Repeated game analysis for cooperative mac with incentive design for wireless networks," *IEEE Trans. Veh. Technol.*, vol. 65, no. 7, pp. 5045–5059, Jul. 2016.

[21] S. Sergi and G. M. Vitetta, "A game theoretical approach to distributed relay selection in randomized cooperation," *IEEE Trans. Wireless Commun.*, vol. 9, no. 8, pp. 2611–2621, Aug 2010.

[22] Z. Ding and H. Poor, "Cooperative energy harvesting networks with spatially random users," *IEEE Signal Process. Lett.*, vol. 20, no. 12, pp. 1211–1214, Dec. 2013.

[23] B. Varan and A. Yener, "Incentivizing signal and energy cooperation in wireless networks," *IEEE J. Sel. Areas Commun.*, vol. PP, no. 99, pp. 1–1, Dec. 2015.

[24] Y. Xiao, Z. Han, and L. Dasilva, "Opportunistic relay selection for cooperative energy harvesting communication networks," in *IEEE Global Telecommun. Conf. (GLOBECOM)*, Dec. 2014, pp. 4371–4376.

[25] S. Maghsudi and E. Hossain, "Distributed user association in energy harvesting small cell networks: A competitive market model with uncertainty," *CoRR*, vol. abs/1511.01976, 2015. [Online]. Available: http://arxiv.org/abs/1511.01976

[26] M. Kashef and A. Ephremides, "Optimal partial relaying for energy-harvesting wireless networks," *IEEE/ACM Trans. Netw.*, vol. 24, no. 1, pp. 113–122, Feb. 2016.

[27] L. Ferdouse and A. Anpalagan, "Relay selection based on bayesian decision theory in cooperative wireless networks," *Electrical and Computer Engineering, Canadian Journal of*, vol. 38, no. 2, pp. 116–124, 2015.

[28] Z. Han, *Game Theory in Wireless and Communication Networks: Theory, Models, and Applications*. Cambridge University Press, 2012. [Online]. Available: https://books.google.co.uk/books?id=oSnz5ngb9YkC

[29] M. Schluter, M. Gerdts, and J. J. Ruckmann, "MIDACO: New global optimization software for MINLP," 2011, Online: http://www.midaco-solver.com.

Chapter 5

A Cooperative Clustering Protocol With Duty Cycling for Energy Harvesting Enabled Wireless Sensor Networks

A Cooperative Clustering Protocol With Duty Cycling for Energy Harvesting Enabled Wireless Sensor Networks

Mohammed S. Bahbahani and Emad Alsusa

Abstract

This paper proposes a cooperative clustering protocol based on the low energy adaptive clustering hierarchy (LEACH) approach to enhance the longevity of energy harvesting based wireless sensor networks (EH-WSN). In the proposed protocol, to ensure that any energy consumption associated with the role of the cluster head (CH) is shared between the nodes, the CH role is alternated between the nodes using duty cycling as a function of their individual energy harvesting capabilities. Furthermore, to maintain an energy neutral operation when not acting as a CH, the nodes adopt a data transmission duty cycle and any excess energy is invested in relaying other nodes' packets. To optimize the relaying performance, a novel cross-layer cooperative TDMA scheme is also presented. The optimal number of clusters in an EH-WSN is analyzed in terms of energy consumption, latency and bandwidth utilization. Simulations, performed using GreenCastalia, demonstrate tangible performance enhancements in adopting the proposed protocol over benchmark schemes in terms of throughput and lifetime, particularly under highly constrained energy conditions.

Index Terms

Energy Harvesting, LEACH, Duty Cycle, Routing Protocol, Omnet++, Castalia, Cooperative Networks, IoT.

I. Introduction

Wireless Sensor Networks (WSNs) are expected to mesh a massive number of objects into what is called the $Internet\ of\ Things$ (IoT) [1]. One of the main challenges associated with a wide deployment of WSNs is energy consumption as it is impractical to regularly replace the batteries of thousands of tiny network nodes. Therefore, extending the network lifetime is a major objective in WSN protocols [2]. Many energy conservation techniques including multi-hop, cooperative transmission and duty-cycling were proposed in the literature. Specifically, multi-hop and data aggregation, implemented through clustering, can provide energy savings at the network layer [3], whereas a periodic wake-up and sleep strategy at the MAC layer can extend the network lifetime for a certain QoS requirement as shown in [4]. Cooperative transmission at the physical layer

utilizes the energy wasted in broadcast transmission by creating multiple independent paths between a source and a destination node to improve the channel capacity [5]. Despite the improvements offered by these schemes, nodes eventually die after their energies have been exhausted.

Recently, it was shown that WSN with energy harvesting (EH) capabilities, whereby nodes can harvest energy from the environment, such as solar and wind power, can sustain a perpetual lifetime [6]. Due to the random nature of such energy sources, current protocols designed for battery powered networks must be adapted to EH scenarios [7]. In response, EH clustering protocols were proposed in [8], [9], [10], [11], [12] that extend the LEACH protocol [13], in which cluster heads (CH) aggregate and then forward data packets of their cluster members to the sink node. Unlike LEACH, which evenly distributes the CH role among the nodes, the aforementioned schemes elect CHs based on their residual energies and forecasted harvesting rates. For instance, in [9], a CH decision threshold termed the energy potential (EP) function is computed for each node in terms of its energy harvesting rate and current available energy as well as the potential functions of neighboring nodes. In [12], the optimal percentage of CHs is incorporated into a new CH threshold function that gets updated by the sink throughout the operation of the protocol. Specifically, a search algorithm is used by the sink to compare the current round's average throughput against that in the last round then a regulation factor is updated accordingly. The above solutions do not guarantee a perpetual operation and require the exchange of information among nodes, which creates additional overheads. The protocol in [11] proposes cluster head groups (CHG), in which nodes take turns in becoming the CH to minimize the overheads of the CH selection process. In [8], Yang $et. al.$ analyzed an optimal multi-hop clustering architecture to achieve a perpetual operation in EH-WSNs. Particularly, energy neutrality constraints were defined and used to obtain the minimum network data transmission cycle using convex optimization. Lastly, an EH aware routing protocol based on the gradient model is proposed in [14] for WSNs. Also, a CH selection scheme based on the residual energy of nodes and their relative positions is suggested. Then, a packet forwarding mechanism is presented, that balances the energy consumption among the EH nodes.

Duty cycle based MAC protocols for EH networks were shown to maintain an $Energy\ Neutral\ Operation$ (ENO), in which the consumed energy does not exceed the harvested energy over a given period [15]. An optimal duty cycle design is formulated in [16] as an optimization problem then solved using a low-complexity sub-optimal algorithm. An extensive analysis of different duty cycling strategies based on the battery state, harvesting rate, queue size and channel conditions was given by Niyato, $et\ al.$ in [15]. Specifically, upper and lower thresholds were defined to determine the transitions between sleep and wake-up cycles.

On the other hand, cooperative communication has been considered as a means to achieve spatial diversity gains in WSN, where installing multiple antennas on tiny nodes is infeasible. To this end, a number of researchers have investigated the problems of resource allocation and relay selection for battery powered networks [17] and EH networks [18] at the physical layer. Cooperation at the MAC layer was also shown to provide higher transmission rates and lower delays particularly in fading channels [19]. A contention based cooperative MAC protocol called CoopMAC [20] brings throughput enhancements and reduced delays in fading channels while remains compatible with the IEEE 802.11 standard. Because relaying consumes additional energy, the protocol in [21] maximizes the network lifetime by assigning scores to nodes to evaluate their availability for relaying. Another protocol in [22] incorporates two relays per source node such that the total transmission time when using both relays is less than that of the direct link. Also, a cross layer protocol that leverages cooperation at the MAC and PHY layers is presented in [23]. Specifically, a source node broadcasts its coded data bits in the first half of a time-slot, which is overheard by a potential relay node. Scheduling based cooperative MAC protocols based on $time\ division\ multiple\ access$ (TDMA) were also investigated in the literature. In [24], the nodes listen in timeslots, not allocated to themselves, to the transmission of the active node and the non-acknowledgement (NACK) of the destination. Only, if a NACK is received and the active node's packet was decoded correctly, the relay node will retransmit the packet in the next allocated time slot of the following TDMA frame. A different technique is proposed in [25], where mini-slots are used to reserve cooperative resources to avoid conflicts between sources, relays and destinations. Also, cooperation enabled clustering protocols were proposed in [26], [27] and [28]. The protocol in [26] introduces cooperative cluster heads (CCH) that are selected to maximize the spatial diversity. Non-cluster members may become CCHs to participate in relaying the CH packet to the sink using a space time block code (STBC) technique. In [28], the lifetime of a battery power WSN is extended using an optimized clustering algorithm that determines the optimal locations of CH nodes. EH nodes can then be used to relay the NCH packets to the CHs.

In this paper[1], clustering, duty cycling and cooperative transmission are combined into a novel cross-layer design for EH-WSNs. The new protocol named $Energy\text{-}Harvesting$ and $Cooperative\ LEACH$ (ECO-LEACH), modifies the LEACH technique by replacing its probabilistic CH selection process with a duty cycle based one to efficiently regulate the frequency at which a node undertakes the CH role. Besides the inherent duty cycling used by the TDMA scheduler in LEACH, another duty cycle is adopted here, by which the cluster members can skip certain allocated timeslots to maintain an ENO state.

[1]A conference version of this paper is published in the International Wireless Communication and Mobile Computing Conference (IWCMC 2017). [29].

Moreover, each node follows another duty cycle to select the TDMA frames in which it is available to act as a relay. To complete the protocol, a novel cooperative TDMA scheme is proposed whereby a time-slot is split into two sub-slots. All potential relays listen to the active node's transmission in the first sub-slot then the best relay transmits the received packet to the destination in the second sub-slot. The selection of the above duty cycles accounts for the node's energy harvesting rate, packet arrival rate and the optimal percentage of CHs in the network. Hence, a rigorous analysis of the optimal CH percentage (OCHP) is given, which unlike in the case of LEACH, may not necessarily minimize the network energy consumption. Instead, the optimal percentage is the one that minimizes the latency while simultaneously achieves the ENO state and bandwidth requirements. Simulations of the proposed protocol, assuming a solar energy source with random shadows, were performed using $GreenCastalia$ [30], an extension of $Castalia$ [31] and $OMNET$++ [32] simulators. The results obtained show significant improvements in throughput, latency and network lifetime compared with the conventional LEACH as well as a generic energy-aware LEACH protocol. Remarkably, these gains can be realized for both EH and battery powered networks. The contributions of this work can be listed as follows:

- Formulated the optimal CH percentage problem for EH clustering based networks that guarantees ENO, while satisfying the bandwidth and latency requirements. The problem is then solved using an iterative method for which complexity is bounded by the number of nodes in the network.
- Proposed a distributed CH selection scheme, using the OCHP, based on duty cycling that adapts to the energy harvesting rates. This deterministic CH selection in ECO-LEACH is compatible with rapidly changing energy sources such that the required CH percentage can be maintained over a few number of rounds. In contrast, LEACH requires a number of rounds equal to the number of nodes before the required CH percentage is maintained. Another feature of the proposed CH selection is the absence of harvesting rate information exchanged between the nodes as in [9]. Instead, only the average nodes' harvesting rates are required. Moreover, the proposed protocol is applicable in non-homogeneous networks, in which nodes have different capabilities and QoS requirements.
- Proposed a data transmission duty cycle to ensure ENO when the OCHP problem has no feasible solution.
- Proposed a novel TDMA-based cooperative mechanism based on sub-slots along with a relaying duty cycle design that utilizes the energy unconsumed in data transmission. The sub-slot based relaying scheme has a lower latency compared to [25], as the relayed transmission starts immediately after the direct one.

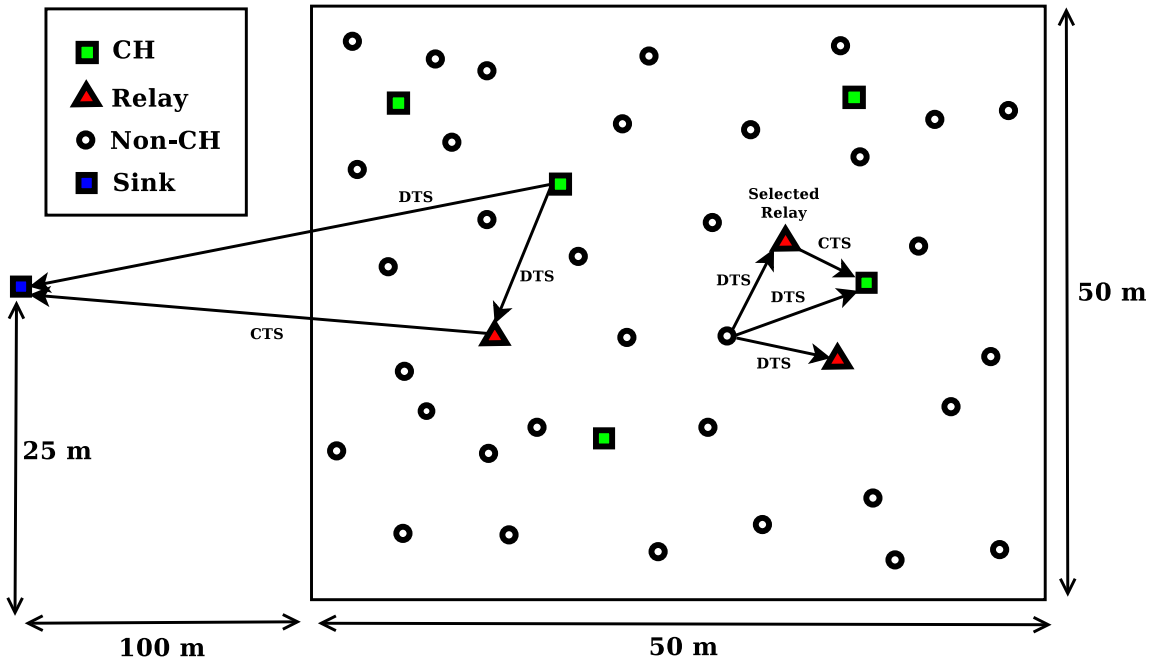

Fig. 1. Network Model

In summary, the proposed protocol first determines the OCHP (assuming nodes transmit in every allocated timeslot) since it is the most energy consuming role. If no feasible solution is found the data transmission phase of LEACH is regulated through duty cycling to maintain the ENO constraint. Any remaining energy is then invested in cooperative relaying by following another ENO duty cycle. This algorithm is thus unique and to our best knowledge has not been discussed in the literature.

The remaining sections of the paper will be organized as follows. The network and energy models are defined in Section II. Section III explains the operation of the conventional LEACH protocol. The proposed ECO-LEACH is then explained in Section IV. Numerical evaluations of the proposed protocol and benchmark schemes are analyzed in Section V. Finally, concluding remarks and possible future work are stated in Section VI. Throughout the paper, the functions $ceil(x)$ and $floor(x)$ will be used to round the value x to the smallest following and largest previous integer value respectively, whereas the $[x]_0^1$ limits the value of x between 0 and 1.

II. System Model and Assumptions

A. Network Model

The network topology, as shown in Fig. 1, consists of $N = 100$ stationary nodes randomly positioned in a square of dimension $M = 50m$ and a sink node placed 125 meters away from the center of the square. These positions guarantee that all

nodes can reach the sink when transmitting at the maximum power level P_{tx}^{max}. A log-normal shadowing radio model is assumed with its temporal variation obtained from real measurements available within the $Castalia$ simulator. It is also assumed that the sink node transmits a short beacon at the beginning of the network operation so that each node can estimate its path loss to the sink and select the minimum required power level to reach the sink node, that is, P_{tx}^{sink}. Although node mobility is not considered in this work, the channel temporal variation created by the movement of surrounding objects is considered. The channel is assumed to be reciprocal, and its instantaneous gain can be estimated from the $received\ signal\ strength\ indicator$ ($RSSI$) value in the received packet. It is noteworthy that $RSSI$ estimation has to be longer than the channel coherence time in order to estimate the pathloss. Also, note that the pathloss estimation may need to be recalculated at defined periods of several seconds to minutes as the nodes are assumed to be stationary.

B. Energy Model

In this work, a solar energy source is assumed, which has an intensity I_o that varies throughout the day but remains nearly constant within periods shorter than 30 minutes [16]. In addition, the average solar intensity $\bar{I}_o$ over a given time horizon in the future may be forecasted using the exponentially weighted moving average prediction model ($EMWA$) in [33]. Despite being exposed to the same intensity at any given time, each node z has a different harvesting efficiency $\varepsilon_z \in [0, 1]$. To create a more realistic scenario, it is assumed that shadows created by objects, such as clouds, may reduce the solar intensity by an opacity factor ϕ_z uniformly distributed between 0 and 1 [15]. The arrivals of shadows are modeled as a Poisson process with an inter-arrival rate $\mathcal{T}$ being constant for all nodes. This rapid fluctuation in the harvesting rate caused by the shadows is important to demonstrate the effectiveness of the proposed protocol in maintaining the required CH percentage over shorter periods compared to LEACH. Therefore, the overall harvesting power of a node z becomes $\eta_z = \phi_z \varsigma_z \varepsilon_z I_o$, where ς_z is the solar cell area of node z. Thus, over a long period, the mean harvesting power of node z becomes $\bar{\eta}_z = 0.5\varsigma_z \varepsilon_z \bar{I}_o$. Finally, the average mean harvesting power of all nodes in the network denoted by $\bar{\eta} = 0.5\bar{\varsigma_z}\bar{\varepsilon_z}\bar{I}_o$ is assumed to be common knowledge among all nodes in the network with $\bar{\varsigma_z}$ and $\bar{\varepsilon_z}$ being the nodes average solar cell size and harvesting efficiency respectively.

III. The LEACH Protocol

The operation of LEACH, described in details in [13], consists of multiple rounds. Each round begins with a short setup phase followed by a long data transmission phase.

During the setup phase of a round t, each node declares itself as a CH with a probability that maintains the CH percentage at π after $\frac{1}{\pi}$ rounds have passed. Once a node becomes a CH, it will never become a CH again until all other nodes have taken their turns. CHs then invite non-CH nodes to join their clusters by broadcasting $invitation$ beacons. A non-CH (NCH) node joins a cluster based on the $RSSI$ of the received beacon and selects its transmit power P_{tx}^{CH} such that the received power at the CH is just above the sensitivity of the receiver. Upon receiving join requests, a CH creates then broadcasts a TDMA schedule to its cluster members.

The data transmission phase (steady state) of a round consists of multiple TDMA frames. In each time slot of a TDMA frame, a single node ($active\ node$) sends its data packet to the CH at a time, while other nodes switch to sleep mode. In the last timeslot of a frame, the CH aggregates then transmits the received packets to the sink node at power P_{tx}^{sink}. This process repeats until the round is over. To eliminate possible collisions between clusters, each cluster randomly selects a unique channel (frequency/code) from a pool of available channel resources.

Despite the performance gains over direct transmission, the uniform distribution of CHs does not consider the residual energy of each node. Hence, nodes that become CHs first will deplete their energies soon reducing network connectivity that in turn causes higher transmit power by the remaining nodes ultimately reducing the network lifetime.

IV. Proposed Protocol Description

The proposed ECO-LEACH protocol extends LEACH by replacing its CH selection process while introducing duty cycling (illustrated in Fig. 4) and cooperative transmission. Each of these features is separately discussed as follows.

A. Cooperative Transmission Protocol

In the proposed cooperative scheme, a time-slot of duration T_s is evenly split into a direct transmission sub-slot (DTS) followed by a cooperative transmission sub-slot (CTS) as illustrated in Figures 2 and 3 below. During a DTS, the active node transmits its data packet to the CH and cooperating nodes. The CH responds with an $acknowledgement$ (ACK) beacon if the packet was successfully received (Fig 2). Otherwise, a $non-acknowledgement$ beacon (NACK) is sent, as shown in Fig 3. The reception of a NACK at potential relay nodes initiates a contention process, whereby a relay node replies with a $relay\ advertisement\ beacon$ (RAB) after a delay inversely proportional to the RSSI of the received NACK. All potential relays that receive the RAB beacon, while waiting to send their RAB beacons, will back off and remain silent in the CTS sub-slot. Because some relays may be hidden from others, a $relay\ acknowledgement\ beacon$ (RACK)

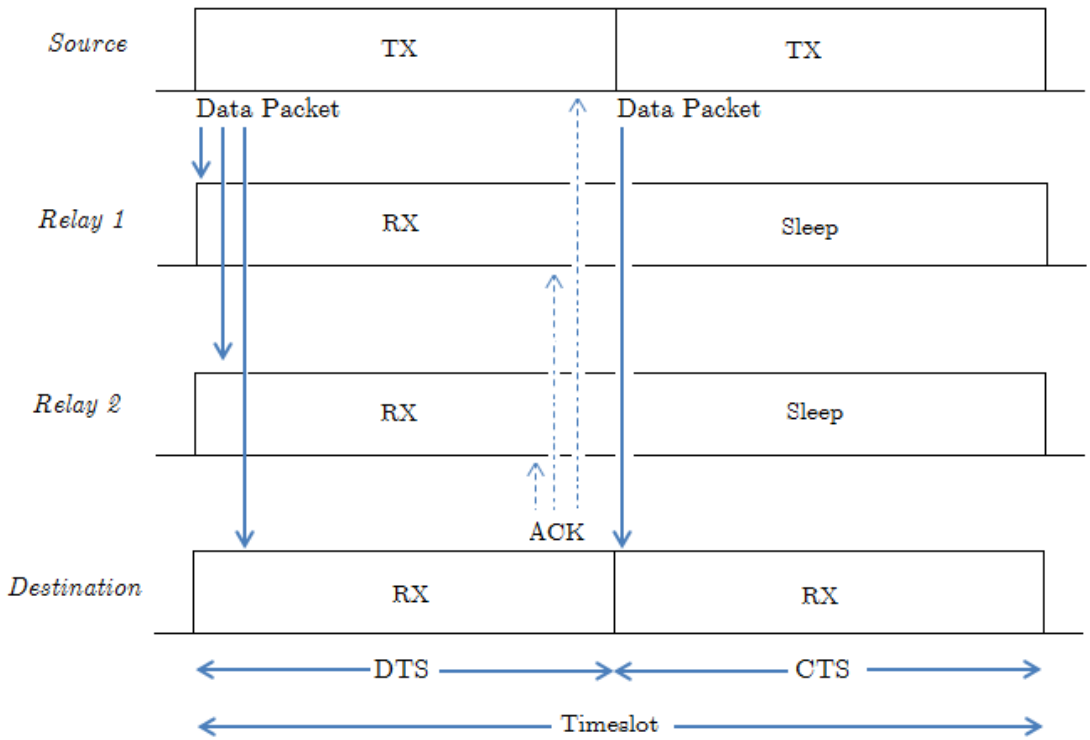

Fig. 2. Proposed Cooperative TDMA Scheme - Case 1

is broadcasted by the destination upon receiving the first RAB so that relays will only transmit upon receiving a RACK destined to themselves [34]. The selected relay then transmits the relayed packet in the CTS sub-slot of the current time-slot. In case an ACK beacon is transmitted by the destination in the DTS, all potential relays will sleep during the CTS sub-slot. To fully utilize the allocated time-slot, the active node may transmit another data packet in the CTS as the second packet is likely to be successful without cooperation due to the correlated channels of consecutive sub-slots (Fig. 2). Clearly, the above scheme implements a decode-and-forward incremental relaying protocol [35] with the opportunistic single relay selection in [34]. It is noteworthy to mention that different cooperative schemes such as space time block code (STBC) can be implemented without affecting the above strategy. However, stringent time synchronization among relays is necessary, which is generally complex to implement.

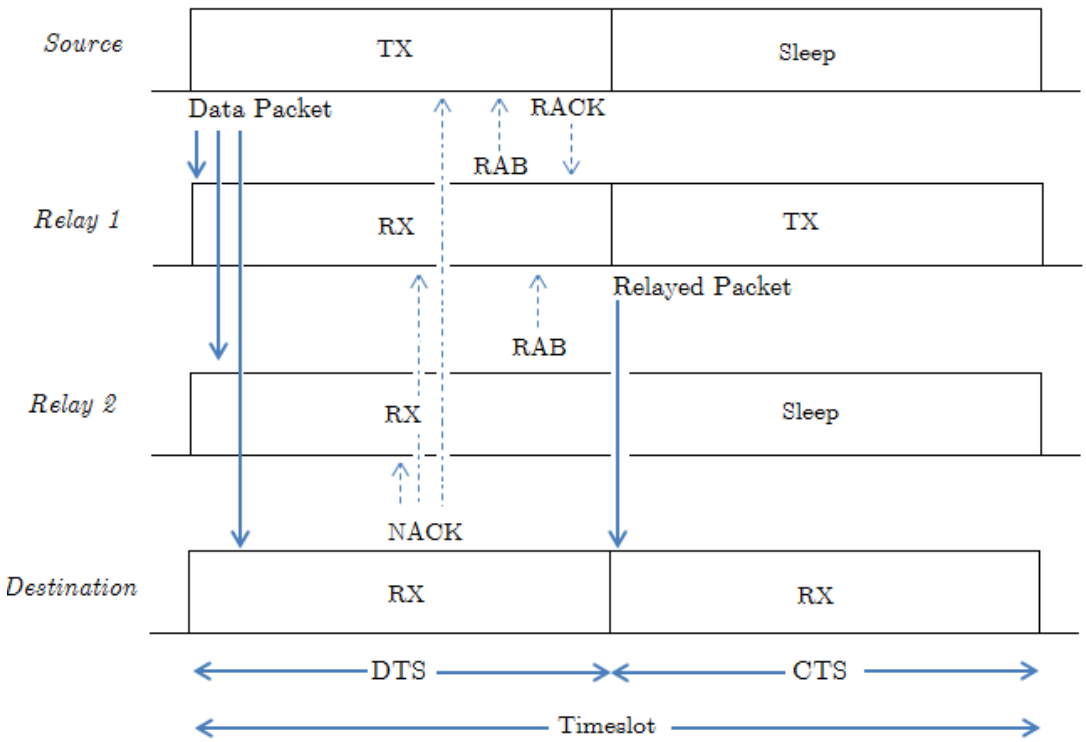

Fig. 3. Proposed Cooperative TDMA Scheme - Case 2

$$D_{CH} = \begin{cases} ceil(\frac{E^r_{CH} L_{hor}}{\bar{\eta}_z T_r L_{hor} \alpha_{CH}}) & \frac{E^r_{CH} L_{hor}}{\bar{\eta}_z T_r L_{hor} \alpha_{CH}} \geq 1 \\ 1 & \frac{E^r_{CH} L_{hor}}{\bar{\eta}_z T_r L_{hor} \alpha_{CH}} < 1 \end{cases} \tag{1}$$

$$E^r_{net}(k) = k(E^r_{CH}(k) + E^r_{NCH}(k)) =$$

$$\frac{L_r}{N}(k^2 P^{sink}_{tx} T_s + (kN - k^2)(P_{rx} T_s + E_{agg}) + (N-k) T_s \frac{M^2}{2\pi}) \tag{2}$$

B. Cluster Head Duty Cycle Design

Unlike the random CH selection in LEACH, in this work, a node follows a CH duty cycle (D_{CH}) that determines how often it will become a CH in a given time horizon L_{hor} defined as the number of rounds over which the average harvested energy can be predicted. For instance, if $D_{CH} = 3$ the node becomes a CH only once every 3 rounds in L_{hor} as shown in Fig. 4. The CH duty cycle is calculated at the beginning of each

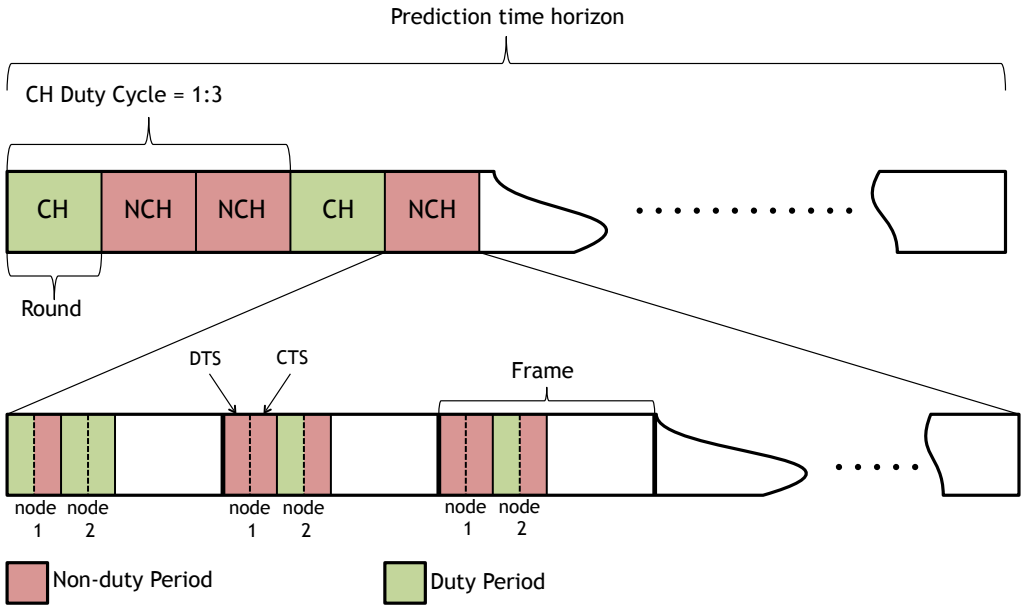

Fig. 4. Duty Cycle Structure

L_{hor} rounds as shown in (1) above. In this function, $T_r = L_r T_s$ is the round duration, L_r is the number of timeslots in a single round and $\alpha_{CH} \in (0, 1]$ is the proportion of the harvested energy allocated to the CH role. Also, E^r_{CH} is the average energy consumed by a CH node in a single round. When the allocated CH energy per round is greater than E^r_{CH}, D_{CH} takes its minimum value of 1. Otherwise, D_{CH} will be the ratio of the required energy to the allocated energy rounded to the next integer value. At the start of each round, the node determines if its duty round has come using a CH-DC counter that counts up to D_{CH} and then resets to 1. To maintain the targeted percentage of CHs, each node starts its CH-DC counter with a random integer value between 1 and D_{CH} such that 1 indicates the duty round. If a node enters the duty round with insufficient energy, the duty round is temporarily shifted to the next round and so on. Therefore, a node's likelihood to become a CH in a given round is the inverse of its D_{CH}. Hence, to maintain the targeted percentage of CHs $\pi = \frac{k}{N}$, where k denotes the number of CHs, the factor α_{CH}, given in (3) below, is used to limit the CH-DCs of nodes when their mean harvesting rate $\bar{\eta}$ is too high causing them to afford to turn into CHs more often than required.

$$\alpha_{CH} = \left[\frac{E^r_{CH}\pi}{\bar{\eta} T_r} \right]^1_0 . \tag{3}$$

C. Optimal Cluster Head Percentage

The number of cluster heads has different effects on the network throughput, latency, bandwidth utilization and lifetime. First, the throughput and latency affect the number of cluster heads as follows. Given the packet arrival rate ρ (packets/second) and the maximum latency tolerated by the application layer Δ^{max} (seconds), the maximum possible frame duration would be $T_f^{max} = \min(\frac{1}{\rho}, \Delta^{max})$ leading to a minimum number of $k^{min} = ceil(NT_s/T_f^{max})$ CHs. On the other hand, the number of available orthogonal channels defines the maximum number of clusters, k^{max}, above which collisions will occur. Thus, the optimal number of CHs, k^{opt}, lies in the interval [k^{min},k^{max}] and maintains an average network energy consumption $E^r_{net}(k^{opt})$ below the total energy harvested by all nodes in the network E^r_{har} during a single round. To find $E^r_{net}(k)$, we first calculate the average energy spent by a CH during a given round as a function of k as:

$$E^r_{CH}(k) = N_f(E^{sink}_{tx} + (L_c - 1)E_{rx} + E_{agg}) + E_{setup}, \tag{4}$$

where $L_c = \frac{N}{k}$ is the average cluster size, $N_f = \frac{L_r k}{N}$ is the average number of TDMA frames in a given round, whereas E_{agg} and E_{setup} are the energies consumed in data aggregation and cluster setup respectively. Similarly, the energy needed by all NCH nodes per round in terms of k becomes [36]:

$$E^r_{NCH}(k) = N_f(L_c - 1)T_s\bar{P}^{CH}_{tx}, \tag{5}$$

where the term $\bar{P}^{CH}_{tx} = \frac{M^2}{2\pi k}$ approximates the average squared distance (path loss) to the CH assuming uniformly distributed nodes. Also, it is assumed that each NCH utilizes all its allocated data transmission slots. Thus, the network energy consumption is given in (2) shown above. With more clusters (smaller average cluster size) the node-to-node distance is reduced causing less energy spent by the NCH nodes in conveying their data packets to their CHs. However, data aggregation is reduced and more energy consuming CHs are introduced. Therefore, the OCHP is unique to the network topology and parameters, which can be formulated as:

$$k^{opt} = \max k \tag{6}$$

s.t.

$$E^r_{net}(k) \leq E^r_{har} = L_r\, T_s \sum_{z=1}^{N} \eta_z \tag{7}$$

$$k \leq k^{max}, k \geq k^{min} \tag{8}$$

$$k \in \{1, \ldots, N\} \tag{9}$$

The optimization problem above gives the highest k (maximum spectral efficiency) that maintains the ENO (constraint (7)) for any value of k in the range defined by constraints (8) and (9)[2]. Unlike the OCHP analysis in [36], the proposed optimal solution may not necessarily minimize the network energy consumption, as some values of $k \neq k^{opt}$ may result in a lower energy consumption. However, these values may degrade the system performance, since by having more clusters than orthogonal channels, backoffs induced by CSMA at the MAC layer may result in longer delays and more collisions. Conversely, choosing a value of k below k^{min} leads to more dropped packets due to buffer overflow and timeouts.

The solution to the non-linear integer programming problem formulated above can be centrally obtained by evaluating $E^r_{net}(k)$ starting from k^{max} until a value that satisfies the constraint in (7) is found. Thus, the solution has a linear complexity in the number of nodes. However, a feasible solution may not exist if $E^r_{net}(k) > E^r_{har}$ $\forall k \in \{k^{min}, k^{min}+1, \ldots, k^{max}-1, k^{max}\}$, in which case reducing the data transmission duty cycle is necessary as will be discussed next.

Due to the absence of a central station in many WSN scenarios, the OCHP can be obtained in a distributed fashion, where each node independently determines k^{opt} assuming the knowledge of the network parameters and the mean average energy harvesting $\bar{\eta}$ instead of $\sum_{z=1}^{N} \eta_z$ in (7). Each node then substitutes k^{opt}/N in (3) to find its CH-DC. Henceforth, the OCHP will refer to the distributed OCHP. As the harvesting rate changes with time, the OCHP is dynamically updated at the beginning of each L_{hor} period as will be demonstrated in Section V.

[2]It is assumed that the network parameters are set such that $k^{min} \leq k^{max}$ and k^{min},$k^{max} \in \{1, \ldots, N\}$.

D. Data Transmission Duty Cycle Design

A periodic wake-up/sleep strategy is inherently implemented in TDMA, as nodes sleep in non-allocated timeslots. In LEACH, this will cause each cluster member to undergo an average duty cycle of 1:L_c. However, if the predicted harvested energy is still insufficient to maintain an ENO, the duty cycle should be further reduced by skipping the allocated slot in certain TDMA frames. In addition, the duty cycle should also adapt to the packet arrival rate ρ since switching to transmit mode with no data packet to send results in an unnecessary energy waste. Hence, a data transmission duty cycle D_{DT}, based on the harvesting power and the packet arrival rate, is proposed that defines the number of TDMA frames to skip after each data transmission. For example, in Fig. 4, node 1 utilizes its allocated slot only once every 3 TDMA frames, hence its D_{DT} is 3, whereas node 2 with $D_{DT} = 1$ uses its timeslot in every frame. A node z computes its D_{DT} at the beginning of every round by first finding the expected remaining harvested energy per NCH round given as:

$$E_{NCH}^{rem} = (\bar{\eta}_z T_s L_r L_{hor} - E_{CH}^{r}(L_{hor} - L_{NCH}))/L_{NCH} \tag{10}$$

where $L_{NCH} = L_{hor} - \frac{L_{hor}}{D_{CH}}$ is the number of NCH rounds in L_{hor}. The node then computes a duty cycle with respect to the harvesting rate and another for the data arrival rate as:

$$D_{DT}^{ene} = \begin{cases} ceil(\frac{E_{tx}^{CH} N_f}{E_{NCH}^{rem}}) & 1 \leq (\frac{E_{tx}^{CH} N_f}{E_{NCH}^{rem}}) \leq N_f \\ 1 & (\frac{E_{tx}^{CH} N_f}{E_{NCH}^{rem}}) < 1 \end{cases}, \tag{11}$$

$$D_{DT}^{data} = \begin{cases} floor(\frac{N_f}{\rho T_r}) & 1 \leq (\frac{N_f}{\rho T_r}) \leq N_f \\ 1 & (\frac{N_f}{\rho T_r}) < 1 \end{cases}, \tag{12}$$

where $E_{tx}^{CH} = P_{tx}^{CH} T_s$ is the energy consumed in transmitting a packet to the CH. Hence, D_{DT} is found as:

$$D_{DT} = \begin{cases} 0 & \max(D_{DT}^{ene}, D_{DT}^{data}) > N_f \\ \max(D_{DT}^{ene}, D_{DT}^{data}) & 1 \leq \max(D_{DT}^{ene}, D_{DT}^{data}) \leq N_f \end{cases} \tag{13}$$

Similar to the CH-DC design, when the average energy available in an NCH round is greater than that consumed when the node transmits in every frame in the round and that the number of generated packets is greater than N_f, then D_{DT} is set to 1. Conversely, if the energy available for data transmission is less than that needed for a single data transmission or the number of generated packets is less than 1, the node will not join any CH and will remain silent in the whole round, that is, $D_{DT} = 0$. For

any intermediate values, the node will be active once every D_{DT} frames. Again, a DC counter is employed to keep track of the duty cycle as in CH-DC.

E. Relaying Duty Cycle Design

In certain TDMA frames, a node may act as a potential relay according to the cooperative strategy explained in Section IV-A. Particularly, the node may relay packets of other cluster members to the CH during their allocated time-slots at power P_{tx}^{CH} and may also relay the aggregated packet of the CH to the sink at power P_{tx}^{sink}. Hence, we define the relaying duty cycle D_{RL} as the number of frames in which the node becomes a potential relay only once. According to the example in Fig. 4, node 1 never acts as a relay and hence its relaying DC is zero, whereas the D_{RL} of node 2 is 3. The relaying duty cycle is computed at the beginning of each round, after calculating D_{DT}, by first finding the remaining energy from E_{NCH}^{rem}, after subtracting the energy reserved for data transmission, as:

$$E_{NCH-R}^{rem} = E_{NCH}^{rem} - \frac{N_f}{D_{DT}} E_{tx}^{CH} \tag{14}$$

Thus, the relay transmission duty cycle can be given as:

$$D_{RT} = \begin{cases} 0 & \frac{E_{RL}^{f} N_f}{E_{NCH-R}^{rem}} > N_f \\ ceil(\frac{E_{RL}^{f} N_f}{E_{NCH-R}^{rem}}) & 1 \leq \frac{E_{RL}^{f} N_f}{E_{NCH-R}^{rem}} \leq N_f \\ 1 & \frac{E_{RL}^{f} N_f}{E_{NCH-R}^{rem}} < 1 \end{cases}, \tag{15}$$

where $E_{RL}^{f} = P_{rx}(L_c - 1)\frac{T_s}{2} + P_{tx}^{CH}(L_c - 2)\frac{T_s}{2} + P_{tx}^{Sink}\frac{T_s}{2}$ is the energy needed by a node to act as a relay during a single frame. Similar to the above DCs, a relaying DC counter is employed.

V. Simulations

The proposed protocol was simulated using $Castalia$, an extension of OMNET++. The default log-normal shadowing radio model of $Castalia$ was used with a path loss exponent of 2.0. In addition, the temporal channel model of $Castalia$, based on real channel measurements, was adopted to demonstrate the spatial diversity gains of cooperative transmission. The transceiver $CC1000$ was assumed at the physical layer, which allows for transmit power levels ranging from -20 dB to 10 dB consuming 15.9 to 80.1 mW respectively. The sensitivity of the chip is -95 dBm, while the receive power consumption is 22.2 dBm. In sleep mode, the chip consumes only 0.6 μW and transitions between states take up 0.2 ms consuming power up to 0.5 μW. At the MAC layer, the conventional CSMA protocol with an exponential back off was adopted, which was

necessary to avoid collisions during cluster setup [13]. The parameters of ECO-LEACH and the topology settings, specified in Table I, were used in all simulations unless stated otherwise. The energy harvesting model was implemented using $GreenCastalia$ [30], an extension to $Castalia$ that simulates energy sources, storage, harvesters and managers. Each node has a single ideal rechargeable battery with a capacity of 3 mAh[3]initially charged with 5% of its full capacity, whereas the sink node was assumed to be non-energy constrained. A single solar energy source was used with an intensity defined per simulated scenario. In addition, the mean arrival rate of shadows $\mathcal{T}$ was set to 1 second. Further, the solar cell efficiency of each node was randomly selected with a mean of 0.22. The proposed algorithms including the proposed protocol and other benchmark schemes are briefly described as follows:

- Conventional LEACH (C-LEACH):

This simulated version of LEACH follows the protocol described in Section III with a few modifications. First, in each time-slot, only a single data packet may be transmitted occupying the whole duration of the time-slot [15], as this approach is used to simplify the simulation of the proposed cooperative protocol below. Also, a node can only declare itself a CH if an amount of E^r_{CH} is available in its battery. In addition, the node can only transmit a packet if a minimum of $P^{CH}_{tx}T_s$ of energy is available.

- Energy-Aware LEACH (EA-LEACH):

Instead of comparing the proposed solution to specific EH protocols in the literature, a generic energy-aware LEACH termed EA-LEACH was simulated. This is due to the protocols in the literature having different energy models and assumptions. Moreover, these reference protocols were evaluated in MATLAB, which is less accurate in simulating upper layer protocols. In this generic protocol, the CH selection incorporates the energy harvesting status of all nodes in the network such that nodes with more relative harvesting rates becomes CHs more often with no restriction on the number of times a node can become a CH. Hence, a node z becomes a CH based on the following probability function:

$$\mathcal{P}_z(t) = \frac{N\pi(E^{bat}_z + E^{har}_z)}{\sum_{i=1}^{N} E^{bat}_i + E^{har}_i}, \tag{16}$$

where E^{bat}_i and E^{har}_i are the residual energy and harvesting rate of node i.

- Proposed Protocol Without Cooperation (ENCO-LEACH):

The proposed protocol described in Section IV is simulated without the cooperation feature in ENCO-LEACH. Hence, this protocol only benefits from the proposed CH

[3]The small capacity used is due to the relatively short simulation time (5000 sec) compared with the real deployment.

Table I
SIMULATION PARAMETERS

N	100	Number of Nodes
T_s	100 ms	Time slot Duration
L_r	500 timeslots	Round Length
L_{hor}	10 rounds	Prediction Time Horizon
E_{agg}	5 nJ/bit	Aggregation Energy
ς_z	1.54 cm^2	Solar Cell Size
ρ	0.5 packet/s	Data Packet rate
T_{sim}	5000 s	Simulation time
$\Delta_{\max}$	5 s	Max. Delay
θ	20	Number of Orthogonal Channels
	2000 bit	Data Payload

selection and data transmission duty cycles as well as the OCHP derived in Section IV-C.

- Proposed Protocol With Cooperation (ECO-LEACH):

Here, the full proposed protocol including cooperative diversity is simulated. Since data packets are sent with half the number of bits during a sub-slot, twice the number of packets are generated with respect to the ENCO-LEACH protocol to ensure a fair comparison.

Different scenarios averaged over 1000 iterations were created to evaluate the performance of the above protocols based on the throughput, latency and lifetime as shown below. In this context, the average network throughput is defined as the number of packets successfully delivered to the sink, within the maximum delay period, divided by the total number of packets generated by all nodes over the simulation period $((N-1)T_{sim})$. For example, if the packet arrival rate is 1 packet/second, a throughput of 40% means that 2000 packets were ultimately delivered to the sink by each node on average. Since the energy consumption is always maintained below the harvested energy in an ENO, maximizing the throughput also maximizes the energy efficiency. As for the lifetime, it is defined as the time until the first node in the network depletes its battery.

The first objective was to verify the OCHP solution proposed in Section IV-C. As depicted in Fig. 5, the OCHP follows the harvesting power (and solar intensity) within the feasible range defined by the maximum number of orthogonal channels (10 and 20 channels) and the packet arrival rate of 0.5 packet/sec[4]. The simulated number of CHs selected in the proposed protocol is shown to closely follow the OCHP for all intensities. The small error seen is due to some nodes being unable to become CHs, after being selected, due to insufficient residual energies. Specifically, in the period 0 to 1000s, the

[4]A low packet arrival rate is common in many surveillance and environmental monitoring WSN applications [37].

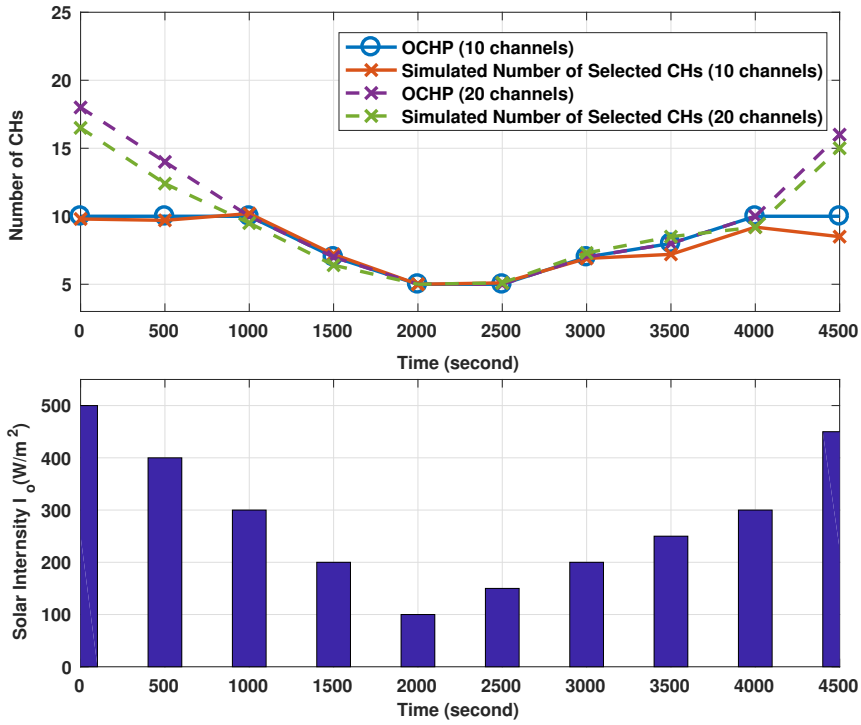

Fig. 5. Optimal CH Percentage for Different Solar Intensities

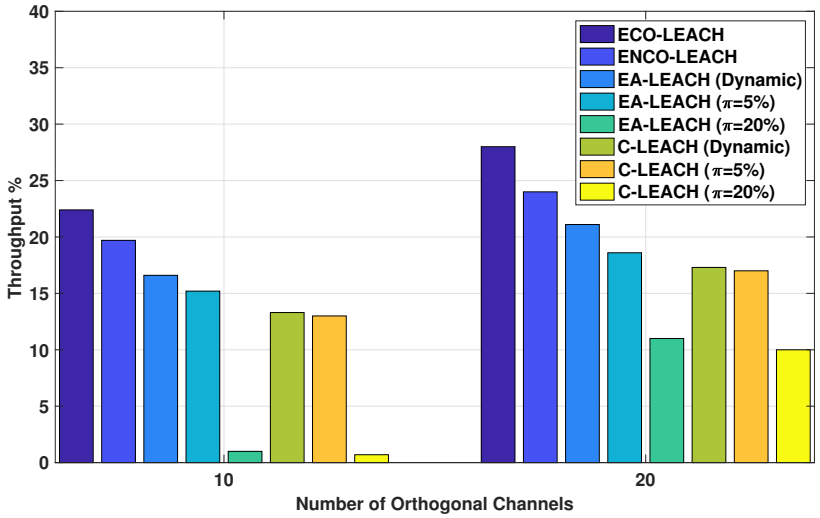

Fig. 6. Dynamic vs. Static CH Percentage

optimal CH number drops from 17 to 10 CHs as the harvested energy is not enough to support 20 CHs even when 20 channels are available. However, with 10 available channels, the number of CHs saturates at 10 for the same period since $k_{max} = 10$. The CH number falls as the energy harvested is further reduced between 1000s and 2500s.

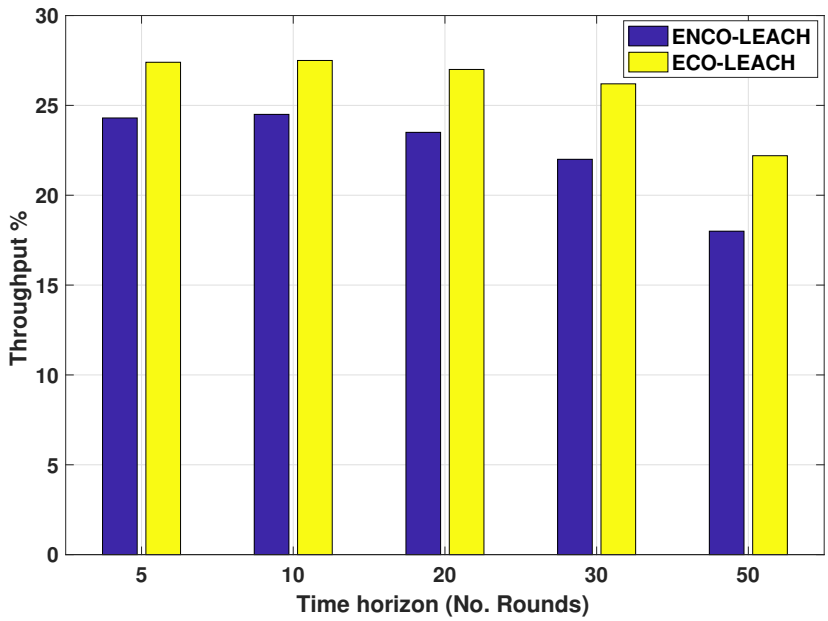

Fig. 7. Average Network Throughput vs. Time Horizon

Since the number of CHs supported is below 10, the available channels, being 10 or 20, cannot be utilized and thus the curves overlap. The reverse is then observed when the harvested energy increases from 2500s onward.

The throughput of the proposed protocol with the dynamically computed OCHP compared against the benchmark protocols, equipped with either static or dynamic CH percentage, is depicted in Fig. 6 for different number of orthogonal channels using the same intensity distribution in Fig 5. Both C-LEACH and EA-LEACH are seen to benefit from the dynamic OCHP compared to static CH percentage fixed at extreme values of 5% and 20%. Also, a sharp fall in throughput is seen for the static 20% case as the number of selected CH is far more than the number of available orthogonal channels. Notably, the proposed protocols outperform the benchmark ones even when they adopt the proposed dynamic OCHP mechanism.

In Fig. 7, the throughput of the proposed protocol is analyzed for several time horizon values, assuming the same intensity distribution above. By extending the time horizon beyond 10 rounds, the performance starts to deteriorate, as the actual energy harvested during each round deviates from the predicted value used to compute the CH-DC at the beginning of each L_{hor} period. Consequently, the harvested energy will not be optimally invested in maintaining the ENO. Note that the solar intensity in Fig 5 remains constant for 10 rounds. Conversely, making the time horizon unnecessarily short will increase the CH setup overheads, which in turn, reduce the network throughput.

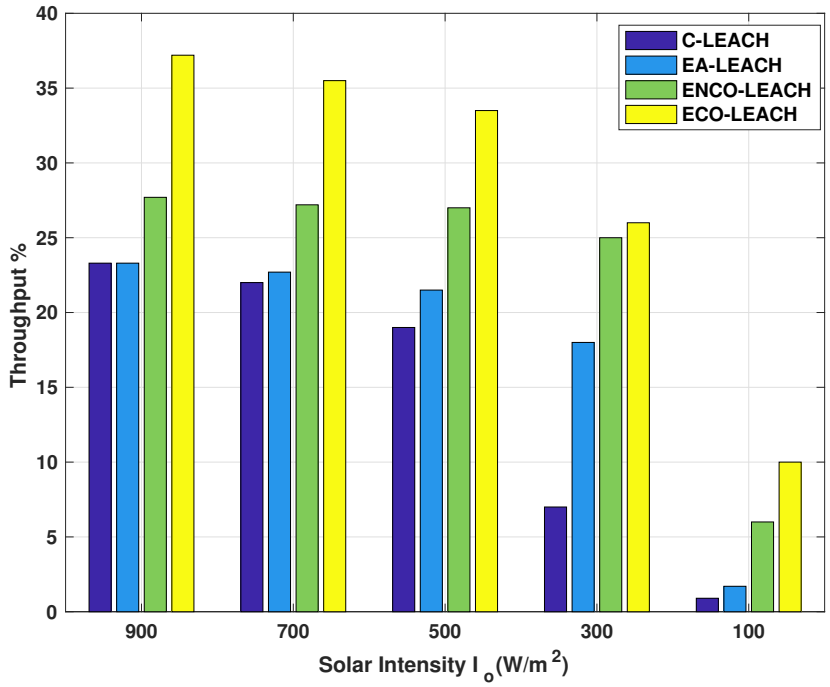

Fig. 8. Average Network Throughput vs. Solar Intensity ($\theta = 10$)

Fig. 8 compares the network throughput of the proposed protocol with and without cooperation against the benchmark protocols for different solar intensities. At high intensities, it is seen that EA-LEACH has a negligible advantage over C-LEACH as almost all nodes are capable of becoming CHs, whereas the proposed ENCO-LEACH outperforms the aforementioned protocols by around 19% due to its DT-DC. A further gain of 35% is obtained when utilizing cooperative relaying . At 300 W/m^2, the performance of ECO-LEACH is seen to fall to near that of ENCO-LEACH as less energy is left for relaying after allocating energy to the CH and data transmission roles. In turn, fewer relays will be available in each time slot reducing the diversity gain and hence the channel capacity. At lower intensities, however, the small portion of energy allocated to relaying has a more significant effect on the throughput as clusters tend to be fewer and larger in size. When this occurs, the average NCH to CH distance increases making the direct transmission less reliable. It is also evident that the gains achieved by the proposed protocol over C-LEACH and EA-LEACH are more significant at lower solar intensities. Specifically, a gain of nearly 500% is achieved by ECO-LEACH with respect to EA-LEACH at 100 W/m^2 compared with only 60% at 900 W/m^2.

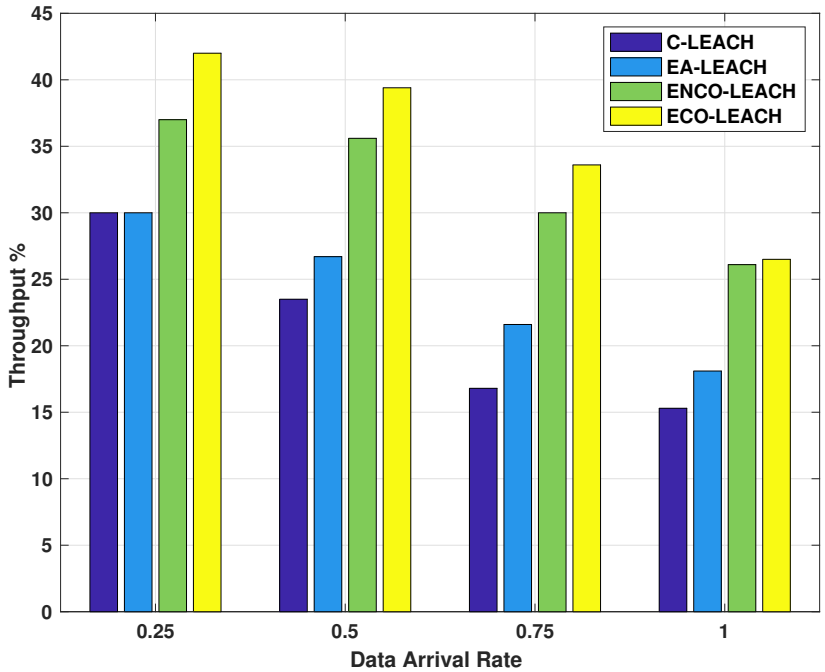

Fig. 9. Average Network Throughput vs. Packet Arrival Rate ($I_o = 500W/m^2$)

The effect of varying the data packet arrival rate on the performance of the different simulated protocols is shown in Fig. 9 for a fixed solar intensity of 500 W/m^2. In general, all the protocols perform worse with higher packet arrival rates due to the relatively low harvesting rate which limits the number of packets that can be transmitted. However, the throughput of the proposed protocol drops by only 26% when the arrival rate is doubled compared to a 32% loss by EA-LEACH. It is also seen that the gain from cooperation diminishes at higher packet arrival rates due to the lower relaying duty cycle resulting from a relatively higher data transmission DC.

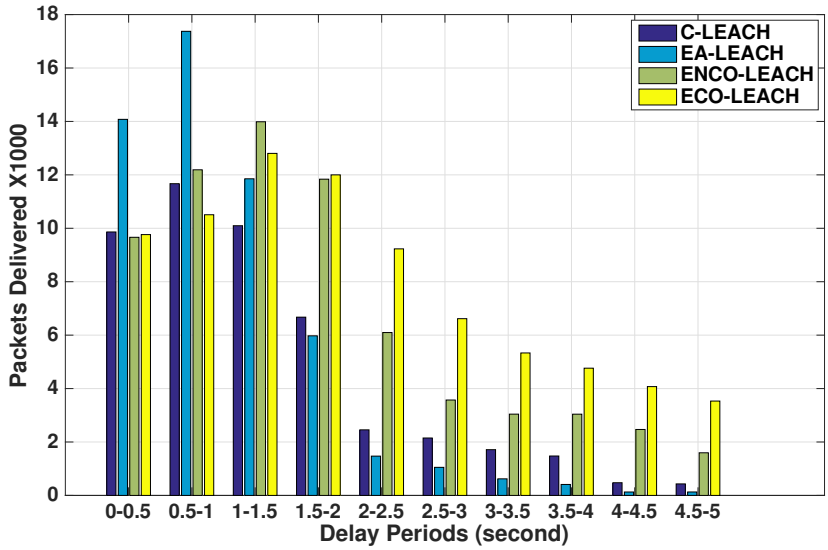

Fig. 10. Number of delivered packets vs. Delay periods ($I_o = 500W/m^2$)

The latency in delivering packets to the sink node is evaluated for the different protocols in Fig 10, assuming a solar intensity of 500 W/m^2. It is shown that the proposed protocol introduces longer delays than the benchmark schemes. This is explained by the reduced data transmission DC in order to adapt to the harvesting rate and maintain the ENO. It is also seen that cooperation introduces a further delay as failed packets are not transmitted until the following sub-slots. Despite that, more packets are delivered using the proposed protocol within the maximum delay period of 5 seconds, leading to a higher throughput as the energy is evenly spread throughout the duration of the simulation.

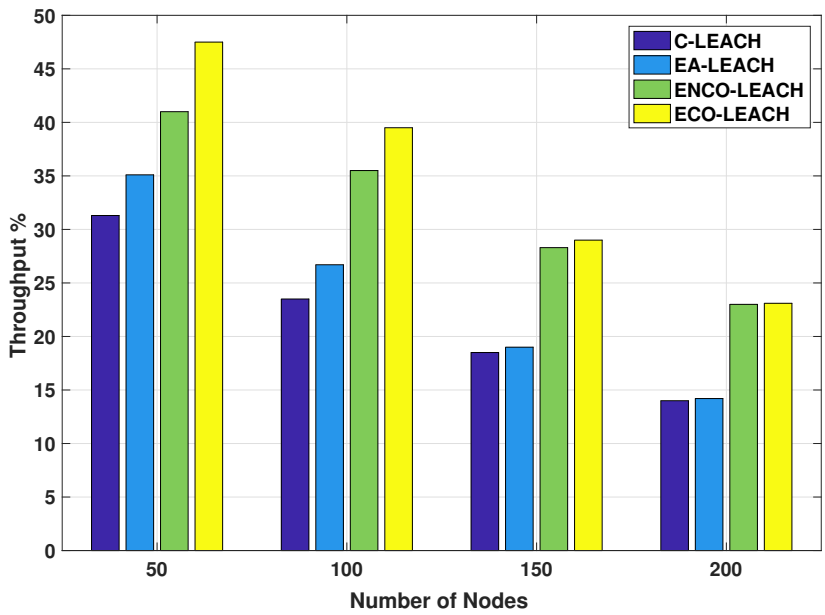

Fig. 11. Average Network Throughput vs. Number of Nodes ($I_o = 500W/m^2$)

The effect of increasing the number of nodes and hence the network density on the performance of ECO-LEACH is demonstrated in Fig. 11. Generally, increasing the nodes degrades the average throughput in all protocols due to larger clusters formed (as k_{max} is limited by the available channels) and thus longer delays. Also, the highly dense collision domain leads to more backoffs and collisions. Meanwhile, the gain obtained from the proposed protocol is more evident at high N as the reduced DT duty cycle lowers the effect of collisions and interference. However, the gain from cooperation diminishes as N increases since the reduced node-to-node distance decreases the spatial diversity gain.

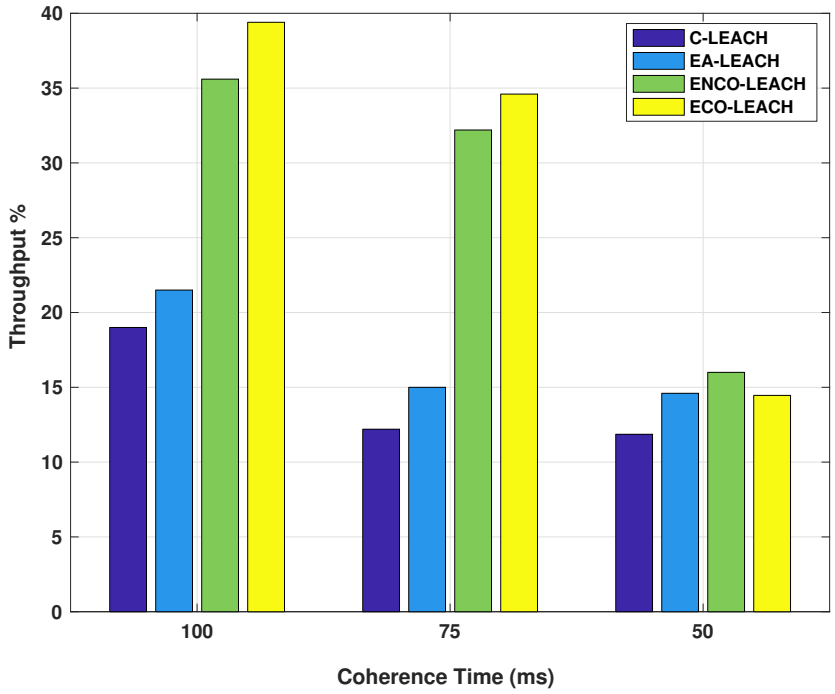

Fig. 12. Average Network Throughput vs. Channel Coherence Time ($I_o = 500W/m^2$)

To evaluate the impact of the fading channel on the performance of the proposed protocol, throughput simulations were run with different channel coherence times as shown in Fig. 12. The shorter the coherence time of the channel the worse is the network performance in all protocols, as the $RSSI$ based CH selections will turn invalid after the channel changes during a single round of the protocol. It is also seen that the cooperative protocol's performance drops with shorter coherence times until it becomes worse than ENCO-LEACH at $T_c = 50ms$. Again, this is explained by the fact that the best relay selected in the DTS sub-slot may not be the best relay in the following RTS.

Finally, figures 13 and 14 evaluate the performance of the proposed protocol with battery powered nodes in terms of throughput and lifetime. In this scenario, L_{hor} is set to equal the simulation duration and the expected harvested energy $\bar{\eta}_z T_r L_{hor}$ in all duty cycle calculations is replaced by the initial battery charge. It is seen that the proposed protocols outperform the benchmark schemes for all values of initial energy due to the novel duty cycling and cooperative schemes. Specifically, at a low initial charge, the throughput is nearly doubled by using the proposed scheme, whereas the lifetime is extended by almost 5 folds. As the initial charge is increased, the performance of ENCO-LEACH and the benchmark protocols become closer as they all reach the maximum lifetime of T_{sim} at 4 (mAh) of initial charge. However, the proposed scheme is still superior in terms of throughput due to the DT-DC. As for ECO-LEACH, it is seen that

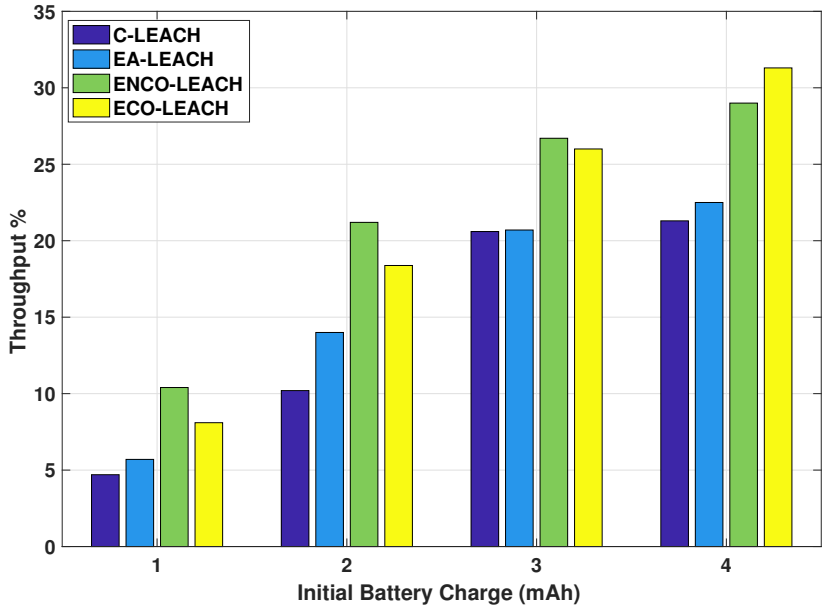

Fig. 13. Average Network Throughput vs. Initial Battery Charge

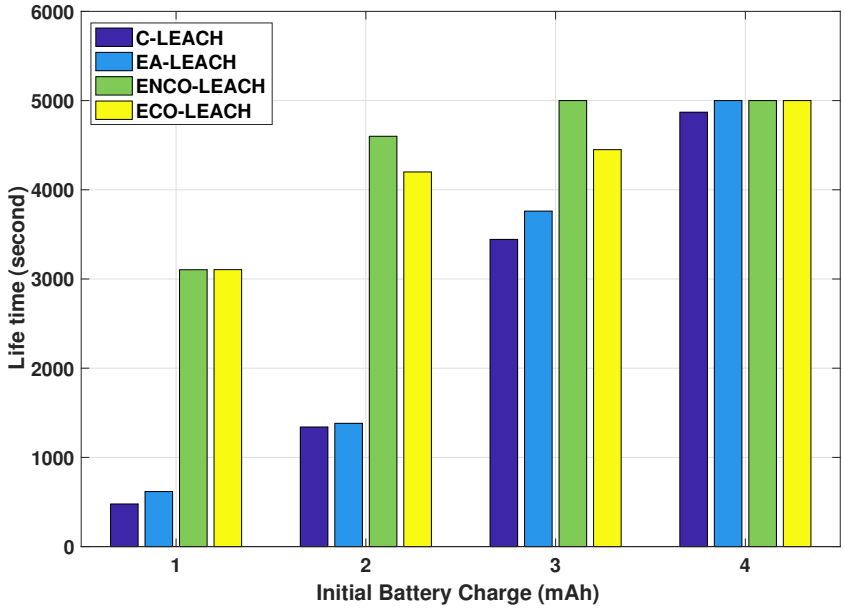

Fig. 14. Network Lifetime vs. Initial Battery Charge

no gain from cooperation is obtained for low values of initial residual energy. This is because all the available energy is used for the node's own data transmissions as it is given priority over relaying others packets. The small degradation in the performance of ECO-LEACH at low initial charge is due to the doubling of the packet generation

rate as described above.

VI. Conclusion

A novel clustering protocol that incorporates duty cycling and cooperative transmission is proposed for energy harvesting WSNs. The duty cycle for the CH assignment that guarantees a targeted CH percentage was derived and its optimal value was investigated. An efficient DC that ensures a perpetual network operation was developed. Besides, a cross-layer cooperative transmission strategy was designed to enable nodes to relay undelivered packets from cluster members to CHs and also from CHs to the sink node. The results obtained using event driven simulations have demonstrated an enhanced network performance in terms of throughput and lifetime with respect to the conventional LEACH as well as a generic energy-aware LEACH in EH and conventional battery powered WSNs. As a future development, this protocol can be extended to include the node's position and mobility in the duty cycle designs. In addition, hierarchical and multi-hop clustering can be integrated to support large network deployments such as the IoT.

References

[1] Q. Chi, H. Yan, C. Zhang, Z. Pang, and L. D. Xu, "A reconfigurable smart sensor interface for industrial WSN in IoT environment," *IEEE Trans. Ind. Inf.*, vol. 10, no. 2, pp. 1417–1425, May 2014.

[2] N. A. Pantazis, S. A. Nikolidakis, and D. D. Vergados, "Energy-efficient routing protocols in wireless sensor networks: A survey," *Commun. Surveys Tuts.*, vol. 15, no. 2, pp. 551–591, Second 2013.

[3] C. Wei, J. Yang, Y. Gao, and Z. Zhang, "Cluster-based routing protocols in wireless sensor networks: A survey," in *International Conf. Comput. Sci. and Netw. Technol. (ICCSNT), 2011*, vol. 3, Dec 2011, pp. 1659–1663.

[4] O. Yang and W. Heinzelman, "Modeling and performance analysis for duty-cycled MAC protocols with applications to S-MAC and X-MAC," *IEEE Trans. Mobile Comput.*, vol. 11, no. 6, pp. 905–921, June 2012.

[5] M. Bahbahani, M. Baidas, and E. Alsusa, "A distributed political coalition formation framework for multi-relay selection in cooperative wireless networks," *IEEE Trans. Wireless Commun.*, vol. 14, no. 12, pp. 6869–6882, Dec. 2015.

[6] J. Zheng, Y. Cai, X. Shen, Z. Zheng, and W. Yang, "Green energy optimization in energy harvesting wireless sensor networks," *IEEE Commun. Mag.*, vol. 53, no. 11, pp. 150–157, November 2015.

[7] S. Sudevalayam and P. Kulkarni, "Energy harvesting sensor nodes: Survey and implications," *Commun. Surveys Tuts.*, vol. 13, no. 3, pp. 443–461, 2011.

[8] L. Yang, Y. Lu, Y. Zhong, X. Wu, and S. X. Yang, "A multi-hop energy neutral clustering algorithm for maximizing network information gathering in energy harvesting wireless sensor networks," *Sensors*, vol. 16, no. 1, p. 26, 2016. [Online]. Available: http://www.mdpi.com/1424-8220/16/1/26

[9] M. Xiao, X. Zhang, and Y. Dong, "An effective routing protocol for energy harvesting wireless sensor networks," *IEEE Wireless Commun. Netw. Conf. (WCNC)*, pp. 2080–2084, April 2013.

[10] S. M. Bozorgi, M. G. Amiri, A. S. Rostami, and F. Mohanna, "A novel dynamic multi-hop clustering protocol based on renewable energy for energy harvesting wireless sensor networks," *2015 2nd International Conf. on Knowledge-Based Engineering and Innovation (KBEI)*, pp. 619–624, Nov 2015.

[11] S. Peng and C. P. Low, "Energy neutral clustering for energy harvesting wireless sensors networks," *IEEE International Conf. Netw. (ICON)*, pp. 1–6, Dec 2013.

[12] J. Meng, X. Zhang, Y. Dong, and X. Lin, "Adaptive energy-harvesting aware clustering routing protocol for wireless sensor networks," *International Conf. on Commun. and Netw. in China (CHINACOM)*, pp. 742–747, Aug 2012.

[13] W. R. Heinzelman, A. Chandrakasan, and H. Balakrishnan, "Energy-efficient communication protocol for wireless microsensor networks," in *Proceedings of the 33rd Annual Hawaii International Conf. on Syst. Sci.*, Jan 2000, pp. 10 pp. vol.2–.

[14] D. Wu, J. He, H. Wang, C. Wang, and R. Wang, "A hierarchical packet forwarding mechanism for energy harvesting wireless sensor networks," *IEEE Commun. Mag.*, vol. 53, no. 8, pp. 92–98, Aug 2015.

[15] D. Niyato, E. Hossain, and A. Fallahi, "Sleep and wakeup strategies in solar-powered wireless sensor/mesh networks: Performance analysis and optimization," *IEEE Trans. Mobile Comput.*, vol. 6, no. 2, pp. 221–236, Feb 2007.

[16] J. Hsu, S. Zahedi, A. Kansal, M. Srivastava, and V. Raghunathan, "Adaptive duty cycling for energy harvesting systems," *Proceedings of International Symposium on Low Power Electron. Des.*, pp. 180–185, Oct 2006.

[17] Y. Jing and H. Jafarkhani, "Single and multiple relay selection schemes and their achievable diversity orders," *IEEE Trans. Wireless Commun.*, vol. 8, pp. 1414 – 1423, Mar. 2009.

[18] M. S. Bahbahani and E. Alsusa, "Relay selection for energy harvesting relay networks using a repeated game," in *IEEE Wireless Commun. Netw. Conf. (WCNC)*, April 2016, pp. 1–6.

[19] N. Newalkar, S. Silakari, and P. K. Shukla, "Comparative analysis of co-operative MAC schemes," in *Cloud and Services Computing (ISCOS), 2012 International Symposium on*, Dec 2012, pp. 42–48.

[20] P. Liu, Z. Tao, S. Narayanan, T. Korakis, and S. S. Panwar, "CoopMAC: A cooperative MAC for wireless LANs," *IEEE J. Sel. Areas Commun.*, vol. 25, no. 2, pp. 340–354, February 2007.

[21] J. Liu, W. Wang, Z. Zheng, X. Zhang, C. Chen, and X. Shen, "Lifetime extended cooperative MAC protocol for wireless LANs," in *Global commun. conf. (GLOBECOM), 2012 IEEE*, Dec 2012, pp. 5476–5481.

[22] M. Khalid, Y. Wang, I. h. Ra, and R. Sankar, "Hybrid cooperative MAC protocol for wireless ad hoc networks," in *International Conf. Comput. Netw. Commun. (ICNC)*, Jan 2012, pp. 1015–1019.

[23] F. Liu, T. Korakis, Z. Tao, and S. Panwar, "A MAC-PHY cross-layer protocol for ad hoc wireless networks," in *IEEE Wireless Commun. Netw. Conf. (WCNC)*, March 2008, pp. 1792–1797.

[24] N. Hu, Y. D. Yao, and Z. Yang, "Analysis of cooperative TDMA in rayleigh fading channels," *IEEE Trans. Veh. Technol.*, vol. 62, no. 3, pp. 1158–1168, March 2013.

[25] H. Jiao and Y. L. Frank, "A mini-slot-based cooperative MAC protocol for wireless mesh networks," in *2010 IEEE Globecom Workshops*, Dec 2010, pp. 89–93.

[26] A. and H. Y. Kong, "Energy efficient cooperative LEACH protocol for wireless sensor networks," *J. Commun. Netw.*, vol. 12, no. 4, pp. 358–365, Aug 2010.

[27] X. Li, M. Chen, and W. Liu, "Application of STBC-encoded cooperative transmissions in wireless sensor networks," *IEEE Signal Process. Lett.*, vol. 12, no. 2, pp. 134–137, Feb 2005.

[28] G. X. Zhang, Pengfei and H.-P. Tan, "Clustering algorithms for maximizing the lifetime of wireless sensor networks with energy-harvesting sensors," *Computer Networks*, vol. 57, no. 4, pp. 2689–2704, 2013.

[29] M. S. Bahbahani and E. Alsusa, "DC-LEACH: A duty-cycle based clustering protocol for energy harvesting WSNs." IEEE Int. Commun. Conf. (ICC), Submitted, Oct. 2016.

[30] D. Benedetti, C. Petrioli, and D. Spenza, "GreenCastalia: An energy-harvesting-enabled framework for the Castalia simulator," *Proceedings of ACM ENSSys 2013*, pp. 7:1–7:6, Nov 2013. [Online]. Available: http://dl.acm.org/citation.cfm?id=2534215

[31] A. Boulis, "Castalia: A simulator for wireless sensor networks and body area networks user's manual." NICTA, 2011. [Online]. Available: https://castalia.forge.nicta.com.au

[32] A. Varga and R. Hornig, "An overview of the OMNeT++ simulation environment," in *Proceedings of the 1st International Conference on Simulation Tools and Techniques for Communications, Networks and Systems & Workshops*, ser. Simutools '08. ICST, Brussels, Belgium, Belgium: ICST (Institute for Computer Sciences, Social-Informatics and Telecommunications Engineering), 2008, pp. 60:1–60:10. [Online]. Available: http://dl.acm.org/citation.cfm?id=1416222.1416290

[33] A. Kansal, J. Hsu, S. Zahedi, and M. B. Srivastava, "Power management in energy harvesting sensor networks," *ACM Trans. Embed. Comput. Syst.*, vol. 6, no. 4, Sep. 2007. [Online]. Available: http://doi.acm.org/10.1145/1274858.1274870

[34] A. Bletsas, A. Khisti, D. Reed, and A. Lippman, "A simple cooperative diversity method based on network path selection," *IEEE J. Sel. Areas Commun.*, vol. 24, no. 3, pp. 659–672, Mar. 2006.

[35] S. S. Ikki and M. H. Ahmed, "Performance analysis of cooperative diversity with incremental-best-relay technique over rayleigh fading channels," *IEEE Trans. Commun.*, vol. 59, no. 8, pp. 2152–2161, August 2011.

[36] W. Heizelman, "Application-specific protocol architectures for wireless networks." *PhD Thesis, MIT*, Jun 2000.

[37] K. Doddapaneni, P. Shah, E. Ever, A. Tasiran, F. A. Omondi, L. Mostarda, and O. Gemikonakli, "Packet arrival analysis in wireless sensor networks," in *2015 IEEE 29th International Conf. on Advanced Information Netw. and Applications Workshops*, Mar 2015, pp. 164–169.

Chapter 6

CrowdConnect: A Network Connectivity Enhancement Solution for Crowded Sport Venues

CrowdConnect: A Network Connectivity Enhancement Solution for Crowded Sport Venues

Mohammed S. Bahbahani and Emad Alsusa

Abstract

In sports stadia and similar crowded venues, where a huge number of fans are seated in a confined area, maintaining a good network quality of experience (QoE) becomes a difficult task. Currently, enhancing the cellular network capacity is approached using small cells, distributed antenna systems and high-density WiFi. These solutions are expensive, unscalable and require huge investments by stadium owners and mobile operators. Hence, we propose a novel cost effective solution based on user coordination in accessing the cellular network, such that only a subset of users enable their cellular data connectivity at a time. Using the relaxed network, the connected devices can obtain then share match specific application data with the disconnected users, using peer-to-peer (P2P) WiFi, in a hierarchical fashion. To eliminate any free-riding behaviour, a limited punishment strategy in a finitely repeated game is proposed and shown to yield a subgame-perfect Nash equilibrium under certain conditions. Additionally, a dynamic cluster-based P2P network design is presented that can adapt to any particular scenario. Simulations performed in MATLAB confirm the improvement in QoE achieved by the proposed scheme, particularly when it is adopted by more than half of the fans.

Index Terms

Stadium connectivity, QoE, Clustering, Repeated game, Symmetric Nash Equilibrium, Large Games.

I. Introduction

The growing demand for wireless network connectivity coupled with the increasing user traffic has created many dense and congested network situations, such as shopping malls, musical concerts and sports venues, where maintaining a high QoE is hard to achieve. Among these scenarios, a football stadium network is the most challenging as tens of thousands of fans are seated shoulder to shoulder resulting in high call-blocking rates, excessive delays, and long video-buffering times [1], [2]. These issues are largely due to the macro base station (BS) being overwhelmed by myriads of simultaneous requests. More specifically, the limited number of resource blocks (RB) at the LTE BS

are acquired by the users via a contention process, in which the users are allocated RBs based on policies set by the network operator [3], [4]. Thus, many users may not obtain any RBs, while others can only access a few, as the total resources are divided among a large number of contenders. Meanwhile, the number of simultaneous connections allowed by the BS, even with scheduling, will be a small fraction of the total stadium attendees. Moreover, the associated inter-user interference will further worsen the network throughput. Furthermore, the fan's correlated behaviour in accessing the network resources is predicted to cause sudden traffic increase (spikes) at certain times of the event.

To enhance the network capacity, and in turn, the quality of experience, cellular network operators employ distributed antenna systems (DAS) [5], whereby multiple low power directional antennas, interconnected with high-speed optical fibre, target small sectors of the stadium, each using the entire LTE bandwidth. Alternatively, the cellular traffic can be offloaded to a stadium-owned high-density (HD) Wi-Fi network fed with a high-speed broadband connection [6]. Both solutions require expensive hardware and software systems, sophisticated site planning, costly maintenance and upgrades.

Recently, specific smartphone applications (Apps) have emerged to create a more engaging fan experience in the stadium. These Apps provide match statistics, audio commentary, video replays, polls and much more [7]. To facilitate the delivery of such services, while addressing the connectivity problem, these Apps build a mesh network via P2P connectivity to allow the sharing of match-specific contents among the fans. Inspired by these schemes, we propose a novel software-based solution to the stadium connectivity problem, by which fans limit the frequency of accessing the cellular network and share any acquired resources among themselves. Specifically, randomly selected groups of fans switch-off their cellular connectivity at a time during certain periods of the match. Given the relaxed network, the connected users, acting as the cluster heads (CH), can obtain the App data at a faster rate then share it with the disconnected users through a proposed cluster-based P2P network design. The network topology changes dynamically throughout the match according to instructions defined at a common server, which the fans can access before attending the stadium. To minimise interference, the Bluetooth, the 2.4 and 5 GHz bands of WiFi are employed at each level of the hierarchical cluster network.

To analyse the selfishness of fans in using the proposed App and to ensure fairness, a non-cooperative game theoretic model with symmetric mixed strategies are proposed, in which fans (the players in the game) enable their cellular data with a given probability. Being a large game (large number of players), the equilibrium is shown to be stable due to the ex-post Nash property. Additionally, a limited punishment strategy in a finitely repeated interaction is designed to enforce cooperation and to support the most

efficient equilibrium. The existence, convergence and complexity properties of the game equilibria are analysed, while accounting for player irrationalities and strategy errors. The performance of the proposed solution, named CrowdConnect (CC), is then verified using extensive MATLAB simulations under various parameters and scenarios. The results show substantial performance enhancements when a significant proportion of the fans adopt the proposed scheme and when the percentage of errors is moderate. The contributions of this work can be summarised as follows:

- Proposed a novel game strategy based on software defined networking concepts to enhance the stadium connectivity at a minimum cost.
- Proposed a dynamic cluster-based topology that adapts to the particular scenario and to the fan behaviour.
- Modelled the free-rider incentives in the proposed scheme as a non-cooperative large game.
- Proposed a punishment strategy that maintains cooperation in finitely repeated large games and verified its equilibrium.

The remaining sections of this paper can be summarised as follows. Section II reviews the art on stadium connectivity solutions. The motivations behind the proposed solution are discussed in Section III before the proposed scheme is explained in Section IV. Then, the stadium network model and topology are discussed in sections V and VI respectively. Section VIII introduces the game theoretic model used to implement the proposed strategy. To verify the proposed solution, simulations are conducted in section IX, and then analysed in section X. Finally, concluding remarks and future work are suggested in section XI.

II. Related Work

A. Distributed Antenna Systems and Small Cells

A distributed antenna system is a MIMO system, in which multiple antennas are co-located at one side of the radio link, whereas spatially scattered access points (AP), connected with optical fibre, comprise the other end of the link [5]. As a result, the DAS system extends the coverage of the outside Macro base station to the inside of the signal attenuating stadium structure. Despite being limited by the cell capacity, the SINR performance is enhanced through the diversity-multiplexing tradeoff of MIMO [8]. Therefore, performance optimisation and designs for stadium DAS have been recently investigated in the literature. In [9], the optimal distributed antenna selection is investigated considering both signal and interference strengths. A stadium scenario also shows that power allocation can further enhance the capacity. The optimal designs of a 2D antenna system including beam pointing directions is analysed in [10]. The

results show that it is sufficient to use four antennas with sectoring by pointing the beams towards the nearest stadium stands. Another distributed antenna system, designed at Bell Labs, is shown to outperform legacy DAS in both indoor and outdoor stadia [1]. By considering a 3D stadium model, the optimal number, location, orientation and power level were investigated and simulated using the OPNET software based on the LTE system. In practice, DAS systems have been widely used by network operators to enhance cellular coverage in stadia besides small cells and WiFi offloading. Claimed as the most connected stadium in the world, the Wembley stadium in London contains an advanced DAS system installed by EE to boost 4G internet access to all fans [11].

B. High-Density WiFi (HD-WiFi)

In a high-density (HD) WiFi network, a large number of users and access points (AP) coexist in the same coverage area limiting the user capacity due to interference and collisions. Unlike a coverage-based WiFi design, an HD WiFi benefits from the 5GHz band of WiFi due to its shorter range and more non-overlapping channels. To mitigate interference and maximise the user's QoE, the number of APs, their locations, power levels, frequency channel reuse and application requirements must all be optimised. For instance, the number of APs should not be too high increasing the co-channel interference nor too low sacrificing the wireless coverage. In addition, the channel frequency assignment to APs should minimise the interference as explained in [12].

Among the several HD WiFi networks deployed for sports stadia, Agile Stadium Solution [12] developed by Huawei is implemented at Borussia Dortmund stadium in Germany. By utilising 3D site planning, 5GHz RF and MIMO, over 80,000 fans can enjoy the speeds of a 1.75 Gbps broadband internet backhaul connection. Cisco has developed another HD-WiFi solution based on their own components. The proposed design is scalable, reliable, secure and includes specially designed algorithms for services including video replays, ticketing and secure point-of-sale infrastructure [13].

C. Wireless Ad-hoc Mesh Networks

Wireless mesh networks (WMN) have recently emerged to mitigate dead zones and increase the capacity of cellular and WiFi hotspots at low cost [14]. In a mesh network, each node connects to its surrounding nodes so data packets can traverse the network in a multi-hop fashion through distributed algorithms and protocols until the packets reach internet gateway nodes. Applications of mesh networks vary from public emergency control, social networks and other situations with absent network infrastructure. Cisco has developed a mesh network system based on Cisco Aironet APs for secure enterprise, campus and metropolitan WiFi networks [15]. Particularly, a mesh network is created

among WiFi APs running the Cisco Adaptive Wireless Path Protocol (AWPP) to carry wireless LAN client traffic.

On the other hand, a mesh network can be established between the mobile devices themselves using WiFi-Direct technology without requiring fixed mesh APs [16]. The WiFi Direct standard facilitates the seamless setup of infrastructure or ad-hoc WiFi hotspots and the discovery of nearby services on the go without an actual AP. In detail, a node can create a group, and become its group owner (GO), or join other groups using the WiFi-Direct protocol. Access credentials are exchanged through the protocol setup phase granting access to specific services declared by the group. Legacy WiFi devices may still join the groups as legacy APs. With this technology, scalable and secure P2P mesh networks have been demonstrated by many applications including chatting Apps and stadium solutions. For instance, $TribeHive$ [17], allows fans to share their cellular data connection to obtain match application data using WiFi P2P connectivity employing a delay-tolerant protocol. Specifically, when a device cannot obtain the match data from the cellular network due to congestion or poor signal, the data is requested from a nearby device with better signal strength. This scheme, however, was only demonstrated to support low data rate text-based match applications and not a general Internet access.

D. Software Defined Networks

A newly proposed strategy for future networks is the decoupling of the network control plane (routing decisions) from the data flow plane (forwarding decisions) through virtualization. In a software-defined network (SDN), routers and switches are only responsible for the forwarding of packets, whereas the routing of packets is controlled externally by a centralised controller [18]. This technique improves the WAN link utilisation through dynamic routing and traffic engineering and also enables efficient protocol evolution. In wireless mesh networks, many design challenges can be overcome using SDN concepts. Efficient resource allocation, congestion control and load balancing are among the major problems, which require a global network view that is hard to obtain in conventional distributed algorithms. However, the centralised control of an SDN suffers from compromised network reliability as a result of link failure or network partitioning. Thus, fault tolerance support using fault detection and redundancy is essential [18]. For a detailed comparison of existing SDN schemes for WMN, the reader may refer to [18].

III. Motivations

The motivations behind the proposed solution are listed as the follows:

A. Infeasibility of Stadium Network Infrastructure Enhancements

A football stadium is only occupied during games, each lasting for nearly two hours. Since a stadium can only host a maximum of two games per week, due to the requirements of the football pitch, the utilisation of the stadium wireless network will be as low as $(2\times2)/(24\times7) = 2.4\%$. In other words, the expensive DAS or HD-WiFi hardware are not used for 97% of the time. Therefore, enhancing the stadium network is infeasible to mobile operators as the investment may be directed to more profitable areas. The other reason behind the infeasibility of such investment is the rapid evolution of wireless technologies demanding frequent updates of expensive systems. For instance, a new generation of cellular telephony and an enhanced WiFi release emerge almost every ten years. Due to the above, having a sustainable software-based solution for infrequently used dense networks is appealing.

B. Correlated User Activity

Since all fans are engaged with the same event, their behaviour in accessing the wireless network will be correlated and hence, may follow an impulsive pattern. In other words, more fans are expected to access the network at the halftime break or during stoppage time. On the other hand, during periods of intensive action, the fans will ignore their phones and the demand for data traffic will reduce significantly. This unique feature of the stadium network may benefit from a dynamic network structure that adapts to the correlated user behaviour and match events unlike many conventional networks.

C. Data Broadcasting and Aggregation

In addition to voice calls and a general Internet access, fans may be interested in event specific applications, including real-time match statistics and video replays. As these applications provide common data to all fans, broadcasting downlink data using a cluster-based network design may exponentially reduce the overall data traffic, whereas aggregating certain uplink traffic by the cluster heads will further improve the network throughput.

IV. Proposed Method Description

When the cellular network capacity fails to meet the demands of the high number of fans, cooperation and coordination can lead to a better QoE. Coordination in accessing the network resources is achieved by reducing the number of simultaneously connected devices at a given moment so that a subset of fans can obtain usable data rates at a time assuming smartphones are only used occasionally. This strategy can be implemented by

switching off the cellular data connectivity of the user's device during certain periods of the sports event. Thus, instead of obtaining low data rates continuously, the user is better off obtaining useful data rates in certain periods, while being completely disconnected in the remaining periods. Users satisfaction can be further enhanced through the sharing of common match-specific application data among fans through WiFi and Bluetooth (BT) connectivity. Specifically, a hierarchical cluster-based ad-hoc P2P network structure is formed, such that a connected device (CD) forwards the obtained match application data to the disconnected cluster member devices (DD). As a result, the match applications are always available to both CDs and DDs.

To implement the above strategy, a distributed algorithm is proposed to reside as an App on the user's device. The objective of the distributed algorithm is to determine the optimal cellular enabled (CE) state of a user in each period of the network lifetime (match duration) taking into account the incentives of following this action as well as possible human error. The actions of fans (CE states) are modelled as a finitely repeated game, where the best response strategies of players form a perfect Nash equilibrium, by which a user has no incentives to deviate from, as will be shown in Section VIII below. Besides, a centralised algorithm, located on a common server, determines the optimal cluster formation that maximises the average QoE given the recommended actions above and the various system parameters. Each user can download the solution of the centralised algorithm before the beginning of the match. Both algorithms rely on several network status and parameters, including the cellular capacity, the number of attendees and the number of App users.

V. Stadium Network Model and Assumptions

We model a football stadium as a set of S sectors each being a two-dimensional grid of H rows and M columns, as shown in Fig. 1. Each element in the grid represents a seat, which may be occupied by a user (a fan) holding a single mobile device as indicated by the binary variable $\mathcal{I}^U_{i,j,s} \in \{0,1\}$, where i, j and s are the row, column and sector indices respectively. Hence, the stadium has $N^C = SHM$ seats out of which $N^U = \sum_{s=1}^{S}\sum_{i=1}^{H}\sum_{j=1}^{M}\mathcal{I}^U_{i,j,s}$ seats will be occupied for the duration of the whole match. Each seat covers a square area of $d_o^2\ m^2$, where d_o is the distance between the centres of two adjacent seats. Also, we denote by $c^l_{i,j}$, a square cluster of $(2l+1)^2$ seats surrounding, and including seat (i,j), where l is the cluster diameter in the number of seats.

Then, the stadium cellular network is modelled as follows. A total of O network operators are assumed to provide cellular connectivity in the stadium, each providing a cell capacity of $\mathcal{C}$ Mbps. Without loss of generality, it is assumed that the operators have equal shares of the market, hence, the number of attending users per operator becomes $N^O = \frac{N^U}{O}$. Out of these users, $N = \Upsilon^{App}N^O$ will use the proposed solution,

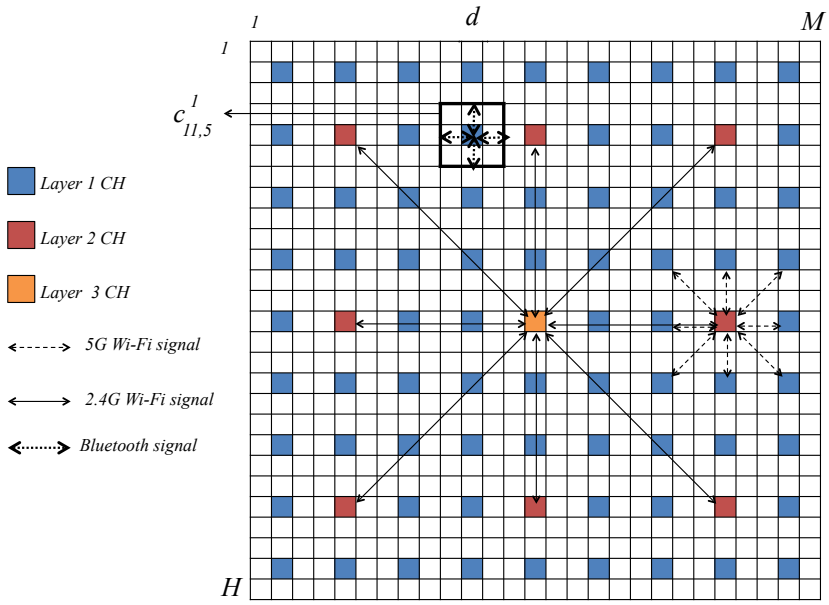

Fig. 1. Stadium Network Model

where Υ^{App} is the percentage of users adopting the proposed solution. Additionally, we use the variable τ to refer to the number of simultaneously active users at a given moment. To simplify the model, we assume that users have similar device capabilities and signal strengths as the base station may be located either very far from the stadium or small cells are installed above the seating areas with direct $Line\ of\ Sight$ (LOS) to each device. Moreover, each user is assumed to have an unlimited cellular data plan and the cellular enabled status (CE) can be toggled at any time period t as indicated by the binary variable $\mathcal{I}^{C}_{i,j,s}(t) \in \{0, 1\}$. However, a node has a continuously enabled WiFi/Bluetooth interface, which can connect to a maximum of n^{max}_{W} nodes at a time using P2P connectivity.

VI. Hierarchical Cluster Based Network Topology

To enable the sharing of cellular data among the nodes, a dynamic hierarchical cluster-based network design is proposed using P2P connectivity. Similar to LEACH [19], the network is divided into clusters of equal size, where a node located near the centre of a cluster acts as a cluster head (CH) connecting the other cluster members (CM). Using

WiFi-Direct [16] or Bluetooth [20], the CMs can exchange match application data with the CHs. In turn, the CHs may be members of an upper layer of clusters as shown in Fig. 1[1]. Hence, a CH acts as a router that forwards uplink data traffic received from its CMs directly to the Internet, if its cellular interface is enabled, or through the CH of the above layer otherwise. Similarly, the downlink traffic received from the Internet or the upper CH is passed down to the node's CMs. The number of layers and their sizes depend upon the percentage of CDs, the maximum possible P2P connections per device as well as other system parameters and QoE requirements. Given the availability of the above information at a common server, the network topology is determined by the algorithm described below.

A. Network Hierarchical Design

The layer structure of the P2P network topology is determined by Algorithm 1 described as follows. The minimum number of layers is first initialised to 0, indicating an infeasible network topology. Also, the total available capacity C^B is initialised given the targeted percentage of CDs denoted as p. The first step in the design is to find the minimum number of clustering layers, below K_{max}, that ensure all DDs are connected to CDs either directly or through CHs (lines 3 to 7). If a feasible K_{min} exists, the number of CMs per cluster, n_W, is then found in line (9). The cluster size (area) per layer l_k and the throughput per layer C_k^B are then obtained in lines (11) to (17). Starting at layer $k = 1$, the minimum distance from the CH covering n_W^{max} users, given the percentage of App users, gives the cluster size. This process is repeated for the remaining $k > 1$ layers except that Υ^{App} will be replaced by the density of CHs of the lower layer, that is, $\frac{n_W^{max}}{((2l_{k-1}+1)^2-1)}$. Having obtained the cluster size of a given layer, the capacity of the CH to a cluster edge CM link C_k^B is obtained from known WiFi capacity versus distance measurements [21]. Due to the contention process in the WiFi MAC layer, the capacity is divided by the number of CMs in the cluster to obtain the user throughput as in line (17). The end-to-end throughput is then found as the minimum layer capacity. This value is further divided by the number of layers (line 19) in case a half-duplex transmission is assumed.

B. Interference Minimising Design

The performance of WiFi and BT connectivity is severely degraded when a high number of users contend for the channel leading to longer back off times and more collisions. To counteract the effect of interference, a 3-layer cluster-based heterogeneous network design is proposed, in which BT, 5Ghz and 2.4Ghz WiFi are deployed at layers

[1]In this figure, a fully occupied stadium is assumed, in which all users adopt the proposed scheme.

Algorithm 1 P2P Network Topology

INITIALIZE: $K_{min} = 0$, $C^B = O\mathcal{C}p$
FOR $i \in \{1, \ldots, K_{max}\}$
    IF ($\frac{1}{p} \leq n_W^{max^i}$)
        $k_{min} = i$
        BREAK
    END IF
END FOR
IF($k_{min} > 0$)
    $n_W = \frac{k_{min}}{p}$
END IF
FOR $k \in \{1, \ldots, k_{min}\}$ %For each level
    FOR $l_k \in \{1, \ldots, L_{max}\}$ %Find cluster size
        IF($n_W \leq ((2l_k + 1)^2 - 1)\Upsilon_{app}$)
            BREAK
        END IF
    END FOR
    $C^B \leftarrow min(C^B, \frac{C_k^B}{n_W})$
END FOR
$C^B \leftarrow C^B / k_{min}$

1, 2 and 3 respectively. BT is adopted at the bottom layer due to the small cluster size, which is compatible with the short range of a BT picocell. Thus, a layer-1 CH acts as a BT master connecting the CMs (BT slaves) using TDMA. Collisions between adjacent clusters are hence minimised through frequency hopping of BT. At the second layer, 5Ghz WiFi is more appropriate due to its shorter range and many non-overlapping channels that are better utilised by the relatively smaller clusters of layer-2 compared to layer-3. Hence, the transmission of all adjacent clusters can be made orthogonal eliminating co-channel interference (CCI). Finally, the legacy 2.4Ghz WiFi is used for the larger layer-3 clusters, as the three non-overlapping channels of 2.4Ghz WiFi are sufficient to eliminate the co-channel interference (CCI). Note that this scheme only supports a specific range of p and n_W^{max} values and requires 5Ghz enabled WiFi devices.

C. Network Topology Design

Having determined the clustering structure, the topology is then determined using P2P connectivity in offline mode. That is, the topology is predetermined by a centralised algorithm located at a server from which the fans can download a topology file before attending the stadium. The offline software-defined mode reduces the computational burden at user's device and utilises information including users locations, device capabilities and application preferences. The topology file dictates the roles of a user (CH and CE status), at each period in the match, as well as the identities (seat coordinates)

Table I
Service A APPLICATIONS [12]

Application	Throughput (Kbps)	Payoff
Text Messaging	60	1
Voice (VoIP)	100	3.5
Web browsing	300	5
Video Streaming	500	6

Table II
Service B APPLICATIONS

Application	Throughput (Kbps)	Payoff
Match Stats.	60	1
Polls and games	100	3.5
Picture Download	300	4
Video Replays	500	4.5

and roles of the devices it connects to. It also includes alternative (back-up) CHs in case the suggested CH is not responding. During the match, each user adopts the topology file as follows. If the user's role at layer-1 is CH, the user becomes a BT master node and waits for BT slaves to join, whose IDs are listed in the topology file. Otherwise, the user connects to the BT master also included in the topology file. In case the BT master is unavailable, the user tries the next backup BT master and so on. At the upper layer, assuming the persistent mode of WiFi-Direct [16], the user becomes a GO if labelled as a layer-2 CH in the topology file and waits for listed CM peers to join its group. Instead, if the user is a layer-1 CH but not a CH at layer-2, it will try to join the specified GO (layer-2 CH) using 2.4GHz WiFi. The same procedure is then followed for layer-3 using the 5Ghz WiFi band. Note that layer-1 and layer-2 CHs will concurrently communicate with their peers and CHs using interfaces (BT,2.4G) and (2.4G,5G) respectively, which may be achieved through time-sharing. To ensure fairness and to extend users' battery charge, the CH role is rotated among the cluster members following each period of the network operation time.

VII. IN-MATCH APPLICATIONS

Using the cellular data connectivity, a fan can access different Internet applications, henceforth denoted by $Service\ A$. On the other hand, match specific application data, henceforth denoted by $Service\ B$, may be acquired either through the cellular data connection or from the P2P network, depending on the user's CE status. Tables I and II above list five classes of applications per service with minimum throughput requirements

[12] and realised game payoffs. A description of popular in-match applications ($Service\ B$) is given as follows.

A. Match Statistics

A basic in-match application is the real-time broadcast of match statistical information, which may include team squad, substitutions, and results of other games being played at other venues. This service is generally text-based, requires low data rates and dominated by downlink traffic.

B. Match Video Replays

Another proposed application is the broadcast of video clips of important match events, such as goal replays [7]. The video files can either be streamed or downloaded using the UDP or TCP protocols respectively. High data rates are necessary to deliver the relatively larger video files within 1-2 minutes from the time they were recorded. Meanwhile, the latency in packet delivery can be tolerated due to video buffering. The associated traffic mostly occurs in the downlink (Server to fan).

C. Match Polls

At certain points in the match, a poll may be conducted, where fans are requested to vote over certain topics such as the $man\text{-}of\text{-}the\text{-}match$. A poll is initiated by a question, which can be either stored in the user's App or fetched to the user's device during the match. The fans then respond to the poll within a given period and then, the result is broadcasted back to the users. Data aggregation may be utilised by summing the votes at each CH, so that only the sum is sent back to the server or the CH in the layer above.

VIII. Network Resource Sharing as a Repeated Game

Since fans are decision makers concerning their CE status and due to the lack of coordination and binding agreements among them, we model the behaviour of fans as a repeated non-cooperative game, wherein each period a stage game is played as described below.

A. Stage Game Description

A stage game is represented by the tuple $\mathcal{G}$ ={$\mathcal{N}$, $\mathcal{A}$, $\mathcal{U}$}, where $\mathcal{N}$ is a set of N players (the fans), $\mathcal{A} = \{0, 1\}$ is the action space indicating the player's CE status, and $\mathcal{U}^{\mathcal{G}} = \{U_1^{\mathcal{G}}, \ldots, U_N^{\mathcal{G}}\}$ is the vector of utilities. The utility of a player n is the payoff received at the end of the stage game, as a function of his action $a_n \in \mathcal{A}$, minus the cost incurred by the chosen action. This is expressed as:

$$\alpha(\mathbf{a}) = \begin{cases} \alpha_1 & 0 = Y_0 \leq \sum_{i=1}^{N} a_i \leq Y_1 \\ \alpha_2 & Y_1 < \sum_{i=1}^{N} a_i \leq Y_2 \\ \vdots & \vdots \\ \alpha_{L-1} & Y_{L-2} < \sum_{i=1}^{N} a_i \leq Y_{L-1} \\ \alpha_L & Y_{L-1} < \sum_{i=1}^{N} a_i \leq Y_L = N \end{cases}, \tag{2}$$

$$\beta(\mathbf{a}) = \begin{cases} \beta_1 & 0 = Y_0 \leq \sum_{i=1}^{N} a_i \leq Y_1 \\ \beta_2 & Y_1 < \sum_{i=1}^{N} a_i \leq Y_2 \\ \vdots & \vdots \\ \beta_{L-1} & Y_{L-2} < \sum_{i=1}^{N} a_i \leq Y_{L-1} \\ \beta_L & Y_{L-1} < \sum_{i=1}^{N} a_i \leq Y_L = N \end{cases}, \tag{3}$$

$$U_n^{\mathcal{G}}(a_n, \mathbf{a_{-n}}) = \begin{cases} \frac{\alpha(a_n, \mathbf{a_{-n}}) + \beta(a_n, \mathbf{a_{-n}})}{2} - \delta & a_n = 1 \\ \beta(a_n, \mathbf{a_{-n}}) & a_n = 0 \end{cases}, \tag{1}$$

where $\alpha(\cdot)$ and $\beta(\cdot)$ represent the payoffs obtained from services A and B respectively as a function of players actions such that $\mathbf{a_{-n}} = \{a_1, a_{2,}, a_{n-1}, a_{n+1}, \ldots, a_N\}$ is a set of actions taken by all players except from n. Upon choosing $a_n = 1$ (CE enabled), a player can utilise both services, while incurring a cost of δ that accounts for the extra energy loss from enabling the cellular interface. The factor $\frac{1}{2}$ comes from the fact that a player can only use one of the services at a time. However, by disabling cellular data ($a_n = 0$), a player can only enjoy Service B. The payoffs of services A and B are given by (2) and (3) respectively at the top of the page, where the values $\alpha_L \leq \ldots \leq \alpha_1$ and $\beta_L \leq \ldots \leq \beta_1$ represent $L \leq N$ distinct payoffs defined by the values $Y_x = xN/L$ $\forall x \in \{0, \ldots, L\}$. These payoffs reflect the fan's relative QoE, as they depend on the number of supported applications based on the received throughput. For the scenarios considered in Section IX, the payoffs per application are shown in tables I and II above. For example, if the user throughput is 350 Kbps, the payoff from service A will be 9.5, being the sum of the payoff values for each of the text, VoIP and web browsing applications. Likewise, service B will yield a payoff of 8.5.

The user throughput of Service A is given by $C_{\mathbf{a}}^{A} = \frac{\mathcal{C}}{1+(\sum_{i=1}^{N} a_i + (1-\Upsilon^{app})N^O)\tau}$, which is taken, for simplicity, as the cellular capacity divided by the number of CDs, assuming all non-App-users are CDs. As for Service B, the throughput is obtained by invoking Algorithm 1 using $p = \frac{\sum_{i=1}^{N} a_i}{N}$. Since the utility only depends on the number of players selecting each action ($\sum_{i=1}^{N} a_i$) regardless of the identities of players, the game is considered as symmetric [22]. This property induces a special equilibrium notion that

is discussed next.

B. Stage Game Equilibria

According to [22], the symmetric stage game defined above has a pure strategy Nash equilibrium in which i players select action $a_n = 1$, while the remaining $N - i$ players select $a_n = 0$. It was proven by Nash [22] that a symmetric game must have a symmetric Nash equilibrium in mixed strategies, in which all players choose $a_n = 1$ with the same probability $p \in [0, 1]$. Specifically, when $N-1$ players adopt the symmetric mixed Nash equilibrium strategy p, the remaining player will be indifferent between choosing any value of p as in the following equation:

$$\frac{(\alpha_1 + \beta_1)}{2} \sum_{i=0}^{Y_1 - 1} \mathcal{X}(N, i, p) + \cdots + \frac{(\alpha_L + \beta_L)}{2} \sum_{i=Y_{L-1}}^{Y_L - 1} \mathcal{X}(N, i, p) - \delta$$

$$= \beta_1 \sum_{i=0}^{Y_1} \mathcal{X}(N, i, p) + \cdots + \beta_L \sum_{i=Y_{L-1}+1}^{Y_L} \mathcal{X}(N, i, p), \tag{4}$$

$$\mathcal{X}(N, i, p) = \begin{pmatrix} N-1 \\ i \end{pmatrix} p^i (1-p)^{N-1-i}, \tag{5}$$

where $\mathcal{X}(N, i, p)$ is the probability that i players actually select $a_n = 1$ upon playing the mixed strategy p. The left hand side term of (4) represents the expected payoff gained by a deviating player who chooses the pure action $a_n = 1$ when the remaining players adopt the symmetric mixed strategy p, whereas the right side term denotes the expected payoff when the player selects $a_n = 0$. Since the solution of (4) is complex and the number of players is large, we apply an approximate equilibrium notion based on the law of large numbers [23], which states that the larger the number of random experiments (large N), performed with a given probability p, the more likely the outcome ($\sum_{i=1}^{N} a_i$) will be close to the expected value pN. Thus, (4) can be approximated by:

$$\frac{\alpha(p(N-1)+1) + \beta(p(N-1)+1)}{2} - \delta = \beta(p(N-1)). \tag{6}$$

Hence, for any $x \in \{0, \ldots, L\}$ for which $\frac{\alpha_x + \beta_x}{2} - \delta = \beta_x$, there exist a continuum of equilibria $[\frac{Y_{x-1}}{N-1}, \frac{Y_x}{N-1} - \frac{1}{N-1}]$ yielding the same approximate payoff of α_x or β_x. Due to the approximation in (6), the equilibrium is near Nash by an error of ϵ and hence denoted as $\epsilon - Nash$. Under the above equilibria, a player's gain from the deviation is limited by ϵ as given by the following theorem [24]:

Definition 1 : $\epsilon -$ **Nash Equilibrium** : A symmetric mixed strategy p^* is an $\epsilon - Nash$ equilibrium if:

$$U_n^{\mathcal{G}}(p^*) \geq U_n^{\mathcal{G}}(p, p_{-n}^*) - \epsilon \qquad \forall n \in \mathcal{N} \ , \forall p \in [0,1], \epsilon \geq 0, \tag{7}$$

where ϵ is the magnitude of the difference between the expected payoffs of actions $a = 1$ and $a = 0$, given as:

$$\epsilon = abs(\frac{(\alpha_1 + \beta_1)}{2} \sum_{i=0}^{Y_1 - 1} \mathcal{X}(N, i, p) + \cdots + \frac{(\alpha_1 + \beta_1)}{2} \sum_{i=Y_{L-1}}^{Y_L - 1} \mathcal{X}(N, i, p) - \delta$$
$$-\beta_1 \sum_{i=0}^{Y_1} \mathcal{X}(N, i, p) + \cdots + \beta_L \sum_{i=Y_{L-1}+1}^{Y_L} \mathcal{X}(N, i, p)). \tag{8}$$

As N increases, the error ϵ decreases as shown in the following proposition.

Proposition 1 : For any $\epsilon - Nash$ symmetric equilibrium p^*, the value of ϵ tends to 0 as N approaches ∞.

Proof: Assuming the symmetric equilibrium lies in the middle of the interval of α_x ($p^* = \frac{Y_x + Y_{x-1}}{2(N-1)}$), applying $Chebyshev's\ inequality$ [25] results in the following:

$$Pr(|X - Np^*| \geq \frac{N}{2L}\sqrt{(1-p^*)Np^*}) \leq \frac{4L^2}{N^2}, \tag{9}$$

where $Y_x = \frac{N}{L}$, Np^* is the mean and $\sqrt{(1-p^*)Np^*}$ is the standard deviation of the binomial random variable $\mathcal{X}$. Hence, for fixed L and p^*, increasing N reduces the probability of the outcome exceeding the range Y_{x-1}, Y_x which in turn reduces the expected gain from payoffs $(|\alpha_1 - \beta_1|, \ldots, |\alpha_{x-1} - \beta_{x-1}|, |\alpha_{x+1} - \beta_{x+1}|, \ldots, |\alpha_L - \alpha_L|)$ and, thus, ϵ approaches zero. ■

$Corollary$ **1** : For a given equilibrium payoff, the error ϵ takes a minimum value when the symmetric equilibrium is in the middle of the interval Y_{x-1}, Y_x.

The relationship between the number of $\epsilon - Nash$ symmetric equilibrium points and the payoff functions in the proposed stage game is summarised by the following remarks.

Remark 1. If $\alpha_x = \beta_x \ \forall x \in \{0, \ldots, L\}$, then any p constitutes a $\epsilon - Nash$ equilibrium.

Remark 2. If $\alpha_x \neq \beta_x \ \forall x \in \{0, \ldots, L\}$ then no symmetric $\epsilon - Nash$ equilibrium exists.

Besides its simplicity, the aforementioned equilibrium is also characterised as being nearly $ex - post\ Nash$ [26]. That is, in equilibrium, no player will consider revising his action even after the actions of all players have been revealed. This $ex - post$ property of the equilibrium ensures its stability against possible deviations.

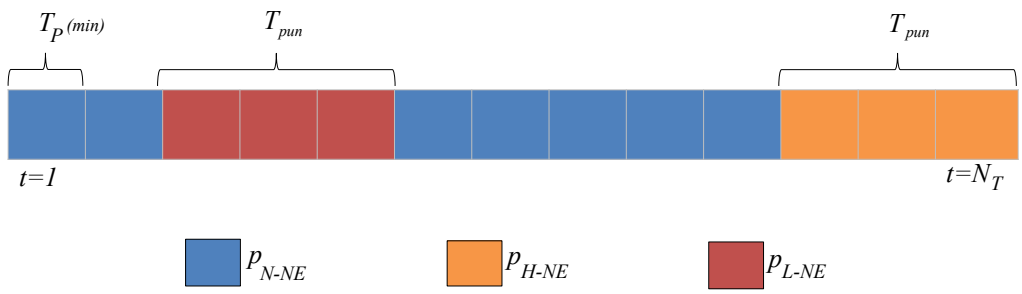

Fig. 2. Repeated Game Model

C. Repeated Game Model

The non-cooperative equilibria of the stage game discussed above may not support all the efficient and network performance maximising values of p. Meanwhile, repeated interactions among players were proven to sustain a cooperative behavior and enforce efficient (QoE maximising) equilibria [27]. For example, the grim-trigger strategy, in which players cooperate until a defection is observed, is a proven equilibrium in a discounted infinitely repeated game according to the folk theorems. On the other hand, a finitely repeated game with a unique stage game Nash equilibrium has a unique sub-game perfect equilibrium, in which the non-cooperative NE is played in every period. Interestingly, a cooperative play can be sustained in finitely repeated games when the stage game has multiple equilibria, such that the worst of which is used as a punishment in the last stage of the repeated game [28]. Since the fans interact over a finite period (the match duration), a finitely repeated game approach is followed as described below.

In a finitely repeated game denoted by $\mathcal{G}^R$, the match duration of T_M minutes is divided into N_T periods each of length $T_P = \frac{T_M}{N_T}$ minutes. In each period $t \in \{1, \ldots, N_T\}$, the stage game $\mathcal{G}_t^R$, described in Section VIII-A, is played and the utility to a player n in the repeated game is the average utility received over all the periods, which is, $U_n^{\mathcal{G}^R} = \frac{1}{N_T} \sum_{t=1}^{N_T} U_n^{\mathcal{G}_t^R}(a_n^t, \mathbf{a}_{-n}^t)$ [2]. Also, a public signal $y^t = \sum_{n=1}^{N} a_n^t \in \mathcal{Y} = \{0, \ldots, N\}$ indicating the collective actions taken by all players in period t becomes common knowledge at the beginning of period $t+1$, leading to a game of $imperfect\ monitoring$ [29], [30]. Moreover, a strategy vector $s_n = \{a_n^1, \ldots, a_n^{N_T}\}$ represents the action plan

[2]It is assumed that the action taken by a player n at period t (a_n^t) remains fixed for the duration of that period. In reality, the CE status of a fan may not remain constant over the whole period. Hence, the action a_n^t is considered to be 1 if the CE remains enabled for a defined fraction of the period t.

Algorithm 2 Limited Punishment Strategy

```
INITIALIZE:,
FOR n ∈ {1, ..., N}
    FOR t ∈ {1, ..., N_T}
        IF (t = 1)
            a_n^t ← p_{N−NE}
        ELSE IF (y^{t−1} > y^{thr} AND a_n^{t−1} = p_{N−NE})
            IF (t > N_T − 2T_pun)
                a_n^{t,...,N_T} ← p_{L−NE}, t ← N_T
            ELSE
                a_n^{t,...,t+T_pun−1} ← p_{L−NE}, t ← t + T_pun − 1
            END IF
        ELSE IF (t = N_T − T_pun + 1)
            a_n^{t,...,N_T} ← p_{H−NE}, t ← N_T
        ELSE
            a_n^t ← p_{N−NE}
        END IF
    END FOR
END FOR
```

of player n throughout the repeated game for all possible histories of play up to any stage t, denoted as $\mathbf{h^t} = \{\mathbf{a^1}, \ldots, \mathbf{a^t}\}$. Also, the strategy profile of all players in the game is defined by $\mathbf{s} = \{s_1, \ldots, s_N\}$. Next, we propose a symmetric strategy $\mathbf{s^{pun}}$ based on a limited punishment, described in algorithm 2, by utilising a high and a low utility stage game Nash equilibria denoted by p^*_{H-NE} and p^*_{L-NE}, respectively. In the first stage of the game, all players select the cooperative and efficient non-NE action p_{N-NE}, which yields a higher utility than both p_{H-NE} and p_{L-NE} (assuming $y^0 = 0$). At stage $t = 2$, given the number of remaining stages is above $2T_{pun} < N_T$ and that the signal y^1 exceeds a common threshold $y^{thr} \in \{p^*N, p^*N + 1, \ldots, N\}$, the players will defect from cooperation by selecting p^*_{L-NE} in the next T_{pun} periods before returning to play p_{N-NE} in period $t = 2 + T_{pun}$. Otherwise, the players will play p_{N-NE} in stage $t = 2$, then consider the same punishment strategy for period $t = 3$ and so on. In the last $T_{pun} + 1$ stages of the repeated game, the strategy $\mathbf{s^{pun}}$ is played as follows. Given the signal $y^{N_T - T_{pun} - 1}$ is below the threshold, the higher utility NE p_{H-NE} will be played in all the remaining stages of the repeated game. Otherwise, the low utility NE strategy p_{L-NE} will be triggered as before. An illustrative example of the repeated game is shown in Fig. 2, in which the players cooperate until stage $t = 2$ after which the punishment is triggered until stage $t = 5$. In the last T_{pun} periods, the high utility Nash is played since the users cooperate at $t = N_T - T_{pun}$.

$$U_n^{\mathcal{G}_t^R}(\mathbf{a_n}^{\mathbf{N-NE}}) = (p_{N-NE}\alpha_1 + (1-p_{N-NE})\beta_1)\sum_{i=0}^{Y_1}\mathcal{X}(N,i,p_{N-NE}) + \cdots$$

$$+(p_{N-NE}\alpha_L + (1-p_{N-NE})\beta_L)\sum_{i=Y_{L-1}}^{Y_L}\mathcal{X}(N,i,p_{N-NE}) \tag{10}$$

$$U_n^{\mathcal{G}_t^R}(1,\mathbf{a_{-n}}^{\mathbf{N-NE}}) = \alpha_1\sum_{i=0}^{Y_1-1}\mathcal{X}(N-1,i,p_{N-NE}) + \cdots + \alpha_L\sum_{i=Y_{L-1}}^{Y_L-1}\mathcal{X}(N-1,i,p_{N-NE}) \tag{11}$$

$$Pr(y^t \leq y^{thr}|a_n = p_{N-NE}) = \sum_{i=0}^{y^{thr}}\mathcal{X}(N,i,p_{N-NE}) \tag{12}$$

$$Pr(y^t \leq y^{thr}|a_n = 1) = \sum_{i=0}^{y^{thr}-1}\mathcal{X}(N-1,i,p_{N-NE}) \tag{13}$$

D. Existence of Sub-game Perfect Nash Equilibria

The strategy profile $\mathbf{s^{pun}}$ described above yields a sub-game perfect Nash equilibrium (SPNE) of the finitely repeated game $\mathcal{G}^R$ if the strategy constitutes a Nash equilibrium in every sub-game of $\mathcal{G}^R$, that is, the continuation play following each possible history. In the context of $\epsilon - Nash$, a near SPNE ($\epsilon - SPNE$) is defined as follows:

Definition 2 : A strategy profile $\mathbf{s}$ forms an $\epsilon - SPNE$ if it constitutes an $\epsilon - Nash$ equilibrium at every sub-game $\mathcal{G}_t^R$ $\forall t \in \{1,\ldots,N_T\}$ and any history $\mathbf{h^t}$ [31].

Proposition 2 : The limited punishment strategy $\mathbf{s^{pun}}$ forms an $\epsilon - SPNE$ of the game $\mathcal{G}^R$ for given values of T_{pun} and y^{thr}.

Proof: To show that $\mathbf{s^{pun}}$ is an $\epsilon - SPNE$ of $\mathcal{G}^R$, we prove, using backward induction, that every sub-game in $\mathcal{G}^R$ forms an $\epsilon - Nash$ equilibrium. Starting at period $t = N_T - T_{pun} + 1$, for which $N_T \geq T_{pun}$, any sub-game, given any history, will form an $\epsilon - Nash$ equilibrium, since either p^*_{H-NE} or p^*_{L-NE} will be played at periods $t = N_T - T_{pun} + 1$ to $t = N_T$ according to $\mathbf{s^{pun}}$. Considering the sub-games at the preceding period $t = N_T - T_{pun}$ (if $N_T > T_{pun}$), for all histories ending with $y^{t-1} \leq y^{thr}$ or has all of $y^{t-T_{pun}-1},\ldots,y^{t-1}$ above y^{thr} (signaling the end of a punishment period), then playing p_{N-NE} is an equilibrium of the continuation play given that a unilateral deviation is non-profitable, as given by the following inequality:

$$U_n^{\mathcal{G}_t^R}(1, \mathbf{a_{-n}}^{\mathbf{N-NE}}) - U_n^{\mathcal{G}_t^R}(\mathbf{a_n}^{\mathbf{N-NE}}) \leq (Pr(y^t > y^{thr}|a_n = 1)$$

$$-Pr(y^t > y^{thr}|a_n = p_{N-NE}))(U_n^{\mathcal{G}_{t+1}^R}(\mathbf{a_n}^{\mathbf{H-NE}}) + U_n^{\mathcal{G}_{t+1}^R}(\mathbf{a_n}^{\mathbf{L-NE}}))T_{pun}, \tag{14}$$

where the LHS term in (14) is the expected utility gain obtained by player n in the current round upon a unilateral deviation to $p = 1$. Precisely, $U_n^{\mathcal{G}_t^R}(1, \mathbf{a_{-n}}^{\mathbf{N-NE}})$, given at the top of the page, is the stage utility of playing $a_n = 1$, while the rest of players adopt p_{N-NE}, whereas $U_n^{\mathcal{G}_t^R}(\mathbf{a_n}^{\mathbf{N-NE}})$ is the utility when all players, including n, adopt p_{N-NE}. The RHS term is the expected loss from the deviation that may be incurred over the remaining periods of the game. Generally, the loss is proportional to the difference between the probabilities of triggering the punishment corresponding to the actions $p = p_{N-NE}$ and $p = 1$. For any history, in which $y^{t-1} > y^{thr}$, at period $t = N_T - T_{pun}$, playing the punishment strategy p_{L-NE} until the end of the game is clearly an $\epsilon - Nash$ equilibrium.

Next, we show that adopting p_{N-NE} at periods $t = N_T - T_{pun} - k$ starting with $k = 1$ ($k < N_T - T_{pun}$) and working recursively until $t = 1$, for the same histories used above, is a best response if the conditions (15) and (16) below are satisfied for $k > T_{pun}$ and $k \leq T_{pun}$, respectively.

$$U_n^{\mathcal{G}_t^R}(1, \mathbf{a_{-n}}^{\mathbf{N-NE}}) - U_n^{\mathcal{G}_t^R}(\mathbf{a_n}^{\mathbf{N-NE}}) \leq (Pr(y^t > y^{thr}|a_n = 1)$$

$$-Pr(y^t > y^{thr}|a_n = p_{N-NE}))U_n^{\mathcal{G}_{t+1}^{Sub}}(\mathbf{a_n}^{\mathbf{N-NE}}) + (Pr(y^t > y^{thr}|a_n = 1)$$

$$-Pr(y^t > y^{thr}|a_n = p_{N-NE}))U_n^{\mathcal{G}_t^R}(\mathbf{a_n}^{\mathbf{L-NE}})(N_T - t), \tag{15}$$

$$U_n^{\mathcal{G}_t^R}(1, \mathbf{a_{-n}}^{\mathbf{N-NE}}) - U_n^{\mathcal{G}_t^R}(\mathbf{a_n}^{\mathbf{N-NE}}) \leq (Pr(y^t > y^{thr}|a_n = 1)$$

$$-Pr(y^t > y^{thr}|a_n = p_{N-NE}))(U_n^{\mathcal{G}_{t+1}^{Sub}}(\mathbf{a_n}^{\mathbf{N-NE}}) - U_n^{\mathcal{G}_{t+T_{pun}}^{Sub}}(\mathbf{a_n}^{\mathbf{N-NE}}))$$

$$+(Pr(y^t > y^{thr}|a_n = 1) - Pr(y^t > y^{thr}|a_n = p_{N-NE}))U_n^{\mathcal{G}_t^R}(\mathbf{a_n}^{\mathbf{L-NE}})T_{pun}. \tag{16}$$

In the above inequalities, $U_n^{\mathcal{G}_t^{Sub}}(\mathbf{a_n}^{\mathbf{N-NE}})$ is the expected utility of the sub-game equilibrium starting at period t, given as:

$$U_n^{\mathcal{G}_t^{Sub}}(\mathbf{a_n}^{\mathbf{N-NE}}) = \begin{cases} \mathcal{I}_1 & : t = N_T - T_{pun} \\ \mathcal{I}_2 & : N_T - 2T_{pun} \leq t < N_T - T_{pun} \\ \mathcal{I}_3 & : 1 \leq t < N_T - 2T_{pun} \end{cases}, \tag{17}$$

where $\mathcal{I}_1$, $\mathcal{I}_2$ and $\mathcal{I}_3$ are given respectively as:

$$\mathcal{I}_1 = U_n^{\mathcal{G}_t^R}(\mathbf{a_n}^{\mathbf{N-NE}}) + (Pr(y^t \leq y^{thr}|a_n = p_{N-NE})U_n^{\mathcal{G}_t^R}(\mathbf{a_n}^{\mathbf{H-NE}})$$

$$+Pr(y^t > y^{thr}|a_n = p_{N-NE})U_n^{\mathcal{G}_t^R}(\mathbf{a_n}^{\mathbf{L-NE}}))T_{pun},$$

$$\mathcal{I}_2 = U_n^{\mathcal{G}_t^R}(\mathbf{a_n}^{\mathbf{N-NE}}) + ((Pr(y^t \leq y^{thr}|a_n = p_{N-NE})U_n^{\mathcal{G}_{t+1}^{Sub}}(\mathbf{a_n}^{\mathbf{N-NE}})$$

$$+(Pr(y^t > y^{thr}|a_n = p_{N-NE})U_n^{\mathcal{G}_{t+1}^{Sub}}(\mathbf{a_n}^{\mathbf{L-NE}}))(N_T - t),$$

$$\mathcal{I}_3 = U_n^{\mathcal{G}_t^R}(\mathbf{a_n}^{\mathbf{N-NE}}) + ((Pr(y^t \leq y^{thr}|a_n = p_{N-NE})(U_n^{\mathcal{G}_{t+1}^{Sub}}(\mathbf{a_n}^{\mathbf{N-NE}}) - U_n^{\mathcal{G}_{t+T_{pun}}^{Sub}}(\mathbf{a_n}^{\mathbf{N-NE}}))$$

$$+(Pr(y^t > y^{thr}|a_n = p_{N-NE})U_n^{\mathcal{G}_t^R}(\mathbf{a_n}^{\mathbf{L-NE}}))T_{pun}.$$

In the RHS of (15), the low utility NE is triggered for the remaining $N_T - t$ periods, since the next T_{pun} will end within the last T_{pun} periods. However, when $t < N_T - 2T_{pun}$, the triggered punishment will end before the last T_{pun} periods and hence the loss in utility is the difference in the expected utility over the next T_{pun} periods, as in (16). By working backwards until $t = 1$, while substituting the result of each sub-game $U_n^{\mathcal{G}_{t+1}^{Sub}}$ into $U_n^{\mathcal{G}_t^{Sub}}$, as in (17), it can be shown that every sub-game forms an $\epsilon - Nash$ equilibrium and hence the game $\mathcal{G}^R$ has an $\epsilon - SPNE$ for the values of T_{pun} and y^{thr} that satisfy (15) and (16) at every sub-game. Thus, for a given threshold value, the values of T_{pun} that sustain the equilibrium are obtained as:

$$T_{pun} \geq \frac{U_n^{\mathcal{G}_t^R}(1, \mathbf{a_{-n}}^{\mathbf{N-NE}}) - U_n^{\mathcal{G}_t^R}(\mathbf{a_n}^{\mathbf{N-NE}})}{(Pr(y^t > y^{thr}|a_n = 1) - Pr(y^t > y^{thr}|a_n = p_{N-NE}))U_n^{\mathcal{G}_t^R}(\mathbf{a_n}^{\mathbf{L-NE}})}$$

$$- \frac{U_n^{\mathcal{G}_{t+1}^{Sub}}(\mathbf{a_n}^{\mathbf{N-NE}}) - U_n^{\mathcal{G}_{t+T_{pun}}^{Sub}}(\mathbf{a_n}^{\mathbf{N-NE}})}{U_n^{\mathcal{G}_t^R}(\mathbf{a_n}^{\mathbf{L-NE}})}. \tag{18}$$

■

In addition to the equilibrium $\mathbf{s^{pun}}$, a trivial equilibrium, in which a stage game Nash equilibrium is played in all periods also forms a SPNE. This result is outlined in the following:

Proposition 3 : The symmetric strategy $\mathbf{s^{NE}} = \{s_1^{NE}, \ldots, s_N^{NE}\}$, where $s_i^{NE} = \{p_{H-NE}^1, \ldots, p_{H-NE}^{N_T},\}$, constitutes an $\epsilon - SPNE$ of $\mathcal{G}^R$.

Proof: Since an ϵ-NE is played in every stage, then $\mathbf{s^{NE}}$ forms an $\epsilon - SPNE$ by definition. ■

E. Uniqueness of the Game Equilibrium

A game with a unique equilibrium is preferred for its outcome, and hence, player utilities can be anticipated. As the stage game in Section VIII-A has multiple equilibrium points, most of which yielding identical payoffs, the repeated game will have multiple equilibria, in which any stage game equilibrium is played in every period. Besides these inefficient equilibria, the $\mathbf{s^{pun}}$ strategy supports many $\epsilon - SPNE$ equilibria for a range of y^{thr} and T_{pun} values. To cope with the existence of multiple equilibria, the App can enforce the most efficient equilibrium by instructing users with the best response action at each period.

F. Complexity of Game Equilibria

Computing the stage game Nash equilibria requires evaluating the utility of all symmetric equilibrium points in the set $P = \{0, \frac{1}{N}, \frac{2}{N}, \ldots, \frac{N-1}{N}, 1\}$. For each value $p \in P$, the utility obtained by unilaterally deviating to any other mixed strategy $\widehat{p} \in P \setminus p$ is calculated. Therefore, the complexity of finding all the NE is $O(N^2)$. These equilibria are then sorted to obtained the most efficient p_{H-NE} and the least efficient p_{L-NE} NE needed by $\mathbf{s^{pun}}$. As for the repeated game equilibria, the trivial equilibrium $\mathbf{s^{H-NE}}$ brings no additional computational burden. However, the $\mathbf{s^{pun}}$ equilibrium requires evaluating the conditions (15) and (16) for all sub-games and all possible combinations of T_{pun} and y^{thr} yielding the maximum utility of $\mathcal{G}^R$.

G. Player Irrationality and Game Noise

The assumption of rationality is common to any game theoretical modelling. This requirement simply asserts that players always select the strategy that maximises their utilities. As the players in the proposed game are the fans, failure in undertaking their best response actions will be likely, as they may not randomise their actions exactly according to the equilibrium mixed strategy. In addition, the player's perception of the QoE, and thereby, the signal used to trigger the punishment may not be accurate and

Table III
SIMULATION PARAMETERS

N^C	90,000	Stadium Capacity
O	4	Number of Operators
T_M	100 mins	Match Duration
N_p	25	Number of Periods
T_{pun}	4	No. of Punishment Periods
$\mathcal{C}$	300 Mpbs	Cell Capacity
n_W^{max}	8	Max. WiFi connections
L	5	Number of QoE levels
τ	40%	Simultaneous Users
η	10%	Game Noise
δ	0	Cellular Energy Cost
Itr	1000	Number of Iterations

homogeneous. Thus, it is proposed that an App residing on a fan's device monitors the QoE signal and computes the fan's best response action at the beginning of each period of the repeated game. Thus, fans can either fulfil the best response action suggested by the App or deviate from it when they do not trust the recommended action or due to human error in manually changing the CE status. In both cases, the error is modelled as a game noise η, defined as the probability of deviating from the best response action at a given period. Hence, given a symmetric strategy p and a noise value of η, the expected number of players selecting action $a = 1$ becomes $pN(1-\eta)+(1-p)\eta N$. In words, it is the proportion of non-deviating players who undertake action $a = 1$ plus erroneous players who were supposed to choose $a = 0$. By assuming a symmetric noise that is common knowledge among players, the noise is incorporated in the stage game Nash equilibrium by updating (6) to:

$$\alpha(p(N-1)(1-\eta)+(1-p)(N-1)\eta+1) = \beta(p(N-1)(1-\eta)+(1-p)(N-1)\eta). \quad (19)$$

Accordingly, the repeated game equilibrium strategies are updated as follows. As for $\mathbf{s^{NE}}$, the corrected stage game NE with highest utility is played in all periods of the repeated game. In the finite punishment strategy, the cooperative action p_{N-NE} is adjusted to $p^{\eta}_{N-NE} = (p_{N-NE}-\eta)/(1-2\eta)$ in order to compensate for the noise. Thus, playing p^{η}_{N-NE} by all players results in an average of Np_{N-NE} players choosing $a = 1$ despite the noise. However, p_{N-NE} must always be greater than η.

IX. Numerical Evaluation

In this section, extensive MATLAB simulations of the stadium network performance, with and without the proposed scheme, are presented and denoted by (CC) and (No-CC), respectively. Additionally, the performance of CC with selfless players was simulated and denoted by SCC, where a fan always follows the CE state that maximises the overall network performance, as instructed by the App. The parameters listed in table III were used in all simulation scenarios unless specified otherwise[3]. Many scenarios were simulated to quantify the performance gains of CC according to different performance metrics, including the average user throughput, utility and CE percentage. For a given CE percentage, the overall throughput and utility represent the combined values obtained from both services (A and B). That is, if the CE percentage is 0.3, the overall throughput will be $0.3 \times C^A + 0.7 \times C^B$. Henceforth, the combined throughput and utility will be simply denoted by the throughput and the utility, respectively.

Figures 3, 4 and 5 compare the average utility, throughput and CE percentage for different number of attendees and App users, assuming a game noise of 10% and a percentage of simultaneous users of 40%. The throughput and the utility are seen to drop together with more attending fans but improve as more fans opt for the proposed solution. Remarkably, a performance gain is only realised by CC when at least 60% of the fans are using the App. Specifically, with a 70% stadium occupancy, the throughput is doubled when CC is adopted by 60% of the fans, whereas an increase by more than five folds is obtained when all the fans use CC. This improvement is also reflected in the game utility. Unlike CC, No-CC brings a zero utility to the players when the stadium occupancy exceeds 70%, since the resulting throughput does not support any Internet application. However, the throughput achieved by CC is sufficient to support the first two applications of both services when cellular data is enabled for 20% of the time ($p = 0.2$) as shown in Fig 5.

[3]Note that the excess cellular energy cost δ was omitted as a realistic value was not available. Obtaining this value requires surveying users preferences, which may be conducted in future work.

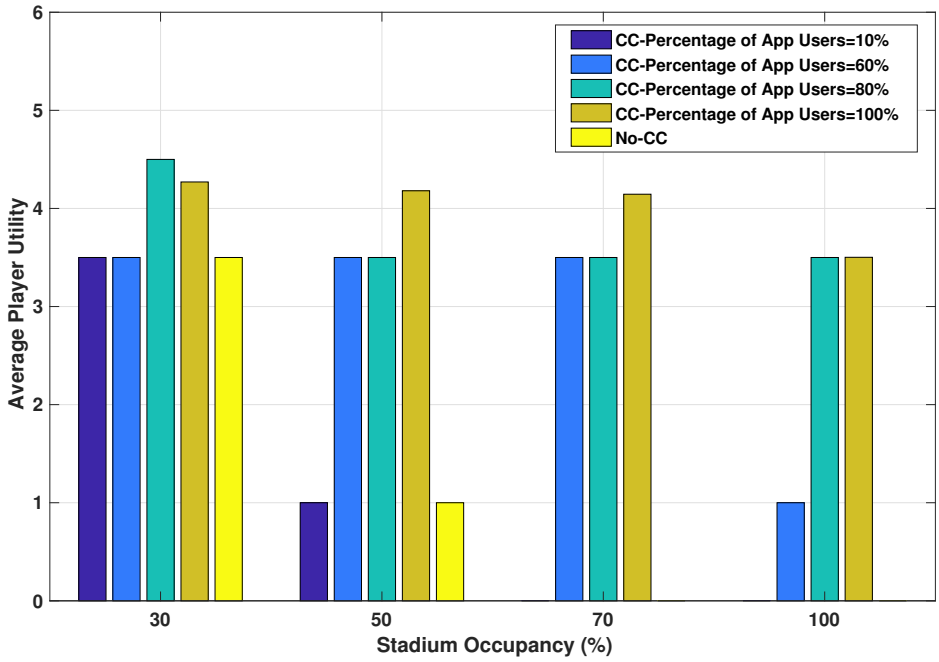

Fig. 3. Average Utility vs. Stadium Occupancy

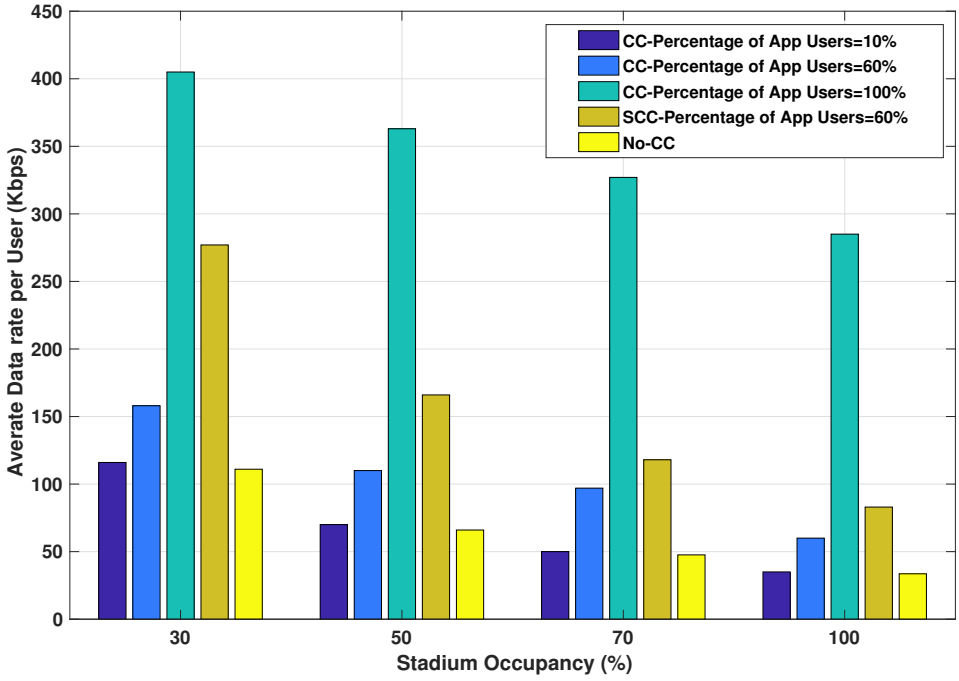

Fig. 4. Average Throughput vs. Stadium Occupancy

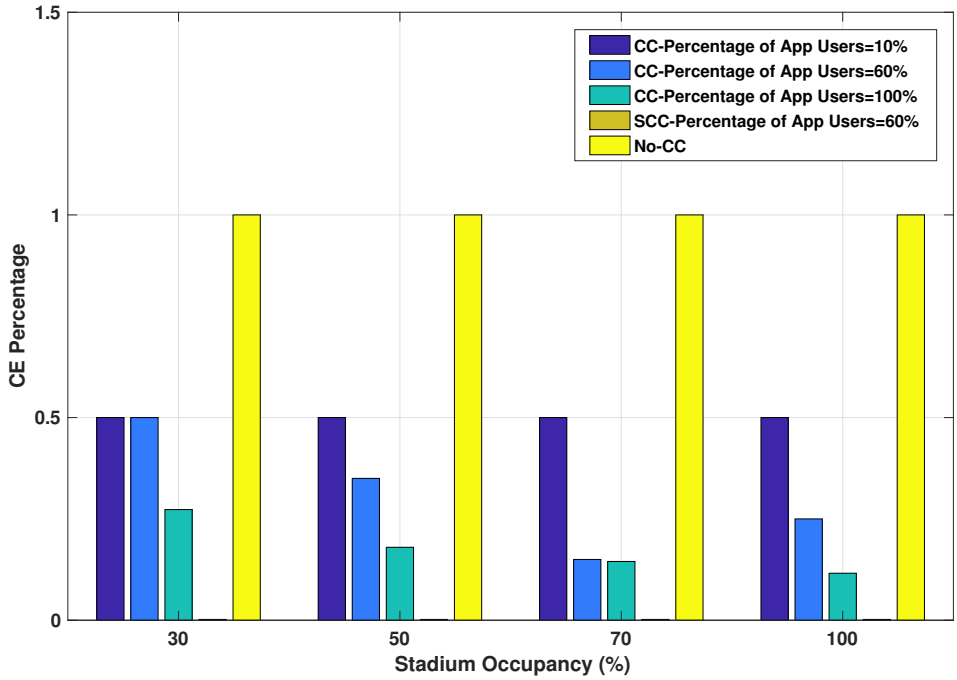

Fig. 5. CE Percentage vs. Stadium Occupancy

The impact of human error in adopting the selected equilibrium strategy, represented by the game noise, is depicted in figures 6, 7 and 8 for different percentages of App users, assuming a fully occupied stadium and that $\tau = 40\%$. An inverse relationship between the game noise and the network performance is observed for all Υ^{App} values except for the case of $\Upsilon^{App} = 100\%$, in which an improvement in utility is observed when the noise is 20%. This is explained by noting the stage game Nash equilibria associated with 10%, 20% and 30% values of noise. For both 10% and 30% noise, the efficient equilibria are the intervals $p = [0.1251, 0.625]$ and $p = [0, 0.7499]$, respectively, both resulting in a utility of 3.5. However, the case of $\eta = 0.2$ supports a higher utility of 4.5 using the equilibrium $p = 0$. Despite that $p = 0$ is adopted, the players' actual actions result in a CE percentage of 0.2 due to the 20% noise, as seen in Fig. 8.

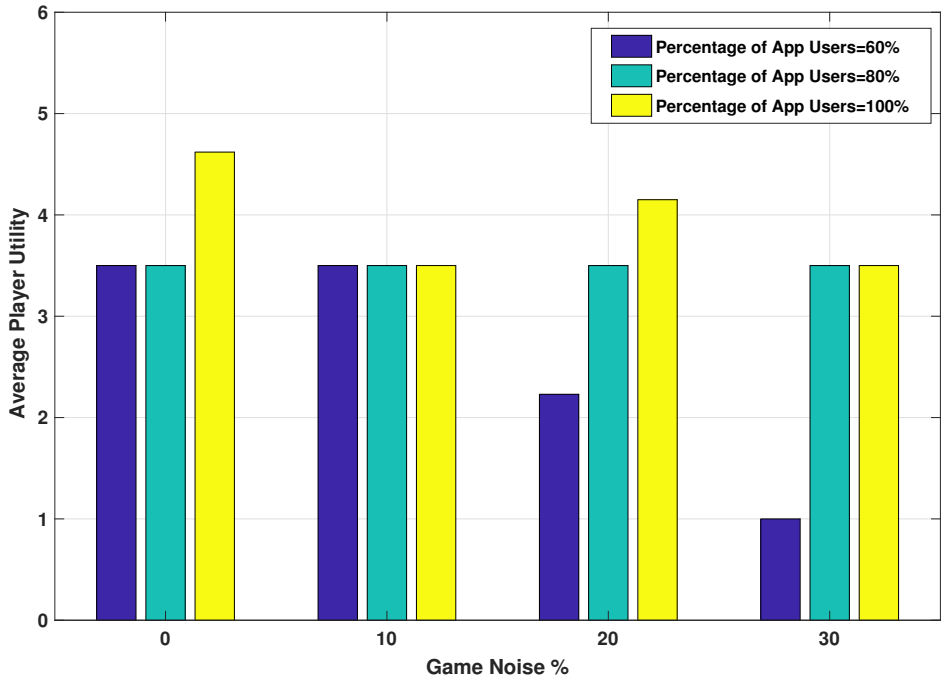

Fig. 6. Average Utility vs. Game Noise ($N^U = 0.7N^C$)

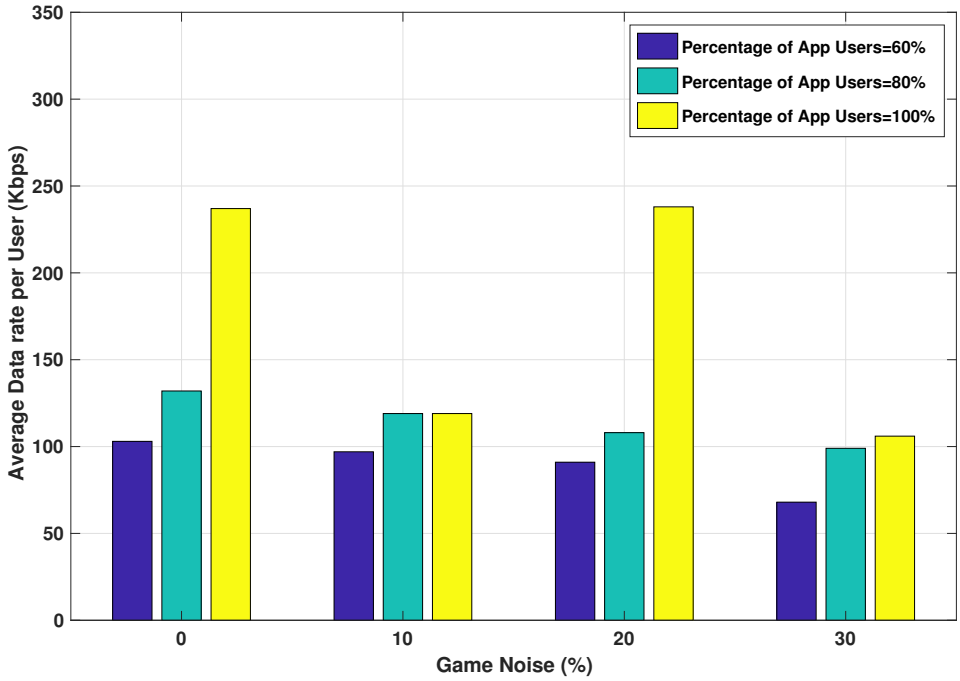

Fig. 7. Average Throughput vs. Game Noise ($N^U = 0.7N^C$)

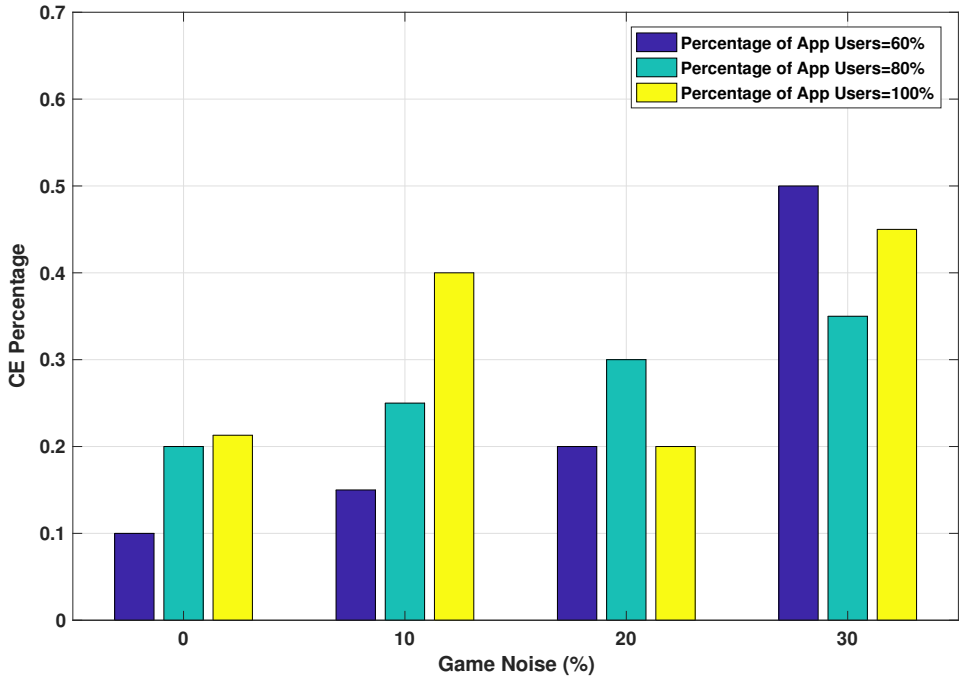

Fig. 8. CE Percentage vs. Game Noise ($N^U = 0.7N^C$)

The next parameter that affects the network performance is the number of simultaneous users that may vary considerably over the course of the match, as will be explained in Section X below. Figures 9 to 11 demonstrate the performance of CC, SCC and No-CC as a function of the percentage of simultaneous users. A similar trend to that of varying the stadium occupancy is seen when the proportion of simultaneous users is raised. At low demand for cellular data ($\tau = 0.1$), CC only outperforms No-CC in utility when Υ^{App} exceeds 80%. In terms of CE percentage, CC requires the fans to switch off the cellular interface with an average probability of 0.4 for $\Upsilon^{App} = 0.6$ and 0.225 for $\Upsilon^{App} = 0.8$, wherein SCC the probability is nearly zero for all values of τ.

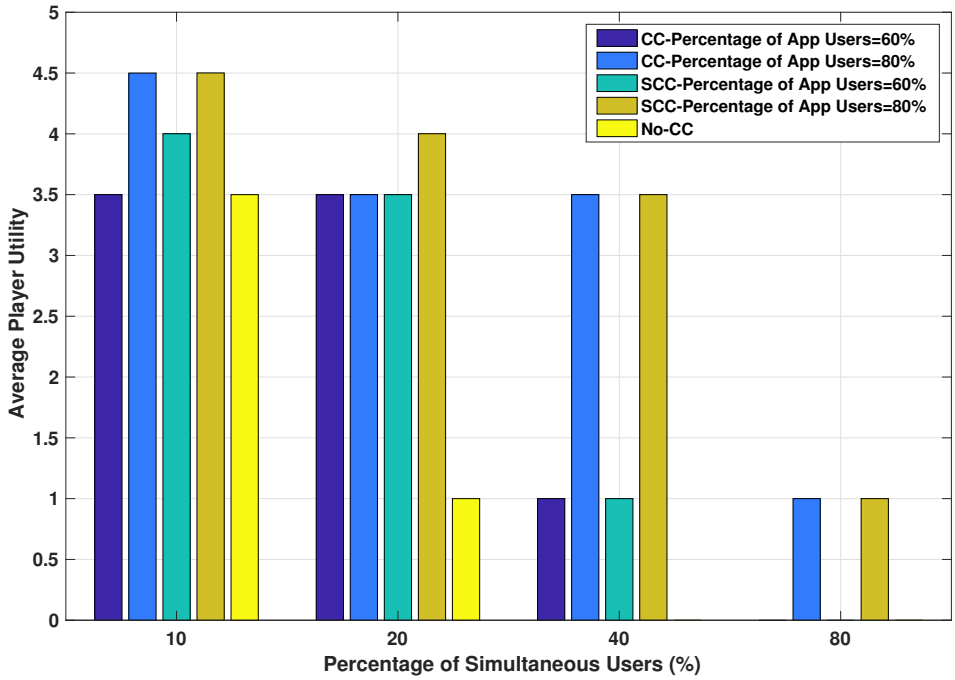

Fig. 9. Average Utility vs. Number of Simultaneous Users

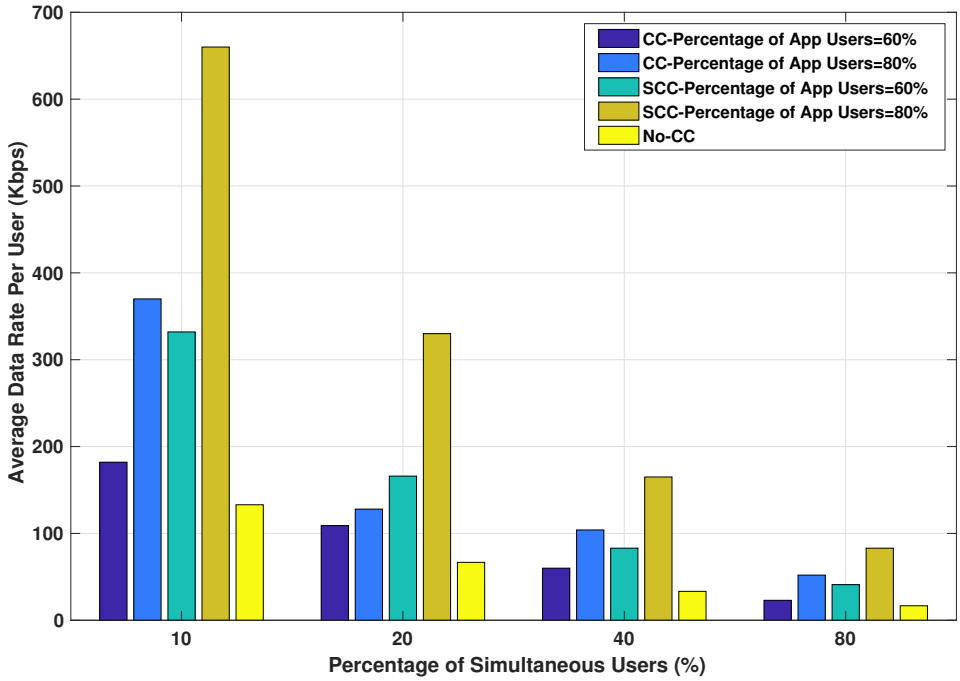

Fig. 10. Average Throughput vs. Number of Simultaneous Users

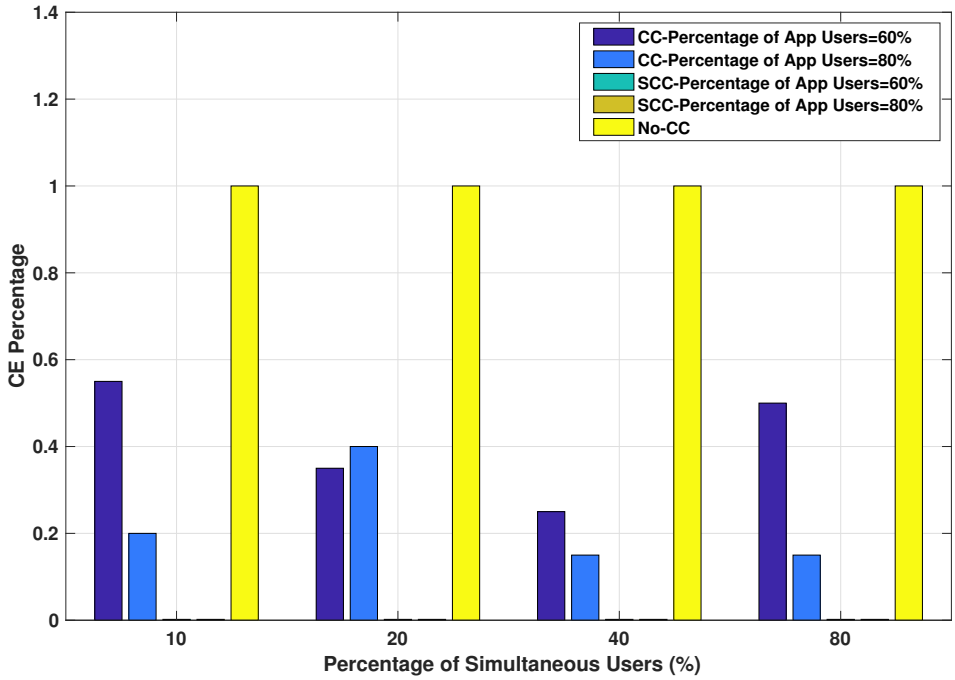

Fig. 11. CE Percentage vs. Number of Simultaneous Users

In all the above simulations, the number of QoE levels L was set to 5 as shown in the above tables I and II. Changing the number of levels affects the stage game equilibria, as the values of $x \in \{0, \ldots, L\}$, for which α_x and β_x are equal, will be affected. For instance, assuming the scenario in Fig. 12, the utility vectors become $\alpha = \{1, 3.5, 3.5, 3.5, 6\}$, $\beta = \{1, 3.5, 3.5, 3.5, 4.5\}$ for 5 QoE levels. For 10 levels, the vectors will be $\alpha = \{1, 1, 1, 3.5, 3.5, 3.5, 3.5, 3.5, 5, 6\}$, $\beta = \{1, 1, 1, 3.5, 3.5, 3.5, 3.5, 3.5, 4, 4.5\}$. In turn, the repeated game equilibria will change as they depend on the stage game equilibria. Meanwhile, increasing the number of levels also increases the probability of triggering the punishment as the levels become closer reducing the expected reward from the deviation. Hence, more efficient equilibria may be supported. As a result, specific values of L may be optimal as shown in figures 12 to 14 below. Particularly, with 10 levels, the throughput reaches a maximum of 350 Kbps per user, and then falls to 150 Kbps when the levels are increased to 100, given $\Upsilon^{App} = 1$. A further increase in the number of levels does not result in any improvement. Practically, a small number of QoE levels is more desirable as it is difficult for individuals to distinguish the performance difference between closely spaced performance levels.

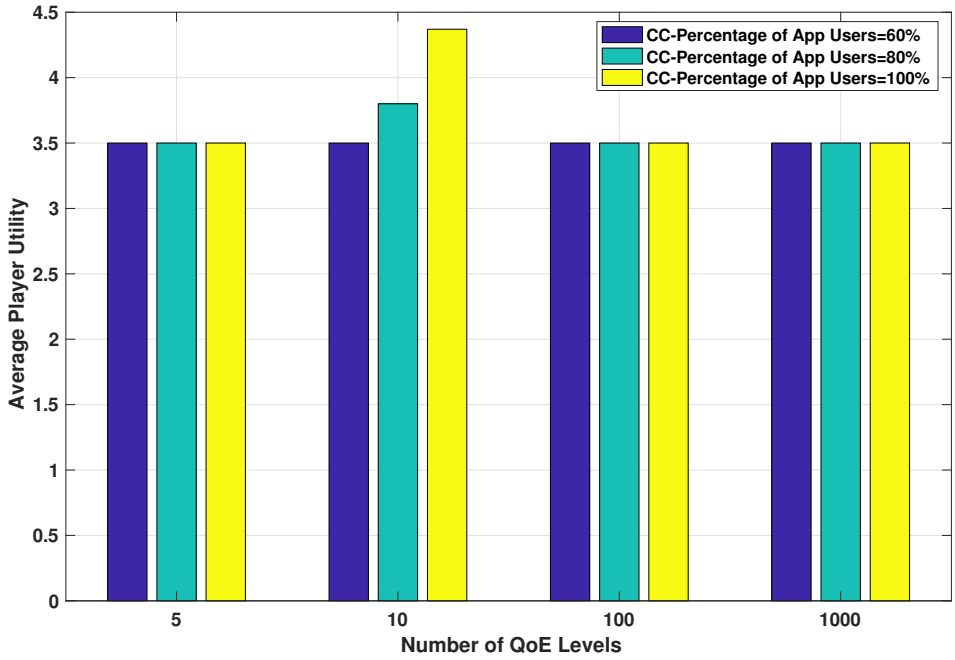

Fig. 12. Average Utility vs. QoE Levels

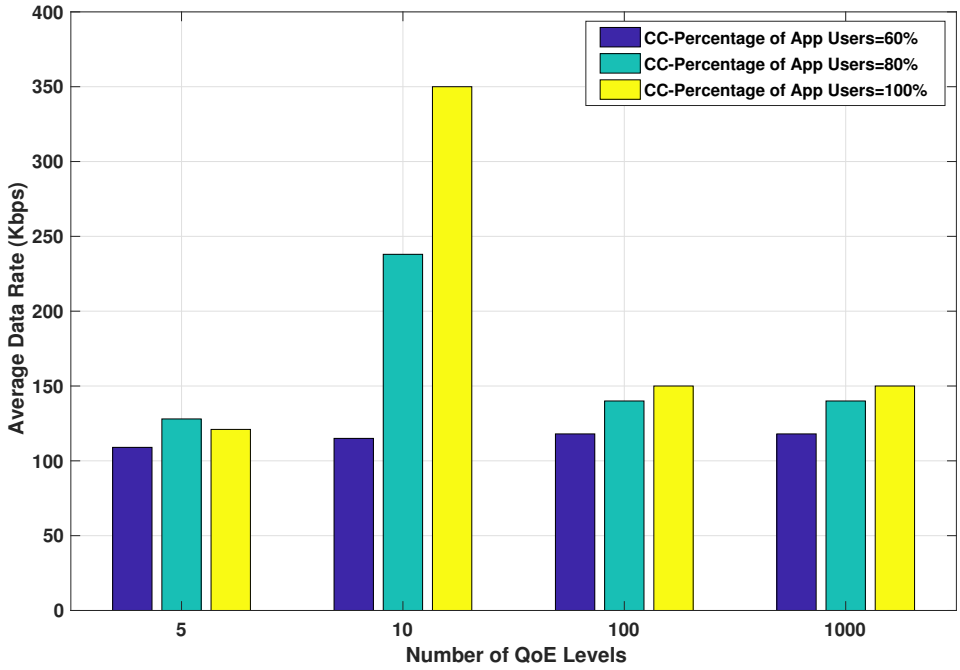

Fig. 13. Average Throughput vs. QoE Levels

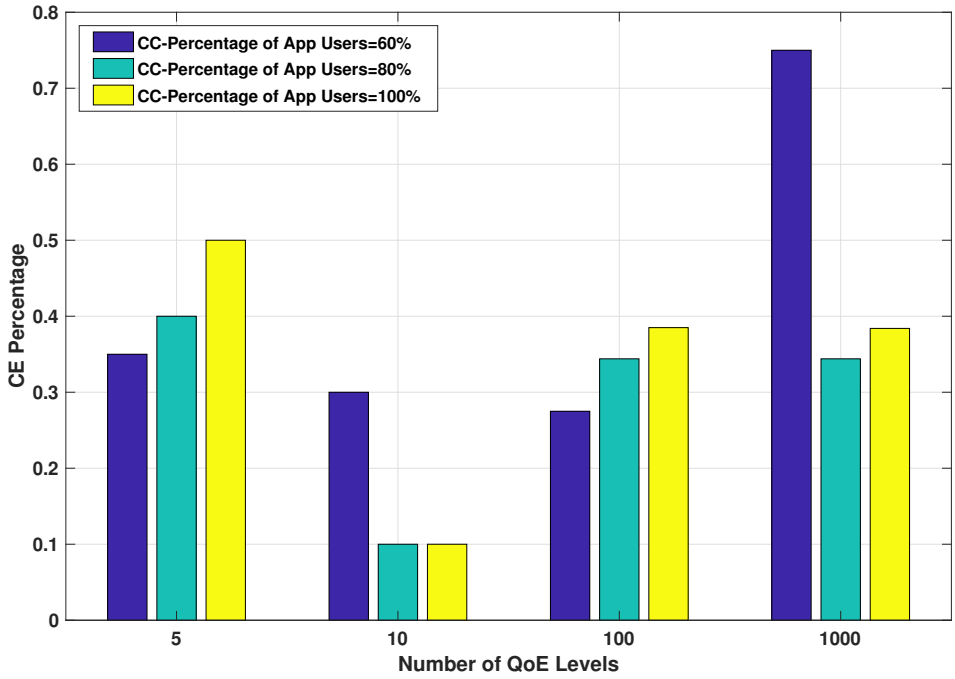

Fig. 14. CE Percentage vs. QoE Levels

X. Discussion

A. Dynamic Network Optimisation

The parameters investigated above do not remain constant over the duration of a football match but may vary considerably as follows. Starting with the stadium occupancy, it is usually observed that fans gradually enter the stadium a few minutes prior to kick-off until a few minutes into the first half of the football match. Later, some fans may leave their seats near the half-time break and then, return to their seats as the second half is about to start. Also, some fans may leave the venue before the final whistle depending on the match score. Moving to the percentage of simultaneous users, we expect that fans tend to use their mobile phones more often during stoppage time or when the events flow at a slow pace. In contrast, the fans are distracted from their devices during critical moments, such as a penalty shoot-out and injury time. Finally, mistakes in following the recommended CE action will be more likely to occur at critical moments and during loud fan chants, as the fans may not hear the CE change notifications.

To deal with the above situations, the match duration may be broken down into several periods, wherein each period, the game parameters above are assumed to remain constant. Thus, each period can be considered as a finitely repeated game on its own. In addition, statistical and machine learning models, such as the *probabilistic neural*

$network$ model [32], may be employed to predict the fan's behaviour, given a match scenario, based on historical data. For instance, if one team has virtually no chance of winning based on historical results, and the match is about to end, the algorithm would predict a high value of τ and the optimal strategies is computed accordingly.

B. Practicality of the Proposed Scheme

A real deployment of the proposed scheme will face many practical challenges. The first difficulty is in achieving a high percentage of App users, as the very first group of fans to join the scheme may not perceive any gain in performance and hence may opt out before more users join in. Even with effective marketing campaigns, persuading a large proportion of the fans (above 60%) to join the scheme at once would seem impossible. However, there are plenty of marketing strategies around this problem, such as providing special discounts on tickets purchased through the designated App or offering subscribers the chance to enter a prize draw if they abide to the App requests. The other obstacle is in the restrictions enforced by mobile phone developers (iOS and Andriod) on many of the settings required by the proposed scheme. For instance, current mobile operating systems (OS) prevent the control of cellular data or WiFi/Bluetooth enable status programmatically. That is, the user has to manually set his CE status introducing possible errors and user inconvenience. Moreover, the peer-to-peer connectivity of iOS and Andriod systems are not entirely compatible with each other, since iOS does not implement the WiFi-Direct standard. To address the first problem, the arrival of application data, such as a new video replay, can be aligned with the CE status changing times so as to minimise the inconvenience. To address the second issue, two segregated and parallel P2P networks may be created for each of iOS and Andriod devices assuming the two platforms are equally popular. Besides the above restrictions, the transmit power and frequency band of the WiFi interface cannot be controlled by software. Thus, the interference minimising topology discussed in VI-B above may not be fully implemented. Hence, we rely on mobile phone manufacturers to relax the above restrictions in the future or to integrate the proposed scheme into the OS by including a "Crowd Mode", for example, that can be enabled by the user.

C. Extending the Stadium WiFi Network

It is noteworthy to mention that the proposed solution can be used to enhance the performance of the stadium owned WiFi network instead. Thus, service A will refer to the Internet access provided by the fixed WiFi network and the CE status will be irrelevant. Instead, the strategy of a user would be its association with the stadium WiFi Access point (AP), such that only a proportion of the users connect to it in a given time

period. Since a full control of the WiFi network is now possible, the user incentives to deviate will be different. Specifically, the collective punishment of playing the low utility NE for T_{pun} periods will be unnecessary as each defecting user (now identifiable by the App) can be individually punished by blocking him from using both the services for T_{pun} periods. Implementing this adjustment requires a minor modification to the game model and its analysis, which can be investigated in a future work.

XI. Conclusion

In this work, the stadium connectivity problem is addressed using a software-defined network approach. A cluster based ad-hoc network with minimum interference is proposed to facilitate the delivery of match application data using BT and WiFi technologies. In this scheme, the in-match applications help to sustain a Nash equilibrium in which the fans reduce their cellular data usage to obtain the optimal trade off between Internet access and exclusive match applications. To sustain cooperative behaviour, a finitely repeated game with limited punishment was proposed and its equilibrium conditions were analysed and shown to exist, given the specific values of the game parameters. It was shown through simulations that adopting the proposed strategy theoretically improves the QoE without the need to increase the cellular capacity with expensive DAS or HD-WiFi. Yet, when CC is combined with these technologies or with the upcoming 5G systems, further gains can be harvested. Many aspects of the behavioural game, including the human error in adopting the optimal strategies were considered. However, actual experiments are still necessary to verify the feasibility of the proposed scheme. Due to the lack of time and budget, real experimentations will be performed in future works.

References

[1] D. Calin, A. Ã. Kaya, B. H. Kim, K. Yang, and S. Yiu, "On the high capacity light radio metro cell design for stadiums," *Bell Labs Technical Journal*, vol. 18, no. 2, pp. 77–97, Sep 2013.

[2] A. Ã. Kaya, D. Calin, and H. Viswanathan, "On the performance of stadium high density carrier wi-fi enabled lte small cell deployments," in *2015 IEEE Wireless Commun. and Netw. Conf. (WCNC)*, Mar 2015, pp. 855–860.

[3] G. Y. Lin, S. R. Chang, and H. Y. Wei, "Estimation and adaptation for bursty lte random access," *IEEE Transactions on Vehicular Technology*, vol. 65, no. 4, pp. 2560–2577, April 2016.

[4] V. K. S. Tripathi and A. Kuma, "Lte e-utran and its access side protocols," 2011. [Online]. Available: http://go.radisys.com/rs/radisys/images/paper-lte-eutran.pdf

[5] H. Hu, Y. Zhang, and J. Luo, *Distributed Antenna Systems: Open Architecture for Future Wireless Communications*, 1st ed. Boston, MA, USA: Auerbach Publications, 2007.

[6] M. N. Islam, S. Subramanian, A. Partyka, and A. Sampath, "Coverage and capacity of 28 ghz band in indoor stadiums," in *2016 IEEE Wireless Commun. and Netw. Conf.*, Apr 2016, pp. 1–7.

[7] J. Cao and C. Williamson, "Towards stadium-scale wireless media streaming," in *14th IEEE International Symposium on Modeling, Analysis, and Simulation*, Sep 2006, pp. 33–42.

[8] W. Choi and J. G. Andrews, "Downlink performance and capacity of distributed antenna systems in a multicell environment," *IEEE Trans. Wireless Commun.*, vol. 6, no. 1, pp. 69–73, Jan 2007.

[9] Y. Li and J. Zhang, "Hot-spot wireless access exploiting shadowing diversity of distributed antennas," in *2008 IEEE International Symposium on Broadband Multimedia Systems and Broadcasting*, March 2008, pp. 1–5.

[10] R. Maslennikov, A. Trushanin, O. Testov, M. Vechkanov, A. Antipova, T. A. Thomas, A. Ghosh, and E. Visotsky, "Azimuth and elevation sectorization for the stadium environment," in *2013 IEEE Global Communications Conference (GLOBECOM)*, Dec 2013, pp. 3971–3976.

[11] "Wembley stadium tour:deep inside ee's' largest das deployment." Think Small Cell. [Online]. Available: https://www.thinksmallcell.com/Enterprise/wembley-stadium-tour-deep-inside-ee-s-largest-das-deployment.html

[12] "Agile stadium solution." Huawei Technologies Co., Ltd., 2014. [Online]. Available: http://enterprise.huawei.com/ilink/cnenterprise/download/

[13] "Cisco stadiumvision." Cisco Systems, Inc., 2013. [Online]. Available: http://www.cisco.com/c/en/us/products/video/stadiumvision/index.html

[14] V. Gabale, B. Raman, P. Dutta, and S. Kalyanraman, "A classification framework for scheduling algorithms in wireless mesh networks," *IEEE Commun. Surveys Tut.*, vol. 15, no. 1, pp. 199–222, First 2013.

[15] "Cisco wireless mesh." Cisco Systems Inc. [Online]. Available: http://www.cisco.com/c/en/us/td/docs/wireless/technology/mesh/8-0/design/guide/mesh80.html

[16] D. Camps-Mur, A. Garcia-Saavedra, and P. Serrano, "Device-to-device communications with wi-fi direct: overview and experimentation," *IEEE Wireless Commun.*, vol. 20, no. 3, pp. 96–104, Jun 2013.

[17] "Tibehive connect - incrowds." Cisco Systems Inc. [Online]. Available: https://incrowdsports.com/stadium-connectivity/

[18] I. T. Haque and N. Abu-Ghazaleh, "Wireless software defined networking: A survey and taxonomy," *IEEE Commun. Surveys Tut.*, vol. 18, no. 4, pp. 2713–2737, Fourthquarter 2016.

[19] W. R. Heinzelman, A. Chandrakasan, and H. Balakrishnan, "Energy-efficient communication protocol for wireless microsensor networks," in *Proceedings of the 33rd Annual Hawaii International Conf. on Syst. Sci.*, Jan 2000, pp. 10 pp. vol.2–.

[20] F. Mazzenga, D. Cassioli, A. Detti, I. Habib, P. Loreti, and F. Vatalaro, "Performance evaluation in bluetooth dense piconet areas," *IEEE Trans. Wireless Commun.*, vol. 3, no. 6, pp. 2362–2373, Nov 2004.

[21] A. C. A. J. Florwick, J. Whiteaker and J. Woodhams, "Wireless lan design guide for high density client environments in higher education." Cisco Systems Inc., 2013. [Online]. Available: http://www.cisco.com/c/en/us/products/collateral/wireless/aironet-1250-series/design_guide_c07-693245.pdf

[22] Y. V. Shih-Fen CHENG, Daniel M. REEVES and M. P. WELLMAN, "Notes on equilibria in symmetric games," *Proceedings of the 6th International Workshop On Game Theoretic And Decision Theoretic Agents GTDT*, 2004. [Online]. Available: http://works.bepress.com/sfcheng/27/

[23] M. A. Khan and Y. Sun, "Non-cooperative games with many players," in *Handbook of Game Theory with Economic Applications*, ser. Handbook of Game Theory with Economic Applications, R. Aumann and S. Hart, Eds. Elsevier, 2002, vol. 3, ch. 46, pp. 1761–1808. [Online]. Available: https://ideas.repec.org/h/eee/gamchp/3-46.html

[24] E. Cartwright, "Learning to play approximate nash equilibria in games with many players," *FEEM Working Paper No. 85.04*, May 2004. [Online]. Available: https://ssrn.com/abstract=555962 or http://dx.doi.org/10.2139/ssrn.555962

[25] A. Papoulis and S. Pillai, *Probability, random variables, and stochastic processes*, ser. McGraw-Hill electrical and electronic engineering series. McGraw-Hill, 2002. [Online]. Available: https://books.google.com.kw/books?id=YYwQAQAAIAAJ

[26] H. Yu, M. A. Khan, K. P. Rath, and Y. Sun, "Strategic uncertainty and the ex-post nash property in large games," *Theoretical Economics*, vol. 10, no. 1, pp. 103–129, 2015. [Online]. Available: http://hdl.handle.net/10419/150245

[27] Z. Han, *Game Theory in Wireless and Communication Networks: Theory, Models, and Applications*, ser. Game Theory in Wireless and Communication Networks: Theory, Models, and Applications. Cambridge University Press, 2012. [Online]. Available: https://books.google.co.uk/books?id=oSnz5ngb9YkC

[28] M. Osborne, *An introduction to game theory*. New York, NY [u.a.]: Oxford Univ. Press, 2004.

[29] V. Srivastava and L. A. DaSilva, "Equilibria for node participation in ad hoc networks - an imperfect monitoring approach," in *2006 IEEE International Conference on Communications*, vol. 8, June 2006, pp. 3850–3855.

[30] C. A. Kamhoua, N. Pissinou, A. Busovaca, and K. Makki, "Belief-free equilibrium of packet forwarding game in ad hoc networks under imperfect monitoring," in *29th International Performance Computing and Communications Conference, IPCCC 2010, 9-11 December 2010, Albuquerque, NM, USA*, 2010, pp. 315–324.

[31] J. Flesch and A. Predtetchinski, "On refinements of subgame perfect ϵ-equilibrium," *International Journal of Game Theory*, vol. 45, no. 3, pp. 523–542, Aug 2016. [Online]. Available: https://doi.org/10.1007/s00182-015-0468-8

[32] C. M. Bishop, *Neural Networks for Pattern Recognition*. New York, NY, USA: Oxford University Press, Inc., 1995.

Chapter 7

Conclusions and Future Work

7.1 Conclusions

This thesis explored alternative techniques by which efficient and reliable communications across future wireless networks of billions of devices can be realised despite the channel capacity limits. In the conducted research, cooperation was an essential component to yield performance gains through the efficient sharing of resources among the network elements. Since the design of cooperation-aware PHY, MAC and NET protocols are fundamental to reap the full advantages of cooperative diversity, we investigated cross-layer cooperative designs at each of the above layers as follows:

At the physical layer, cooperative diversity was shown to improve the channel capacity without sacrificing bandwidth or transmit power. Besides, the distributed relay management techniques that motivate cooperation were analysed for different network configurations. Specifically, the multi-relay selection problem with power control in a downlink relay channel was addressed, in Chapter 3, using a political coalition formation game. In this game, the relays form stable coalitions of parties to maximise their shares from the source's payment. The resulting ultimate ruling coalition was shown to produce a near optimal network sum-rate performance.

In Chapter 4, the power-level selection problem in the EH relay networks were solved via a repeated Bayesian Stackelberg game while considering the relay's data traffic and energy harvesting capability. A relay cost function that combines the channel, energy, and data arrival states was proposed, which its value is only statistically known by the source. A pair of optimal strategies

and a belief update system were proposed then shown to yield a perfect Bayesian equilibrium.

Each of the game theoretic approaches above is effective for particular applications and scenarios. For example, the coalitional game results in a set of relays that is stable against perturbations in channel conditions but requires orthogonal relay channels as well as the exchange of coalitional strength values. Therefore, the solution is applicable in the downlink of relay-assisted 5G cellular networks as the off-grid relay stations are nearly stationary, being within the vicinity of each other. On the other hand, the RBSG targets energy and bandwidth constrained WSNs by allowing non-orthogonal source-relay negotiations, while only demanding the statistical information of channel and energy states.

Moving to the MAC and NET layers, we proposed a novel TDMA-based cooperative MAC protocol, as outlined in Chapter 5, that opportunistically allocates time resources (sub-slots) to a single relay with the best signal strength. This cooperative MAC scheme was integrated with clustering, energy harvesting, and duty cycling to yield an energy efficient cross-layer protocol named ECO-LEACH. In this protocol, each node determines the cluster-head rounds, data transmission, and relaying time slots by means of duty cycles that guarantee an energy-neutral operation. Unlike other clustering protocols in the literature, the proposed protocol features a built-in algorithm to determine the optimal number of clusters based on the application bandwidth and latency requirements. The performance gains of ECO-LEACH were verified against other benchmark protocols by the realistic network simulator OMNET++ and its extensions; GreenCastalia and Castalia.

The stadium connectivity problem was then considered to demonstrate the practicality of the above cooperative techniques, including game theoretic approaches in real-life scenarios. Since highly dense stadium networks suffer from poor user QoE, the solution proposed, being software-based, relieves the capacity bottleneck at the base station through user coordination. As such, a group of users are instructed to switch-off their cellular interfaces at a time to reduce the traffic load on the base station. Similar to LEACH, the cellular-enabled devices act as CHs of a P2P hierarchical cluster network. The topology of this ad-hoc network is obtained using an offline algorithm that maximises the user QoE by computing the interference minimising clustering

layers and the number of CHs per hierarchical level.

As the above problem involves self-interested individuals, the strategic decisions of fans in adopting the proposed scheme were modelled using a finitely repeated large game with approximate equilibria. A novel limited punishment strategy was proposed and proven to yield an SPNE for a given range of game parameters. Furthermore, the irrationalities of players in undertaking their choices were modelled as game noise embedded in the game dynamics. Finally, MATLAB simulations demonstrated, in principle, the performance improvement that can be realised by adopting the proposed scheme. Nevertheless, actual experimentations in a realistic environment are still necessary to ascertain the feasibility and applicability of the proposed solution as will be explained in the next section.

In summary, the thesis has demonstrated how cooperation among network elements can result in significant performance gains only from the efficient utilisation of the available resources. However, maintaining such cooperation among selfish and independent nodes in a decentralised manner to maximise the social welfare is not a straightforward task. In addition, a full stack of cooperation-aware protocols must be carefully designed. Otherwise, the hidden terminal problem of the MAC layer may be aggravated by the relayed transmission of the PHY cooperative diversity scheme. These issues, usually overlooked in the literature, have been well addressed in this thesis using game theory.

7.2 Future Work

Here, we suggest possible research extensions to each component of this research work as follows:

- Relay Selection via Political Coalition Formation

The main disadvantage of the coalitional game discussed in Chapter 3 is the high complexity of finding the URC despite the iterative elimination and party formation stages. Thus, investigating low-complexity URC algorithms should improve the feasibility of the solution for a broad range of applications and scenarios. Also, the stability property of the URC may occasionally prevent the selection of the sum-rate maximising relays, which explains the suboptimality of the URC performance. Therefore, the sum-rate optimality can

be achieved by the transfer of coalitional strengths across the relays to guarantee stability, as suggested in [20]. For instance, an extension of the PCFG may include a stage where the relays with too high coalitional strength values may reduce their powers to remain in the URC. Remarkably, the scenario is compatible with EH relay networks with wireless power transfer capabilities.

- The RPLS in EH-Relay Networks

In the RBSG proposed in Chapter 4, the closed-form solution of (21) was not derived due to its intractability. Hence, the derivation of the exact solution and its effect on the obtained results may be considered in the future. Another possible extension is the implementation and simulation of the multi-source/multi-destination scenario described in Section 4.7. Consequently, modifications to the network model to include multiple-access DF relays will be necessary. Additionally, the stage game formulation and equilibrium analysis should be updated to reflect the new performance metric, that is, the maximisation of the network sum-rate or the minimum source rate.

- The ECO-LEACH Protocol

The protocol, as discussed in Chapter 5, can be further enhanced by introducing hierarchical clustering, as in CrowdConnect, to improve data aggregation and energy efficiency through multi-hop transmission. Comprehensively, the OCHP should first determine the optimal number of hierarchical layers and the number of CHs per layer based on EH rates, latency, and throughput requirements. Then, each node should compute a CH-DC in order for each layer to maintain the optimal CH percentage and energy neutrality. Moving to the proposed cooperative MAC design, the RS scheme based on timers requires a further analysis of node synchronisation as well as the hidden terminal problem. Additionally, various energy sources and energy model parameters may be experimented with to justify the protocol practicality. Finally, a hardware implementation of ECO-LEACH may be carried out to verify its operation under realistic conditions. Testbeds, based on Zigbee motes [92], can be employed with their PHY, MAC, NET, and application layers reprogrammed to comply with ECO-LEACH operation.

- CrowdConnect

Many practical aspects of the stadium connectivity problem have been ignored to simplify the analysis. Specifically, an entirely symmetric scenario was assumed, in which the network operators have an equal number of subscribers seated uniformly in the stadium while holding identical smartphones with a similar degree of wireless reception. Also, fans were assumed to have similar data plans of unlimited usage allowances, and it was assumed that WiFi was always enabled. When the above assumptions are relaxed in reality, the percentage of CDs has to vary across the network depending on the hardware specifications and connection qualities of users' devices. In turn, the proposed game analysis should be modified to allow for non-symmetric strategies. Also, the interactions between each operator fans may be considered as a separate game. Finally, the valuation of the energy cost parameter in the player utility function should be conducted, possibly through surveys.

The predicted correlation between the cellular usage and the match events has not been quantitatively measured in this work. According to the match events, this relationship can be used to develop a prediction model to adjust the cluster network topology dynamically. Hence, we proposed a procedure for acquiring the correlation mentioned above as follows. A number of smartphones belonging to different operators are placed in various locations of the stadium during a football match. Each smartphone is programmed to measure and record the connection speed at regular intervals (every 1 minute). The values from the smartphones are averaged and compared against the match events. For instance, the average connection speed during the first, second, and last five-minute periods of the half-time break can be obtained. By knowing the number of fans and the peak connection speed in the empty stadium, the number of simultaneous users can be determined for each speed value obtained from the measurements. The results can be averaged over data obtained at different stadia and matches. This experiment can be conducted in future work.

Another possible extension to CC is the development of machine learning models to predict the data usage in the match and update the network topology dynamically. For instance, a probabilistic neural network (PNN) model can be used to predict the number of simultaneous users in the next period to come, given the events that occurred in the match so far. Specifically, historical data from previous matches are used, as the training set, to build the

PNN model. The current network status (QoE) is then entered as inputs to the model to classify the output based on the maximum probability. Thus, the output can be in terms of discrete values of the simultaneous number of users in the next period to come.

Since the main focus was on the proposed coordination game and due to budget and time limitations, only MATLAB simulations were performed, which lacked details of the PHY and MAC layers of the cellular, WiFi, and BT systems. For instance, the user throughput was simply obtained by dividing the total cell capacity by the number of active users. In fact, the resource allocation in LTE is not uniform, as users are allocated resources based on CSI and application QoS priorities. On the other hand, establishing WiFi/BT connections incurs overheads and delays that may affect the expected throughput. Thus, simulating CC with OMNET++ would reveal more details of the real deployment.

Nonetheless, implementing the proposed scheme using actual smartphones in a similarly dense scenario is essential to justify its practicality. Due to the lack of time and budget, the experimental work will be pursued in the future. As a first step, we plan to test the designed solution in a classroom environment, where students will be asked to install the CC App on their smartphones and then connect to a testing WiFi access point, which its traffic can be controlled to simulate different stadium environments.

References

[1] X. Foukas, G. Patounas, A. Elmokashfi, and M. K. Marina, "Network slicing in 5g: Survey and challenges," *IEEE Communications Magazine*, vol. 55, no. 5, pp. 94–100, May 2017.

[2] M. Agiwal, A. Roy, and N. Saxena, "Next generation 5g wireless networks: A comprehensive survey," *IEEE Communications Surveys Tutorials*, vol. 18, no. 3, pp. 1617–1655, 2016.

[3] J. G. Andrews, S. Buzzi, W. Choi, S. V. Hanly, A. Lozano, A. C. K. Soong, and J. C. Zhang, "What will 5g be?" *IEEE Journal on Selected Areas in Communications*, vol. 32, no. 6, pp. 1065–1082, June 2014.

[4] G. Choudhary and A. K. Jain, "Internet of things: A survey on architecture, technologies, protocols and challenges," in *2016 International Conference on Recent Advances and Innovations in Engineering (ICRAIE)*, Dec 2016, pp. 1–8.

[5] L. M. Borges, F. J. Velez, and A. S. Lebres, "Survey on the characterization and classification of wireless sensor network applications," *IEEE Communications Surveys Tutorials*, vol. 16, no. 4, pp. 1860–1890, 2014.

[6] S. M. R. Islam, D. Kwak, M. H. Kabir, M. Hossain, and K. S. Kwak, "The internet of things for health care: A comprehensive survey," *IEEE Access*, vol. 3, pp. 678–708, 2015.

[7] P. Gandotra, R. K. Jha, and S. Jain, "Green communication in next generation cellular networks: A survey," *IEEE Access*, vol. 5, pp. 11 727–11 758, 2017.

[8] D. C. AraÃžjo, T. Maksymyuk, A. L. F. de Almeida, T. Maciel, J. C. M.

Mota, and M. Jo, "Massive mimo: survey and future research topics," *IET Communications*, vol. 10, no. 15, pp. 1938–1946, 2016.

[9] H. I. Kobo, A. M. Abu-Mahfouz, and G. P. Hancke, "A survey on software-defined wireless sensor networks: Challenges and design requirements," *IEEE Access*, vol. 5, pp. 1872–1899, 2017.

[10] V. Havary-Nassab, S. Shahbazpanahi, A. Grami, and Z.-Q. Luo, "Distributed beamforming for relay networks based on second-order statistics of the channel state information," *IEEE Trans. on Signal Processing*, vol. 56, pp. 4306–4316, 2008.

[11] J. N. Laneman, D. N. Tse, and G. W. Wornell, "Cooperative diversity in wireless networks: Efficient protocols and outage behavior," *IEEE Trans. on Info. Theory*, vol. 50, pp. 3062–3080, Dec. 2004.

[12] P. Liu, Z. Tao, Z. Lin, E. Erkip, and S. Panwar, "Cooperative wireless communications: a cross-layer approach," *IEEE Wireless Communications*, vol. 13, no. 4, pp. 84–92, Aug 2006.

[13] S. Atapattu, Y. Jing, H. Jiang, and C. Tellambura, "Relay selection and performance analysis in multi-user networks," *IEEE Journal on Selected Areas in Communications*, vol. 31, no. 8, pp. 740—753, Aug. 2013.

[14] P. Ju, W. Song, and D. Zhou, "Survey on cooperative medium access control protocols," *IET Communications*, vol. 7, no. 9, pp. 893–902, Jun. 2013.

[15] M. Bahbahani, M. Baidas, and E. Alsusa, "A distributed political coalition formation framework for multi-relay selection in cooperative wireless networks," *Wireless Communications, IEEE Transactions on*, vol. PP, no. 99, pp. 1–1, 2015.

[16] T. S. Rappaport, *Wireless Communications: Principles and Practice (2nd Edition)*. Prentice Hall, 2002.

[17] D. Niyato, E. Hossain, M. Rashid, and V. Bhargava, "Wireless sensor networks with energy harvesting technologies: a game-theoretic approach to optimal energy management," *Wireless Communications, IEEE*, vol. 14, no. 4, pp. 90–96, August 2007.

[18] "TibeHive Connect - InCrowds," Accessed: 2017-09-19. [Online]. Available: https://incrowdsports.com/stadium-connectivity/

[19] M. Schluter, M. Gerdts, and J. J. Ruckmann, "MIDACO: New global optimization software for MINLP," 2011, Online: http://www.midaco-solver.com.

[20] D. Acemoglu, G. Egorov, and K. Sonin, "Coalition formation in political games," *NBER Working Paper No. 12749*, Dec. 2004, Accessed: 2017-09-19. [Online]. Available: http://www.nber.org/papers/w12749

[21] A. B. MacKenzie and L. A. DaSilva, *Game Theory for Wireless Engineers*. Morgan and Claypool Publishers, 2006.

[22] W. Saad, Z. Han, M. Debbah, and A. Hjorungnes, "A distributed coalition formation framework for fair user cooperation in wireless networks," *IEEE Trans. on Wireless Comms*, vol. 8, no. 9, pp. 4580 – 4593, Sept. 2009.

[23] M. W. Baidas and A. B. MacKenzie, "Altruistic coalition formation in cooperative wireless networks," *IEEE Transactions on Communications*, vol. 61, no. 11, pp. 4678–4689, Nov. 2013.

[24] Z. Han, *Game Theory in Wireless and Communication Networks: Theory, Models, and Applications*, ser. Game Theory in Wireless and Communication Networks: Theory, Models, and Applications. Cambridge University Press, 2012.

[25] J. Marecki, G. Tesauro, and R. Segal, "Playing repeated Stackelberg games with unknown opponents." in *AAMAS*, W. van der Hoek, L. Padgham, V. Conitzer, and M. Winikoff, Eds. IFAAMAS, 2012, pp. 821–828, Accessed: 2017-09-19. [Online]. Available: http://dblp.uni-trier.de/db/conf/atal/aamas2012.html

[26] C. Kiekintveld, J. Marecki, and M. Tambe, "Approximation methods for infinite Bayesian Stackelberg games: modeling distributional payoff uncertainty." in *AAMAS*, L. Sonenberg, P. Stone, K. Tumer, and P. Yolum, Eds. IFAAMAS, 2011, pp. 1005–1012, Accessed: 2017-09-19. [Online]. Available: http://dblp.uni-trier.de/db/conf/atal/aamas2011.html

[27] L. Ferdouse and A. Anpalagan, "Relay selection based on bayesian decision theory in cooperative wireless networks," *Electrical and Computer Engineering, Canadian Journal of*, vol. 38, no. 2, pp. 116–124, Spring 2015.

[28] R. J. Aumann, "Markets with a continuum of traders," *Econometrica*, pp. 32:39–50, 1964.

[29] D. Schmeidler, "Equilibrium points of nonatomic games," *J. Statist. Phys.*, pp. 7:295ÂŰ–300, 1973.

[30] E. Kalai, "Large robust games," *Econometrica*, pp. 1631ÂŰ–1665, 2004.

[31] E. Kalai and E. Shmaya, "Large repeated games with uncertain fundamentals i: compressed equilibrium," 2013, Accessed: 2017-09-19. [Online]. Available: https://economics.wustl.edu/files/economics/imce/compressed-13-12-1_with_corrections.pdf

[32] E. Cartwright, "Learning to play approximate Nash equilibria in games with many players," *FEEM Working Paper No. 85.04*, May 2004, Accessed: 2017-09-19. [Online]. Available: http://dx.doi.org/10.2139/ssrn.555962

[33] J. Laneman and G. W. Wornell, "Distributed space-time-coded protocols for exploiting cooperative diversity in wireless networks," *IEEE Transactions on Information Theory*, vol. 49, no. 10, pp. 2415–2425, Oct 2003.

[34] K. J. R. Liu, A. K. Sadek, W. Su, and A. Kwasinski, *Cooperative Communications and Networking*. Cambridge University Press, 2008.

[35] G. Levin and S. Loyka, "Amplify-and-forward versus decode-and-forward relaying: Which is better?" *Int. Zurich Seminar on Communications (IZS)*, 2012.

[36] J. Boyer, D. Falconer, and H. Yanikomeroglu, "Multihop diversity in wireless relaying channels," *Communications, IEEE Transactions on*, vol. 52, no. 10, pp. 1820–1830, Oct 2004.

[37] M. Yu and J. Li, "Is amplify-and-forward practically better than decode-and-forward or vice versa?" in *Acoustics, Speech, and Signal Processing, 2005. Proceedings. (ICASSP '05). IEEE International Conference on*, vol. 3, March 2005, pp. iii/365–iii/368 Vol. 3.

[38] A. Khan and V. Kuhn, "On the performance of adaptive relaying with arq," in *Smart Antennas (WSA), 2010 International ITG Workshop on*, Feb 2010, pp. 121–126.

[39] X. Wu and L. L. Xie, "On the optimal compressions in the compress-and-forward relay schemes," *IEEE Transactions on Information Theory*, vol. 59, no. 5, pp. 2613–2628, May 2013.

[40] M. M. Fareed, M. S. Alouini, and H. C. Yang, "Efficient incremental relaying for packet transmission over fading channels," *IEEE Transactions on Wireless Communications*, vol. 13, no. 7, pp. 3609–3620, July 2014.

[41] A. Bletsas, A. Khisti, D. Reed, and A. Lippman, "A simple cooperative diversity method based on network path selection," *IEEE Journal on Selected Areas in Comms*, vol. 24, no. 3, pp. 659–672, March 2006.

[42] Y. Jing and H. Jafarkhani, "Single and multiple relay selection schemes and their achievable diversity orders," *IEEE Transactions in Wireless Communcations*, vol. 8, pp. 1414 – 1423, March 2009.

[43] Y. Zhao, R. Adve, and T. J. Lim, "Improving amplify-and-forward relay networks: Optimal power allocation versus selection," *IEEE Trans. on Wireless Communications*, vol. 6, pp. 3114 – 3123, Aug. 2007.

[44] D. Michalopoulos, G. Karagiannidis, T. Tsiftsis, and R. Mallik, "Wlc41-1: An optimized user selection method for cooperative diversity systems," in *Global Telecommunications Conference, 2006. GLOBECOM '06. IEEE*, 2006.

[45] F. A. Onat, Y. Fan, H. Yanikomeroglu, and H. V. Poor, "Threshold based relay selection in cooperative wireless networks," in *IEEE GLOBECOM 2008 - 2008 IEEE Global Telecommunications Conference*, Nov 2008, pp. 1–5.

[46] L. Fei, Q. Gao, J. Zhang, and Q. Xu, "Relay selection with outdated channel state information in cooperative communication systems," *IET Communications*, vol. 7, no. 14, pp. 1557–1565, September 2013.

[47] W. Su, A. K. Sadek, and K. J. R. Liu, "Cooperative communication protocols in wireless networks: Performance analysis and optimal power allocation," *Wireless Pers Commun*, pp. 181—217, Aug. 2007.

[48] B. Wang, Z. Han, and K. J. R. Liu, "Distributed relay selection and power control for multiuser cooperative communication networks using Stackelberg game," *IEEE Trans. on Mobile Computing*, vol. 8, pp. 975–990, Jul. 2009.

[49] M. W. Baidas and M. S. Bahbahani, "A game-theoretic approach to relay selection in cooperative wireless networks," *Proc. of IEEE International Wireless Communications and Mobile Computing Conference*, pp. 375—380, Aug. 2014.

[50] C.-H. Yu, B. Mume, and O. Tirkkonen, "Distributed multiple relay selection by an auction mechanism," in *Proc. of IEEE Global Communications Conference (GLOBECOM)*, Dec 2012, pp. 4392–4397.

[51] X. Liang, M. Chen, and V. C. M. Leung, "A game-theoretic approach for relay assignment over distributed wireless networks," *Proc. of IEEE Wireless Communications and Networking Conference*, pp. 1557—1562, Jul. 2011.

[52] D. Niyato, P. Wang, W. Saad, Z. Han, and A. Hjorungnes, "Coalition formation games for relay transmission: Stability analysis under uncertainty," pp. 920–925, March 2011.

[53] H. Khayatian, R. Saadat, and J. Abouei, "Coalition-based approaches for joint power control and relay selection in cooperative networks," *IEEE Trans. on Vehicular Technology*, vol. 62, no. 2, pp. 835–842, Feb 2013.

[54] B. Varan and A. Yener, "Incentivizing signal and energy cooperation in wireless networks," *IEEE Journal on Selected Areas in Communications*, vol. 33, no. 12, pp. 2554–2566, Dec 2015.

[55] Y. Mao, J. Zhang, S. Song, and K. Letaief, "Joint link selection and relay power allocation for energy harvesting relaying systems," in *Global Communications Conference (GLOBECOM), 2014 IEEE*, Dec 2014, pp. 2568–2573.

[56] M. Kashef and A. Ephremides, "Optimal partial relaying for energy-harvesting wireless networks," *Networking, IEEE/ACM Transactions on*, vol. PP, no. 99, pp. 1–1, 2014.

[57] T. Li, P. Fan, and K. Letaief, "Outage probability of energy harvesting relay-aided cooperative networks over rayleigh fading channel," *Vehicular Technology, IEEE Transactions on*, vol. PP, no. 99, pp. 1–1, 2015.

[58] K. Tutuncuoglu and A. Yener, "Optimum transmission policies for battery limited energy harvesting nodes," *Wireless Communications, IEEE Transactions on*, vol. 11, no. 3, pp. 1180–1189, March 2012.

[59] K. hao Liu, "Selection cooperation using rf energy harvesting relays with finite energy buffer," in *Wireless Communications and Networking Conference (WCNC), 2014 IEEE*, April 2014, pp. 2156–2161.

[60] Y. Luo, J. Zhang, and K. Letaief, "Relay selection for energy harvesting cooperative communication systems," in *Global Communications Conference (GLOBECOM), 2013 IEEE*, Dec 2013, pp. 2514–2519.

[61] Z. Ding and H. Poor, "Cooperative energy harvesting networks with spatially random users," *Signal Processing Letters, IEEE*, vol. 20, no. 12, pp. 1211–1214, Dec 2013.

[62] Y. Xiao, Z. Han, and L. Dasilva, "Opportunistic relay selection for cooperative energy harvesting communication networks," in *Global Communications Conference (GLOBECOM), 2014 IEEE*, Dec 2014, pp. 4371–4376.

[63] N. Newalkar, S. Silakari, and P. K. Shukla, "Comparative analysis of cooperative MAC schemes," in *Cloud and Services Computing (ISCOS), 2012 International Symposium on*, Dec 2012, pp. 42–48.

[64] P. Liu, Z. Tao, S. Narayanan, T. Korakis, and S. S. Panwar, "CoopMAC: A cooperative MAC for wireless LANs," *IEEE J. Sel. Areas Commun.*, vol. 25, no. 2, pp. 340–354, February 2007.

[65] J. Liu, W. Wang, Z. Zheng, X. Zhang, C. Chen, and X. Shen, "Lifetime extended cooperative MAC protocol for wireless LANs," in *Global commun. conf. (GLOBECOM), 2012 IEEE*, Dec 2012, pp. 5476–5481.

[66] M. Khalid, Y. Wang, I. h. Ra, and R. Sankar, "Hybrid cooperative MAC protocol for wireless ad hoc networks," in *International Conf. Comput. Netw. Commun. (ICNC)*, Jan 2012, pp. 1015–1019.

[67] F. Liu, T. Korakis, Z. Tao, and S. Panwar, "A MAC-PHY cross-layer protocol for ad hoc wireless networks," in *IEEE Wireless Commun. Netw. Conf. (WCNC)*, March 2008, pp. 1792–1797.

[68] N. Hu, Y. D. Yao, and Z. Yang, "Analysis of cooperative TDMA in rayleigh fading channels," *IEEE Trans. Veh. Technol.*, vol. 62, no. 3, pp. 1158–1168, March 2013.

[69] H. Jiao and Y. L. Frank, "A mini-slot-based cooperative MAC protocol for wireless mesh networks," in *2010 IEEE Globecom Workshops*, Dec 2010, pp. 89–93.

[70] W. R. Heinzelman, A. Chandrakasan, and H. Balakrishnan, "Energy-efficient communication protocol for wireless microsensor networks," in *Proceedings of the 33rd Annual Hawaii International Conf. on Syst. Sci.*, Jan 2000, pp. 10 pp. vol.2–.

[71] L. Yang, Y. Lu, Y. Zhong, X. Wu, and S. X. Yang, "A multi-hop energy neutral clustering algorithm for maximizing network information gathering in energy harvesting wireless sensor networks," *Sensors*, vol. 16, no. 1, p. 26, 2016.

[72] M. Xiao, X. Zhang, and Y. Dong, "An effective routing protocol for energy harvesting wireless sensor networks," *IEEE Wireless Commun. Netw. Conf. (WCNC)*, pp. 2080–2084, April 2013.

[73] S. M. Bozorgi, M. G. Amiri, A. S. Rostami, and F. Mohanna, "A novel dynamic multi-hop clustering protocol based on renewable energy for energy harvesting wireless sensor networks," *2015 2nd International Conf. on Knowledge-Based Engineering and Innovation (KBEI)*, pp. 619–624, Nov 2015.

[74] S. Peng and C. P. Low, "Energy neutral clustering for energy harvesting wireless sensors networks," *IEEE International Conf. Netw. (ICON)*, pp. 1–6, Dec 2013.

[75] D. Wu, J. He, H. Wang, C. Wang, and R. Wang, "A hierarchical packet forwarding mechanism for energy harvesting wireless sensor networks," *IEEE Commun. Mag.*, vol. 53, no. 8, pp. 92–98, Aug 2015.

[76] A. and H. Y. Kong, "Energy efficient cooperative LEACH protocol for wireless sensor networks," *J. Commun. Netw.*, vol. 12, no. 4, pp. 358–365, Aug 2010.

[77] X. Li, M. Chen, and W. Liu, "Application of STBC-encoded cooperative transmissions in wireless sensor networks," *IEEE Signal Process. Lett.*, vol. 12, no. 2, pp. 134–137, Feb 2005.

[78] G. X. Zhang, Pengfei and H.-P. Tan, "Clustering algorithms for maximizing the lifetime of wireless sensor networks with energy-harvesting sensors," *Computer Networks*, vol. 57, no. 4, pp. 2689–2704, 2013.

[79] A. Ã. Kaya, D. Calin, and H. Viswanathan, "On the performance of stadium high density carrier wi-fi enabled lte small cell deployments," in *2015 IEEE Wireless Commun. and Netw. Conf. (WCNC)*, Mar 2015, pp. 855–860.

[80] H. Hu, Y. Zhang, and J. Luo, *Distributed Antenna Systems: Open Architecture for Future Wireless Communications*, 1st ed. Boston, MA, USA: Auerbach Publications, 2007.

[81] W. Choi and J. G. Andrews, "Downlink performance and capacity of distributed antenna systems in a multicell environment," *IEEE Trans. Wireless Commun.*, vol. 6, no. 1, pp. 69–73, Jan 2007.

[82] Y. Li and J. Zhang, "Hot-spot wireless access exploiting shadowing diversity of distributed antennas," in *2008 IEEE International Symposium on Broadband Multimedia Systems and Broadcasting*, March 2008, pp. 1–5.

[83] R. Maslennikov, A. Trushanin, O. Testov, M. Vechkanov, A. Antipova, T. A. Thomas, A. Ghosh, and E. Visotsky, "Azimuth and elevation sectorization for the stadium environment," in *2013 IEEE Global Communications Conference (GLOBECOM)*, Dec 2013, pp. 3971–3976.

[84] D. Calin, A. Ã. Kaya, B. H. Kim, K. Yang, and S. Yiu, "On the high capacity light radio metro cell design for stadiums," *Bell Labs Technical Journal*, vol. 18, no. 2, pp. 77–97, Sep 2013.

[85] "Wembley stadium tour:deep inside EE's largest DAS deployment." Think Small Cell, Accessed: 2017-09-19.

[Online]. Available: https://www.thinksmallcell.com/Enterprise/wembley-stadium-tour-deep-inside-ee-s-largest-das-deployment.html

[86] "Agile stadium solution." Huawei Technologies Co., Ltd., 2014, Accessed: 2017-09-19. [Online]. Available: http://enterprise.huawei.com/ilink/cnenterprise/download/

[87] "Cisco stadiumvision." Cisco Systems, Inc., 2013, Accessed: 2017-09-19. [Online]. Available: http://www.cisco.com/c/en/us/products/video/stadiumvision/index.html

[88] V. Gabale, B. Raman, P. Dutta, and S. Kalyanraman, "A classification framework for scheduling algorithms in wireless mesh networks," *IEEE Commun. Surveys Tut.*, vol. 15, no. 1, pp. 199–222, First 2013.

[89] "Cisco wireless mesh." Cisco Systems Inc., Accessed: 2017-09-19. [Online]. Available: http://www.cisco.com/c/en/us/td/docs/wireless/technology/mesh/8-0/design/guide/mesh80.html

[90] D. Camps-Mur, A. Garcia-Saavedra, and P. Serrano, "Device-to-device communications with wi-fi direct: overview and experimentation," *IEEE Wireless Commun.*, vol. 20, no. 3, pp. 96–104, Jun 2013.

[91] I. T. Haque and N. Abu-Ghazaleh, "Wireless software defined networking: A survey and taxonomy," *IEEE Commun. Surveys Tut.*, vol. 18, no. 4, pp. 2713–2737, Fourthquarter 2016.

[92] T. de Almeida Oliveira and E. P. Godoy, "Zigbee wireless dynamic sensor networks: Feasibility analysis and implementation guide," *IEEE Sensors Journal*, vol. 16, no. 11, pp. 4614–4621, June 2016.